UNMASKING OF EPIGENETICALLY SILENCED GENES AND IDENTIFICATION OF TRANSGELIN AS A POTENTIAL METHYLATION BIOMARKER IN BREAST CANCER

A THESIS SUBMITTED TO

THE GRADUATE SCHOOL OF ENGINEERING AND SCIENCE

OF BILKENT UNIVERSITY

IN PARTIAL FULFILLMENT OF THE REQUIREMENTS

FOR THE DEGREE OF

DOCTOR OF PHILOSOPHY

IN MOLECULAR BIOLOGY AND GENETICS

By

Nilüfer Sayar

November, 2015

UNMASKING OF EPIGENETICALLY SILENCED GENES AND IDENTIFICATION OF TRANSGELIN AS A POTENTIAL METHYLATION BIOMARKER IN BREAST CANCER

By Nilüfer Sayar
November, 2015

We certify that we have read this thesis and that in our opinion it is fully adequate, in scope and in quality, as a thesis for the degree of Doctor of Philosophy.

_____
Assoc. Prof. Dr. Işık G. Yuluğ
(Advisor)

_____
Prof. Dr. Mehmet Öztürk

_____
Assist. Prof. Dr. Özlen Konu

_____
Assoc. Prof. Dr. Sreeparna Banerjee

_____
Assist. Prof. Dr. Ebru Erbay

Approved for the Graduate School of Engineering and Science

_____
Prof. Dr. Levent Onural

Director of the Graduate School of Engineering and Science

Abstract

UNMASKING OF EPIGENETICALLY SILENCED GENES AND IDENTIFICATION OF TRANSGELIN AS A POTENTIAL METHYLATION BIOMARKER IN BREAST CANCER

Nilüfer Sayar

PhD in Molecular Biology and Genetics

Advisor: Assoc. Prof. Dr. Işık G. Yuluğ

November, 2015

Tumor suppressor genes (TSG) are frequently silenced in cancer by epigenetic mechanisms, including promoter DNA hypermethylation and repressive chromatin formation by means of histone deacetylation. 5-aza-2'-deoxycytidine (AZA) and Trichostatin A (TSA) are DNA methyl-transferase and histone deacetylase inhibitors, respectively, and are used as anti-cancer agents for induction of epigenetically suppressed genes.

In this study, in an attempt to unmask epigenetically suppressed potential TSGs in breast cancer, two breast carcinoma cells and one non-tumorigenic breast cell line were treated with AZA and TSA, either separately or in combination, and with DMSO as control. Afterwards, high-throughput expression profiling revealed significantly affected genes and pathways in response to epigenetic induction in each cell line. Analysis of 32 candidate genes highlighted Transgelin (*TAGLN*) as a putative TSG that is frequently downregulated by promoter DNA hyper-methylation in breast cancer cell lines, and in 61.9% of normal-paired breast tumors according to bisulfite sequencing; and in 63.02% of unpaired breast tumor tissues as determined by bioinformatics analyses of public microarray data. Both relapse-free and overall survivals of patients were more favorable with lower *TAGLN* methylation. Moreover, *TAGLN* promoter methylation levels diagnosed tumors tissues with 83.14% sensitivity and 100% specificity. qRT-PCR and IHC experiments demonstrated that, TAGLN was persistently downregulated in breast cancer cell lines in comparison to non-tumorigenic cells; and in three independent sets of breast tumor tissues, compared to normal tissues. Furthermore, *TAGLN* expression was associated with good prognostic factors. Functional analyses in breast cancer cells revealed negative effect of

transgelin on colony formation abilities of cells, and analyses with epithelial-to-mesenchymal (EMT) markers implicate an association of transgelin with EMT status of breast cancer.

In short, *TAGLN* downregulation by promoter DNA hypermethylation in breast cancer could serve as a growth advantage to the breast cancer cells, while it could be used as a diagnostic or prognostic biomarker for breast cancer.

Keywords: TAGLN, transgelin, breast cancer, methylation, AZA, TSA, biomarker, EMT

Özet

MEME KANSERINDE EPIGENETIK OLARAK SUSTURULMUŞ GENLERİN AÇIĞA ÇIKARILMASI VE TRANSGELIN GENİNİN POTANSİYEL BİR METİLASYON BELİRTEÇİ OLARAK TANIMLANMASI

Nilüfer Sayar

Moleküler Biyoloji ve Genetik, Doktora

Tez Danışmanı: Assoc. Prof. Dr. Işık G. Yuluğ

Kasım, 2015

Tümör baskılayıcı genler (TBG), kanserde sıklıkla DNA hipermetillenmesi ve histon asetil modifikasyonlarının kaldırılması gibi epigenetic mekanizmalar ile baskılanmaktadır. 5-aza-2'-deoksisitidin (AZA) ve Trikostatin A (TSA), DNA metillenmesini ve histon deasetilaz aktivitesini engelleyen, anti-kanser amaçlı kullanılan ilaçlardır.

Bu çalışmada, meme kanserinde epigenetik olarak baskılanan aday TBG'leri tanımlamak için, iki meme kanseri ve bir normal meme hücre hattı, AZA ve/veya TSA, ve DMSO (kontrol) ile muamele edilip, mikrodizin analizleri ile epigenetik mekanizmalardan etkilenen genler ve yolaklar açığa çıkarılmıştır. 32 aday genin incelenmesi sonucu Transgelin (*TAGLN*) geni meme kanseri hücrelerinde, ve normal eşlerine göre tümörlerin %61.9'unda bisülfit sekanslama yöntemi ile; mikrodizin veri analiz yöntemi ile ise meme tümörlerinin %63.02'sinde metillenme ile baskılanan aday bir TBG olarak öne çıkmıştır. Hastaların yüksek sağkalım oranlarının düşük *TAGLN* metillenme skorları ile ilişkili olduğu, ve *TAGLN* metillenme değerlerinin, tümör dokularını %83.14 hassaslık ve %100 özgünlük değerleri ile tespit edebildiği gösterilmiştir. qRT-PCR ve immün-histokimya analizleri *TAGLN* ifadesinin, meme kanseri hücre hatlarında, ve normal meme dokusuyla kıyaslandığında birbirinden bağımsız üç meme tümörü panelinde anlamlı olarak düşük ifade edildiğini göstermiştir. Ayrıca *TAGLN* gen ifadesinin iyi prognoz faktörleri ile ilişkili olduğu anlaşılmıştır. Meme kanseri hücrelerindeki işlevsel çalışmalar, transgelinin hücrelerin proliferasyon yeteneğini negatif etkilediğini göstermiş olup, epitel-mezenkimal dönüşüm (EMD) belirteçleri ile yapılan analizler ise TAGLN'in meme kanserinde EMD ile ilişkili olabileceğine işaret etmektedir.

Kısaca, *TAGLN* geninin meme kanserinde promotör DNA metillenmesi ile susturulması, kanser hücrelerine büyüme avantajı sağlarken, aynı zamanda meme kanseri tanı ve prognozu için de iyi bir biyo-belirteç olmasını mümkün kılmaktadır.

Anahtar kelimeler: TAGLN, transgelin, meme kanseri, metillenme, AZA, TSA, biyo-belirteç, EMD

To my family, Deniz & Defne…

Acknowledgements

"PhD is like marriage". This is how I started my PhD under supervision of Assoc. Prof. Dr. Işık Yuluğ in 2007. Starting from the first day, until the last, she was always supportive, encouraging, caring and guiding. She open-heartedly shared her advices on both lab and life with me, which helped me get through tough times. Not only for these, but I also thank her for trusting me even when I had difficulties in focusing, for enabling a comfortable atmosphere to work and study independently, never opposing to anything we wanted to try, and for creating what I've become as a researcher.

I am very grateful to Prof. Dr. Mehmet Öztürk for broadening my perspective with excellent ideas and comments, and never retaining his support, trust and guidance. I feel lucky to find chance to study with him. I am indebted to Assist. Prof. Dr. Özlen Konu, who guided and motivated me whenever I needed, even at her busiest schedules, and taught me what I know about statistics and bioinformatics. I am very thankful to Assoc. Prof. Dr. Sreeparna Banerjee since I was an undergraduate senior student, for guiding my first steps in laboratory environment, and later for being in my thesis progress committee and being supportive, motivating and full of ideas and recommendations. I thank Assist. Prof. Dr. Ebru Erbay for devising her precious time at a very busy schedule to evaluate my thesis and being a jury member.

I would like to express my gratitude to Assoc. Prof. Dr. Ali Güre as well, for the illuminating classes he gave, and his ideas for my article. I am also very grateful to all past and present MBG faculty members, who had even the slightest effort for my education.

Past and present members of Yuluğ group deserve the greatest gratitude, especially Bala Gür Dedeoğlu, without whom I would have been like a fish out of water. She taught the very basics of MBG laboratory experience with her never-ending patience and sympathy. I would like to thank Prof. Dr. Önder Bozdoğan, who always advised, and practiced, positive attitude in life, and generously shared his excellent life experiences and insights. I am also thankful to him for his helps for my publication. I cannot express my gratitude and love enough for Dr. Gurbet Karahan, who was the number one element of my "life-support unit", being much more than a friend, a sister, a life companion.

I would like to express my special thanks to the other elements of my "life-support unit", Dr. Sinem Yılmaz-Özcan, Dilan Çelebi-Birand and Gizem Ölmezer, for helping me survive all the challenges, dilemmas, and frustrations of my life, and for always being there, never letting me

feel alone or lost. Special thanks are spared for Emre Yurdusev and Can Birand, for their positive, honest and lovely friendship, and advices on grim realities. I am so much thankful to Dr. Ceren Sucularlı for her support, guidance, love and friendship, for confidently being able to share everything with her, without doubt. I am very lucky to have Dr. Verda Bitirim as a good fellow, late gained but among the most valuable. She enlightened my latest years, and never let me on my own to despair in the most difficult days of my life.

I am pleased to be a part of the MBG family, to have known each and every single individual, not possible to name all, but especially Kerem Mert Şenses, Tamer Kahraman, Buse Özel, Begüm Han, Gözde Güçlüer, Füsun Doldur-Ballı, Deniz Cansen Yıldırım, Merve Mutlu, Azer Aylin Açıkgöz, Gülşah Dal Kılınç, İhsan Dereli, and Büşra Yağabasan; and Füsun Elvan, Bilge Kılıç, Yıldız Karabacak, "Abdullah Amca", and "Yavuz Abi".

I thank Dr. Deniz Atasoy for encouraging me to finish "as soon as possible", for his love and support, for bringing me back to life without even knowing.

Last but never the least, I am deeply grateful for my family: my mother, father, sister and brother-in-law, for their endless love, unconditional support, limitless prayers and explicit trust. It is not even possible to imagine one day without them on my side. Finally my little life-partner Mırık, the strongest psychotherapeutic agent during my PhD, will always be missed and loved.

I was supported by TÜBİTAK BİDEB 2211 and ARDEB scholarships during my PhD, and this project was supported by TÜBİTAK 1001 grant, 107T181.

Table of contents

ABSTRACT III

ÖZET V

ACKNOWLEDGEMENTS VIII

TABLE OF CONTENTS X

LIST OF FIGURES XIV

LIST OF TABLES XVI

ABBREVIATIONS XVII

CHAPTER 1. INTRODUCTION 1

1.1. BREAST CANCER 1

1.1.1. PATHOLOGICAL CLASSIFICATION OF BREAST CANCER 2

1.1.2. HISTOLOGICAL GRADING OF BREAST CANCER 2

1.1.3. MOLECULAR CLASSIFICATION OF BREAST CANCER 3

1.1.4. HEREDITARY BREAST CANCER AND SUSCEPTIBILITY GENES 4

1.2. EPIGENETICS AND CANCER 4

1.2.1. DNA METHYLATION, CPG ISLANDS AND CANCER 4

1.2.2. GENOMIC HYPOMETHYLATION IN CANCER 5

1.2.3. HYPERMETHYLATION OF TUMOR SUPPRESSOR GENE PROMOTERS IN CANCER 6

1.2.4. HISTONES, THEIR MODIFICATIONS AND CANCER 9

1.2.5. EPIGENETIC CHANGES IN BREAST CANCER 10

1.2.6. DNA METHYLATION BASED BIOMARKERS FOR DETECTION OF BREAST CANCER 12

1.2.7. EPIGENETIC DRUGS 13

1.2.8. HIGH THROUGHPUT ASSAYS TO STUDY EPIGENETICS IN CANCER 14

1.3. AZA INDUCED GENES ANALYZED IN THIS STUDY 17

1.3.1. TAGLN 23

1.4. AIM OF THE STUDY 24

CHAPTER 2. MATERIALS AND METHODS 25

2.1. MATERIALS 25

2.1.1. GENERAL LABORATORY CHEMICALS AND REAGENTS 25

2.1.2. CELL CULTURE CHEMICALS AND REAGENTS 28

2.1.3. NUCLEIC ACIDS 29

2.1.4. TISSUE MATERIAL 30

2.1.5. ANTIBODIES 31

2.1.6. PCR PRIMERS 32
2.1.7. EQUIPMENT 36
2.2. SOLUTIONS AND MEDIA 36
2.2.1. ROUTINELY USED LABORATORY SOLUTIONS 36
2.2.2. CELL CULTURE SOLUTIONS AND MEDIA 38
2.3. METHODS 39
2.3.1. GENERAL MAINTENANCE AND HANDLING OF HUMAN CELL LINES 39
2.3.2. AZA AND TSA TREATMENT OF CELL LINES 40
2.3.3. DRUG TOXICITY ANALYSIS USING MTT ASSAY 40
2.3.4. RNA ISOLATION AND DETERMINATION OF QUALITY 41
2.3.5. CDNA PREPARATION FROM RNA SAMPLES 41
2.3.6. RT-PCR 41
2.3.7. QRT-PCR AND EXPRESSION ANALYSES 42
2.3.8. HISTONE ISOLATION FROM CELL PELLETS 43
2.3.9. CYTOPLASMIC PROTEIN ISOLATION FROM CELL PELLETS 43
2.3.10. SDS-PAGE AND COOMASSIE STAINING 43
2.3.11. WESTERN BLOT 44
2.3.12. HYBRIDIZATION OF RNA SAMPLES TO THE MICROCHIPS 44
2.3.13. DATA NORMALIZATION AND QUALITY CONTROL 44
2.3.14. CLASS COMPARISON AND DATA ANALYSIS 45
2.3.15. CPG ISLAND ANALYSES 45
2.3.16. ONCOMINE AND EXPRESSION ATLAS ANALYSES 45
2.3.17. DNA ISOLATION FROM CELL LINES AND TISSUES 46
2.3.18. BISULFITE MODIFICATION OF DNA AND BISULFITE PCR 46
2.3.19. PREPARATION OF COMPETENT *E.COLI* DH5A 46
2.3.20. TRANSFORMATION OF BSP PRODUCTS TO COMPETENT DH5A 47
2.3.21. PLASMID ISOLATION FROM TRANSFORMANTS AND BISULFITE SEQUENCING 47
2.3.22. ANALYSIS OF BISULFITE SEQUENCING DATA 47
2.3.23. ANALYSES OF PUBLIC METHYLATION AND SURVIVAL DATA 48
2.3.24. IMMUNOHISTOCHEMISTRY STAINING OF BREAST TISSUE ARRAYS 49
2.3.25. SIRNA TRANSFECTIONS OF MCF10A AND MCF12A CELLS 49
2.3.26. KILL CURVE ASSAY AND DETERMINATION OF GENETICIN CONCENTRATION 49
2.3.27. OVER-EXPRESSION OF *TAGLN* IN BREAST CANCER CELLS 50
2.3.28. 2D COLONY FORMATION ASSAYS 50
2.3.29. *IN VITRO* WOUND HEALING AND MATRIGEL INVASION ASSAYS 50

2.3.30. IMMUNOFLUORESCENCE (IF) STAINING OF BREAST CANCER AND NT BREAST CELLS 51
2.3.31. FACS ANALYSES 51
2.3.32. SENESCENCE ASSOCIATED B-GALACTOSIDASE (SA-B-GAL) STAINING 52
2.3.33. STATISTICAL ANALYSES 52
CHAPTER 3. RESULTS 53
3.1. MICROARRAY EXPERIMENTS AND BIOINFORMATICS ANALYSES 53
3.1.1. DETERMINATION OF THE EFFECTIVE DOSES OF AZA AND TSA 53
3.1.2. VALIDATION OF DRUG ACTIVITY FOR THE MICROARRAY EXPERIMENT SET UP 56
3.1.3. NORMALIZATION AND QUALITY CONTROL OF THE MICROARRAY DATA 58
3.1.4. TRANSCRIPTIONAL CHANGES IN THE TREATED BREAST CELL LINES 59
3.1.5. FUNCTIONAL ANALYSIS OF GENES ALTERED BY AZA AND/OR TSA TREATMENTS IN BREAST CARCINOMA CELL LINES 60
3.1.6. ANALYSIS OF GENE LISTS AND DETERMINATION OF CANDIDATE GENES 64
3.2. ANALYSES OF SELECTED CANDIDATE GENES 73
3.2.1. VALIDATION OF THE SELECTED GENES IN MICROARRAY SET UP BY QRT-PCR 73
3.2.2. ANALYSIS OF EXPRESSION IN BREAST CELL LINE PANEL BY QRT-PCR 76
3.2.3. EXPRESSION ANALYSIS OF SELECTED GENES IN TREATED BREAST CELL LINES 84
3.2.4. BISULFITE SEQUENCING AND METHYLATION ANALYSIS OF SELECTED GENES 88
3.3. ANALYSES OF SECOND PHASE CANDIDATE GENES 90
3.3.1. SELECTION OF NEW CANDIDATE GENES BASED ON FOLD CHANGES 90
3.3.2. EXPRESSION OF THE SECOND PHASE CANDIDATE GENES IN BREAST CELL LINES 91
3.3.3. BISULFITE SEQUENCING OF THE SECOND PHASE GENES IN BREAST CANCER CELL LINES 94
3.3.4. METHYLATION ANALYSIS OF *S100A2* IN NORMAL BREAST TISSUES 97
3.4. METHYLATION AND EXPRESSION ANALYSES OF *TAGLN* IN BREAST TUMORS 98
3.4.1. METHYLATION ANALYSIS OF *TAGLN* GENE IN BREAST TUMORS 98
3.4.2. EXPRESSION ANALYSIS OF *TAGLN* IN MATCHED TUMOR AND NORMAL TISSUES 100
3.4.3. EXPRESSION AND PROMOTER METHYLATION ANALYSES OF *TAGLN* IN PUBLICLY AVAILABLE MICROARRAY DATA 102
3.4.4. *TAGLN* HYPERMETHYLATION AS A BREAST TUMOR BIOMARKER 105
3.4.5. *TAGLN* EXPRESSION IN INDEPENDENT SETS OF BREAST TUMOR TISSUES 106
3.5. FUNCTIONAL ANALYSES OF TRANSGELIN 110
3.5.1. EFFECT OF *TAGLN* EXPRESSION ON COLONY FORMATION IN BREAST CELL LINES 110
3.5.2. EFFECT OF *TAGLN* OVER-EXPRESSION ON CELL MIGRATION AND INVASION 110
3.5.3. TRANSGELIN AND EPITHELIAL-TO-MESENCHYMAL TRANSITION (EMT) IN BREAST CANCER AND NT CELL LINES 113
3.5.4. SPONTANEOUS EMT MODEL AND *TAGLN* EXPRESSION IN MCF10A NT BREAST CELLS 120
3.5.5. EMT MARKERS IN TRANSGELIN OVER-EXPRESSING CELLS 123

3.5.6. TRANSGELIN AND EMT MARKERS IN BREAST TUMOR AND NORMAL TISSUES 125
3.5.7. *TAGLN* AND SENESCENCE IN MDA-MB-361 CELLS 125
CHAPTER 4. DISCUSSION 127
CHAPTER 5. FUTURE PERSPECTIVES 136
REFERENCES 138
APPENDICES 170
APPENDIX A – GENE LISTS 170
APPENDIX B – COPYRIGHT PERMISSIONS 182

List of figures

FIGURE 1.1: STRUCTURE OF NORMAL BREAST TISSUE, AND DEVELOPMENT OF BREAST CANCER. 1

FIGURE 1.2: EPIGENETIC REGULATION OF TUMOR SUPPRESSOR GENES IN CANCER AND NORMAL CELLS. 6

FIGURE 1.3: A CPG ISLAND HYPERMETHYLATION PROFILE OF HUMAN CANCER. 8

FIGURE 1.4 STRUCTURES OF AZA AND TSA. 13

FIGURE 3.1: DETERMINATION OF THE EFFECTIVE DOSES OF AZA AND TSA IN MCF7 CELLS. 54

FIGURE 3.2: DETERMINATION OF THE EFFECTIVE DOSES OF AZA AND TSA IN MDA-MB-231 CELLS. 55

FIGURE 3.3: DETERMINATION OF THE EFFECTIVE DOSES OF AZA AND TSA IN MCF12A CELLS. 56

FIGURE 3.4: VALIDATION OF EFFECTIVENESS OF AZA AND TSA TREATMENTS BEFORE THE MICROARRAY EXPERIMENT. 57

FIGURE 3.5: QUALITY CONTROL ANALYSES OF THE MICROARRAY DATA USING R. 58

FIGURE 3.6: BREAST CARCINOMA CELL LINE SPECIFIC ALTERATIONS UPON DRUG TREATMENTS. 60

FIGURE 3.7: PATHWAYS SIGNIFICANTLY ENRICHED BY AZA TREATMENT OF BREAST CARCINOMA CELLS. . 61

FIGURE 3.8: PATHWAYS SIGNIFICANTLY ENRICHED BY TSA TREATMENT OF BREAST CARCINOMA CELLS. . 62

FIGURE 3.9: PATHWAYS SIGNIFICANTLY ENRICHED BY A+T TREATMENT OF BREAST CARCINOMA CELLS. . 63

FIGURE 3.10: GENES DOWNREGULATED IN EXPRESSION ATLAS OR ONCOMINE DATABASES. 70

FIGURE 3.11: EXPRESSION OF SELECTED GENES IN A PANEL OF BREAST CANCER AND NON-TUMORIGENIC BREAST CELL LINES. 76

FIGURE 3.12: BISULFITE SEQUENCING OF THE GENES IN TEST CELL LINES. 88

FIGURE 3.13: EXPRESSION OF SECOND PHASE CANDIDATE GENES IN BREAST CELL LINE PANEL. 92

FIGURE 3.14: EXPRESSION OF *TAGLN* GENE IN AZA AND/OR TSA TREATED BREAST CELL LINES. 92

FIGURE 3.15: BISULFITE SEQUENCING OF SECOND PHASE CANDIDATE GENES IN SELECTED CELL LINES AND TISSUE SAMPLES. 94

FIGURE 3.16: METHYLATION OF *S100A2* AND *TAGLN* IN BREAST CANCER AND NT CELL LINES. 97

FIGURE 3.17: *S100A2* METHYLATION IN BREAST TISSUES. 98

FIGURE 3.18: OVERALL *TAGLN* METHYLATION IN TUMOR AND NORMAL TISSUES. 98

FIGURE 3.19: *TAGLN* METHYLATION IN MATCHED NORMAL-TUMOR BREAST TISSUES. 99

FIGURE 3.20: *TAGLN* METHYLATION IN DIFFERENT CLINICAL AND PATHOLOGICAL GROUPS. 100

FIGURE 3.21: *TAGLN* EXPRESSION IN PAIRED NORMAL-TUMOR BREAST TISSUES. 101

FIGURE 3.22: CORRELATION OF *TAGLN* EXPRESSION AND METHYLATION WITH *ANLN* EXPRESSION IN MATCHED TUMOR-NORMAL BREAST TISSUES. 102

FIGURE 3.23: METHYLATION OF *TAGLN* PROBES IN PUBLIC DATA SETS. 103

FIGURE 3.24: EVALUATION OF *TAGLN* METHYLATION WITH CLINICAL PARAMETERS IN PUBLIC DATA. 104

FIGURE 3.25: *TAGLN* AS A SERUM METHYLATION BIOMARKER FOR BREAST TUMORS. 105

FIGURE 3.26: *TAGLN* EXPRESSION IN INDEPENDENT SETS OF BREAST TUMORS. 108

FIGURE 3.27: KAPLAN-MEIER ANALYSES WITH *TAGLN* EXPRESSION IN BREAST CANCER PATIENTS. 109

FIGURE 3.28: COLONY FORMATION IN CELLS WITH ALTERED *TAGLN* EXPRESSION. 111

FIGURE 3.29: EFFECT OF *TAGLN* OVER-EXPRESSION ON MIGRATION AND INVASION OF BREAST CANCER CELLS. 112

FIGURE 3.30: CO-STAINING OF TRANSGELIN WITH VIMENTIN OR E-CADHERIN IN NT BREAST CELLS. 113

FIGURE 3.31: CO-STAINING OF TRANSGELIN WITH VIMENTIN OR E-CADHERIN IN HIGHLY INVASIVE BREAST CANCER CELLS. 114

FIGURE 3.32: CO-STAINING OF TRANSGELIN WITH VIMENTIN OR E-CADHERIN IN LOW INVASIVE BREAST CANCER CELLS. 115

FIGURE 3.33: CO-STAINING OF TRANSGELIN WITH VIMENTIN OR E-CADHERIN IN NON-INVASIVE BREAST CANCER CELLS WITH HIGH LEVELS OF E-CADHERIN EXPRESSION. 116

FIGURE 3.34: CO-STAINING OF TRANSGELIN WITH VIMENTIN OR E-CADHERIN IN NON-INVASIVE BREAST CANCER CELLS WITH MEDIUM LEVELS OF E-CADHERIN EXPRESSION. 117

FIGURE 3.35: CO-STAINING OF TRANSGELIN WITH VIMENTIN OR E-CADHERIN IN NON-INVASIVE BREAST CANCER CELLS WITH LOW LEVELS OF E-CADHERIN EXPRESSION. 118

FIGURE 3.36: QRT-PCR ANALYSES OF EMT MARKERS AND *TAGLN* IN BREAST CELL LINE PANEL. 119

FIGURE 3.37: TRANSGELIN PROTEIN LEVELS IN MCF10A SPONTANEOUS EMT MODEL. 121

FIGURE 3.38: MORPHOLOGIES OF MCF10A CELLS WITH DECREASED TRANSGELIN PROTEIN LEVELS. 122

FIGURE 3.39: EMT MARKERS IN *TAGLN* OVER-EXPRESSING BREAST CANCER CELLS. 124

FIGURE 3.40: CELL CYCLE ANALYSIS USING FLOW CYTOMETRY IN MDA-MB-361 CELLS. 125

FIGURE 3.41: CORRELATION OF TRANSGELIN WITH EMT MARKERS IN BREAST TUMOR TISSUE ARRAY. 126

FIGURE 3.42: SA-B-GAL STAINING IN MDA-MB-361 CELLS. 126

List of tables

TABLE 1.1: COMMON FEATURES OF BREAST CANCER MOLECULAR SUBTYPES 3

TABLE 1.2 : PATHWAYS DISRUPTED BY GENE-PROMOTER HYPERMETHYLATION AND THE ASSOCIATED GENES SILENCED IN CANCER 7

TABLE 1.3: EPIGENETIC STUDIES WHICH USED EXPRESSION MICROARRAYS TOGETHER WITH EPIGENETIC DRUGS 14

TABLE 2.1: CHEMICALS, REAGENTS, ENZYMES, AND KITS USED FOR GENERAL LABORATORY PURPOSES 25

TABLE 2.2: CHEMICALS, REAGENTS, KITS AND MEDIA USED IN CELL CULTURE 28

TABLE 2.3: LIST OF NUCLEIC ACIDS USED FOR GENE EDITING 30

TABLE 2.4: PATHOLOGICAL FEATURES OF NORMAL MATCHED BREAST TUMOR TISSUES 30

TABLE 2.5: ARRAYS PURCHASED FOR IHC AND QRT-PCR ANALYSES 31

TABLE 2.6: ANTIBODIES USED IN THE STUDY 32

TABLE 2.7: PRIMERS USED IN THE STUDY 33

TABLE 2.8: EQUIPMENT USED FOR THE EXPERIMENTS 36

TABLE 2.9: ROUTINELY USED BUFFERS AND SOLUTIONS 36

TABLE 2.10: CELL LINES AND THEIR GROWTH MEDIA 38

TABLE 2.11: SDS-POLYACRYLAMIDE GEL PREPARATION 43

TABLE 2.12: DATASETS USED FOR ANALYSIS OF *TAGLN* EXPRESSION AND PROMOTER METHYLATION IN BREAST CANCER 48

TABLE 3.1: RIN VALUES OF RNAS USED IN MICROARRAY ANALYSIS 57

TABLE 3.2: CORRELATION OF DATA BETWEEN REPLICATES 59

TABLE 3.3: NUMBERS OF PROBE SETS ALTERED UPON TREATMENTS IN EACH CELL LINE 59

TABLE 3.4: EXPRESSION RATIOS OF SELECTED CANDIDATE GENES IN EACH CELL LINE AND TREATMENT 64

TABLE 3.5: CPG ISLAND SEARCH IN THE 2000 BP UPSTREAM AND DOWNSTREAM OF TRANSCRIPTION START SITE OF SELECTED CANDIDATE GENES 68

TABLE 3.6: COMBINATION OF ALL ANALYSES CARRIED OUT FOR CANDIDATE GENES 71

TABLE 3.7: EXPRESSION OF SELECTED GENES IN TREATMENT GROUPS OF TEST CELL LINES 74

TABLE 3.8: QRT-PCR ANALYSIS OF SELECTED GENES IN TREATED BREAST CANCER AND NT CELL LINES 85

TABLE 3.9: EXPRESSION RATIOS OF THE SECOND PHASE CANDIDATE GENES IN MICROARRAY DATA 91

TABLE 3.10: EXPRESSION RATIOS OF THE SECOND PHASE CANDIDATE GENES IN TREATMENT GROUPS 93

TABLE 3.11: *TAGLN* HYPERMETHYLATION IN MATCHED TUMOR AND NORMAL BREAST TISSUES 100

TABLE 3.12: *TAGLN* HYPERMETHYLATION IN PUBLIC TUMOR AND NORMAL BREAST TISSUES 103

TABLE 3.13: CANCER VS. NORMAL ANALYSIS OF *TAGLN* MRNA IN ONCOMINE DATABASE 106

TABLE 3.14: EXPRESSION OF *TAGLN* IN INDEPENDENT TUMOR AND NORMAL TISSUES 107

TABLE 3.15: CORRELATIONS OF EXPRESSIONS OF EPITHELIAL AND MESENCHYMAL MARKERS 120

Abbreviations

ANLN	Annilin
AZA	5-aza-2'-deoxycytidine
A+T	5-aza-2'-deoxycytidine + Trichostatin A
BC	Breast carcinoma
BSP	Bisulfite sequencing PCR
CGI	CpG Island
CK19	Cytokeratin 19
CpG	Cytosine-phosphate-Guanine
DBC	Ductal breast carcinoma
DCIS	Ductal carcinoma *in situ*
DMSO	Dimethyl sulfoxide
DNMT	DNA methyltransferase
EMT	Epithelial to mesenchymal transition
ER	Estrogen receptor
GEO	Gene Expression Omnibus
H3K9Ac	Histone 3 lysine 9 acetylation
HDAC	Histone Deacetylase
Her2	Human epidermal growth factor receptor 2
H-score	Immunohistochemical score
IDC	Infiltrating ductal carcinoma
IF	Immunofluorescence
IHC	Immunohistochemistry
ILC	Infiltrating lobular carcinoma
KM	Kaplan-Meier
LBC	Lobular breast carcinoma
LCIS	Lobular carcinoma *in situ*
MSP	Methylation specific PCR
NAMS	Normalized average methylation score
NT	Non-tumorigenic
OD	Optical density
OS	Overall survival
PR	Progesterone receptor
RFS	Relapse-free survival
ROC	Receiver-operator characteristics
RT	Room temperature
S100A2	S100 calcium binding protein A2
SA-β-Gal	Senescence associated β-galactosidase
SEM	Standard error of means
SMC	Smooth muscle cell
TAGLN	Transgelin
TB	Transformation buffer
TN	Triple negative
TSA	Trichostatin A
TSG	Tumor suppressor gene
TSS	Transcription start site
VIM	Vimentin

Chapter 1. Introduction

1.1. Breast Cancer

Breast cancer is the second most observed cancer throughout the world, and the leading cause of cancer mortality in women. In 2012, 1.67 million new breast cancer cases were diagnosed and 522 thousand deaths were reported due to breast cancer[1]. 29% of new cancer cases have been estimated to be of breast origin for 2015 in the US. The high mortality rates and challenges in treatment of breast cancer patients stems from the highly heterogeneous nature of the disease[2].

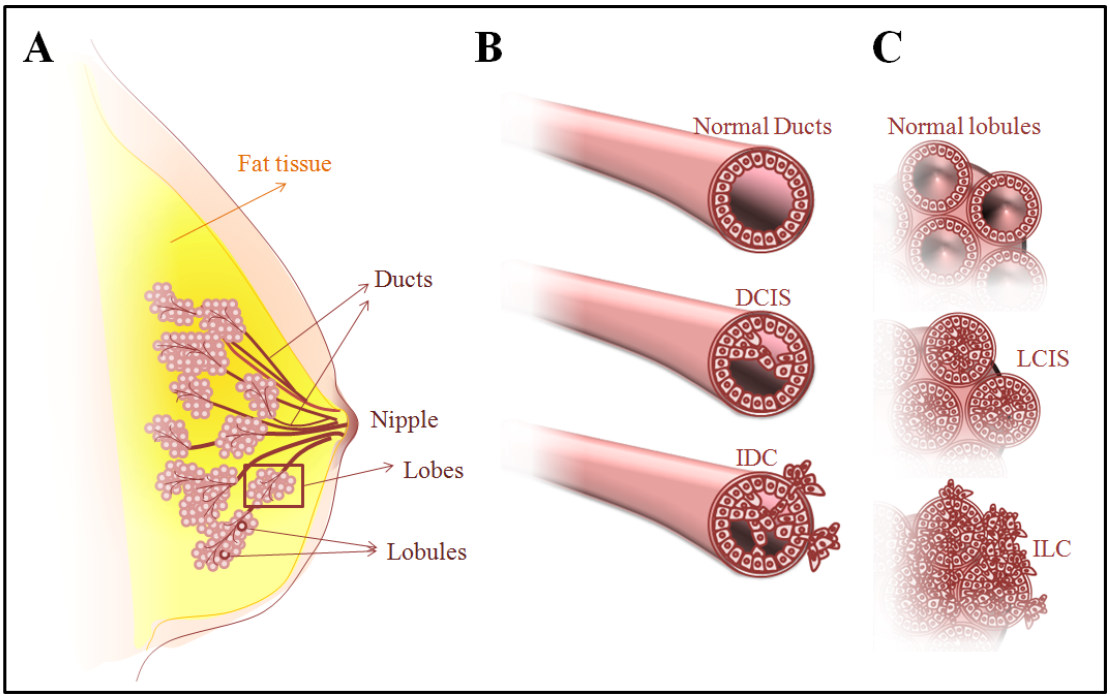

Figure 1.1: Structure of normal breast tissue, and development of breast cancer.

(A) Structure of the normal breast tissue. (B)Development and progression of ductal carcinoma in situ (DCIS) and invasive ductal carcinoma (IDC). (C)Development and progression of lobular carcinoma in situ (LCIS) and invasive lobular carcinoma (ILC). (Copyright, 2015, Nilufer Sayar).

The normal human mammary gland consists of a secretor (glandular) tissue, composed of a branching ductal-lobular system, including milk glands that are called lobules, milk ducts carrying milk from the lobules to the nipple; a fat tissue and a supporting connective tissue, including blood and lymph vessels[3-4]. Approximately 25 ducts originate from the nipple base

and branch into smaller ductules, eventually channeling to the lobules which are arranged into a lobe (Figure 1.1A)[2, 4]. Each duct has two layers of epithelial cells. The inner layer forms the lumen, and the outer layer forms the myoepithelial cells, having properties of smooth muscle cells and providing the contractile force during lactation to excrete milk[2]. Carcinoma of the breast may emerge from any cell along the ductal-lobular system. This results in pathological classification of breast cancer to discriminate between the different original cell types.

1.1.1. Pathological classification of breast Cancer

Although several pathological subtypes have been described by the World Health Organization[5], most of them are very rarely observed. Moreover, breast cancer is a heterogeneous disease, and a breast tumor may be composed of more than one type, such as combination of invasive and *in situ* types. The most common types of breast cancer, and their general features are listed below[6]:

(1) Ductal carcinoma in situ (DCIS, Figure 1.1B) is the most common class of the *in-situ* breast cancers. In this case, the abnormal cell proliferation occurs only in the epithelial cells of the ducts, and the malignant cells do not invade through the duct walls[6]. DCIS can be identified by morphology, and usually is curable.

(2) Lobular carcinoma in situ (LCIS, Figure 1.1C) is the non-invasive cancer of the lobules. The epithelial cells proliferate regularly, without invading the lobular borders[6].

(3) Invasive (or infiltrating) ductal carcinoma (IDC, Figure 1.1B) is the most frequent of the invasive breast cancers, making up ~80% of the cases[5-6]. As in the DCIS, uncontrolled proliferation starts in the ducts, but the neoplastic cells acquire the ability to invade and infiltrate the duct walls, associated basement membrane and the remaining breast tissue. At later stages, metastasis to the other tissues and organs of the body is frequent, usually by establishment of penetrating ducts and tubules[4]. IDC itself can be categorized into several subtypes, including metaplastic, papillary, micropapillary, mucinous, and medullary. These categorized subtypes constitute a~20% of the IDC cases. The rest of the uncategorized cases are usually called as IDC of "Not Otherwise Specified", NOS.

(4) Invasive (or infiltrating) lobular carcinoma (ILC, Figure 1.1C) is the second most observed invasive breast cancer, with ~10% of frequency. It originates in the lobules, like LCIS, but invades through the walls and infiltrates the breast and other tissues, as in IDC.

1.1.2. Histological grading of breast cancer

Invasive breast carcinomas can be grouped into distinct grades based on their histological features, including mitotic activity, tubule formation and nuclear pleomorphism, and basically

define the proliferation and differentiation status of the breast tumors[4, 7]. Among these, mitotic activity index is the most informative one[8]. For each feature, a value of 1-3 is given and the total score is determined by adding each score[9]. According to this, grade 1 tumors have scores up to 5, grade 2 tumors have 6 or 7, and grade 3 tumors have 8 or 9 as scores. Since differentiation states of the tumors decrease with higher grades, poorer prognosis of patients, such as lymph node metastases, death from disease, and recurrence increase with increasing grade[6].

1.1.3. Molecular classification of breast cancer

It is assumed that the gene expression diversities in breast tumors underlie the diversity at phenotypic levels[10-11]. Thus, global expression profiling has been employed to classify breast tumors into separate groups, of usually six intrinsic subtypes[12-16]: luminal A (LumA), luminal B (LumB), HER2/ERBB2- overexpressing (Her2pos), basal-like, normal breast-like and claudin-low. The origin of most of the breast cancer cases are usually luminal cells[17]. Expression levels of estrogen receptor (ER), progesterone receptor (PR), and human epidermal growth factor receptor 2 (Her2) of the tumors are essential to the prognosis of the patients, and selection of the treatment procedures. While the $ER^{(+)}$ LumA types of tumors are associated with the best outcome, claudin low ($ER^{(-)}$, $PR^{(-)}$ and $Her2^{(-)}$; a.k.a. triple negative, TN), Her2pos ($ER^{(-)}$, $PR^{(-)}$, $Her2^{(++)}$) and basal-like (also TN) tumors are known as more aggressive and worse prognosis tumors[13, 18-20]. Over-expression of embryonic stem cell genes have been observed in some of the more undifferentiated class of basal-like breast cancers, which are usually of IDC type[17, 21]. Claudin-low tumors are known for higher expression of epithelial to mesenchymal transition (EMT) genes[22]. Normal breast-like tumors, on the other hand, are intermediate between basal-like and luminal cancers. While some studies characterize these as a distinct subtype of breast tumors, some believe they are resultant of contamination with normal breast tissues[23]. Table 1.1 summarizes the common features of breast cancer molecular subtypes, and the corresponding prognostic states[18].

Table 1.1: Common features of breast cancer molecular subtypes

Molecular subtype	Frequency (%)	ER/PR/Her2 states	Grade	Prognosis
Normal Breast Like	5-10	ER-/+, PR-, Her2-	Low	Intermediate
Luminal A	50-60	ER+, PR+, Her2-	Low	Good
Luminal B	15-20	ER+/-, PR+/-, Her2+/-	Intermediate	Intermediate
Her2+	10-15	ER-, PR-, Her2+	High	Poor
Basal-like	10-30	ER-, PR-, Her2-	High	Poor
Claudin-low	12-14	ER-, PR-, Her2-	High	Poor

Adapted from Eroles et al.[18]

1.1.4. Hereditary breast cancer and susceptibility genes

Approximately 5-10% of breast cancer cases is hereditary, and occurs due to inheritance of autosomal dominant mutations of predisposing genes[24-25]. *BRCA1* and *BRCA2* germ-line mutations are responsible for about 30% of these hereditary cases, and 70-85% of the mutation carriers are expected to develop breast cancer in the future[24, 26]. BRCA1 and BRCA2 proteins function in DNA repair by binding and activating RAD51 protein[27]. There are also other genes associated with familial breast cancer, categorized as high penetrance genes with lower frequencies, and lower-moderate penetrance genes with higher frequencies. *TP53* tumor suppressor gene is a high penetrance gene, its mutation is found in only 1% of breast cancer cases, yet once present, p53 mutation predisposes a woman to a 60-fold increased risk for development of breast cancer[25, 28]. Germ-line mutations in another high penetrance gene, *PTEN*, constitute < 1% of breast cancer cases, with 50% increased risk for breast cancer[29-30]. *CDH1* gene (coding E-cadherin protein) is another example, with frequency of 1.3%, and increased risk for breast cancer of 39%[25, 31]. Among the low-moderately penetrating genes, *CHEK2* gene mutations are observed in 1% of the breast cancer patients, and increase the breast cancer risk by approximately 3 fold[25], whereas a mutation in *ATM* gene gives rise to 2 fold increase[32-33]. Most of these genes cause other syndromes when mutated, like Li-Fraumani (*TP53*), ataxia-telangiectesia (*ATM*), and Cowden (*PTEN*) syndromes.

1.2. Epigenetics and cancer

Cancer is a heterogeneous, complex and multistep disease involving changes in DNA structure, and alterations in gene expressions, which in turn causes an imbalance of oncogenes and tumor suppressor genes (TSG) that are finely orchestrated in a normal cell. These changes might be genetic, and result in small or large differences in the sequence of DNA; or epigenetic, referring to heritable modifications in the pattern of gene expression that do not involve variations in the original nucleotide sequence of a gene[34]. Epigenetic mechanisms include DNA methylation and hydroxy-methylation, histone modifications and chromatin remodeling, and a variety of non-coding RNAs. Deregulation in any step of these events will have specific or global effects on gene expression, thereby resulting in changes that drive initiation, advancement and progression of cancer, relating to all of the hallmarks of a cancer cell[35-37].

1.2.1. DNA methylation, CpG islands and cancer

DNA methylation is the addition of a methyl group, supplied by S adenosyl-methionine, to the 5' carbon of the cytosine bases of CpG dinucleotides, by DNA methyltransferases (DNMTs)[34].

DNMT1 gene is responsible for preserving the methylation motifs of a cell during and after DNA replication[38], and therefore the substrate of DNMT1 is hemi-methylated DNA. DNMT3a and DNMT3b function in *de novo* methylation of DNA. Nevertheless, all three enzymes can accomplish both *de novo* and maintenance methylation functions, separately, or in cooperation[38]. TET proteins, as well as AID, GADD45A, ELP3 and TDG, on the other hand, are responsible for de-methylation of already methylated sequences[39-40].

DNA methylation is one of the most important and well-studied mechanisms for gene expression regulation in mammals. It is essential for transcriptionally inactive heterochromatin formation, by suppressing translocation events and preserving integrity of the genome, X-chromosome inactivation, gene imprinting, and several other mechanisms[41-42].

The frequency of the CpG dinucleotides in the human genome is lower than expected due to spontaneous deamination of the methylated C to U in the germ cells throughout the years of evolution[38]. Yet, there are CpG rich regions in the genome, especially around the promoter regions, first exons and 5' UTR sequences of several genes, which are usually referred to as CpG islands. The definition of CpG islands is usually accepted as 200 – 500 bp sequences, whose G+C content is greater than 50-55%, and whose (observed CpG %) / (expected CpG %) ratio is smaller than 0.6[43-44]. The unmethylated status of a CpG island corresponds to transcriptionally active genes as long as the necessary protein machinery is available for transcription[41]. CpG islands are usually unmethylated in normal cells and are associated with housekeeping or tissue specific genes, and ensure the fine tuning of gene expression regulation in different types of cells[45]. In cancer, these mechanisms can be exploited in two ways:[38] first, by global hypomethylation in the genome and creating genomic instability; and second, hypermethylation of TSG promoter regions (Figure 1.2), thereby avoiding growth and proliferation inhibitory activities of these genes[46].

1.2.2. Genomic hypomethylation in cancer

Genome-wide loss of DNA methylation, genomic hypomethylation, was one of the first epigenetic deregulations to be discovered in human cancer[47]. The hypomethylation levels increase as the tumor progresses from benign to an invasive type. Since the many gene promoters are usually unmethylated in a normal cell, a high proportion of the methylated CpGs are located around and at the repeated sequences, such as transposable elements. Thus, global hypomethylation serves as a mechanism to activate not only normally hypermethylated oncogenes, but it also turns on the normally inactive transposable elements, in addition to imprinted genes, and genes on the inactive X chromosome [34, 48]. Specifically, long interspersed nucleotide element-1(*LINE-1*) and Alu transposable elements are associated with DNA

hypomethylation in almost all known human cancers. Hypomethylation of *LINE*-1 elements results in activation of its retro-transposition and unexpected insertions may affect nearby genes and promoters, resulting in activation of proto-oncogenes. Alternatively, insertion of a repetitive element into a promoter region may result in methylation of the region, resulting in possible inactivation of TSGs[49].

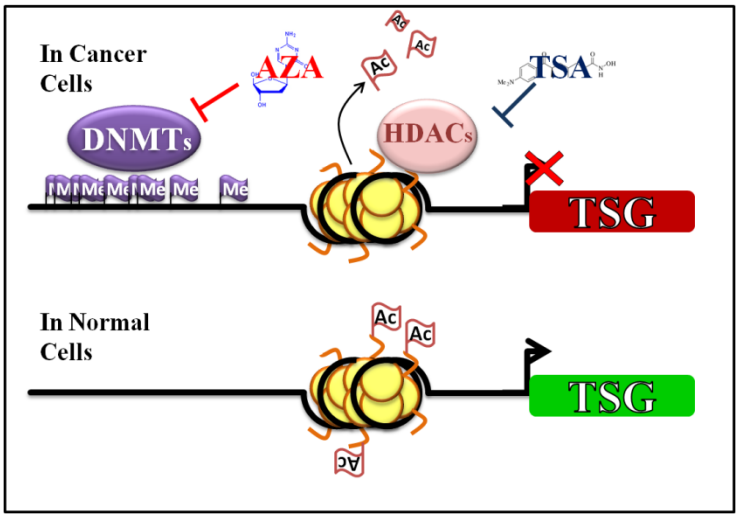

Figure 1.2: Epigenetic regulation of tumor suppressor genes in cancer and normal cells.

Promoter regions of the TSGs become hypermethylated by DNMTs in cancer, and the associated histones are de-acetylated by the HDACs, all resulting in inactivation of the TSGs, which are actively transcribed in normal cells, where the promoter region is clear of methylation signals, and the histone tails are acetylated.

1.2.3. Hypermethylation of tumor suppressor gene promoters in cancer

Although the genes bearing a CpG island in their promoter regions account for ~60% of the human genes, most of these sequences remain unmethylated in a normal cell. However, in cancer, promoter DNA hypermethylation of many genes, especially of TSGs have been frequently observed[42]. Among the very first genes reported to by hypermethylated in its promoter region was *RB* gene in retinoblastoma, which was the followed by E-cadherin, calcitonin, *P15INK4B* and ERβ[50-54]. Later on, many other known TSGs have been determined to be inactivated by promoter DNA hypermethylation in every type of human cancers[55-60]. *APC* and *RASSF1A* genes are examples of these genes[61-63]. The increase in search for TSG methylation in cancers in the latest years revealed that the hypermethylated genes involved in initiation and progression of cancers could be involved in several pathways, contributing to all hallmarks of cancer including: carcinogen metabolism, cell cycle, DNA repair, apoptosis, cell adhesion, angiogenesis, and immune evasion (Table 1.2)[34, 38, 41, 47]. Evidently, these sequences

specifically become methylated after clonal selection of randomly methylated genes, as they start to provide growth advantages to these cancer cells by deregulation of associated pathways[42]. To date, majority of the genes causing familial cancers have been detected to undergo silencing by hypermethylation in non-familial cancers as well[64]. *BRCA1* is a well-known example, as its hypermethylation is now documented in 10-50% of women with sporadic breast cancer[65-66]. *MLH1* gene is another example, which is hypermethylated in both sporadic and hereditary colorectal cancers[67].

Table 1.2 : Pathways disrupted by gene-promoter hypermethylation and the associated genes silenced in cancer

Pathway	**Genes**
Cell cycle	*RB*, p16, p15, p14, p73, 14-3-3
DNA repair	*MLH1, O6-MGMT, GSTP1, BRCA1, WRN*
Apoptosis	*DAPK1, CASP8, TMS-1*
Senescence	*TERT, TERC*
Tumor-cell invasion	E-cadherin, *VHL, APC, LKB1, TIMP-3, THBS1*
Vitamin response	*RARB2, CRBP1*
Tyrosine kinase cascades	*SOCS-1, SOCS-3, SYK*
Transcription	*GATA-4, GATA-5, ID4, RUNX3, TWIST, RARβ*
Homeobox genes	*PAX6, HOXA9*
Hormone response	*ER, PR, AR*, Prolactin receptor, *TSHR*
Signal transduction	*LKB1/STK11, RASSF1A, APC, ErbB2, NOREIA, APC, DKK-1, IGFBP-3, WIF-1, SFRP1*
Other pathways	*GSTP1, THBS-14, COX-2, SRBC, RIZ1, TPEF/HPP1, SLC5A8*, Lamin A/C, *HIC-1*
microRNAs	miR-127 (targeting *BCL6*), miR-124a (targeting *CDK6*)

Adapted from Herman et al., Esteller et al., and Choi et al.[34, 38, 68]

In the case of oncogenes, deregulation of one copy of the proposed gene is sufficient for the tumorigenesis in a predisposing environment. However for the disruption of the function of a

TSG, both alleles of the involved gene should be inactivated, grounding the basis for Knudson's two hit hypothesis[69-70]. The first allele of the TSG is usually inherited, generating the first hit. The second allele is usually lost via a somatic mutation. With the discovery that TSGs can also be inactivated by hypermethylation of their promoter DNA, a new player had its place in the Knudson's two hit hypothesis. According to this, abnormal hypermethylation of the TSG promoter in the sporadic cancers usually provides the first hit, and the second hit is the loss of the second copy by other means, or by a second hypermethylation event[69-70]. In the case of familial cancers, DNA hypermethylation usually serves as the second hit[34]. Aptly, the hypermethylation of the TSG occurs only in the wild type in hereditary cases, *i.e.,* the already mutated copy does not undergo hypermethylation to ensure redundancy is avoided[48]. This provides a selective advantage to the cancer cells, as both of the copies are inactivated.

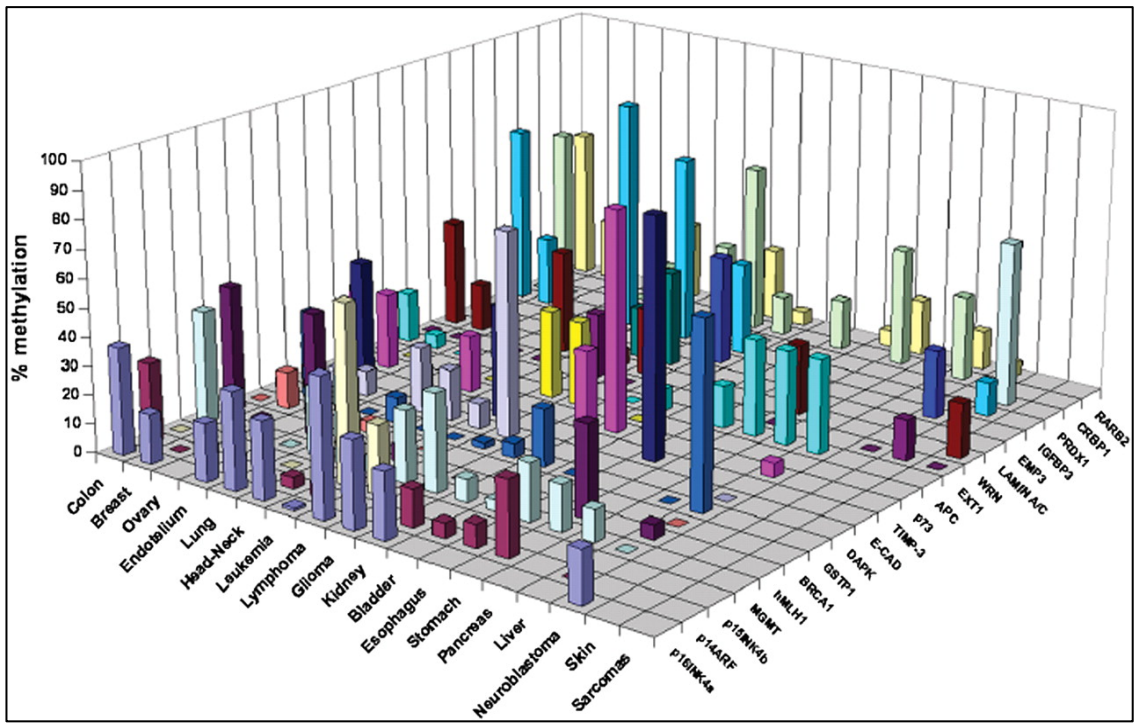

Figure 1.3: A CpG island hypermethylation profile of human cancer.

The profiles of hypermethylation of the CpG islands in TSG are specific to cancer type. The figure shows the frequently methylated TSGs, and their methylation frequencies in the indicated cancers. Taken from: Manel Esteller, Epigenetic gene silencing in cancer: the DNA hypermethylome, Human Molecular Genetics, 2007,16, R1, R50-R59, by permission of Oxford University Press.[38]

Hypermethylation of TSGs is a common event in human tumors, and each tumor has its own specific "DNA hypermethylome". They can be classified according to their hypermethylation

profiles (Figure 1.3), which could be maintained even after long periods of culturing[38, 60]. *BRCA1*, for example, is predominantly hypermethylated in breast and ovarian cancer, while *hMLH1* hypermethylation is definitive for colon cancer, and *TIMP3* hypermethylation is frequent in renal cancer.

Global methylation levels in a specific tumor may be higher than others as well. Gastrointestinal tumors are an example for the highest levels of hypermethylation in their genomes, possibly due to repeated exposure to external carcinogenic substances[38]. The methylation phenotypes of the tumors could be so distinct that an unknown type of tumor could be recognized based on the methylation levels of a number of selected genes[48].

1.2.4. Histones, their modifications and cancer

In eukaryotes, DNA is not naked in the nucleus, but is highly packed with several proteins into a structure called "nucleosome", in which 147 bp length of DNA is wrapped around a core of 8 histones, consisting of two copies of H2A, H2B, H3 and H4 histones, a histone octamer. These basic units are linked by a "linker DNA", whose length is variable across species. The nucleosome structure ensures regulation of chromatin accessibility and gene expression[71]. Two mechanisms are in general responsible for this regulation; first, the chromatin remodeling complexes, functioning in displacement or translocation of the histone octamers; and second, the modification of associated histones. The histones are negatively charged to be bound by DNA, and these histone modifications cause differences in charge of the octamers, changing the interaction of the histone core with the surrounding DNA. These modifications provide binding sites for many other proteins and transcription factors as well[72].

Several histone modifications have been detected to date, functioning in transcriptional activation or repression, cell proliferation regulation, DNA damage response, ribosomal gene expression, telomere silencing, spindle functioning and many other processes[73]. These modifications include acetylation, methylation, phosphorylation, hydroxylation, SUMOylation, ubiquitination and other modifications to the histones H2A, H2AX, H2B, H3, H3.3, H4, H1 and CEN-PA. Most commonly studied modifications are methylation and acetylation of N-terminal tails. Usually, lysine 4 methylation on histone H3 (H3K4me) and acetylation of histones H3 and H4, are related to open chromatin conformation and active transcription, whereas methylations, such as H3K9me or H3K27me, are usually related to transcriptional repression[74]. Histone deacetylases (HDACs) remove the acetyl groups added by histone acetyltransferases (HATs) from the histones, resulting in repression of gene transcription. In cancer, increased activity of HDACs result in repression of several TSGs (Figure 1.2), thereby providing growth advantages

to the cells[75]. Several genes have been identified to be repressed by deacetylation of associated histones in cancer, including *NDRG2*, *GRHL1*, RARβ, p53[76-80].

It is accepted that the chromatin conformations and DNA methylation levels are connected. One of the elements known for this connection is MeCP2, which binds to the methylated DNA and recruits HDACs and HMTs and other chromatin modifiers to the promoter region of the associated gene, and facilitates formation of repressive chromatin, hence repression of transcription from the promoter[81]. Thus, it is common to observe same genes to be both hypermethylated by their promoter DNA, and de-acetylated and methylated by their associated histones in a specific type of cell, tissue or cancer type.

1.2.5. Epigenetic changes in breast cancer

In breast cancer, multiple genes are hypermethylated compared to non-cancerous tissue. These include genes involved in apoptotic regulation (*RASSF1A, TWIST1*), uncontrolled proliferation and growth (*CCND2*, p16, RARβ, ERα, *PGR*), DNA repair (*BRCA1*), and tissue invasion and metastasis (*CDH1*)[82]. These genes are not only hypermethylated in tumor cells, but show increased epigenetic silencing in tumor stroma, including the normal cells at the periphery of the tumors. Among these, *RASSF1A* is widely accepted as a breast cancer biomarker, since it is methylated in 60-77% of breast tumors but rarely in normal tissue. Moreover, *RASSF1A* methylation can be detected in blood based samples[82]. In addition, *BRCA1* methylation, observed at nearly 10% of sporadic breast cancer patients, is a prognostic biomarker of breast cancer given that *BRCA1* promoter methylation was more frequent in invasive than *in situ* carcinoma, and higher *BRCA1* methylation levels may correlate positively with the tumor stage[82]. Promoter hypermethylation of this gene may serve as the second hit for gene silencing in patients with an inherited *BRCA1* genetic mutation. hMLH1 and MSH2 are other repair related genes which become hypermethylated in breast cancer[81]. Another gene which is implicated in breast cancer epigenetics is the gene encoding for ERα, *ESR1* gene. Majority of breast cancer cases demonstrate a certain level of methylation in the *ESR1* gene promoter DNA, although the methylation and gene repression are correlated in only ~30% of tumors[82]. An important element of chromatin remodeling complex, *SWI/SNF* gene was also found to be methylated in metastatic breast cancer, whereas *ZEB2* and *SNAIL*, which are known EMT markers, were hypo-methylated[83]. Moreover, it was shown that *DNMT* expression was increased in $ER^{(-)}$ breast cancer cells[81].

Promoter DNA hypermethylation can also be associated with hormone receptor status of breast cancer[82]. Investigation of promoter methylation profiles of 12 hypermethylated genes enabled identification of positive association of ER status with high *HIN-1* and *RASSF1A* methylation.

HIN-1 methylation levels were positively, and *CDH 13* methylation levels were negatively associated with PR status. 58% of TN breast tumors were positively correlated with *CDH13* methylation[82, 84]. A more recent study identified two sets of genes; the first set's promoter methylation levels were associated with hormone receptor positive, LumA subtype tumors, whereas the second set was highly methylated in poorer prognosis tumors such as TN and basal-like tumors[85]. Another study identified LumB tumors to have a hypermethylator phenotype, and basal-like tumors to have decreased levels of methylation in the promoter regions, compared to other subtypes[86]. These results suggest the existence of an interaction between DNA methylation and hormone receptor status, and subtypes of breast cancer. Somatic and germ-line mutations present in a specific subtype can be assumed to predispose a cell to certain epigenetic alterations[87]. Studies suggest that ERα$^{(-)}$ tumors have more methylated regions than ERα $^{(+)}$ tumors, probably since loss of ERα results in occupation of ER target gene promoters by polycomb proteins, which mainly function in epigenetic silencing[82]. This could also be explained by the fact that ER positivity is associated with methyl CpG binding protein 2 (MeCP2) over-expression[42].

Genomic hypomethylation is also observed in breast cancer, and is associated with several clinical features such as stage, tumor size and histological grade[88-89]. Some proto-oncogenes implicated in proliferation, metastasis or drug resistance have been found to be upregulated in breast cancer through the hypomethylation of their promoters[89]. Cancer/testis antigens, which are normally suppressed in the adult tissues, for example, become hypomethylated and expressed in breast cancer. *MAGE*, which is associated with metastasis of different types of cancers and poor prognosis, is an example of these genes[81]. Metastasis related genes such as *SNCG, S100A4* and *PLAU* were also shown to be activated by hypomethylation in metastatic breast cancer[81]. Park *et al.* showed that Alu and *LINE-1* regions were hypomethylated in breast cancer, *LINE-1* demethylation being earlier than Alu hypomethylation; and that hypo-methylation was more severe in HER2 subtypes, and was associated with the genomic instability of *HER2* amplified breast cancer[90]. Another mechanism was shown by Hon *et al*., in which genomic hypomethylation in HCC1954 breast cancer cells resulted in repressive chromatin formation, enriched with H3K9me3 and H3K27me3 modifications, and repression of expression of many genes, including known TSGs such as *MGMT, DCC, DLC1, PYHIN1, THBS2, HRG, DACH1,* and *CST5*[40].

Elsheikh *et al.* studied the histone lysine acetylation and methylation, and arginine methylation marks with IHC in breast tumor samples, and found that majority of breast tumors (79%) had lower levels of acetylated histone marks, with even lower levels in higher tumor grades[91]. Intermediate to low levels of lysine acetylation and methylation, and arginine methylation were

detected in basal-like and HER2 tumors, which have unfavorable prognosis[91]. The observed decrease in the global acetylation levels in breast cancer could be due to the increased expression of several HDACs in breast cancer[92]. EZH2, which is responsible for gene repression by H3K27me3, is also known to be over-expressed in breast cancer, and this over-expression resulted in HDAC induction, and increased invasion potentials of breast cancer cells[93]. Moreover, several genes were identified by deacetylation of the histones in their promoter regions by HDACs, including E-cadherin, RARβ and ERα, *ARHI* and *BRCA1*[94-97].

1.2.6. DNA methylation based biomarkers for detection of breast cancer

It is known that dying tumor cells shed their DNA into the blood stream and body fluids, and circulating cell free DNA (cfDNA) could be detected from the peripheral blood/plasma/serum of cancer patients[98]. Thus, it possible to identify frequently hypermethylated genes from these non-invasive and easily accessible sites, using easy and quick techniques such as methylation specific PCR (MSP) [98-101]. Analysis from serum or plasma is more patient-friendly than biopsies, detection could be earlier than scanning techniques like mammography or CT scan, and could be repeated easily without side effects during the follow-up period[102]. Furthermore, using hypermethylated genes as biomarkers have several advantages including stability of DNA compared to RNA and protein, quick and sensitive techniques for detection (like methylation specific PCR, MSP), and specificity of DNA hypermethylation events for neoplastic cells[103]. To date, several genes have been detected as hypermethylated in serum and/or plasma of different types of cancer patients, including *RASSF1A, CCDN2, GSTP1* and *DAPK1*[99-100]. Among a high number of genes, *RASSF1A* is the most studied and the most powerful biomarker candidate, with highest detected sensitivity-specificity ratios of 75% and 100%, respectively and average sensitivity of 56%[104-105]. The most powerful candidates after *RASSF1A* are *CDH1, CCND2, ESR1* and *APC*[105]. GHSR gene was also shown to distinguish normal cells from IDC with 90% specificity and 96% sensitivity[106]. Many studies also combine the discriminative power of these genes, and create panels for the detection of breast cancer. Radpour *et al*. show that when eight genes (*APC, BIN1, BRCA1, CST6, GSTP1, P16, P21* and *TIMP3*) were examined for hypermethylation in serum of breast cancer patients, 92.6% of the early stage and 88.9% of the late stage breast cancer patients had hypermethylation of at least one of these genes in the plasma, and 91.7% and 100% of early and late stage patients, respectively, had at least one hypermethylated gene in the serum[99]. The search for diagnostic and prognostic biomarkers for breast cancer in blood based samples is growing, and a panel with fewer number of genes, with higher specificity and sensitivity values is still in need.

1.2.7. Epigenetic drugs

The most commonly used epigenetic drugs to treat cancer are DNMT inhibitors, and HDAC inhibitors. The first drug used to inhibit DNA methylation was 5-azacytidine (Vidaza), which causes covalent arrest of DNMTs, resulting in cytotoxicity. The analogue 5-aza-2'-deoxycytidine (Decitabine, AZA, Figure 1.4A) is one of the most commonly used DNMT inhibitors in cell culture[48]. Although sometimes it is considered as a "demethylating" agent, AZA does not actively de-methylate the CpGs, but inhibits the process as it is incorporated into the DNA as a cytidine analog during DNA synthesis, by formation of a covalent bond between the 6th carbon in the AZA structure and the Cys-thiol in the active site of the DNMT enzyme. The AZA-DNMT adduct that forms during this process in known to be stable and inactive, and thus, following the DNA synthesis, the newly formed strand becomes unmethylated[107]. AZA can also be used to treat the cancer patients, especially those with hematological malignancies, such as MDS (myelodysplastic syndrome)[48].

Histone deacetylase inhibitors, HDACis, affect many biological pathways including proliferation, apoptosis, cell cycle, and differentiation. Thus, they are also used as a therapy against several types of malignancies[75]. HDACis result in increased acetylation of histones, which in turn result in the activation of suppressed TSGs in a cancer cell. Trichostatin A (TSA, Figure 1.4B) is a natural compound including a hydroxamic-acid in its structure isolated from *Streptomyces hygroscopicus*. The mechanism of inhibition of HDACs by TSA is not very well known. However, chemical structure analyses of TSA binding to a HDAC like enzyme, called HDLP, revealed that binding of TSA results in association of its functional hyroxamic acid chain with the Zn^{+} cation at the active site of the enzyme, and blockade of the entrance pocket of the enzyme by TSA's polar cap at the other end, and eventually inhibition of the enzyme by the drug[108]. TSA is known to induce apoptosis by downregulation of anti-apoptotic protein Bcl2, and induce p53 and VHL under hypoxic conditions, to prevent angiogenesis[75]. TSA, SAHA and valproic acid are among HDACis which are used to restore histone acetylation in cultured cells for epigenetic studies[48].

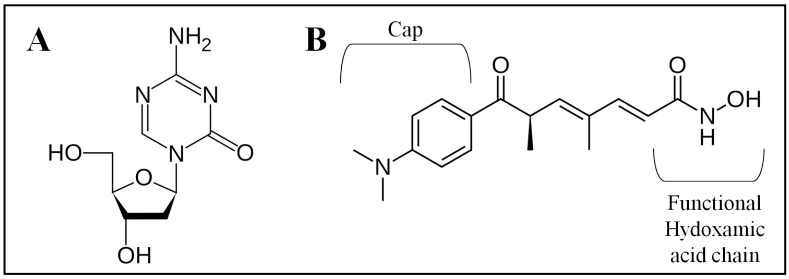

Figure 1.4 Structures of AZA and TSA.

(A) Structure of AZA. (B) Structure of TSA.

1.2.8. High throughput assays to study epigenetics in cancer

After the human genome project was complete, new genome-wide systems were designed in an attempt to discover novel epigenetically regulated genes in cancer. Affymetrix HGU-133 plus 2.0 (GPL570) platform, for example, covers more than 47,000 transcripts, with 54,675 probe sets, enabling high-throughput analysis of gene expression changes in certain conditions, such as treatments with DNMT inhibitors and HDACis, that was first discovered by Suzuki *et al.*[109]. After this initial study, several groups studied epigenetic mechanisms in cancer using microarray studies in combination with epigenetic drugs (Table 1.3). Although there are two microarray studies on AZA treatment of breast cancer (GSE22250[110] and GSE8007[111]), none of them included analysis of expression before and after direct administration of AZA and/or TSA on both cancer and non-tumorigenic cell lines. Dataset GSE8007 included only the data of human mammary epithelial cells (HMECs), which were treated with AZA. GSE22250 on the other hand, included AZA treatment of 7 breast cancer cell lines, however, neither duplicates were included for the experiments, nor was there a non-tumorigenic cell line to compare with, creating a requirement for such a study in the field of breast cancer epigenetics.

Table 1.3: Epigenetic studies which used expression microarrays together with epigenetic drugs

Name	Study Name/Explanation	Platform code*
GSE1793	AZA treated melanoma cells[112]	GPL80
GSE2097	AZA and TSA treatment of cervical carcinoma cell lines[113]	GPL1753
GSE2932	AZA treated prostate cancer cells[114]	GPL2624
GSE3168	AZA treatment of oral cancer cells	GPL127, GPL128, GPL129
GSE4089	AZA treated prostate cancer cell lines[114]	GPL3295
GSE4465	HDACI treatment of hepG2 cells[115]	GPL570
GSE4717	AZA treatment of three short term cultured glioblastomas[116]	GPL96
GSE4763	AZA and TSA treatment of HCT116 cells[117]	GPL1708
GSE5230	AZA and TSA treatment of human hepatoma cells[118]	GPL570

Table 1.3: Epigenetic studies which used expression microarrays together with epigenetic drugs

Name	Study Name/Explanation	Platform code*
GSE5816	AZA treatment of lung cancer cells[119]	GPL570
GSE6695	AZA treatment of lung cancer cells[119]	GPL570
GSE7132	AZA and TSA treatment of tumor endothelial cells[120]	GPL885
GSE7454	AZA treatment of U-2OS (osteosarcoma) cells[121]	GPL96, GPL570
GSE7687	AZA treatment in colorectal cancer cell lines[122]	GPL1291
GSE8007	AZA treatment of breast cancer[111]	GPL3348
GSE8388	AZA treatment of classical Hodgkin lymphoma cells[123]	GPL96
GSE8645	TSA treatment of LNCaP Prostate Cancer cells	GPL5694
GSE9118	AZA treatment of melanoma cells [124]	GPL96
GSE9764	AZA treatment of carcinoma associated fibroblasts[125]	GPL570
GSE10455	AZA treatment of colorectal cancer[126]	GPL4133
GSE10952	TSA treatment in colon cancer cells [127]	GPL6104
GSE14315	AZA treatment of lung cancer cells	GPL570
E-MEXP-403	TSA treatment of Burkitts lymphoma cell lines	GPL96
E-MEXP-1269	AZA/TSA treatment of multiple myeloma cell lines[128]	GPL96
GSE22250	AZA treatment of breast cancer cells[110]	GPL570
GSE22563	AZA treatment of renal cell carcinoma[129]	GPL570
GSE24224	AZA treatment of leukemia cells[130]	GPL570
GSE29060	AZA treatment of colorectal cancer cells	GPL570
GSE30985	AZA treatment of colorectal cancer cells	GPL570
GSE32323	AZA treatment of colorectal cancer cells[131]	GPL570
GSE32496	AZA treatment of lung cancer cells[132]	GPL570

Table 1.3: Epigenetic studies which used expression microarrays together with epigenetic drugs

Name	Study Name/Explanation	Platform code*
GSE34042	AZA treatment of prostate cancer cells[133]	GPL570
GSE44244	AZA treatment of L428-PAX5 cells[134]	GPL6244
GSE44537	AZA treatment of neuroblastoma SKNAS induced cancer stem cells[135]	GPL570
GSE45437	AZA treatment of pediatric ependymoma cells[136]	GPL570

** Explanation of platform codes could be obtained from GEO (http://www.ncbi.nlm.nih.gov/geo/). GPL570 stands for Affymetrix Hgu 133 Plus 2.0 arrays.*

Besides expression microarrays and epigenetic drugs, other methods have been developed for identification of genome-wide methylation and histone modification events in cancer. Here, some of the pioneering and high impact studies on breast cancer have been listed:

Rodenhiser *et al.*(2008) studied the genome-wide methylation events in metastatic breast cancer cell line MDA-MB-468LN compared to its non-metastatic counterpart, MAD-MB-468GFP, using human gene promoter tiling microarray platforms, and identified several genes hyper- or hypo-methylated in metastatic breast cancer[83]. These microarray platforms had TSS sequences of more than 25,500 genes, and as a result of the study 2,209 and 1,235 genes were found to be significantly ($P < 0.05$) hyper- and hypo-methylated in the metastatic cell line, respectively. They identified *EGFR, CDH1* and *CST6* epithelial genes to be hypermethylated and *ZEB1* mesenchymal gene to be hypomethylated in the metastatic cells.

Ruike *et al.* (2010) performed MeDIP-Seq (methylated DNA sequencing) in 8 breast cancer and one non-tumorigenic breast cell lines[137]. MeDIP technique is based on immunoprecipitation of methylated DNA using methyl-cytosine specific antibodies, combined with high throughput DNA sequencing. They identified global DNA hypomethylation in especially CpG poor areas of the genome, without any preference for genic loci. However, hypermethylation events were observed at gene rich loci with CpG rich regions, being more concentrated on TSS distant locations compared to proximal locations in the promoter regions; and the expression of the genes were positively correlated with methylation events in the distal regions, while were negatively correlated in the proximal regions. They also analyzed the methylome of epithelial and mesenchymal (induced by TNFα and TGF-β) MCF7 cells, and identified only minor effect

of EMT on the methylome of MCF7 cells, resulting more in hypo- than hyper-methylation in gene associated CpGs.

Dedeurwaerder *et al.* (2012) used Illumina HumanMethylation27 BeadChip methylation microarrays to analyze genome-wide methylation levels in 236 breast tumors and 12 normal tissues[110]. They identified a group of immune related genes, which could be used as prognostic markers for breast cancer. They also showed that, ER $^{(+)}$ and ER $^{(-)}$ IDC tumors were clustering separately according to their methylation statuses, and genes whose expressions were correlated with *ESR1* gene had higher methylation levels in ER $^{(-)}$ breast tumors.

Hon *et al.* (2012) combined shotgun sequencing of bisulfite treated DNA and ChIP-seq data to study both DNA methylome and histone modifications in HCC1954 breast cancer and non-tumorigenic HMEC cells[40]. They identified global loss of methylation and sequence specific hypermethylation events in the cancer cell line compared to HMECs, and most of these alterations were observed in the regions that are partially methylated in HMEC cells. Interestingly, they revealed that the hypomethylation events were coupled to repressive chromatin marks such as H3K9me3 and H3K27me3, and that these histone marks were mutually exclusive with methylated CpG rich regions. On the other hand, H3K36me3, which is an active transcription mark, was associated with methylated CpG rich regions. At genic regions, hypomethylated regions were higher in the cancer cell line compared to the HMECs. They also found that the loss of DNA methylation occurred mostly in the late replicating sequences by passive mechanisms, instead of active de-methylation by demethylating proteins.

Lin *et al.* (2015) used whole-genome bisulfite sequencing in IDC, fibroadenoma, normal breast tissues and in MCF7 cell line[138]. They also used the methylation data by Hon *et al*[40]. They showed that the methylation levels were lower in non-tumorigenic and breast cancer cell lines compared to normal or tumor breast tissues[138]. When they compared normal breast, fibroadenoma and HMEC to breast cancer samples, they concluded that the low-methylated-CGIs were fewer in the latter. Among the methylomes, normal breast had the least number of hypomethylated regions. They also reported aberrant expression of X-linked genes due to hypermethylation of the *XIST* promoter.

1.3. AZA induced genes analyzed in this study

DST (BPAG1)

DST is a major component of the hemidesmosome, functions in attachment of intermediate filaments to actin cytoskeleton, or to hemidesmosomes. *DST* expression has been shown to be

downregulated in IDC of breast[139], in naso-pharyngeal carcinoma cells [140], and in basal cell carcinoma[141].

COL4A6

COL4A6 encodes a subunit of collagen-4 of the basement membranes. COL4A6 protein has been shown to be an inhibitor of angiogenesis and tumor growth[142], and its decreased levels are associated with invasive growth properties in colorectal cancer and esophageal squamous cell carcinoma[143-144], and increased levels associate with decreased human endothelial cell proliferation in mice[142]. *COL4A6* downregulation is observed in pancreatic carcinoma, prostate cancer, bile duct carcinoma, and others [145-147]. Moreover, methylation of this gene has been shown in colon carcinoma[148].

AXIN2

Axin2 is functions in the Wnt signaling pathway. Axin2, is involved in efficient TGFβ signaling[149], regulates EMT in breast cancer cells[150], and regulates chromosome cohesion[151]. *AXIN2* gene mutations are common in several types of cancer[152-154]. Epigenetic silencing of *AXIN2* by promoter hypermethylation was also shown in MSI^{+} colorectal cancer, lung, and neuroendocrine tumors[155-157].

ZMAT3 (Wig-1)

ZMAT3 gene encodes a dsRNA-binding zinc finger protein[158], which can bind siRNAs and miRNAs[159]. ZMAT3 has functions in p53 dependent growth suppression and cell cycle arrest[158, 160-161].

RIOK3

RIOK3 is an atypical serine-threonine protein kinase. RIOK3 interacts with CASP10 and negatively regulates the NF-KB pathway[162]. *RIOK3* expression is significantly lower in invasive malignant melanomas and has been found to be methylated in prostate cancer[163-164]; however, it is associated with cell migration and invasion as well, in pancreatic ductal adenocarcinoma and MDA-MB-231 cells[165-166].

PPP1R15A (Gadd34, MyD116)

PPP1R15A, growth arrest and DNA damage-inducible gene 34 (Gaddd34) expression correlates positively with apoptosis[167-169], and is decreased in mouse and human mammary tumors[170]. Gadd34 has roles in regulation of p21 expression, and suppression of cellular proliferation and migration[171-172].

CASP9

CASP9 is processed by APAF1 for its activation and apoptosome formation, and cleaving of effector caspases[173]. Rare mutations have been found in gastric, colorectal and lung adenocarcinomas[174].

NFKBIA (IKBA)

NFKBIA inactivates NFKB by preventing its translocation to nucleus. It induces or increases susceptibility to apoptosis[175]. *NFKBIA* has been found to be downregulated in mouse and human mammary tumors[170, 176], and is methylated in osteosarcoma cells[121]. Polymorphisms are found in several types of tumors[177].

CDC14B

CDC14B activates G2/DNA-Damage checkpoint, maintains the fidelity of centrosome duplication, and controls the cell cycle progression[178-181]. *CDC14B* has been found to be downregulated in HCC cells and clear cell renal carcinoma[182-183].

ADAMTSL4

ADAMTSL4 peptides inhibit proliferation and migration of human umbilical vein endothelial cells *in vitro*[184], and over-expression of *ADAMTSL4* in ovarian cancer induces apoptosis[185]. The gene has been found to be downregulated in BCR-Abl positive acute lymphoblastic leukemia[186].

FOXO1

FOXO1:PAX3 translocation has been associated with alveolar rhabdomyosarcoma[187-188]. In liver, *FOXO1* deletion is required for cell proliferation and regeneration[189]. *FOXO1* is downregulated in breast tumors, is related to inhibition of cell cycle progression and metastasis, and activation of apoptosis[190-193]. Loss or downregulation of *FOXO1* expression has been shown in different types of cancers[194-197]. On the contrary, elevated *FOXO1* levels were shown in malignant and drug resistant breast cancer cells[198-199].

ACVR1C

ACVR1C is a TGFβ –type I signaling receptor[200], which initiates apoptosis through classical TGFβ pathway, and is known to regulate Bax/Bcl-2 and Xiap[201-203]. ACVR1C regulates cell proliferation[204-206], and lack of expression is associated with breast tumor progression and gallbladder cancer metastasis[207-208].

NR4A3

NR4A3 is a steroid hormone receptor, and a transcription factor. Increased *NR4A3* expression is related to inhibition of cell growth and proliferation, and to apoptosis[209-212]. NR4A3 is accepted as a tumor suppressor in hematologic malignancies[213-214].

EGR2

EGR2 is a transcription factor, widely accepted as a tumor suppressor. EGR2 has an important role in PTEN induced apoptosis[215]. *EGR2* gene expression is downregulated in several cancer types with different mechanisms[216-220]. However, *EGR2* was also reported to be associated with induction of *ERBB2* expression in breast cancer [221].

BTG1

BTG1 protein regulates cell growth and proliferation[222]. In chronic lymphocytic leukemia, it is undergoes t(8;12)(q24;q22) chromosomal translocation[223]. Increase in *BTG1* expression arrests cells at G0/G1 phases, and induces apoptosis in ovarian, granulosa, breast and brain microglia cells[224-228]. BTG1 inhibits metastasis and cell proliferation, and negatively correlates with progression in breast cancer[227-229].

EPB41L2 (4.1 G)

EPB41L2 regulates cell growth[230]. *EPB41L2* expression was downregulated in lung cancer and expression levels were related to the differentiation status[231-232].

DUSP5

Dual specificity phosphatases (DUSPs) negatively regulates MAPK signaling by inactivating Erk1 and Erk2 proteins[233-234]. Increased expression of *DUSP5* is associated with suppressed cellular growth in several cancer cell lines, and decreased expression was observed in prostate and gastric cancers[235-237].

BEX4

BEX4 is an X-linked gene, and is highly expressed in brain. It has been found to be suppressed in ovarian cancer by DNA hypermethylation[238].

NDRG4

N-myc downregulated-4 (NDRG4) is thought to be involved in the regulation of mitogenic signaling and control of cell growth[239]. Its expression is decreased in colorectal and pancreatic cancers by promoter DNA hypermethylation[240-242].

IQGAP2

IQGAP2 has a Ras-GTPase activating domain (Ras-GAP) and regulates cell morphology and motility. Expression of *IQGAP2* has been found to be decreased in gastric cancer by promoter hypermethylation, resulting in tumor invasion and poor prognosis[243-244]. *IQGAP2* is downregulated and associated with better prognosis in HCC[245-246].

GSTM1

GSTM1 is a cytoplasmic Glutathione-S-transferase. *GSTM1* deficiency is associated with increasing susceptibility to carcinogens and increase in DNA adducts[247-250]. Both under- and over-expression of *GSTM1* was found to be a risk factor for breast cancer[251-252]. *GSTM1* null phenotype is related to lung, head and neck, gastric, colorectal, liver, nasopharyngeal, and laryngeal cancers[253-261]. Polymorphisms are associated with several types of cancers. *GSTM1* gene has been reported to be downregulated in primary tumors of prostate by DNA methylation[262-263].

GSTM2

GSTM2 is also a cytoplasmic Glutathione-S-transferase. It is downregulated in Barrett's adenocarcinomas by promoter DNA hypermethylation[264]. Its expression is not detectable in colon cell lines[265].

HMOX1

Heme-oxygenase 1 functions in heme catabolism. HMOX1 has anti-proliferative, pro-apoptotic and anti-invasion effects on rat and human breast cancer[266-267]. *HMOX1* expression is associated with better survival in colorectal cancer, and poorer survival in breast cancer patients[268-269]. Other studies related *HMOX1* expression to upregulation of *MMP1*, and *VEGF,* resulting in increased metastasis and invasiveness in MCF7 cells[270-271].

F11R

F11R protein functions in the structure of tight junctions, and inhibits cellular motility and invasion. F11R has been found to be downregulated in invasive breast tumors and in renal cell carcinoma and low expression levels are associated with poor outcome in breast cancer[272-274]. However, its expression has also been reported to be related to poor prognosis, tumor growth and metastasis in breast cancer[275-280].

BMP2

BMP2 functions in Smad signaling pathway, and induces apoptosis in colon tumor cells[281-283]. BMP2 prevents degradation of PTEN tumor suppressor, suppresses mitosis and proliferation of

breast cancer cells[284-286]. *BMP2* gene has been found to be silenced by promoter methylation in gastric cancer, and has been shown to be downregulated in ovarian cancer[287-288]. However, it has also been reported to induce angiogenesis and migration, and to prevent apoptosis in breast cancer[289-291].

INSIG1

This gene is an insulin induced gene, and encodes an endoplasmic reticulum membrane protein. *INSIG1* gene has been found to be downregulated through methylation in gastric cancer[292].

NETO2

NETO2 is a predicted trans-membrane protein similar to a rat protein that tunes glutamate signaling in the brain. Downregulation of this gene was reported in human breast tumors and carcinoma cell lines[293].

ID2

Inhibitor of DNA binding 2 (ID), is a regulator of transcription with dominant negative helix-loop-helix (HLH) domains. The protein has been found to be under-expressed in breast cancer and to favor differentiation of breast epithelial cells, and to reduce their proliferative and invasive potential[294-295], while other studies identified this gene to be variably expressed in breast cancer cell lines[296], yet others identified ID2 as stimulant of invasive potential, proliferation, and predictor of poor prognosis in breast cancer[297-299].

S100A2

S100 proteins are involved in cell cycle and differentiation. *S100A2* expression has been found to be diminished in breast carcinoma, and hypermethylation of its promoter region has been observed in one biopsy sample and in T47D breast cancer cell line[300-301]. CpG methylation has also been detected in promoter region of this gene in lung and head and neck cancers[302-303]. S100A2 inhibits proliferation of *BRCA1* mutant basal-like breast cancer cells and invasive potentials of gastric cancer cells[304-305]. Contradictory to these findings S100A2 protein levels are elevated in highly metastatic tumors of breast cancer patients and basal-type breast cancers[306-307].

AKAP12

AKAP12 serves as a scaffold protein in signal transduction. Over-expression of this gene results in reduced levels of MMP9 and suppressed MAPK pathway, and inhibition of metastatic and invasive potential of colorectal carcinoma, pancreatic ductal adenocarcinoma, and squamous

cell carcinoma[308-312]. Downregulation and methylation of this gene have been shown in several types of cancer[313-317].

TGFBI

This protein plays a role in cell-collagen interactions and is induced by TGF-beta. While some studies indicate that TGFBI induces cell adhesion and apoptosis, and reduces colony formation and tumor growth and metastasis[318-320], others may indicate just the opposite[321]. *TGFBI* promoter has been found to be hypermethylated in ovarian, prostate, and lung cancers, and in neuroblastoma[322-324]. Consistent with its predicted tumor suppressive role, deficiency of TGFBI in mice causes spontaneous tumor development[325].

1.3.1. TAGLN

TAGLN gene is located on chromosome 11q23.2. The transcripts have two variants, each consisting of 5 exons and differing only in the 5'-UTR region; thus, encoding the same protein. The structure consists of a calponin family repeat and a calponin homology domain, which are required for actin binding. *TAGLN* gene has homologs in zebrafish, frog, dog, chicken, cow, mouse, rat, and chimpanzee.

Transgelin is a protein that interacts closely with actin cytoskeleton, as well as protein kinase C delta, and is majorly expressed in smooth muscle cells (SMCs)[326-329]. It has functions in formation of podosomes and focal adhesion in SMCs, and loss of TAGLN is associated with increased TNFα mediated NFKB activation in mice arteries[330-333]. Transgelin is linked to senescence of fibroblasts and apoptosis of prostate cancer and glomerular cells, and has functions in inhibiting invasion and migration of prostate and colon cancer cells, and migration of SMCs, partly through negative regulation of metastasis mediator MMP9[330-332, 334-341]. Transgelin downregulation has been documented in different types of cancer, including breast, colon, prostate, and gall bladder cancers[342-348]; yet is upregulated in gastric, pancreatic and metastatic colon cancers, and oral squamous cell carcinoma according to different studies[349-353]. Several studies identify transgelin as a mesenchymal protein, and some studies indicate increase in its expression levels upon epithelial-to-mesenchymal transition (EMT)[354-355]. *TAGLN* is known to be induced by TGF-β[356-359], which induces EMT in cancer cell lines[360].

Promoter DNA methylation was found to control transcription of *TAGLN* in SMCs, and methylation in promoter region was detected in hepatocytes and colorectal carcinoma[361-363]. Regulation of its transcription through H3K27me3 by EZH2 polycomb repressor protein has been shown in endothelial cells[364]. A recent study identifies TAGLN as a marker for triple negative breast cancer[365]. Transcriptional regulation by methylation, expression, and function of

TAGLN have never been studied before in a comprehensive panel of breast cancer cell lines and tumors before, and our study is the first to accomplish these analyses[366].

1.4. Aim of the study

Epigenetic changes in cancer, especially silencing of TSGs, are now accepted as one of the hallmarks of cancer. There are several studies employing high throughput methylation analyses linking epigenetics to mRNA expression levels in many types of cancers. One study (GEO ID: GSE22250) used breast cancer cell lines treated with AZA for microarray profiling, yet the treatments did not have duplicates, and there was no non-tumorigenic cell line to compare the carcinoma cell lines' data. Thus, a detailed and high throughput analysis of effects of AZA and/or TSA treatment on expression profiles in breast cancer compared to normal cells was still a missing point in literature.

The initial aim of this study was to discover epigenetically downregulated potential TSGs in breast cancer, by combining epigenetic drug treatments (AZA and TSA) with high throughput gene expression analyses, and comparing the differences in gene expression levels between drug and control treatments, and between cancer and non-cancer cells.

The second aim of the thesis was to identify the expression and methylation statuses of selected candidate genes in breast cancer cells. qRT-PCR experiments were used to confirm the microarray expression results, and to identify expression patterns of the selected genes in breast cancer cells. As a gold standard method for DNA methylation analysis, bisulfite sequencing was employed to reveal methylation patterns of the promoter regions of the genes.

Upon identification of *TAGLN* as a potential TSG that is hypermethylated in breast cancer, third aim of the study emerged as identification of expression and methylation patterns of this gene in different sets of breast tumor tissues, and determination of *TAGLN* gene's potential as a methylation based biomarker. Moreover, uncovering effects of *TAGLN* methylation and expression on patients' survival and prognosis outcomes, and gaining insights into functions of this protein in breast cancer were aimed.

Chapter 2. Materials and Methods

2.1. Materials

2.1.1. General laboratory chemicals and reagents

General laboratory chemicals and reagents include substances that are routinely used in the laboratory, in common techniques such as PCR, western blotting, bacterial growth etc. Table 2.1 lists these materials, with catalog numbers and the companies providing them.

Table 2.1: Chemicals, reagents, enzymes, and kits used for general laboratory purposes

Name	Catalog#	Company (Country)
Molecular Biology Grade Water	SH30538	Thermo Scientific (USA)
Nucleospin RNA extraction kit	740955	Macherey Nagel (Germany)
DEPC	A0881	Applichem (Germany)
TRI Reagent	RT 111	Molecular Research Center (USA)
Phenol:Chloroform:Isoamyalcohol, 25:24:1	AM9730	Life Sciences (USA)
4-Bromoanisole	BN 191	Molecular Research Center (USA)
DNA-free™ Kit	AM1906	Life Sciences (USA)
RevertAid First Strand cDNA Synthesis Kit	K1622	Thermo Scientific (USA)
DyNAmo HS SYBR Green qPCR Kit	F-410L	Thermo Scientific (USA)
Nucleospin Tissue-DNA extraction kit	740952	Macherey Nagel (Germany)
Proteinase K	P2308	Sigma Aldrich (USA)
EpiTect Bisulfite Conversion	59104	Qiagen (Germany)
Taq DNA Polymerase and buffers	EP0402	Thermo Scientific (USA)
dNTP Set, 100 mM Solutions	R0182	Thermo Scientific (USA)

Table 2.1: Chemicals, reagents, enzymes, and kits used for general laboratory purposes

Name	Catalog#	Company (Country)
Agarose	BHE500	Prona (Spain)
Bromophenol blue	B5525	Sigma Aldrich (USA)
Xylene Cyanol	X4126	Sigma Aldrich (USA)
Glucose	G7021	Sigma Aldrich (USA)
Ethidium Bromide	17898	Thermo Scientific (USA)
Gene Ruler 1 kb DNA Ladder	SM0311	Thermo Scientific (USA)
Gene Ruler 50 bp DNA Ladder	SM373	Thermo Scientific (USA)
QIAquick Gel Extraction kit	28704	Qiagen (Germany)
pGEM-T Easy vector system	A1360	Promega (USA)
Yeast extract	1702	Conda (Spain)
NaCl	31434	Sigma Aldrich (USA)
Agar (microbiology grade)	05039	Sigma Aldrich (USA)
Bacto-tryptone	1612	Conda (Spain)
Pipes	A1079	Applichem (Germany)
Ampicillin	A0839	Applichem (Germany)
Kanamycin	60615	Sigma Aldrich (USA)
IPTG for molecular biology	A4773	Applichem (Germany)
X-Gal	R0404	Thermo Scientific (USA)
PureLink Quick Plasmid Miniprep Kit	K210011	Thermo Scientific (USA)
Proteinase inhibitor cocktail	P8340	Sigma Aldrich (USA)
Triton X-100	T8787	Sigma Aldrich (USA)
2-mercaptoethanol	M3148	Sigma Aldrich (USA)
EDTA	A3562	Applichem (Germany)

Table 2.1: Chemicals, reagents, enzymes, and kits used for general laboratory purposes

Name	Catalog#	Company (Country)
Acrylamide	A9099	Sigma Aldrich (USA)
Bis-acrylamide	M7279	Sigma Aldrich (USA)
SDS	71725	Sigma Aldrich (USA)
Ammonium per sulfate	A3678	Sigma Aldrich (USA)
TEMED	1610801	Biorad (USA)
PageRuler Prestained Protein Ladder, 10 to 170kDa	26616	Thermo Scientific (USA)
Brilliant Blue R	B0149	Sigma Aldrich (USA)
Glacial acetic acid	27225	Sigma Aldrich (USA)
Tris (Trizma Base)	T1503	Sigma Aldrich (USA)
Glycine	G8898	Sigma Aldrich (USA)
Roche PVDF Membranes 0.2uM	3010040001	Roche (USA)
Bovine Serum Albumin Fraction V (BSA)	10735078001	Roche (USA)
Tween-20	822184	Merck /Germany)
ECL Prime System	RPN2232	Life Sciences (USA)
Bond-Epitope Retrieval Solution 1	AR9961	Leica Microsystems (Germany)
Bond Polymer Refine Red Detection kit	DS9390	Leica Microsystems (Germany)
Mounting medium for IHC	CS70330	Dako (Denmark)
Sulforhodamine B (SRB)	230162	Sigma Aldrich (USA)
Trichloroacetic acid (TCA)	33731	Sigma Aldrich (USA)
K-ferrocyanide	P3289	Sigma Aldrich (USA)
K-ferricyanide	P3667	Sigma Aldrich (USA)

Table 2.1: Chemicals, reagents, enzymes, and kits used for general laboratory purposes

Name	Catalog#	Company (Country)
Nuclear fast red	N3020	Sigma Aldrich (USA)
Crystal Violet	V5265	Sigma Aldrich (USA)
Giemsa	453616	Carlo Erba (Spain)
Propidium Iodide (PI)	421301	Biolegend (USA)
Rnase A	R6513	Sigma Aldrich (USA)

2.1.2. Cell culture chemicals and reagents

Chemicals, media and reagents that are used in the cell culture experiments included in this study have been listed in Table 2.2.

Table 2.2: Chemicals, reagents, kits and media used in cell culture

Name	Catalog #	Company (Country)
DMEM, High Glucose	SH30243	GE Healthcare (UK)
DMEM, Low Glucose	SH30021	GE Healthcare (UK)
DMEM:HAM's F-12 1:1	SH30023	GE Healthcare (UK)
RPMI 1640	SH30027	GE Healthcare (UK)
McCoy's 5A medium	F 1015	Biochrom (Germany)
OptiMEM I	11058	Thermo-Fischer Scientific (USA)
Fetal Bovine Serum	CH30160	GE Healthcare (UK)
L-glutamine	SH30034	GE Healthcare (UK)
Non-Essential Amino Acids	SH30238	GE Healthcare (UK)
Penicillin/Streptomycin	SV30010	GE Healthcare (UK)
Sodium Pyruvate (100mM)	11360	Thermo-Fischer Scientific (USA)

Table 2.2: Chemicals, reagents, kits and media used in cell culture

Name	Catalog #	Company (Country)
Hydrocortisone	H4001	Sigma Aldrich (USA)
Epidermal Growth Factor	E9644	Sigma Aldrich (USA)
Insulin	I9278	Sigma Aldrich (USA)
PBS	SH30256	GE Healthcare (UK)
Trypsin/EDTA (0.25%)	SV30031	GE Healthcare (UK)
5-aza-2' deoxycytidine	A3656	Sigma Aldrich (USA)
Trichostatin A	T8552	Sigma Aldrich (USA)
Dimethyl sulfoxide (DMSO)	A1584	Applichem (Germany)
Vybrant MTT Cell Proliferation Assay kit	V13154	Thermo-Fischer Scientific (USA)
UltraCruz™ Mounting Medium for IF	SC24941	Santa Cruz Biotechnology (USA)
Lipofectamine RNAiMAX transfection reagent	13778	Thermo-Fischer Scientific (USA)
Lipofectamine 2000 transfection reagent	11668	Thermo-Fischer Scientific (USA)
Growth Factor Reduced Matrigel Matrix Basement Membrane	356230	Becton Dickinson (USA)
Transwell Permeable Support invasion chambers	3422	Corning (USA)

2.1.3.Nucleic acids

Nucleic acids, such as siRNAs and over-expression vectors used in the experiments related to the study have been listed in Table 2.3. Description of the vectors and sequences of the siRNAs have also been provided.

Table 2.3: List of nucleic acids used for gene editing

Name	Catalog#	Company	Description/Target sequence
pCMV6-Entry	PS100001	OriGene (USA)	Mammalian vector with C-terminal Myc-DDK Tag
pCMV6-TAGLN	RC215789	OriGene (USA)	TAGLN (Myc-DDK-tagged)-Human transgelin (TAGLN), transcript variant 2
siGENOME Human TAGLN siRNA, SMARTpool	M-003714-02-0020	Thermo Scientific (USA)	siRNA 1- AGAAAGCGCAGGAGCAUAA siRNA2- CCAGACUGUUGACCUCUUU siRNA3- CCAAAAUCGAGAAGAAGUA siRNA4- UGUCCUCCUUGGCGGCAAA
siGENOME Non-Targeting siRNA #2	D-001210-02-20	Thermo Scientific (USA)	UAAGGCUAUGAAGAGAUAC

2.1.4. Tissue material

This study includes analyses with 21 tumors and their matched normal tissues. The pathological features of these tumors are listed in Table 2.4.

Table 2.4: Pathological features of normal matched breast tumor tissues

Patient code	Lymph node	Grade	Stage	ER status	PR status	Her2 status
#003	1	1	N/A	1	1	0
#043	0	2	N/A	1	1	1
#044	1	2	2B	0	1	1
#047	1	2	4	1	0	1
#055	0	2	N/A	1	1	1
#057	0	N/A	2B	0	0	0
#073	1	2	N/A	1	0	1
#076	1	3	2A	0	0	1
#082	0	1	2B	1	0	1
#083	1	2	2B	1	0	1

Table 2.4: Pathological features of normal matched breast tumor tissues

Patient code	Lymph node	Grade	Stage	ER status	PR status	Her2 status
#084	1	3	N/A	0	0	0
#085	0	2	2A	0	1	1
#090	1	2	2B	1	1	1
#096	0	1	2A	0	1	0
#113	1	1	3B	1	0	1
#124	1	1	2A	1	0	1
#137	1	N/A	3A	1	1	N/A
#133	N/A	N/A	N/A	N/A	N/A	N/A
#161	1	2	2A	1	0	0
#164	0	2	2B	1	1	0
#168	1	2	2B	0	1	1

ER: Estrogen receptor. PR: Progesterone receptor. Her2: Erbb2 receptor amplification. N/A: Information regarding the pathological feature is missing. 1: Positive for the given condition. 0: Negative for the given condition. Adapted from Sayar et al.[366]

In addition to the tumor tissues, arrays described in Table 2.5 were also used to be analyzed with IHC and qRT-PCR methods.

Table 2.5: Arrays purchased for IHC and qRT-PCR analyses

Name	Catalog #	Company	Sample Size	Method
BioChain Tissue array #4	Z7020005	BioChain (USA)	68 tumor, 7 normal	IHC
*TissueScan Breast Cancer Tissue qPCR Panel I	BCRT101	OriGene (USA)	41 tumor, 7 normal	qRT-PCR

**cDNA panel was a gift from Assist. Prof. Dr. Özlen Konu.*

2.1.5. Antibodies

Antibodies used in the immunofluorescence (IF), western blot, and immunohistochemistry (IHC) experiments have been listed in Table 2.6.

Table 2.6: Antibodies used in the study

Name of the antibody	Catalog#	Company
Anti-H3K9Ac	07352	Millipore
Rabbit anti-SM22 alpha (TAGLN)	ab14106	Abcam (UK)
Mouse anti-E Cadherin [HECD-1]	ab1416	Abcam (UK)
Mouse anti-Vimentin [V9]	ab8069	Abcam (UK)
Mouse anti-CK19	NCL-CK19	Leica Biosystems
Rabbit anti-calnexin antibody	C4731	Sigma Aldrich (USA)
Anti-rabbit IgG-HRP	6154	Sigma-Aldrich (USA)
Anti-mouse IgG-HRP	M7001	Dako (Denmark)
Donkey polyclonal Secondary Antibody to Mouse IgG - H&L (Alexa Fluor® 488), pre-adsorbed	ab150109	Abcam (UK)
Donkey anti-Rabbit IgG (H+L) Secondary Antibody, Alexa Fluor® 568 conjugate	A10042	Life Sciences (USA)

2.1.6. PCR Primers

Primers that have been used for RT-PCR, qRT-PCR, bisulfite sequencing and plasmid amplification have been presented in Table 2.7, together with the associated amplicon size, optimized Tm values for the annealing step of PCR reaction, and calculated qRT-PCR efficiency percentages. All primers (if not otherwise stated) were purchased from and synthesized by Iontek (Istanbul) or Sentromer (Istanbul). All primers were solved in ddH_2O upon arrival, to be 100µM (except for T7 and SP6 primers), and were kept at -20°C.

Table 2.7: Primers used in the study

Primer Name	PCR[a]	Primer Sequence	Tm[b] (°C)	Size[c] (bp)	Eff.[d] %
ACTB F ACTB R	RT	CCAACCGCGAGACGATGACC GGAGTCCATCACGATGCCAG	60	124	100
GAPDH F GAPDH R	RT	GGCTGAGAACGGGAAGCTTGTCAT CAGCCTTCTCCATGGTGGTGAAGA	60	140	99
SDHA F SDHA R	RT	TGGGAACAAGAGGGCATCTG CCACCACTGCATCAAATTCATG	60	86	100
ACVR1C F ACVR1C R	RT	CGCGGCCCGGGAACTTCAAA ACACTTCAGTCCTGGCGAGAGC	67	176	104
ADAMTSL4 F ADAMTSL4 R	RT	GCAGCCAGCGCCCTGATGAT GCCCCGGACCCCTTTCAGGA	60	166	98
AKAP12 F AKAP12 R	RT	TCACAGAGGTTGGACAGAGA GTGAACAACCGCTGACTTAG	60	86	100
ANLN F ANLN R	RT	TAAAGCAGGTGATTGTTCGG GTTCTTCATCAACACAGCAG	60	180	100
AXIN2 F AXIN2 R	RT	CTCCAGGCGAACGAGCCAGC ACAGCACCGCTGCTTTGGGG	60	194	100
BEX4 F BEX4 R	RT	GCACAATGAAGCGAGAGATG ATGGTTGTCAGGTTCAGGAG	60	124	97
BMP2 F BMP2 R	RT	GTGCGCAGCTTCCACCATGA TTCGAGTTGGCTGTTGCAGG	60	230	93
BTG1 F BTG1 R	RT	CCATGCATCCCTTCTACACC GCTTTTCTGGGAACCAGTGA	60	183	96
CASP9 F CASP9 R	RT	GTTGCGGCGTCGCTTCTCCT ACTGCAGGTGGCTGGCCTGA	60	170	92
CDC14B F CDC14B R	RT	TTCTGGCAGTGCAGGCATTA GTCTTCCTTCAGCTCTGGTC	60	135	98
COL4A6 F COL4A6 R	RT	AGGGAAGCCGGGCCTGAGAG TGGGCGGCCTCGTTCTCCAT	60	163	96
CST6 F CST6 R	RT	ACATCATCAAGGCGCAGAGC ATGGTTGTCCATCGTGGAGT	60	185	N/A
DAPK1 F DAPK1 R	RT	GATTACTACGACACCGGCGA TCTCCTTCAGGATGCTGACC	60	181	N/A
DST F DST R	RT	TGCAGACGCAGTGGAGCTGG AGCTGTACTTCCGCTGAATGGC	60	153	96
DUSP5 F DUSP5 R	RT	ATCAGCCAGTGTGGAAAACC GGAGCTAATGTCAGCCGTGT	60	249	94
EGR2 F EGR2 R	RT	GTGCACCAGCTGTCTGACAA TCCAACGACCTCTTCTCTCC	60	164	98
EPB41L2 F EPB41L2 R	RT	GCCGCCTGCCCTGCTCTTTT TGGCGATAAGCCCCTGTGGGT	60	191	104
F11R F F11R R	RT	CCAAGGAGACACCACCAGAC AACTGTAGGCTTGGATGGAG	60	217	94
FOXO1 F	RT	CAAGAGCAGCTCGTCCCGCC	60	188	98

Table 2.7: Primers used in the study

Primer Name	PCR[a]	Primer Sequence	Tm[b] (°C)	Size[c] (bp)	Eff.[d] %
FOXO1 R		TTGAATTCTTCCAGCCCGCCGA			
GSTM1 F	RT	CATGGACAACCATATGCAGC	60	194	99
GSTM1 R		TACGGTGGAGGTCAAGGACA			
GSTM2 F	RT	GCCAAACTCTGCTATGACCC	60	168	102
GSTM2 R		GTTTCTCTCAAGGACATCATAAG			
HMOX1 F	RT	AGGGCCAGGTGACCCGAGAC	60	147	92
HMOX1 R		CAGCCTTGCGGTGCAGCTCT			
ID2 F	RT	GCCGCTGACCACCCTCAACAC	60	216	102
ID2 R		ACTTGTCCTCCTTGTGAAATGGTTG			
INSIG1 F	RT	TTGCACGACCACTTCTGGAG	60	251	92
INSIG1 R		CTCTGCAACAGGCGATGATG			
IQGAP2 F	RT	GGGACAGAACACCCTGCGCC	67	150	101
IQGAP2 R		GGCAACTTGCTGGCCTCTCCA			
NDRG4 F	RT	GTGCTAGTTAGGCCGGAGAG	60	159	94
NDRG4 R		TGTGATTGGCATCGGAGTGG			
NETO2 F	RT	AGGGATTGCCGTGGCCCAAA	60	184	103
NETO2 R		TTGACGTGGAGCAGCTTCCAAA			
NFKBIA F	RT	ACCACCCCGCACCTCCACTC	60	170	100
NFKBIA R		GCGAGGTGAAGGGCAGTCCG			
NR4A3 F	RT	GCCTTAGCCTGCCTGTCAGCAC	67	139	97
NR4A3 R		TGGGCTCCAGAGCCTGTCCC			
PPP1R15A F	RT	CCCCTCCGACTGCAAAGGCG	60	135	105
PPP1R15A R		CCCTGCCCAGACAGCCAGGA			
RIOK3 F	RT	GGAGACAATCACTGGCTGTA	60	122	95
RIOK3 R		CCTTGATGGCACATTCTG			
S100A02 F	RT	CTGCCACCTGGTCTGCCACAGAT	60	220	103
S100A02 R		CTCATCCAGGCTGCCCATCAGC			
SFRP1 F	RT	CCGAGATGCTTAAGTGTGAC	60	163	99
SFRP1 R		CTCGCTGGCACAGAGATGTT			
TAGLN F	RT	TGCGAGCCCTGAGGAAGCCT	60	220	104
TAGLN R		TCAGAATCACGCCATTCTTCAGCCA			
TGFBI F	RT	CGCTCCATGGCGCTCTTCGT	60	151	103
TGFBI R		ACACGTTGGGGCCGTGCTG			
ZMAT3 F	RT	AGAGGCTGGGTCGAGCTGGG	60	124	98
ZMAT3 R		TGAGAAGCAAGGTCTTCAAATCGGA			
ADAMTSL4 F	BSP	GGTTTAGGGGTTTTAGTGG	56	253	N/A
ADAMTSL4 R		AAAATTATCCRAAACCACC			
AKAP12 F	BSP	TTTTGGAGGTTTTTTAGGGTTTT	60	454	N/A
AKAP12 R		ACTACACCCCAAACTTTCTCTACCT			
CASP9 F	BSP	GATGGGAGGTTTGGTTTTG	54	321	N/A
CASP9 R		CACCTACAACTCTTCCACCAAC			
CDC14B F	BSP	TGGAGGATATAGAAGAAATAAAAGTT	54	259	N/A
CDC14B R		AACCCCAAAAAAACTATTCC			

Table 2.7: Primers used in the study

Primer Name	PCR[a]	Primer Sequence	Tm[b] (°C)	Size[c] (bp)	Eff.[d] %
COL4A6 F	BSP	GGGGAGGGAAATTTTTAGATTA	56	264	N/A
COL4A6 R		TAAAAAAAACCAACAACCCAA			
FOXO1 F	BSP	GAGTGTGTGAAAGAGAAAAATATTTT	52	343	N/A
FOXO1 R		CTCCAACTAACAAAACCRC			
PPP1R15A F	BSP	TTGATTTTGAGTTGAGAGAGAA	60	252	N/A
PPP1R15A R		CACAATAACCACTAAACTTTTATAACC			
S100A2 F	BSP	TTTGGAAGAATTTTTTGTGAAG	58	405	N/A
S100A2 R		AAACAACCCCTACACTAAAACC			
TAGLN F	BSP	GGGGTTAGAGAATAGTGAAGTAGGAGTA	58	407	N/A
TAGLN R		ACACTCACAAAACTTCCTCAAAACT			
TGFBI F	BSP	TTTTGGTTTGAGGAAGATTGT	56	369	N/A
TGFBI R		AACCCAAAACCAAAACCA			
ZMAT3 F	BSP	TGTTTGGATTTTAATGATTGGA	58	401	N/A
ZMAT3 R		TATCAAAAATCAATCCAACCC			
SP6	P	ATTTAGGTGACACTATAG	47	N/A	N/A
T7	P	TAATACGACTCACTATAGGG	47	N/A	N/A
Primers designed and kindly provided by Dr. Özgür Şahin's group:					
CDH1 F	RT	CCCGGGACAACGTTTATTAC	58	72	92
CDH1 R		GCTGGCTCAAGTCAAAGTCC			
CDH2 F	RT	ACAGTGGCCACCTACAAAGG	58	201	105
CDH2 R		CCGAGATGGGGTTGATAATG			
FN F	RT	CTGGCCGAAAATACATTGTAAA	58	114	91
FN R		CCACAGTCGGGTCAGGAG			
KRT18 F	RT	TGATGACACCAATATCACACGA	58	112	98
KRT18 R		GGCTTGTAGGCCTTTTACTTCC			
MMP9 F	RT	GAACCAATCTCACCGACAGG	58	67	103
MMP9 R		GCCACCCGAGTGTAACCATA			
SNAI2 F	RT	TGGTTGCTTCAAGGACACAT	58	66	93
SNAI2 R		GTTGCAGTGAGGGCAAGAA			
ZEB1 F	RT	GGGAGGAGCAGTGAAAGAGA	58	70	96
ZEB1 R		TTTCTTGCCCTTCCTTTCTG			
ZEB2 F	RT	AAGCCAGGGACAGATCAGC	58	74	100
ZEB2 R		CCACACTCTGTGCATTTGAACT			
ZO1 F	RT	CAGAGCCTTCTGATCATTCCA	58	69	98
ZO1 R		CATCTCTACTCCGGAGACTGC			

[a] Purpose of PCR, RT: qRT-PCR or RT-PCR, BSP: Bisulfite sequencing, P: Plasmid PCR. [b] Annealing temperature optimized for given efficiency values. [c]Amplicon size. [d]Eff: Efficiency

2.1.7. Equipment

Equipment used for the completion of the experiments have been listed in Table 2.8.

Table 2.8: Equipment used for the experiments

Name of the instrument	Company
PCR Thermal cycler	Applied Biosystems (USA)
AutoFlow NU-8500 Water Jacket CO_2 Incubator	NuAire (USA)
AxioCam MRc5 image capture device	Carl Zeiss (Germany)
Centrifuges 5810 and 5810 R	Eppendorf (Germany)
Stratagene Mx3005P Real-Time PCR System	Agilent (USA)
Bond Max equipment	Leica Microsystems (Germany)

2.2. Solutions and media

2.2.1. Routinely used laboratory solutions

Buffers and solutions that are commonly used in the laboratory have been listed in Table 2.9

Table 2.9: Routinely used buffers and solutions

Buffer	For 100 ml aqueous solution (if not otherwise stated)
50X TAE	24.2 g Tris-base; 1.86 g EDTA; 5.71 ml glacial acetic acid.
6X Loading Dye	0.012 g Bromophenol blue; 0.012 g Xylene cyanol; 8ml 0.5M EDTA; 80ml glycerol
10X PBS	2.56 g $Na_2HPO_4.7H_2O$; 8.0 g NaCl; 0.2 g KCl; 0.2 g KH_2PO_4
10X TBS	1.22 g Tris-base; 8.78g NaCl. pH = 8.0

Table 2.9: Routinely used buffers and solutions

Buffer	For 100 ml aqueous solution (if not otherwise stated)
30% Acryl:Bis-acryl solution	29 gr acrylamide; 1 gr bis-acrylamide (in dark).
5X Running Buffer	1.5 g Tris-base; 7.2 g glycine; 0.5 g SDS
Lysis buffer (1ml)	67.5 µl 2M NaCl; 45 µl 1M Tris-HCL (pH = 8.0); 10 µl Triton X-100, 100 µL 10X Proteinase inhibitor.
5x Protein Loading Buffer	0.001g Bromophenol blue; 2g SDS; 62.5 mM Tris-HCL (pH:6.8); 15% glycerol. 5% β-mercaptoethanol is prior to loading.
Coomassie Staining Buffer	0.25 g Coomassie Brilliant Blue; 45 ml MetOH; 10 ml glacial acetic acid
Destaining Solution	20% MetOH; 7% glacial acetic acid
Wet Transfer Buffer	0.6 g Tris-Base; 2.88 g glycine; 15% Methanol
Crystal Violet Solution	0.5% crystal violet; 25% MetOH
Fixation Solution for IF	2% Formaldehyde; 100 ml 1X PBS
Permeabilization Solution for IF	0.2% Triton X-100; 100 ml 1X PBS
Na-P Buffer	25.5 µl 1M Na_2HPO_4; 74.5 µl NaH_2PO_4
SA-B-Gal Solution	20 µl 200mM Citric acid;20 µl Na-P buffer; 5 µl 100mM K-ferrocyanide; 5 µl 100mM K-ferricyanide; 7.5 µl 2mM NaCl; 2 µl 100mM MgCl2; 2.5 µl 40mg/ml X-gal.
LB	1 g Tryptone; 0.5 g yeast extract;1 g NaCl; 2.5 g Bacto agar (for plates)

Table 2.9: Routinely used buffers and solutions

Buffer	For 100 ml aqueous solution (if not otherwise stated)
Transformation Buffer	1.09 g $MnCl_2.4H_2O$; 0.22 g $CaCl_2.2H_2O$; 1.87 g KCl; 2 ml 0.5M Pipes (pH 6.7)
SOC medium	2 g Tryptone; 0.5 g Yeast extract; 1ml 1M NaCl solution; 0.25 ml 1M KCl solution ; 97 ml ddH2O. After autoclaving : sterile 1ml 1M MgCL2; sterile 1ml 1M MgSO4; sterile 1ml 2M glucose

2.2.2. Cell culture solutions and media

Cell lines and their growth media have been listed in Table 2.10.

Table 2.10: Cell lines and their growth media

Cell Line	Medium
BT20	Basic DMEM
BT474	Basic DMEM; 10µg/ml insulin
CAL51*	Basic DMEM (high glucose) ; 10% FBS
CAL85-1*	Basic DMEM; 1mM Sodium pyruvate
CAMA-1	Basic DMEM
EFM19*	Basic RPMI
HCC1143*	Basic RPMI; 10% FBS
HCC-1937	Basic RPMI-1640; 1mM sodium pruvate
HDQP1*	Basic DMEM
JIMT-1*	Basic DMEM
MCF10A*	Basic DMEM/Ham's F12; 10µg/ml insulin; 20 ng/ml EGF;0.5 mg/ml hydrocortisone

Table 2.10: Cell lines and their growth media

Cell Line	Medium
MCF12A	Basic DMEM/Ham's F12; 10µg/ml insulin; 20 ng/ml EGF;0.5 mg/ml hydrocortisone
MCF7	Basic DMEM
MDA-MB-157	Basic DMEM; 1mM Sodium pyruvate
MDA-MB-231	Basic DMEM
MDA-MB-361	Basic DMEM; 1mM Sodium pyruvate
MDA-MB-453	Basic DMEM
MDA-MB-468	Basic DMEM
SKBR-3	Basic McCoy's 5A Medium
T47D	Basic RPMI; 1mM Sodium pyruvate
ZR-75-1	Basic RPMI-1640, 4.5g/L glucose

** Cell lines kindly provided by Elif Erson Bensan, METU, Ankara. Other cell lines were purchased from ATCC. Basic Media consist of the given medium; 10% FBS; 1% Penicillin/Streptomycin; 1% Non-essential amino acids.*

2.3. Methods

2.3.1. General maintenance and handling of human cell lines

Cells are preserved in liquid nitrogen tanks in sterile screw capped cryo-vials. When needed, frozen cells can be cultured as follows: The vial is immersed in 37°C water bath until almost completely thawed and then directly transferred to 37°C growth medium (Table 2.10), followed by centrifugation at 1500 rpm for five minutes at room temperature (RT). After removal of the supernatant, cells are washed with growth medium, and are transferred to T25 tissue culture flasks. All cells are maintained in CO_2 incubators, providing 5% CO_2 and 37°C environment. Cells can be split 1:2 to 1:5 depending on the cell type in approximately two days; and if not split, the growth medium is changed in every three days. When necessary, cells can be detached from the flasks, after washing with 1X sterile PBS, with addition of 0.25% Trypsin/EDTA for 3

min, at volumes adequate to cover the entire surface. When the cells are to be frozen, the detached cells are transferred into freshly prepared freezing medium, consisting of 90% FBS and 10% DMSO, and are directly transferred to -20 freezers. After 1 hour, the cells are moved into -80 freezers for overnight, and finally they are transferred to liquid nitrogen tanks. All cell culture practices are done in sterile environment, using sterile technique under cell culture laminar flow hoods.

2.3.2. AZA and TSA treatment of cell lines

For each treatment, 500.000 cells/100-mm-cell-culture-plate (for the cases of MCF12A, 750.000 cells/plate) were cultured, and 10 ml medium was used for each.

5-aza-2'deoxycytidine (AZA) was dissolved in DMSO as described in the user manual. For decision of the concentration 100nM, 250nM, 500nM, 750nM, 1µM, 3µM and 5µM were used to treat the cells for 4 days. After the effective concentration was determined, a final concentration of 5µM was used to treat the cells immediately after plating, and the cells were incubated for 4 days with everyday media change.

Trichostatin A (TSA) was also dissolved in DMSO, and for determination of concentration, 25nM, 50nM, 75nM, 100nM and 400nM concentrations were used to treat the cells for 1 day. After the effective concentration was determined, cells were treated with 400nM TSA for 1 day. The drug was added 24 hours after the cells were plated.

For treatment with both agents, the cells were plated, 5µM AZA was added immediately, the medium and drug was changed every day, and in the 74th hour, 400 nM TSA was added together with AZA. The cells were collected at 94th hour. The trial concentrations for combined treatment were 5µM AZA + 50nM TSA, 5µM AZA + 75nM TSA, 5µM AZA + 100nM TSA, and 5µM AZA + 400nM TSA.

Cells were also treated with equivalent amounts of DMSO (controls), or were grown without any treatment (mock). Cells were harvested and centrifuged at 1500 rpm for 5 min at +4°C to be kept as pellets at -80°C for use of RNA, DNA or protein isolation.

BT-20, BT-474, CAL-51, MCF10A, MDA-MB-361, MDA-MB-453, MDA-MB-468, SK-BR-3, ZR-75-1 cell lines were plated to be 750.000/plate, and were treated with AZA and/or TSA as described above.

2.3.3. Drug toxicity analysis using MTT assay

Cells were plated into 24-well plates to be 11.000 cells/plate (or 16.000 cells/plate for MCF12A) and effects of different doses of AZA and/or TSA were tested on each cell line. For

AZA, 750nM, 1µM, 3µM and 5µM were tested while for TSA 25nM, 75nM, 100nM and 400nM were tested. After 5µM was chosen for AZA treatment, effects of addition of 50nM, 75nM, 100nM and 400nM TSA were tested to this concentration of AZA, for AZA+TSA (A+T) treatments. Drug and medium refreshments were done as in the cell treatment protocol. MTT test was applied according to the user protocol, in triplicates.

2.3.4.RNA Isolation and determination of quality

RNA isolation from the cell lines was carried out with MN Nucleospin RNA kit as described in the kit's user protocol. The quantification of the RNA was carried out with NanoDrop ND-1000 spectrophotometer using 2µl of RNA sample, and the quality of the RNA was determined with Agilent 2100 Bioanalyzer by calculating the RNA Integrity Number (RIN) values.

For RNA isolation from tissues, 60 µm thick sections were dissected from tumor(~5 slices) and normal tissues (~10 slices), and were transferred into eppendorf tubes with 1ml TRI reagent to be homogenized by a homogenizer, followed by 21-gauge fine needle homogenization. 50 µl 4-bromoanisole was added to the homogenized tissues after 5 min incubation at RT. The mixture was vortexed for 15 sec and incubated at RT for 3 min followed by centrifugation at 12,000g for 15 min at +4°C. The aqueous phase was carefully transferred into a new tube, was added 0.5 ml 2-propanol and was left at RT for 10 min. The centrifugation was repeated with same conditions, and the supernatant was carefully discarded to leave the RNA pellet, which was washed twice with 75% EtOH followed by 5 min centrifugation at 7500g at +4°C. Finally, the pellet was left for air dry under the hood. Afterwards, 25 – 50 µl DEPC treated molecular biology grade water is added onto the dried RNA pellets, and the quantity and quality were determined with ND-1000 spectrophotometer using 2µl of RNA sample. Remaining samples were kept in -80°C freezers.

2.3.5. cDNA preparation from RNA samples

cDNA was prepared from 1µg of RNA from each sample, using RevertAid 1st strand cDNA synthesis kit (Thermo Scientific), using oligo-dT primers for cell line RNAs, and random hexamers for tissue RNAs. Quality and quantity of cDNAs were tested by carrying out PCR with *GAPDH* primers (Table 2.7). The cDNAs were kept at-20°C for later use.

2.3.6.RT-PCR

Reverse transcriptase-PCR (RT-PCR) was performed using the following PCR mixture: 17.4 µl H_2O; 2.5 µl 10X *Taq* Buffer with KCl; 1.5 µl 25mM $MgCl_2$; 0.5 µl dNTP mix; 1 µl forward primer; 1 µl reverse primer; 0.2 µl *Taq* polymerase; 1 µl cDNA. A negative control was always

included, which does not include cDNA. Final 25 µl mix was placed in thermal cycler, and typically 25-30 cycles of 15 sec at 90°C; 15 sec at Tm (Table 2.7); 15 sec at 72°C was applied. The PCR products were run in 2% or 3% agarose gels including 30ng/ml EtBr for 15 min, and were visualized under UV light.

2.3.7.qRT-PCR and expression analyses

Expression of selected genes was quantified using the primers designed in Primer.exe programs and in the Primer-BLAST of NCBI (http://www.ncbi.nlm.nih.gov). The primers (Table 2.7) were designed to exclude any genomic DNA amplification such that either a long intron was included between the forward and the reverse primers, or at least one of the primers was designed to include an exon-exon junction. Efficiency of the primers was assigned by generation of a dilution series (7 dilutions from 1 to 1/15625, as powers of 1/5) of pooled cDNA, then running a qRT-PCR reaction for each concentration. Plotting the Ct values against the $\log_5$(DNA content) resulted in a linear graph, whose slope was used to calculate the efficiency value (Eff) of each primer, as listed in Table 2.7.

$$Eff = 5^{-1/slope}$$
$$\%Eff = [(5^{-1/slope}) - 1]\times 100 \qquad \text{Eq (1)}$$

qRT- PCR assays were performed in duplicates, using DyNAmo™ HS SYBR® Green qPCR Kit. The reaction volume was 20 µl, including 1µl of cDNA and 0.8 µl of the indicated primers (10pmol/µl each) and 10 µl of master mix. The reaction conditions were as follows: Initial denaturation for 5 minutes at 94°C, 40 cycles of denaturation (94°C, 20 sec), annealing (Tms as in Table 2.7, 15 sec) and elongation (72°C, 15 sec), and a final elongation of 5 min at 72°C. The Ct values (cycle number at which the fluorescence exceeds the fixed threshold) of the duplicates were averaged and the expression values of the target gene were normalized to the housekeeping control gene *GAPDH* for the cell lines, and to the geometric means of *ACTB* and *SDHA* for the tissue samples[367]. The relative expression values were compared using the equation given in Eq(2). The qRT-PCR experiments were done in Stratagene Mx3005P Real-Time PCR System.

$$Relative\ expression = \frac{Eff(target)^{-Ct(target)}}{Eff(reference\ gene)^{-Ct(reference\ gene)}} \qquad \text{Eq (2)}$$

2.3.8. Histone isolation from cell pellets

Cell pellets were resolved inside the TEB Buffer consisting of filtered PBS, 0.5% Triton X100, 1X protease inhibitor, and 0.02%NaN_3; and cells were ruptured by gentle agitation on ice for 10 min. After centrifugation for 10 min at 2000 rpm and 4°C, supernatant was discarded and pellet was resuspended in TEB buffer. The solution was again centrifuged for 10 min at 2000 rpm at 4°C, and the supernatant was discarded. The obtained pellet was resuspended in 0.2N HCl solution and was rotated overnight at 4°C for continuous mixing. The solutions were then centrifuged for 10 min at 2000 rpm and 4°C, and the supernatant was kept as the histone proteins.

2.3.9. Cytoplasmic protein isolation from cell pellets

Depending on the size of the pellets, 30-100 µl lysis buffer (Table 2.9) was added onto the cells on ice, and were mixed by pipetting. The pellets were incubated on ice for 30 min with occasional vortexing, and then were centrifuged at 13,000 rpm, for 30 min at +4°C. Supernatant, the cell lysate, was the used for western blot experiments.

2.3.10. SDS-PAGE and coomassie staining

15-18% SDS-polyacrylamide gels were prepared for histones, and 12% gels were used for other proteins, as shown in Table 2.11.

Table 2.11: SDS-Polyacrylamide gel preparation

Resolving Gel				**Stacking Gel**	
Constituent	**12% (ml)**	**15% (ml)**	**18% (ml)**	**Constituent**	**5% (ml)**
H_20	3.3	2.3	1.3	H_20	3.4
30% Acrylamide-bisacrylamide mix	4.0	5.0	6.0	30% Acrylamide-bisacrylamide mix	0.83
Tris Buffer (pH 8.8)	2.5	2.5	2.5	Tris Buffer (pH 6.8)	0.63
10% SDS	0.1	0.1	0.1	10% SDS	0.05
15% APS	0.1	0.1	0.1	15% APS	0.05
TEMED	0.004	0.004	0.004	TEMED	0.005

Gels were run in 1X running buffer (Table 2.9) at 80V for 15 min, followed by 120V until the loading dye reaches the end of the gel. For histone proteins, Coomassie staining was used as equal loading, thus double gels were loaded with equal amounts of proteins, and one gel was stained with Coomassie solution (Table 2.9). Briefly, gels were immersed in Coomassie solution for 1 hour with constant shaking, and then were left overnight in the destaining solution with shaking.

2.3.11. Western blot

The proteins which were run in SDS-PAGE were transferred to nitrocellulose membranes using wet transfer system (Biorad) and wet transfer buffer (Table 2.9). The histone proteins were transferred overnight at 14V, or for 3 hours at 80 V. Other proteins were transferred at 60V for 2 hours. After the transfer, the membrane is incubated in blocking solution, including 5% BSA or skim milk powder in 1X TBS with 0.3% Tween-20 (0.3% TBS-T) for 1 hr on shaker (slow). After 1 hour, the membrane is transferred to primary antibody solution, consisting of 5% skim milk powder or BSA, 0.3% TBS-T and primary antibody (Table 2.6) for 1-3 hours at RT or overnight at +4°C, on shaker (slow). After the incubation, the membrane is washed three times with 0.3% TBS-T, for 10 min each, on shaker (fast). The membrane is placed into the secondary antibody solution, containing 5% skim milk powder and 1:5000 diluted secondary antibody in 0.3% TBS-T for 1 hr. After the incubation the membrane is washed again as before, and is developed using ECL prime system as described, visualization is performed in dark room with X-ray films.

2.3.12. Hybridization of RNA samples to the microchips

For hybridization to Affymetrix Hgu-133 Plus 2.0 gene chips, the concentration of the RNAs was adjusted to be 5 µg/8µl. Preparation of the samples and hybridizations of each sample to the gene chips were done following the standard Affymetrix protocol, in the Microarray Hybridization Facility, at Bilkent University. Shortly, RNA samples were converted to cDNA (One-cycle cDNA synthesis kit, Affymetrix), generated cDNAs were re-converted to RNA and the cRNA were labeled with biotin (IVT Labeling Kit, Affymetrix), and the fragmented cRNA were hybridized to the microchips. Scanning of the microchips was done using GCOS software, and .CEL files were obtained as a result.

2.3.13. Data normalization and quality control

Data were extracted from the .CEL files using BRB-ArrayTools 3.8.0, developed by Dr. Richard Simon and the BRB-ArrayTools Development Team, and were normalized with justRMA method. Quality control analyses were performed using the “Affy Data Quality

Control" utility of the software, which analyses the signals obtained from the probe sets corresponding to the 5' and 3' ends of *GAPDH* and *ACTB* mRNAs. Scatter plots were generated between the replicates of each sample using "Scatter Plot" function (experiment vs. experiment) to reveal the consistency between the replicates, as another step of quality control. Quality control was also performed using R 2.10.0, and box-plots before and after RMA normalization were generated. Normalized data is uploaded to the Gene Expression Omnibus (GEO) database under the accession number GSE71363.

URL for accession: http://www.ncbi.nlm.nih.gov/geo/query/acc.cgi?acc=GSE71363.

2.3.14. Class comparison and data analysis

Intensities of probes in control and treatment groups were compared using the "Class Comparison" function of BRB-ArrayTools, which applies t-test with a random variance model for small sample sizes. Gene lists were generated for each cell line and each treatment group, selecting the genes upregulated or downregulated by >1.5 fold at $P < 0.05$ for global analyses and $P < 0.001$ for candidate selection. Then, the gene lists were intersected using the "Intersect gene lists" utility of the software. The utility also performs subtraction, so probe sets which were also altered in the non-tumorigenic cell line MCF12A were subtracted from the gene lists of MCF7 and MDA-MB-231 using this function. Pathway annotation of the genes and gene lists were performed using DAVID Bioinformatics Resources 6.7, "Functional Annotation Clustering" tool[368-369]. Human Genome U133 Plus 2 Array was selected as the background for the enrichment analyses.

2.3.15. CpG island analyses

Candidate genes were screened for presence of CpG islands (CGI) in their promoter proximal locations using MethPrimer[370] and CpG Island Searcher[371]. For this, sequences between ±2000 bp locations with respect to the transcription start sites (TSS) were searched for presence of a CGI, using the search parameters: % GC is >55% Observed CpG/Expected CpG is <0.6, Length > 200bp and the gap between adjacent islands is >100bp. If one of the algorithms found a CGI in the given region, the candidate gene was accepted as $CGI^{(+)}$. If none of the algorithms could define a CGI in the examined sequence, the gene was removed from the candidate gene list.

2.3.16. Oncomine and Expression Atlas analyses

The expression states of the candidate genes were examined in Oncomine[372] and Expression Atlas (https://www.ebi.ac.uk/gxa/) databases. $P < 0.05$ threshold was applied for cancer vs. normal comparisons in both databases. If a gene was found to be downregulated in breast cancer

tissues or cell lines compared to the normal tissues or NT cells, respectively, its candidacy was strengthened. If a gene was found to be strongly over-expressed in several breast cancer studies, the gene was removed from the candidate gene lists.

2.3.17. DNA isolation from cell lines and tissues

Cells were grown to 70-80% confluency and were harvested by trypsinization. DNA isolation was done using MN-Nucleospin Tissue kit, following the kit's user protocol, with elution in ddH_2O. The quantification of DNA samples was carried out with NanoDrop ND-1000 spectrophotometer. The DNA samples were kept at -40°C.

For DNA isolation from tissue samples, 60 µm thick sections were dissected from tumor (~5 slices) and normal tissues (~10 slices), and the dissected sections were processed using Nucleospin Tissue kit (Macherey Nagel), as described in the user protocol.

2.3.18. Bisulfite modification of DNA and bisulfite PCR

Bisulfite modification of the DNAs was carried out with Epitect Bisulfite Kit (Qiagen), following the user protocol. Primers for PCR of bisulfite modified genomic DNA (BSP) were specially designed for bisulfite sequencing (Table 2.7), using Methyl Primer Express v1.0 software (Applied Biosystems). Bisulfite sequencing PCR (BSP) conditions and mixes were optimized for each primer set, and as positive control of the reaction, Epitect Methylated and Unmethylated Bisulfite Treated DNA were used.

2.3.19. Preparation of competent *E.coli* DH5α

E.coli single colonies were grown in 15 ml LB at 37°C with constant agitation of 225 rpm overnight, and the next day, the bacteria were transferred to 200ml fresh LB and were incubated with constant agitation at 225 rpm until the optical density (OD) of 0.6 is obtained. At this step, the bacteria at the log phase were taken into sterile ultracentrifuge tubes and incubated on ice for 10 min, followed by centrifugation at 2500 g for 10 min at +4°C. 64 ml transfer buffer (TB, ice-cold, Table 2.9) was added onto the pellet after the supernatant was discarded, and the bacteria were resuspended by pipetting, followed by a second centrifugation under the same conditions. This time, the bacteria pellet was resuspended with 8ml ice-cold TB with 7% DMSO, on ice. The obtained competent cells are immediately frozen in liquid nitrogen as 150- 200 µl aliquots in eppendorf tubes, and were kept at -80 freezers.

2.3.20. Transformation of BSP products to competent DH5α

BSP products were run in 1.2% agarose gels, and were visualized under UV light. The bands at the correct sizes (Table 2.7, Amp. size) were cut out with a blade, and gel extraction procedure was applied according to the supplied protocol using QIAquick Gel Extraction kit (Qiagen). Gel extracted, pure PCR products were ligated into the pGEM-T Easy vector (Promega) using the kit contents and provided protocol. Each time, positive and negative controls were included as described in the protocol. Usually 1 hr was given at RT for ligation to take place, or if necessary overnight incubation at +4°C could also be applied. After the ligation is complete, the whole ligation mix was used to transform the competent *E.coli* DH5α using the protocol supplied by the pGEM-T Easy vector system (Promega); however, instead of 50 µl of competent cells, 150 – 200 µl was used. 100 – 200 ml transformed bacteria was spread over LB-agar plates containing 100 µg/ml ampicillin, 0.5 mM IPTG and 80 µg/ml X-Gal. The plates were incubated overnight at 37°C prior to blue – white selection.

2.3.21. Plasmid isolation from transformants and bisulfite sequencing

Successful transformants were selected using ampicillin as selective antibiotic, and the presence of insert was assured by blue-white selection. 5 – 6 white colonies were selected from each plate and were grown overnight in liquid LB at 37°C with constant agitation at 225 rpm. Afterwards, plasmids were isolated from the overnight cultures using PureLink Quick Plasmid Miniprep Kit (Invitrogen), following the user protocol. Quantification of plasmid concentration was done with NanoDrop ND-1000 spectrophotometer. Confirmation of the insert of the PCR product was carried out with PCR using T7 promoter and SP6 primers, whose complementary sequences are present in the pGEM-T Easy Vector, at 47 °C, using regular PCR conditions. Confirmed plasmids were sent for sequencing to Iontek (Istanbul) or Genoks (Ankara), with SP6 primers.

2.3.22. Analysis of bisulfite sequencing data

The sequencing data was analyzed using the web based Quantification of Methylation Analysis (QUMA) tool[373], which aligns the sequenced bisulfite and downloaded genomic sequences, calculates the efficiency of bisulfite treatment, percentage of methylation, and significance of the difference between given two groups, and generates lollipop and other graphical figures. Poorly converted clones*, i.e.* the conversion of non CpG Cs to Ts is lower than 95%, or sequences resulting in mismatches more than 10 bases were excluded from the analyses. Mann-Whitney test was used to compare methylation frequencies of unpaired samples and Wilcoxon signed rank test was applied to compare the methylation percentages of the paired samples.

2.3.23. Analyses of public methylation and survival data

Publicly available breast cancer methylation microarray (GPL8490 Illumina Human-Methylation-27 BeadChip) data sets GSE20713 super-series (GSE20712 and GSE22249) and GSE31979 were downloaded from GEO database (n = 338 tumors and 33 normal tissues). Mean of the methylation scores of the two probes (cg24619694 and cg06950730) corresponding to +445 and -561 positions from the TSS of *TAGLN* gene, respectively, were analyzed. The data from two separate datasets were combined and normalized in GraphPad Prism 6.0, assigning 0 for the lowest methylation scores and 100 for the highest. The remaining scores were distributed accordingly, fitting on a sigmoidal curve. As a result, normalized average methylation scores (NAMS) were obtained to be used for further analyses. Group comparisons were done with Mann-Whitney test. For Spearman correlation of methylation scores and the expression values, expression data corresponding to 90 tissues in GSE20713 methylation dataset were downloaded (GSE20711) from GEO. ROC analyses were performed using the NAMS values of 338 breast tumor and 33 normal tissues. For survival analyses depending on the methylation scores, best cut off was determined testing cut-offs between NAMS = 60 and 90, with intervals of 5. NAMS > 80 was selected for the best cut-off for calculation of 10 years RFS[374]. *P* values were calculated using Gehan-Breslow-Wilcoxon test. All analyses were performed in GraphPad Prism 6.0. Datasets used for the expression and promoter methylation analyses of *TAGLN* gene are listed in Table 2.12.

Table 2.12: Datasets used for analysis of *TAGLN* expression and promoter methylation in breast cancer

GEO Accession #	Data	Year	Normal Tissues	Tumor Tissues	Type of sample
GSE20711[110]	Expression	2011	2	88	Tumor and normal breast tissues
GSE20712[110]	Methylation	2011	4	119	Tumor and normal breast tissues
GSE22249[110]	Methylation	2011	8	117	Tumor and normal breast tissues
GSE31979[375]	Methylation	2011	21	103	Tumor and normal breast tissues
GSE52621[375]	Methylation	2014	6	11	Breast cancer sera, normal breast tissue
GSE58119	Methylation	2014	282	0	Serum

Survival analyses depending on the expression levels of *TAGLN* gene were performed in the breast cancer cohort of web based Kaplan-Meier (KM) plotter, with the best cut-off option[376]. Expression data of the 205547_s_at probe set corresponding to *TAGLN* mRNAs was used for the survival analyses.

2.3.24. Immunohistochemistry staining of breast tissue arrays

Immunohistochemical staining (IHC) of the tissue arrays were carried out with automatic Bond Max equipment by Prof. Dr. Önder Bozdoğan. Antigen retrieval steps were performed in Bond-Epitope Retrieval Solution 1 with for TAGLN antibody (1:500) and E-cadherin antibody (1:100), Vimentin antibody (1:100) and CK19 antibody (1:100) at 100°C. Detection was carried out with Bond Polymer Refine Red Detection kit. Stained slides were dehydrated and covered with mounting medium and cover-slips. Digital images of the slides were evaluated using the H-score method[377]. Statistical differences between groups were calculated with Mann-Whitney test while correlations were tested with Spearman correlation, in GraphPad Prism 6.0.

2.3.25. siRNA transfections of MCF10A and MCF12A cells

TAGLN gene was silenced in MCF12A and MCF10A cells with siGENOME Human *TAGLN* siRNA (Thermo Scientific) using RNAiMAX transfection reagent (Table 2.3). For control, siGENOME Non-Targeting siRNA #2 (Thermo Scientific) was used for transfection of the cells. Reverse transfection protocol supplied by the manufacturer was applied, by plating 100.000 cells per well of a 6-well tissue culture plate and transfecting with 50nM siRNA in 5 µl lipofectamine. The downregulation of the transgelin protein was assessed with western blot experiments.

2.3.26. Kill curve assay and determination of Geneticin concentration

For determination of Geneticin concentration to be used as selective antibiotic for stable cell line generation, kill curve assays were performed. 0 µg/ml, 100 µg/ml, 200 µg/ml, 300 µg/ml, 400 µg/ml and 500 µg/ml Geneticin concentrations were tested with MDA-MB-361 and MDA-MB-157 cells. Cells were treated with given concentrations of Geneticin for two weeks, changing the media every 3 – 4 days. After two weeks, SRB assay was performed to calculate the survival proportions of the cells. For the SRB assay, cells were washed with PBS once, and then fixed with 250 µl ice-cold 10% TCA for 1 hr at +4°C, in dark. After the incubation is over, wells were washed 5 times with ddH_2O and left for air dry. 0.04 g SRB dye was dissolved in 10 ml 1% acetic acid, and 250 µl of the solution was added to each well. Plates were incubated for 10 min at RT in dark, washed 5 times with 1% acetic acid solution and were left for air dry. Finally, 0.5X TBS was added (500 µl/well) and the colored solution was read at 495 – 525 nm

to obtain absorbance values. The concentrations at which all the cells were killed were determined to be used for the stable clone generation.

2.3.27. Over-expression of *TAGLN* in breast cancer cells

TrueORF-Gold pCMV6-Entry-*TAGLN* (Origene) was used for transfection of MDA-MB-361 and MDA-MB-157 cells in order to over-express *TAGLN* gene. As control, empty pCMV6-Entry vector (Origene) was used. Lipofectamine 2000 reagent (Invitrogen) was used for the transfections using the protocol supplied. Briefly, 1.5 µg vector was transfected in 5 µl of Lipofectamine 2000 reagent to 250,000 cells, and after three days, the cells were transferred into 150 mm petri dishes, including pre-determined concentration of selective antibiotic Geneticin (Life Technologies). Single cells were allowed to form colonies for 20-30 days, with change of media and antibiotics every three days. After colonies were formed, they were picked up with 200 µl pipettes, and were transferred to 6-well plates including growth media with Geneticin. As the cells proliferated, half were harvested for validation of over-expression, and the rest was left to grow. The cells successfully over-expressing transgelin protein were scaled-up until they can occupy T75 flasks and were then frozen for further use.

2.3.28. 2D Colony formation assays

MDA-MB-157, MDA-MB-361, MCF10A and MCF12A cells were cultured to be 2,000/well of a 6-well plate, in at least triplicates and were left to grow for 2 – 4 weeks, until colonies visible to eye formed, with change of media every 3 – 4 days. Then, the cells were fixed with ice-cold MetOH for 10 min in freezer, and then stained with 0.5% crystal violet solution for 15 min. Wells were washed with ddH_2O at least 5 times and left for air dry. Then, the photos of the wells were taken with scanner, and the colonies were counted. Image J was used to determine the number and size of the MDA-MB-361 colonies, which were round and compact. Colony numbers of other cells were determined manually, and hence, the size could not be calculated. Statistical significance of differences between the number and size of the colonies were determined with t-test in GraphPad Prism 6.0.

2.3.29. *In vitro* wound healing and Matrigel invasion assays

For wound healing assay, MDA-MB-157 cells were plated to be 150.000/well and MDA-MB-361 cells were plated to be 250.000/well of 24-well plates in normal growth medium. The next day, scratches were drawn with 200 µl pipette tips, and the media was replaced with 0.5% FBS containing media. Photos were taken at 0 hr and 24 hr. The area of the scratches in the 0^{th} and 24^{th} hour were determined using Image J, and the differences between control and *TAGLN* over-expressing groups were tested for significance using Mann Whitney test.

For the Matrigel invasion assays, Matrigel (BD) was diluted 1:5 with ice cold serum free media on ice, using cold pipette tips, and the bottom of the Transwell Permeable Support invasion chambers were covered with a thin layer of diluted ice cold Matrigel (50 µl). The plates with chambers covered with Matrigel were incubated at 37°C to harden and settle. Then, 150,000 cells were added to the upper chamber in 100 µl 0.5% FBS containing media; and 270 µl of 10% FBS containing media was added to the lower chamber. The set up was incubated in CO_2 cell culture incubator for 48 hr; and then the upper chambers were removed from the set up, the matrigel, cells and media at the upper chamber were removed carefully with cotton swabs, then inserts were washed with PBS, and were stained with Giemsa solution for 2min at RT. The membranes were cut out from the chambers, were mounted with glycerol on to the cover-glasses with bottom part facing the cover-slips. Then the cells passing through the Matrigel and the membrane were counted under the light microscope.

2.3.30. Immunofluorescence (IF) staining of breast cancer and NT breast cells

Cells were plated to be ~50% confluent on cover-slips in 6-well plates, and allowed to settle and grow for two days. Then, cells were fixed with fixation solution (Table 2.9) for 15 min under the hood, followed by 3 times wash with 1X PBS. Then the cell membranes were permeabilized using permeabilization buffer (Table 2.9) for 10 min at RT. After one wash with 1X PBS, plates were incubated with blocking solution including 1% BSA and 0.1% Tween-20, for 1 hr at RT. Primary antibody incubation was carried out overnight at +4°C, in humidified atmosphere. Following day, the plates were washed 3 times with 0.1% PBS-T, and were incubated with secondary antibody solution for 45 min at RT. Washing was repeated as before, and finally the slides were washed with ddH_2O, removed from the plates, and were mounted using 10 µl of mounting medium (Santa-Cruz).

2.3.31. FACS analyses

300,000 cells were plated in wells of 6-well plates and were grown in normal growth conditions for 24 hr. After 24 hr, cells were trypsinized, counted and collected in PBS, followed by centrifugation at 1500 g for 5 min, at +4°C. After the PBS is discarded, 1.5 ml PBS was added onto the pellets. The tubes were vortexed vigorously, while at the same time 3.5 ml ice-cold EtOH was added drop-wise. The tubes were incubated on ice for 30 min, with occasional vortexing, and then were transferred to +4°C, or were directly stained with propidium iodide (PI). For this, final concentration of 20 µg/ml RNase A was added, and the mixture was incubated at 37°C for 10 min. Then 40 µg/ml PI was added, and cells were incubated at RT for 30 min. After the incubation period was over, cells were transferred to FACS tubes, and FACS analyses were performed.

2.3.32. Senescence associated β-galactosidase (SA-β-Gal) staining

MDA-MB-361 cells were plated to be 2,000/well of 6-well plates, on cover-slips, and allowed to grow for 30 days. After 30 days, cells were washed with 1x PBS, and were fixed with 3% formaldehyde for 5 min. After washed twice with 1X PBS, cells were incubated with SA-β-gal solution (Table 2.9) at 37°C for 18 hr, in dark. After the incubation, plates were washed twice with PBS and were fixed again, with ice cold MetOH for 5 min. Fixed cells were stained with nuclear fast red for 5 min, washed with ddH_2O and were mounted over glass slides.

2.3.33. Statistical Analyses

All statistical analyses were performed in GraphPad Prism 6.0 software, if not otherwise stated. Comparison of methylation levels in paired samples were analyzed with Wilcoxon signed rank test, whereas Mann-Whitney test was applied for the unpaired data. Comparison of data for qRT-PCR, 2D colony formation, Matrigel, *in vitro* wound healing, FACS and SA-β-Gal assays were performed with two tailed t-test. All correlation analyses were calculated by Spearman method. Gehan-Breslow-Wilcoxon test was applied for survival analyses.

Chapter 3. Results

3.1. Microarray experiments and bioinformatics analyses

3.1.1. Determination of the effective doses of AZA and TSA

To determine the most effective, yet non-toxic, doses of 5-aza-2'deoxycytidine (AZA) and Trichostatin A (TSA), MCF7, MDA-MB-231 and MCF12A cell lines were treated with different concentrations of AZA and/or with TSA. For AZA treatment 100nM, 250nM, 500nM, 750nM, 1μM, 3μM and 5μM concentrations were tested, while for TSA 25nM, 50nM, 75nM, 100nM and 400nM were used. Figure 3.1, Figure 3.2, and Figure 3.3 show the experiments carried out in MCF7, MDA-MB-231, and MCF12A cell lines, respectively.

Efficiency of the DNA methylation inhibitor AZA's dose was determined by semi-quantitative RT-PCR of the genes previously known to be hypermethylated in breast cancer (*DAPK1* or *CST6* and *SFRP1*), and the concentrations at which the highest induction in the genes' expression levels were observed were determined to be greater than 1μM (Figure 3.1A and Figure 3.2A). For concentration determination of TSA, a histone deacetylase inhibitor, Western blot analyses were done using antibodies specific to acetylated histone 3 lysine 9 residue (H3K9Ac) with the histone proteins extracted from MCF7 cells. The concentration at which the most increase was observed in acetylated H3K9 was determined to be 400nM (Figure 3.1B and Figure 3.2E and Figure 3.3D). To determine the most effective dose with the lowest impact on cell viability, MTT assays were performed in the cells treated with the selected doses (Figure 3.1D and Figure 3.2B and Figure 3.3). Since 5μM AZA restored the expression of *SFRP1* gene in both cell lines and of *DAPK1* in MCF7 cell line, and did not have very toxic effects on the cells' viabilities (Figure 3.1A and D, Figure 3.2A and B), it was chosen for the further experiments. Similarly, 400nM TSA concentration was chosen for further analyses (Figure 3.1E and Figure 3.2C). For the combination of the drugs, 5μM AZA was tested in combination with 50nM, 75nM, 100nM and 400nM TSA. Figure 3.1C and F show that 5μM AZA+400nM TSA (A+T) successfully restored the expression of *SFRP1* and *CST6* genes, and was not very toxic to the cells (Figure 3.1E). Thus, 5μM AZA, 400nM TSA and 5μM AZA+400nM TSA were selected to treat the cells for the microarray analyses.

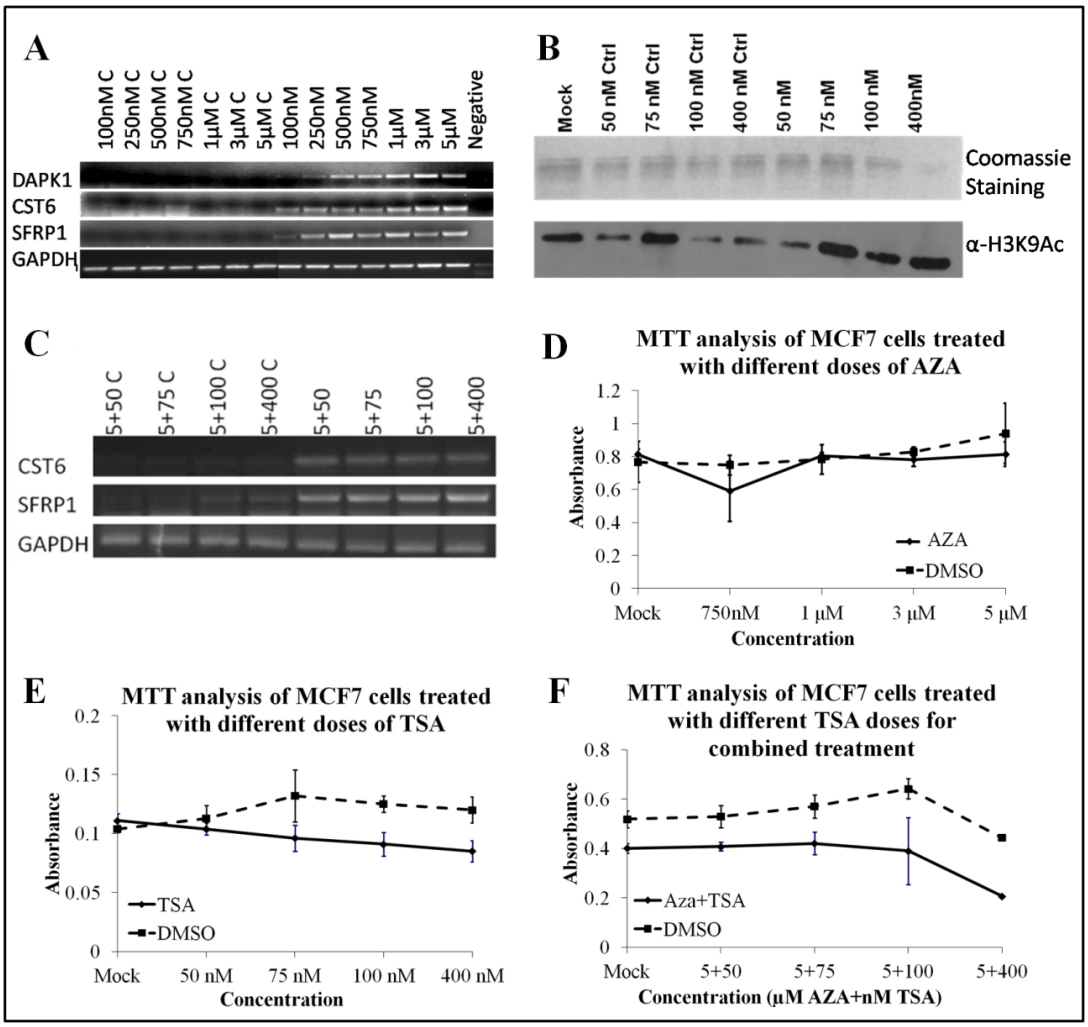

Figure 3.1: Determination of the effective doses of AZA and TSA in MCF7 cells.

(A) RT-PCR of DAPK1, CST6 and SFRP1 in MCF7 cells treated with different AZA concentrations. DMSO controls are indicated with "C" after the given doses. ***(B)*** *Western blot experiments carried out with H3K9Ac antibody after histone extraction from MCF7.* ***(C)*** *AZA+TSA trials by means of RT-PCR on the expression of CST6 and SFRP1 genes. 5+X indicates that 5µM AZA was used with given concentration (nM) of TSA. DMSO controls are indicated with C after the given doses.* ***(D-F)*** *MTT analyses of MCF7 cells treated with different concentrations of AZA (D); TSA (E); AZA+TSA (F).*

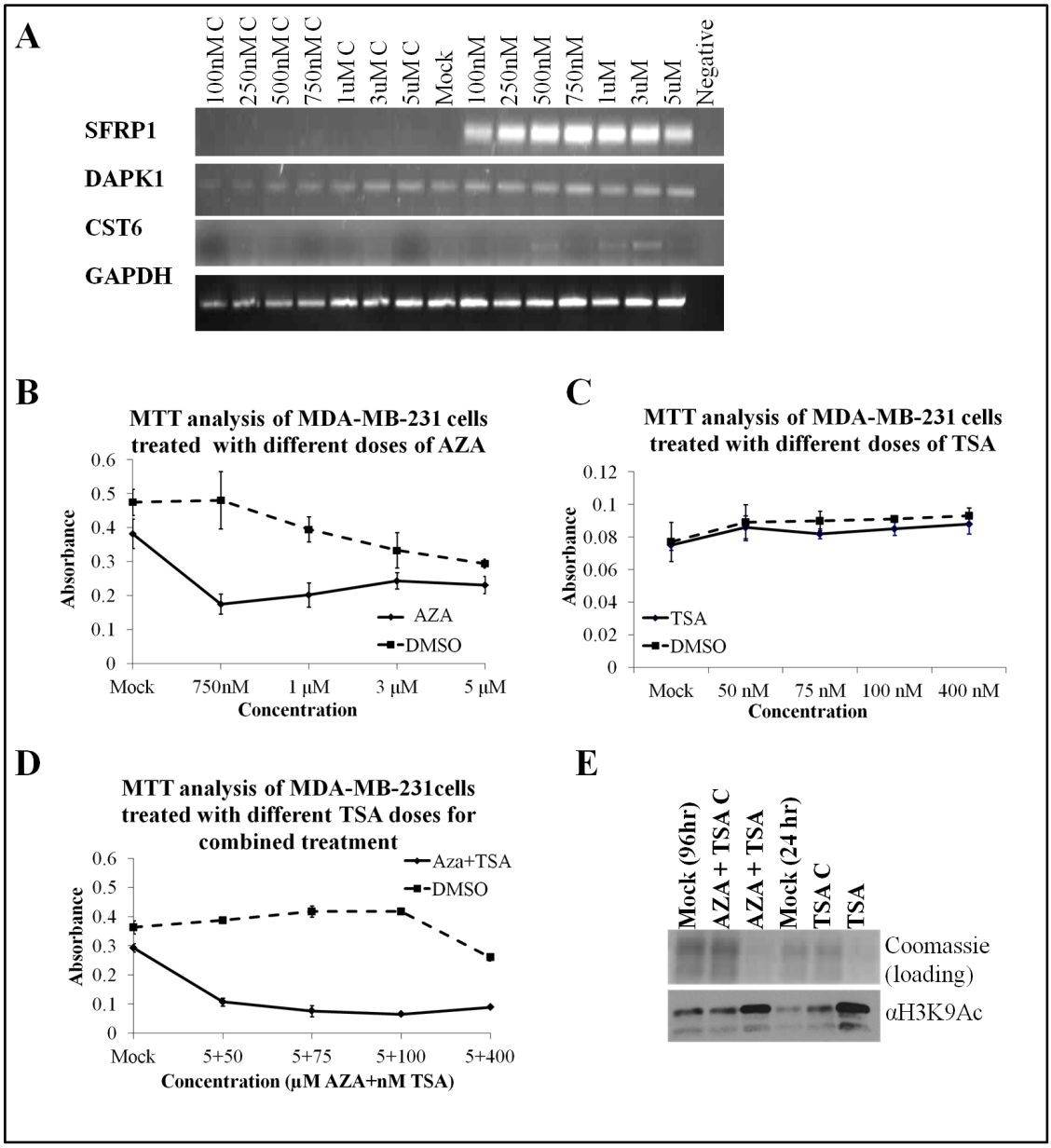

Figure 3.2: Determination of the effective doses of AZA and TSA in MDA-MB-231 cells.

(A) RT-PCR of SFRP1, DAPK1 and CST6 in MDA-MB-231 cells treated with different AZA and DMSO (with "C) concentrations. ***(B-D)*** *MTT analyses of MDA-MB-231 cells treated with different concentrations of AZA (B); TSA (C); and AZA+TSA (D).* ***(E)*** *Western blot experiments carried out with H3K9Ac antibody after histone extraction from 400nM TSA and/or 5µM AZA treated MDA-MB-231 cells and corresponding control cells.*

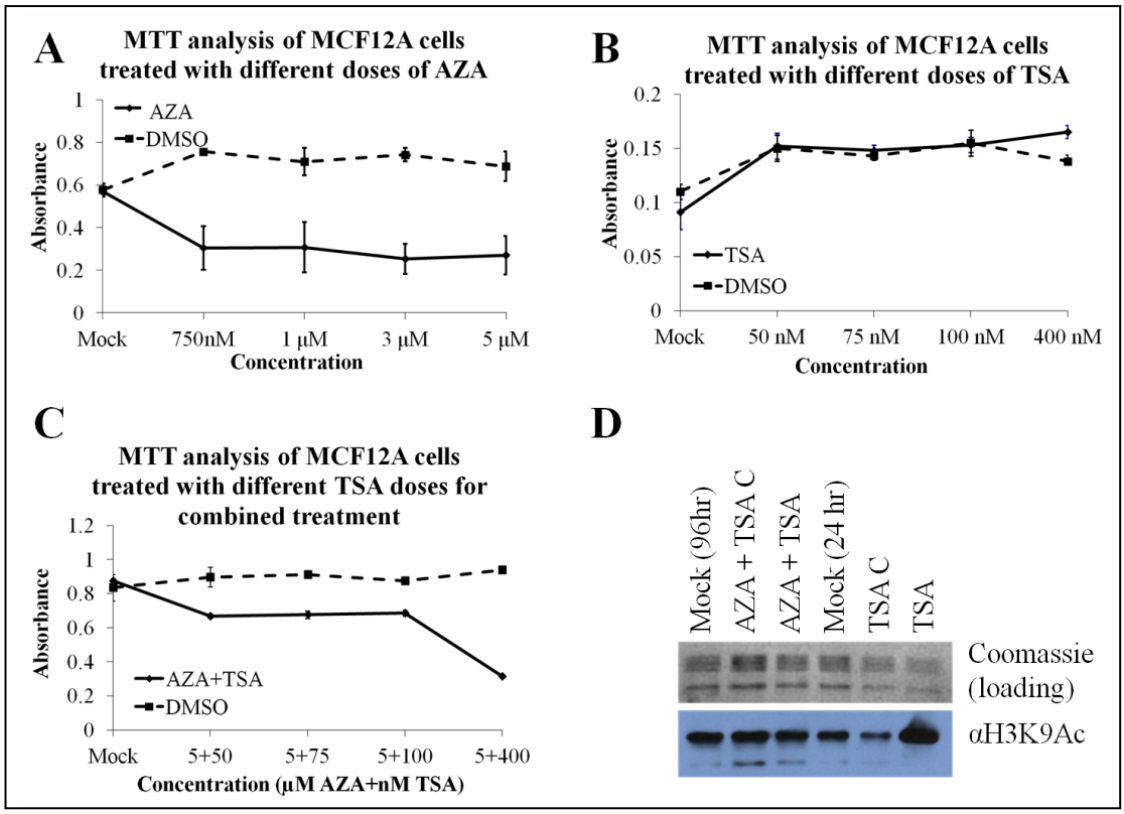

Figure 3.3: Determination of the effective doses of AZA and TSA in MCF12A cells.

(A-C) *MTT analysis of MCF12A cells treated with different concentrations of AZA (A); TSA (B) and AZA+TSA (C).* ***(D)*** *Western blot experiments carried out with H3K9Ac antibody after histone extraction from 400nM TSA and/or 5µM AZA treatedMCF12A cells.*

3.1.2. Validation of drug activity for the microarray experiment set up

After determination of the least toxic, but effective doses, MCF7, MDA-MB-231 breast cancer cells and non-tumorigenic (NT) mammary epithelial cell line MCF12A were treated with 5µM AZA, 400nM TSA or a combination of the two. After collection of RNA from each sample, and detection of integrity by Agilent 2100 Bioanalyzer (Table 3.1), affectivity of the treatments were validated by carrying out semi-quantitative RT-PCR of the genes whose expression is known to be repressed by DNA methylation in breast cancer, namely *SFRP1* and *DAPK1* genes. Figure 3.4A shows that the expressions of the genes, which are normally under-expressed in MCF7 or MDA-MB-231 cell lines were induced after the cells were treated with AZA, or with AZA+TSA, suggesting that the AZA treatments were successful. TSA treatments were validated with western blot analyses with anti-H3K9Ac antibody, and an increase in acetylation level was observed after TSA treatment of cell lines (Figure 3.4)

Table 3.1: RIN values of RNAs used in microarray analysis

Treatment	MCF7 RINs	MDA-MB-231 RINs	MCF12A RINs
Mock R1	10	10	10
Mock R2	9.9	9.9	10
AZA C R1	10	10	10
AZA C R2	10	9.8	10
AZA R1	9.8	10	10
AZA R2	9.9	10	10
TSA C R1	9.8	10	10
TSA C R2	10	10	10
TSA R1	8.8	9.8	10
TSA R2	8.8	10	9.9
A+T C R1	9.7	10	10
A+T C R2	9.1	10	9.8
A+T R1	9.2	10	9.3
A+T R2	9	10	10

A+T, AZA+TSA; R, replicate; C, DMSO treatment; R: replicate

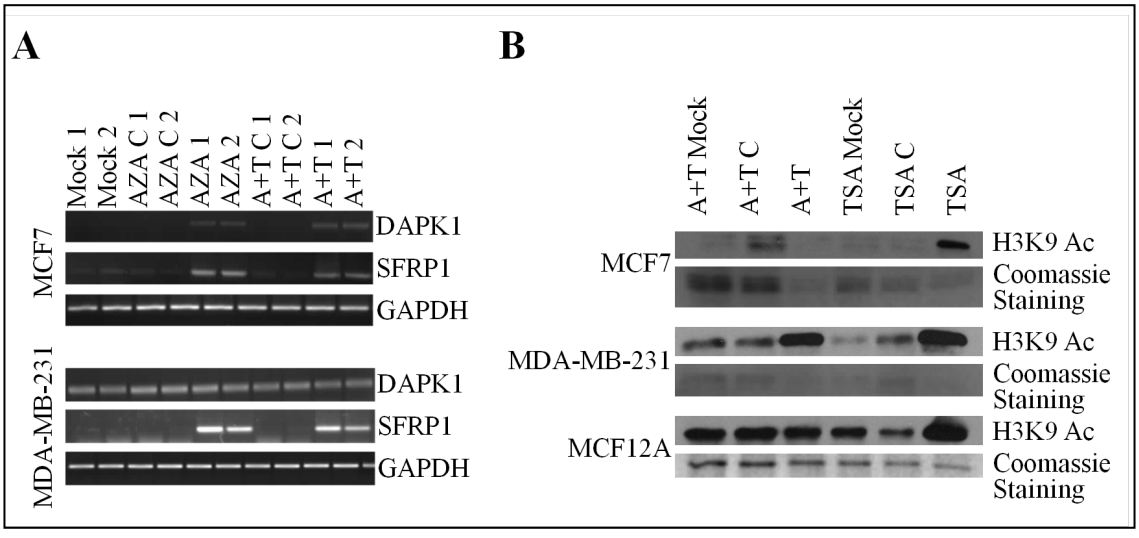

Figure 3.4: Validation of effectiveness of AZA and TSA treatments before the microarray experiment.

(A) *cDNA was prepared from RNA samples which were used for microarray hybridization and RT-PCR was carried out to analyze expression of genes which are normally not expressed in MCF7 and/or MDA-MB-231 cell lines. 1 and 2 designate the replicate numbers for the microarray experiment. DMSO controls are indicated with "C" after the treatment name.* ***(B)****Western blot experiments showing increase in H3K9 acetylation levels upon TSA and A+T treatments. Coomassie staining images were used as loading controls.*

3.1.3. Normalization and quality control of the microarray data

After processing the RNAs for hybridization to the microarrays, expression profiling was performed as described in Materials and Methods section. Data was RMA normalized using BRB-ArrayTools for further analyses. Quality control analyses performed both in R and BRB-ArrayTools revealed that the data were of high quality, the distributions of the normalized data were comparable and within the same range (Figure 3.5A). RNA degradation plots showed that the processed RNAs were intact and their degradation plots were parallel as expected (Figure 3.5B). Moreover, the replicates of the data of each experiment correlated well with each other, with Pearson correlation coefficients ranging from 0.74 to 0.94 (Table 3.2).

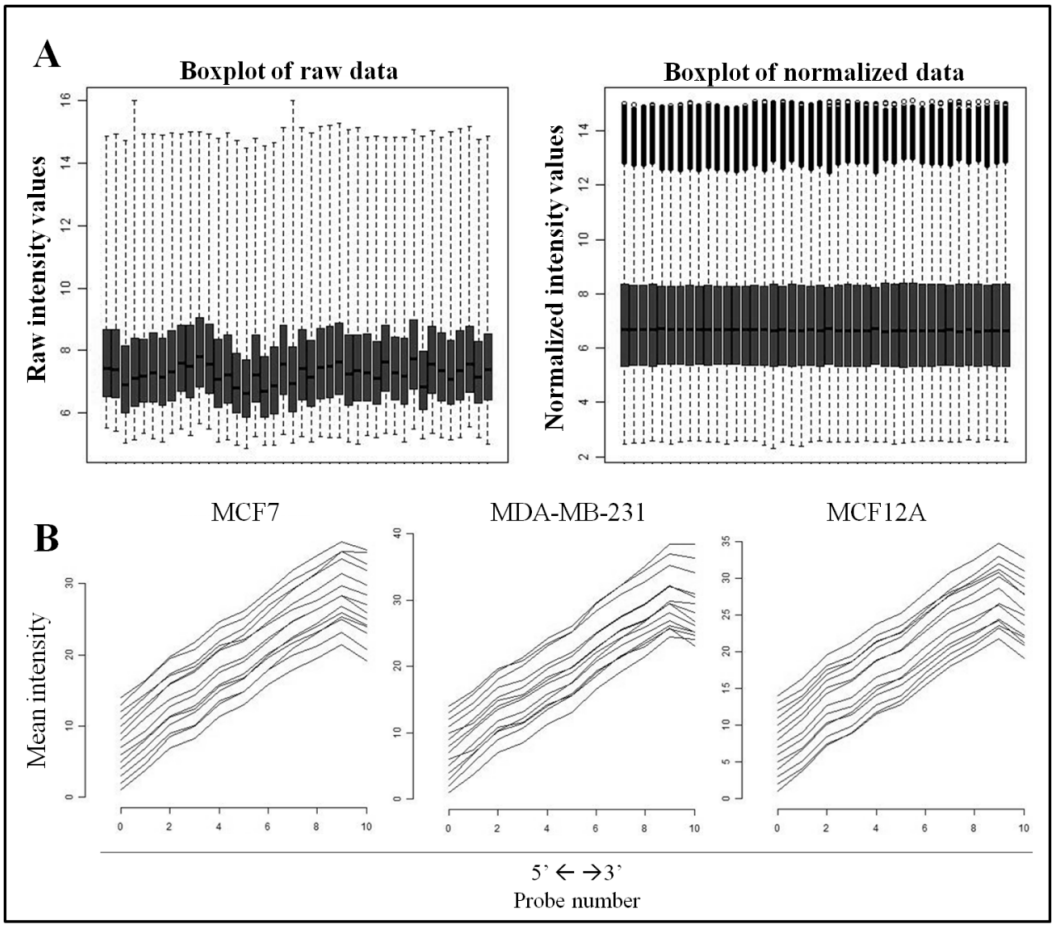

Figure 3.5: Quality control analyses of the microarray data using R.

(A) Box-plot analyses show that the distributions of the intensity values were comparable after the data were normalized by RMA method. (B) RNA degradation plots of MCF7, MDA-MB-231 and MCF12A microarray experiments.

Table 3.2: Correlation of data between replicates

Experiment	Pearson correlation coefficient
MCF7 AZA	0.82496
MCF7 TSA	0.916479
MCF7 A+T	0.937229
MCF12A AZA	0.740181
MCF12A TSA	0.769144
MCF12A A+T	0.892495
231 AZA	0.836972
231 TSA	0.890318
231 A+T	0.942615

3.1.4. Transcriptional changes in the treated breast cell lines

The probe sets which were significantly ($P < 0.05$) changed by at least 1.5 fold upon AZA and/or TSA treatments were determined using BRB-ArrayTools' class comparison function (Table 3.3). Upon all the treatments, the least number of probe sets affected was in the MCF12A cell line. The highest numbers of genes were altered upon treatment with TSA or AZA+TSA (A+T) in each cell line. To obtain breast carcinoma specific alterations, probe sets which were also altered in the same direction by the same drug in MCF12A cells were subtracted from lists of MCF7 and MDA-MB-231 (Figure 3.6). Probe sets commonly altered in both of the breast carcinoma cell lines were also determined. Lowest numbers of common probe sets were observed upon AZA treatment, while the percentages increased with TSA and A+T treatments.

Table 3.3: Numbers of probe sets altered upon treatments in each cell line

Treatment	Alteration[a]	Number of probe sets in:		
		MCF7	MDA-MB-231	MCF12A
AZA	UP	4011	4285	3006
	DOWN	4672	3717	2406
TSA	UP	5803	5908	2221
	DOWN	6948	4851	1545
A+T	UP	7002	3995	2279
	DOWN	8749	3678	1744

[a] *Up/downregulated at P < 0.05(t-test) and 1.5x threshold*

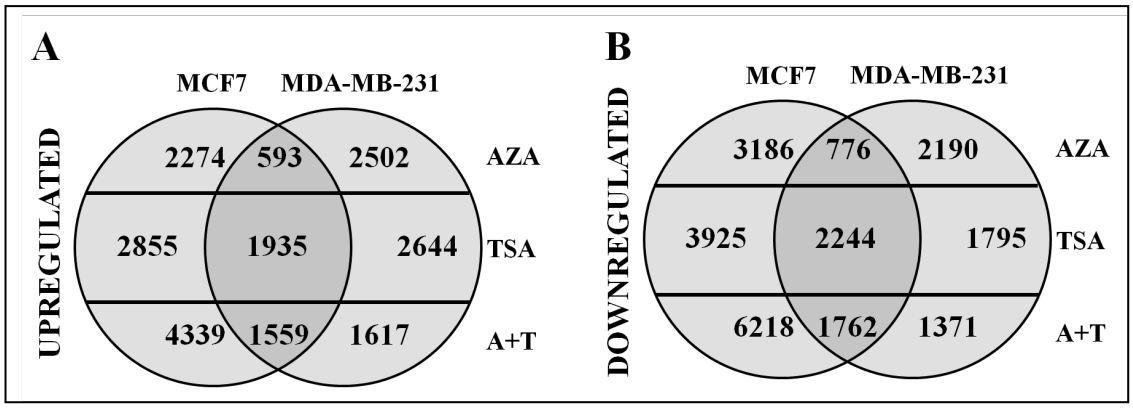

Figure 3.6: Breast carcinoma cell line specific alterations upon drug treatments.

Numbers of probe sets upregulated (A) and downregulated (B) in MCF7 and/or MDA-MB-231 cell lines upon indicated drug treatments (>1.5 fold, P < 0.05). Those commonly upregulated (A) or downregulated (B) in MCF12A (>1.5 fold, P < 0.05) have been subtracted from the list to obtain breast carcinoma specific alterations. T-test was used for comparisons. Please see Appendix A – Gene lists for top 50 probe-sets from each intersection subset.

3.1.5. Functional analysis of genes altered by AZA and/or TSA treatments in breast carcinoma cell lines

DAVID Bioinformatics Resources 6.7, functional annotation tool was used to find out pathways altered upon drug treatments using the gene lists commonly altered in MCF7 and MDA-MB-231 breast cancer cell lines, but not in MCF12A (*i.e.* the gene lists corresponding to the intersections in Figure 3.6A and B). Using the Hgu-133 Plus 2.0 array as background, and the numbers of genes in the given lists, DAVID Functional Annotation Clustering Tool calculates enrichment scores for similar pathways, and the *P* values corresponding to significance of each pathway in the given gene lists. Higher enrichment scores with lower significance values for the included pathways represent the clusters important for the analyses. Thus, top 5 pathway clusters were determined for each drug treatment, in upregulated and downregulated probe-set lists. AZA treatment resulted in upregulation of pathways related to apoptosis, responses to bacterial or extracellular stimuli, and regulation of cell motility (Figure 3.7A). Figure 3.8A shows the pathways upregulated by TSA treatment; and determination of cell symmetry, vasculature, and regulation of apoptosis and migration pathways were top enriched pathways. A+T treatment resulted in induction of pathways involved in regulation of apoptosis, and gene expression and sexual reproduction (Figure 3.9A).

Upon each treatment (Figure 3.7B and Figure 3.8B and Figure 3.9B), the downregulated pathways were mainly enriched in cell cycle and mRNA processing related pathways, indicating negative effect of these drugs on cellular proliferation and metabolism, which could be related to modulation of expression of TSGs.

A

Annotation Cluster 1	Enrichment Score: 4.04	Count	P_Value	Benjamini
GOTERM_BP_FAT	regulation of programmed cell death	40	7.3E-5	3.0E-2
GOTERM_BP_FAT	regulation of cell death	40	8.0E-5	2.7E-2
GOTERM_BP_FAT	regulation of apoptosis	39	1.3E-4	3.2E-2
Annotation Cluster 2	**Enrichment Score: 3.68**	**Count**	**P_Value**	**Benjamini**
GOTERM_BP_FAT	response to lipopolysaccharide	11	2.4E-5	1.7E-2
GOTERM_BP_FAT	response to molecule of bacterial origin	11	6.4E-5	3.3E-2
GOTERM_BP_FAT	response to bacterium	12	5.9E-3	3.3E-1
Annotation Cluster 3	**Enrichment Score: 3.57**	**Count**	**P_Value**	**Benjamini**
GOTERM_BP_FAT	regulation of locomotion	16	1.2E-4	3.5E-2
GOTERM_BP_FAT	regulation of cell migration	14	3.9E-4	6.0E-2
GOTERM_BP_FAT	regulation of cell motion	15	4.3E-4	6.2E-2
Annotation Cluster 4	**Enrichment Score: 2.95**	**Count**	**P_Value**	**Benjamini**
GOTERM_BP_FAT	positive regulation of cell motion	10	8.7E-4	1.1E-1
GOTERM_BP_FAT	positive regulation of locomotion	10	8.7E-4	1.1E-1
GOTERM_BP_FAT	positive regulation of cell migration	9	1.9E-3	1.7E-1
Annotation Cluster 5	**Enrichment Score: 2.59**	**Count**	**P_Value**	**Benjamini**
GOTERM_BP_FAT	response to nutrient levels	14	1.5E-3	1.5E-1
GOTERM_BP_FAT	response to nutrient	11	2.9E-3	2.0E-1
GOTERM_BP_FAT	response to extracellular stimulus	14	3.9E-3	2.5E-1

B

Annotation Cluster 1	Enrichment Score: 20.87	Count	P_Value	Benjamini
GOTERM_BP_FAT	cell cycle phase	62	3.2E-23	6.9E-20
GOTERM_BP_FAT	M phase of mitotic cell cycle	45	5.6E-22	3.9E-19
GOTERM_BP_FAT	mitotic cell cycle	57	6.1E-22	3.3E-19
GOTERM_BP_FAT	nuclear division	44	2.0E-21	8.7E-19
GOTERM_BP_FAT	mitosis	44	2.0E-21	8.7E-19
Annotation Cluster 2	**Enrichment Score: 7.33**	**Count**	**P_Value**	**Benjamini**
GOTERM_MF_FAT	nucleotide binding	123	1.3E-10	8.7E-8
GOTERM_MF_FAT	ATP binding	87	7.5E-9	2.4E-6
GOTERM_MF_FAT	adenyl ribonucleotide binding	87	1.4E-8	2.3E-6
GOTERM_MF_FAT	nucleoside binding	90	4.9E-8	6.3E-6
Annotation Cluster 3	**Enrichment Score: 7.01**	**Count**	**P_Value**	**Benjamini**
GOTERM_BP_FAT	mRNA metabolic process	36	2.8E-8	4.6E-6
GOTERM_BP_FAT	mRNA processing	33	3.3E-8	5.1E-6
GOTERM_BP_FAT	RNA splicing	28	1.0E-6	1.4E-4
Annotation Cluster 4	**Enrichment Score: 3.84**	**Count**	**P_Value**	**Benjamini**
GOTERM_MF_FAT	microtubule motor activity	13	4.6E-6	3.0E-4
GOTERM_BP_FAT	microtubule-based movement	13	3.9E-4	2.2E-2
GOTERM_MF_FAT	motor activity	13	1.7E-3	7.2E-2
Annotation Cluster 5	**Enrichment Score: 3.21**	**Count**	**P_Value**	**Benjamini**
GOTERM_BP_FAT	RNA splicing, via transesterification reactions with bulged adenosine as nucleophile	15	6.1E-4	3.1E-2
GOTERM_BP_FAT	RNA splicing, via transesterification reactions	15	6.1E-4	3.1E-2
GOTERM_BP_FAT	nuclear mRNA splicing, via spliceosome	15	6.1E-4	3.1E-2

Figure 3.7: Pathways significantly enriched by AZA treatment of breast carcinoma cells.

Top 5 clusters of pathways commonly and significantly (A) upregulated and (B) downregulated, upon AZA treatment in MCF7 and MDA-MB-231 cells, by 1.5 fold, $P < 0.05$.

A

Annotation Cluster 1	Enrichment Score: 2.7	Count	P_Value	Benjamini
GOTERM_BP_FAT	determination of left/right symmetry	10	1.8E-3	3.9E-1
GOTERM_BP_FAT	determination of symmetry	10	2.1E-3	3.7E-1
GOTERM_BP_FAT	determination of bilateral symmetry	10	2.1E-3	3.7E-1
Annotation Cluster 2	**Enrichment Score: 2.19**	**Count**	**P_Value**	**Benjamini**
GOTERM_BP_FAT	vasculature development	31	2.9E-3	3.7E-1
GOTERM_BP_FAT	blood vessel development	30	3.9E-3	4.2E-1
GOTERM_BP_FAT	blood vessel morphogenesis	24	2.4E-2	6.5E-1
Annotation Cluster 3	**Enrichment Score: 2.18**	**Count**	**P_Value**	**Benjamini**
GOTERM_BP_FAT	regulation of programmed cell death	76	5.5E-3	4.8E-1
GOTERM_BP_FAT	regulation of cell death	76	6.0E-3	4.7E-1
GOTERM_BP_FAT	regulation of apoptosis	74	8.8E-3	5.2E-1
Annotation Cluster 4	**Enrichment Score: 2.01**	**Count**	**P_Value**	**Benjamini**
GOTERM_BP_FAT	regulation of cell migration	22	7.2E-3	5.2E-1
GOTERM_BP_FAT	regulation of cell motion	24	8.4E-3	5.3E-1
GOTERM_BP_FAT	regulation of locomotion	23	1.5E-2	5.7E-1
Annotation Cluster 5	**Enrichment Score: 1.78**	**Count**	**P_Value**	**Benjamini**
GOTERM_BP_FAT	negative regulation of programmed cell death	37	1.5E-2	5.8E-1
GOTERM_BP_FAT	negative regulation of cell death	37	1.6E-2	5.7E-1
GOTERM_BP_FAT	negative regulation of apoptosis	36	2.0E-2	6.0E-1

B

Annotation Cluster 1	Enrichment Score: 26.7	Count	P_Value	Benjamini
GOTERM_BP_FAT	cell cycle phase	109	2.8E-28	2.8E-25
GOTERM_BP_FAT	mitotic cell cycle	101	1.7E-27	1.3E-24
GOTERM_BP_FAT	cell cycle process	128	1.7E-26	1.0E-23
Annotation Cluster 2	**Enrichment Score: 23.03**	**Count**	**P_Value**	**Benjamini**
GOTERM_BP_FAT	M phase	92	4.9E-26	2.4E-23
GOTERM_BP_FAT	M phase of mitotic cell cycle	71	1.9E-23	8.2E-21
GOTERM_BP_FAT	nuclear division	70	3.1E-23	1.2E-20
GOTERM_BP_FAT	mitosis	70	3.1E-23	1.2E-20
GOTERM_BP_FAT	organelle fission	71	8.1E-23	2.7E-20
Annotation Cluster 3	**Enrichment Score: 20.65**	**Count**	**P_Value**	**Benjamini**
GOTERM_BP_FAT	RNA splicing	79	2.6E-22	7.7E-20
GOTERM_BP_FAT	mRNA metabolic process	92	5.8E-22	1.6E-19
GOTERM_BP_FAT	mRNA processing	81	7.5E-20	1.9E-17
Annotation Cluster 4	**Enrichment Score: 15.65**	**Count**	**P_Value**	**Benjamini**
GOTERM_BP_FAT	nuclear mRNA splicing, via spliceosome	49	2.2E-16	5.1E-14
GOTERM_BP_FAT	RNA splicing, via transesterification reactions with bulged adenosine as nucleophile	49	2.2E-16	5.1E-14
GOTERM_BP_FAT	RNA splicing, via transesterification reactions	49	2.2E-16	5.1E-14
Annotation Cluster 5	**Enrichment Score: 10.96**	**Count**	**P_Value**	**Benjamini**
GOTERM_BP_FAT	RNA transport	33	3.0E-12	5.1E-10
GOTERM_BP_FAT	nucleic acid transport	33	3.0E-12	5.1E-10
GOTERM_BP_FAT	establishment of RNA localization	33	3.0E-12	5.1E-10
GOTERM_BP_FAT	RNA localization	33	7.9E-12	1.2E-9
GOTERM_BP_FAT	nucleobase, nucleoside, nucleotide and nucleic acid transport	34	6.5E-11	9.3E-9
GOTERM_BP_FAT	mRNA transport	29	1.3E-10	1.7E-8

Figure 3.8: Pathways significantly enriched by TSA treatment of breast carcinoma cells.

Top 5 clusters of pathways commonly and significantly (A) upregulated and (B) downregulated, upon TSA treatment in MCF7 and MDA-MB-231 cells, by 1.5 fold, $P < 0.05$.

A

Annotation Cluster 1	Enrichment Score: 3.28	Count	P_Value	Benjamini
GOTERM_BP_FAT	regulation of programmed cell death	82	4.8E-4	1.2E-1
GOTERM_BP_FAT	regulation of cell death	82	5.4E-4	1.1E-1
GOTERM_BP_FAT	regulation of apoptosis	81	5.5E-4	1.1E-1
Annotation Cluster 2	**Enrichment Score: 2.67**	**Count**	**P_Value**	**Benjamini**
GOTERM_BP_FAT	negative regulation of programmed cell death	41	1.9E-3	1.9E-1
GOTERM_BP_FAT	negative regulation of cell death	41	2.0E-3	1.9E-1
GOTERM_BP_FAT	negative regulation of apoptosis	40	2.6E-3	1.9E-1
Annotation Cluster 3	**Enrichment Score: 2.6**	**Count**	**P_Value**	**Benjamini**
GOTERM_BP_FAT	positive regulation of nitrogen compound metabolic process	68	4.3E-4	1.2E-1
GOTERM_BP_FAT	positive regulation of nucleobase, nucleoside, nucleotide and nucleic acid metabolic process	66	4.9E-4	1.1E-1
GOTERM_BP_FAT	positive regulation of gene expression	61	9.7E-4	1.4E-1
GOTERM_BP_FAT	positive regulation of transcription	59	1.3E-3	1.6E-1
Annotation Cluster 4	**Enrichment Score: 2.51**	**Count**	**P_Value**	**Benjamini**
GOTERM_BP_FAT	sexual reproduction	48	2.5E-3	1.9E-1
GOTERM_BP_FAT	reproductive process in a multicellular organism	50	3.2E-3	2.0E-1
GOTERM_BP_FAT	multicellular organism reproduction	50	3.2E-3	2.0E-1
GOTERM_BP_FAT	gamete generation	42	3.7E-3	2.2E-1
Annotation Cluster 5	**Enrichment Score: 2.47**	**Count**	**P_Value**	**Benjamini**
GOTERM_BP_FAT	regulation of transcription factor activity	18	7.7E-4	1.4E-1
GOTERM_BP_FAT	regulation of DNA binding	18	4.6E-3	2.4E-1
GOTERM_BP_FAT	regulation of binding	20	1.1E-2	3.8E-1

B

Annotation Cluster 1	Enrichment Score: 16.82	Count	P_Value	Benjamini
GOTERM_BP_FAT	RNA splicing	66	7.9E-18	1.1E-14
GOTERM_BP_FAT	mRNA processing	71	8.9E-18	8.3E-15
GOTERM_BP_FAT	mRNA metabolic process	76	4.8E-17	3.4E-14
Annotation Cluster 2	**Enrichment Score: 11.04**	**Count**	**P_Value**	**Benjamini**
GOTERM_BP_FAT	nuclear mRNA splicing, via spliceosome	39	9.0E-12	3.6E-9
GOTERM_BP_FAT	RNA splicing, via transesterification reactions	39	9.0E-12	3.6E-9
GOTERM_BP_FAT	RNA splicing, via transesterification reactions with bulged adenosine as nucleophile	39	9.0E-12	3.6E-9
Annotation Cluster 3	**Enrichment Score: 10.4**	**Count**	**P_Value**	**Benjamini**
GOTERM_BP_FAT	mitotic cell cycle	68	9.5E-13	4.4E-10
GOTERM_BP_FAT	cell cycle process	84	1.6E-10	5.4E-8
GOTERM_BP_FAT	cell cycle phase	67	4.3E-10	1.3E-7
Annotation Cluster 4	**Enrichment Score: 7.46**	**Count**	**P_Value**	**Benjamini**
GOTERM_BP_FAT	organelle fission	43	1.3E-8	3.1E-6
GOTERM_BP_FAT	M phase	54	1.5E-8	3.2E-6
GOTERM_BP_FAT	M phase of mitotic cell cycle	42	2.1E-8	3.8E-6
GOTERM_BP_FAT	nuclear division	40	1.1E-7	1.9E-5
GOTERM_BP_FAT	mitosis	40	1.1E-7	1.9E-5
Annotation Cluster 5	**Enrichment Score: 4.65**	**Count**	**P_Value**	**Benjamini**
GOTERM_BP_FAT	modification-dependent macromolecule catabolic process	72	1.9E-6	2.7E-4
GOTERM_BP_FAT	modification-dependent protein catabolic process	72	1.9E-6	2.7E-4
GOTERM_BP_FAT	proteolysis involved in cellular protein catabolic process	73	4.9E-6	5.7E-4
GOTERM_BP_FAT	cellular protein catabolic process	73	5.9E-6	6.6E-4

Figure 3.9: Pathways significantly enriched by A+T treatment of breast carcinoma cells.

Top 5 clusters of pathways commonly and significantly (A) upregulated and (B) downregulated, upon AZA+TSA treatment in MCF7 and MDA-MB-231 cells, by 1.5 fold, $P < 0.05$.

3.1.6. Analysis of gene lists and determination of candidate genes

After the generation of gene lists which are upregulated in response to different treatments and functional analyses of these gene lists, there were still more than 1000 genes to select for candidates among for verification with quantitative real time PCR and bisulfite sequencing. The following criteria were used to narrow down the lists:

(1) The gene should be upregulated upon any treatment in MDA-MB-231 and MCF7 cells, but should not be upregulated in MCF12A cells, at $P < 0.001$.

(2) The function of the gene should be related to a tumor suppressor activity and/or downregulation of the gene should be indicated in some cancer types.

(3) There should not be any available and extended data about tumor specific methylation of the gene in breast cancer.

(4) The gene sequence should have at least one CpG island at the interval region -2000 to +2000 according to the transcription start site.

According to the first 3 criteria, there were 52 genes with functions in diverse biological pathways, and methylation and expression data of some had been previously revealed in other types of tumors (Table 3.4). 6 of these genes (*CDKN1A*[378], *ITGA9*[379], *CLDN6*[380], *TNFRSF10C*[381], *PER1*, and *LAMA3*[382] and *WIF-1*[383]) had already been shown to be methylated in breast cancer.

Table 3.4: Expression ratios of selected candidate genes in each cell line and treatment

Gene symbol	Probe set	Accession Number	MDA-MB-231			MCF7		
			AT*	AZA*	TSA*	AT*	AZA*	TSA*
ABCA1	203504_s_at	NM_005502	0.61	0.52	1.7	5.39	8.39	1.61
ABCA1	203505_at	AF285167	0.58	0.5	1.52	6.13	9.76	1.11
ABCA1	1570279_at	BC034824	0.76	0.6	1.02	0.9	1.24	0.93
ABCA1	216066_at	AK024328	0.91	0.87	1.28	1.01	0.93	1.12
ACVR1C	1552519_at	NM_145259	3.53	1.65	2.39	3.31	2.57	1.86
ACVR1C	1563182_at	BC030101	2.04	1.02	1.45	1.66	1.97	1.24
ADAMTSL4	226071_at	NM_019032	1.88	1.56	3.70	2.41	3.70	0.76
AKR1C1	204151_x_at	NM_001353	1.42	1.01	2.19	2.08	2.38	1.69
AKR1C1	216594_x_at	S68290	1.18	1.02	1.91	1.69	2.34	1.95
AKR1C1	1562102_at	BC014579	1.2	1.05	0.93	0.96	0.93	1.28

Table 3.4: Expression ratios of selected candidate genes in each cell line and treatment

Gene symbol	Probe set	Accession Number	MDA-MB-231			MCF7		
			AT*	AZA*	TSA*	AT*	AZA*	TSA*
AKR1C2	209699_x_at	U05598	1.4	0.97	2.2	2.33	2.47	1.66
AKR1C2	211653_x_at	M33376	1.02	0.76	2.24	1.66	2.74	1.78
AKR1C2	217626_at	BF508244	0.91	0.92	1.03	1.34	1.04	1.52
AKR1C2	1560098_at	CA425039	0.89	0.94	1.33	0.98	0.93	1.02
AXIN2	222696_at	BF684446	3.22	1.2	1.82	5.48	2.81	1.61
AXIN2	224176_s_at	AF205888	2.24	1.06	1.1	2.04	1.75	1.05
AXIN2	224498_x_at	BC006295	1.25	1.06	1.03	1.48	1.11	1.14
AXIN2	222695_s_at	AI818109	1.19	0.98	1.02	1.09	1.12	1.3
BEX4	215440_s_at	AL523320	24.49	10.14	0.93	5.9	8.21	4.29
BMP2	205289_at	AA583044	5.43	3.06	2.31	6.37	1.8	1.22
BMP2	205290_s_at	NM_001200	5.42	2.36	1.78	3.11	1.44	0.98
BTG1	200921_s_at	NM_001731	4.32	2.81	2.18	2.29	1.3	2.76
BTG1	200920_s_at	AL535380	4.65	2.9	2.38	2.32	1.49	2.68
BTG1	1559975_at	BC009050	1.1	0.86	1.07	1.76	1.11	1.35
CASP9	203984_s_at	NM_001229	2.88	1.54	1.55	3.33	2.03	2.11
CAST	212586_at	AA195244	0.66	0.66	1.72	1.06	1.3	1.23
CAST	207467_x_at	NM_001750	1.36	0.86	1.59	2.19	2.16	1.76
CAST	1564010_at	AK026822	1.14	1.61	1.78	1.56	1.21	1.14
CAST	212580_at	BG111635	0.53	0.65	1.82	0.94	1.07	1.02
CDC14B	221556_at	BF792631	1.36	0.78	1.55	5.34	2.21	2.32
CDC14B	208022_s_at	NM_003671	1.38	0.88	1.82	3.59	1.62	2.66
CDC14B	234605_at	AK024886	2.47	1.83	3.21	4.89	2.06	4.36
CDC14B	230887_at	AI921238	2.22	1.19	1.49	1.61	0.97	1.32
CDC14B	221555_x_at	AU145941	1.38	0.92	1.56	2.09	1.69	1.99
CDC14B	211347_at	AF064105	1.08	0.78	2.05	1.4	1.05	1.71
CDC14B	211348_s_at	AF064105	1.15	0.95	1.67	1.41	1.19	1.58
CDC14B	234740_at	AK024886	0.77	0.98	0.93	0.91	1.1	1
CDKN1A	1555186_at	AY008263	0.97	1	0.9	1.12	1.01	1.11
CGREF1	205937_at	NM_006569	3.19	0.96	2.56	10.19	0.81	6.79
CLDN6	237810_at	AW003929	2.86	1.38	0.94	11.91	12.26	1.21
CLDN6	208474_at	NM_021195	1.42	1.17	1.01	2.47	3.24	1.21

Table 3.4: Expression ratios of selected candidate genes in each cell line and treatment

Gene symbol	Probe set	Accession Number	MDA-MB-231			MCF7		
			AT*	AZA*	TSA*	AT*	AZA*	TSA*
COL4A6	210945_at	BC005305	6.49	3.07	1.8	1.46	1.79	1.21
COL4A6	213992_at	AI889941	5.32	8.71	2.38	2.33	5.63	1.14
COL4A6	211473_s_at	U04845	1.6	1.66	1.25	1.12	1.49	1
CXCL14	218002_s_at	NM_004887	4.28	1.31	2.15	3.97	2.43	0.91
CXCL14	222484_s_at	AF144103	3.2	1.13	2.22	3.51	1.82	1.31
CXCL14	237038_at	AI927990	1.02	0.96	1.01	0.86	1.05	1.11
DDIT3	209383_at	NT_029419	5.71	3.20	1.03	7.21	2.02	3.70
DST	204455_at	NT_007592.	3.82	3.93	1.39	7.28	2.57	1.20
DUSP5	209457_at	U16996	2.93	1.59	2.54	8.94	4.89	3.92
EGR2	205249_at	NM_000399	34.73	6.70	3.09	1.86	2.34	9.34
EPB41L2	201718_s_at	BF511685	1.21	0.92	1.75	8.37	2.58	4.73
EPB41L2	201719_s_at	NM_001431	0.81	0.72	1.49	6.81	2.24	4.93
EPB41L2	242092_at	AA019300	0.85	1.03	1.04	1.09	0.91	0.98
F11R	221664_s_at	AF154005	3.12	2.52	3.44	2.52	1.74	2.76
F11R	223000_s_at	AF172398	3.33	2.31	4.81	1.7	1.53	2.15
F11R	224097_s_at	AF191495	2.4	1.84	2.7	3.29	2.14	2.62
F11R	226482_s_at	AI814545	2.65	1.43	3.01	0.97	1.08	1.03
F11R	222354_at	AW675655	1.99	1.7	2.25	1.75	1.51	1.69
FOXO1	202723_s_at	NM_002015	1.98	1.60	1.59	2.09	1.27	1.89
FOXO1	202724_s_at	NM_002015	4.17	1.72	7.08	4.01	1.45	3.45
GPX1	200736_s_at	NM_000581	0.78	0.79	0.69	25.66	37.38	1.2
GSTM1	204550_x_at	NM_000561	1.29	1.14	1.93	1.19	2.24	1.03
GSTM1	215333_x_at	X08020	1.29	1.1	1.91	1.17	2.45	1.09
GSTM2	204418_x_at	NM_000848	1.46	1.07	2.36	1.38	2.59	1.05
HLA-A	213932_x_at	AI923492	1.31	1.39	1.28	2.42	2.31	1.73
HLA-A	215313_x_at	AA573862	1.31	1.49	1.3	3.29	2.92	2.19
HLA-A	217436_x_at	M80469	1.21	1.42	1.36	1.61	1.62	1.68
HLA-B	208729_x_at	D83043	1.42	1.53	1.46	3.1	3.03	1.75
HLA-B	209140_x_at	L42024	1.44	1.59	1.36	3.69	3.89	2.47
HLA-B	211911_x_at	L07950	1.43	1.61	1.44	3.55	3.73	2.00
HMOX1	203665_at	NM_002133	1.65	1.32	1.65	21.31	3.78	19.42

Table 3.4: Expression ratios of selected candidate genes in each cell line and treatment

Gene symbol	Probe set	Accession Number	MDA-MB-231			MCF7		
			AT*	AZA*	TSA*	AT*	AZA*	TSA*
IFNGR1	202727_s_at	NM_000416	2.10	1.30	1.55	1.87	2.12	1.63
IFNGR1	211676_s_at	AF056979	2.17	1.16	1.53	2.03	2.52	1.80
IFNGR1	242903_at	AI458949	2.05	2.03	2.35	0.52	1.11	1.78
IL24	206569_at	NM_006850	15.94	14.15	6.67	0.14	0.12	0.15
IQGAP2	203474_at	NM_006633	6.07	2.72	4.72	5.09	2.00	2.38
IQGAP2	241723_at	AA679303	1.08	1.07	1.00	0.98	0.96	1.24
ITGA5	201389_at	NM_002205	0.98	0.88	0.85	3.09	2.45	1.14
ITGA9	227297_at	AI479176	0.96	0.98	1.23	1.66	2.2	1.14
ITGA9	206009_at	NM_002207	0.86	1.05	0.93	1.08	1.12	1.01
ITGA9	1555336_a_at	BC030198	1.05	0.86	1.00	0.92	1.04	1.26
ITGA9	1555335_at	BC030198	0.92	0.81	0.93	1.08	1.02	0.87
LAMA3	203726_s_at	NM_000227	2.86	0.83	0.93	18.39	2.91	1.18
LAMA3	234608_at	AK024889	1.85	0.77	0.98	3.59	1.29	1.14
LAMA3	1568879_a_at	BC033663	1.00	1.23	0.73	1.14	1.23	1.02
LAMA3	234719_at	AK024889	0.8	0.92	0.88	1.01	1.04	1.4
LAMA3	1560078_at	AL708055	0.95	0.96	1.1	1.11	0.98	0.89
LAMA3	1563772_a_at	AK096422	0.83	0.89	0.82	0.92	1.1	0.92
NDRG4	209159_s_at	AV724216	11.66	2.23	5.3	8.06	1.86	4.55
NEU1	208926_at	U84246	4.02	2.22	3.42	10.7	2.83	11.02
NFKBIA	201502_s_at	AI078167	1.84	1.13	1.23	2.54	2.04	1.39
NLRP1	218380_at	NM_001162	4.05	1.87	0.65	17.91	1.70	24.04
NR4A3	209959_at	NT_008470	3.56	1.82	1.58	5.18	1.57	5.41
PER1	202861_at	NM_002616	2.01	1.43	1.13	3.32	1.15	2.67
PER1	36829_at	NM_002616	1.49	1.18	1.25	1.86	1.24	1.74
PPP1R15A	202014_at	NT_011109	3.93	2.96	0.47	3.35	1.67	2.96
PPP1R15A	37028_at	NT_011109	3.51	2.86	0.49	3.29	1.75	2.62
PYY	207080_s_at	NM_004160	9.66	1.01	0.85	7.67	2.01	1.04
RIOK3	202129_s_at	NM_003831	2.63	1.68	1.82	3.08	1.73	2.62
TAP1	202307_s_at	NM_000593	1.25	1.69	1.47	2.04	5.09	0.86
TNFRSF10C	211163_s_at	AF012536	5.29	1.72	1.58	2.03	2.75	0.9
TNFRSF10C	206222_at	NM_003841	1.65	1.77	1.38	1.49	2.75	0.92

Table 3.4: Expression ratios of selected candidate genes in each cell line and treatment

Gene symbol	Probe set	Accession Number	MDA-MB-231			MCF7		
			AT*	AZA*	TSA*	AT*	AZA*	TSA*
TNFSF15	221085_at	NM_005118	3.56	2.97	5.17	0.2	3.02	0.41
VCL	200931_s_at	NM_014000	0.78	0.51	1.59	2.78	2.07	3.14
VCL	200930_s_at	AA156675	0.94	0.7	1.09	1.08	0.93	0.88
WIF1	204712_at	NM_007191	21.11	7.01	1.22	16.98	8.28	7
WNT5A	205990_s_at	NM_003392	0.86	1	1.02	3.66	2.02	3.47
ZMAT3	219628_at	NM_022470	1.58	1.61	1.40	2.19	3.82	1.24

**Treatment/Ctrl ratios have been shown.*

CpG island search of these 52 genes revealed that, 48 of them had CpG islands either in the expected promoter region (*i.e.* the end of the CpG island is not further from -2000 position) or within the gene (*i.e.* at least 1 base of CpG island and the gene intersect), while *AKR1C1, AKR1C2, IL-24* and *TNFSF15* did not (Table 3.5).

Table 3.5: CpG island search in the 2000 bp upstream and downstream of transcription start site of selected candidate genes

Gene	CpG island in -2000 to +2000	Location of island*
ABCA1	Yes	-726 to 1991
ACVR1C	Yes	-631 to 1136
ADAMTSL4	Yes	-548 to 470
AKR1C1	No	-
AKR1C2	No	-
AXIN2	Yes	-935 to 1991
BEX4	Yes (2)	-1000 to -500 and -100 to 500
BMP2	Yes	-1000 to 1000 and 1500 to 2500
BTG1	Yes (2)	-1030 to 969 and 984 to 1630
CASP9	Yes	241 to 446
CAST	Yes	-707 to1725
CDC14B	Yes	-612 to 1991
CDKN1A	Yes	-650 to 1991
CGREF	Yes (2)	-725 to 870 and 908 to 1668
CLDN6	Yes (2)	-2000 to 623 and 1041 to 1858

Table 3.5: CpG island search in the 2000 bp upstream and downstream of transcription start site of selected candidate genes

Gene	CpG island in -2000 to +2000	Location of island*
COL4A6	Yes	-1011 to -479
CXCL14	Yes	-403 to 1231
DDIT3	Yes (2)	1300 to 1500 and 3300 to 3900
DST	Yes	
DUSP5	Yes	-1030 to 969
EGR2	Yes	-2652 to 1465
EPB41L2	Yes	-707 to 1478
F11R	Yes	200 to 400
FOXO1	Yes	-1016 to 2233
GPX1	Yes	-555 to 1611
GSTM1	Yes	-441 to 558
GSTM2	Yes	-484 to 10
HLA-A	Yes	-47 to 1440
HLA-B	Yes	-441 to 1497
HMOX1	Yes	-71 to 161
IFNGR1	Yes	-517 to 1003
IL24	No	-
IQGAP2	Yes	-1429 to 1231
ITGA5	Yes	-1403 to 1079
ITGA9	Yes	-973 to 1041
LAMA3	Yes	-916 to 1383
NDRG4	Yes	-878 to 1121
NEU1	Yes	571 to 2570
NFKBIA	Yes	-807 to 1288
NLRP1	Yes	-1587 to -117
NR4A3	Yes	-2345 to 3424
PER1	Yes	-82 to 1202
PPP1R15A	Yes	164 to 607
PYY	Yes	-3135 to -191
RIOK3	Yes	-285 to 300
TAP1	Yes	-859 to 1231

Table 3.5: CpG island search in the 2000 bp upstream and downstream of transcription start site of selected candidate genes

Gene	CpG island in -2000 to +2000	Location of island*
TNFRSF10C	Yes	-403 to 946
TNFSF15	No	-
VCL	Yes	-1657 to 98
WIF-1	Yes	-1486 to 718
WNT5A	Yes	-2000 to 2000
ZMAT3	Yes	-271 to 350

**The locations of the CpG islands are presented with respect to the transcription start sites.*

When we carried out analyses in Oncomine[372] (www.oncomine.org) and Expression Atlas[384] (www.ebi.ac.uk), some of the genes were found to be significantly downregulated in breast cancer. While some of the genes could not be found in either of the databases (especially in Expression Atlas), some did not exhibit significant downregulation in breast tumors (especially in Oncomine). Some genes, namely *HLA-A, ITGA9* and *CDC14B*, were found to be down-regulated only when a specific subtype of breast cancer (example: IDC) was selected. When the genes which were upregulated in any of the databases were considered, 27 genes were obtained, and 4 of these had already been identified to be hypermethylated in breast cancer (Figure 3.10).

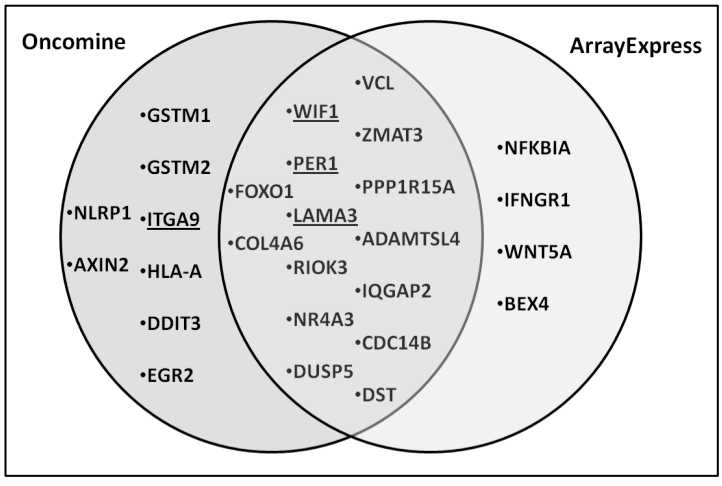

Figure 3.10: Genes downregulated in Expression Atlas or Oncomine databases.

When the selected candidate genes were evaluated in the Oncomine and Expression Atlas databases, a total of 27 genes were found to be downregulated in breast cancer samples compared to normal breast. 4 of them, WIF-1, LAMA3, PER1 and ITGA9 (underlined) had already been found to be methylated in breast cancer by at least one study[379, 382-383, 385-386].

When all of the analyses on candidate genes were combined in a single table, most of the genes seemed to provide the criteria for being a candidate gene (Table 3.6). According to this table, *ACVR1C, AXIN2, ADAMTSL4, BEX4, BMP2, BTG1, CASP9, CDC14B, COL4A6, DST, DUSP5, EGR2, EPB41L2, F11R, FOXO1, GSTM1, GSTM2, HMOX1, INSIG1, IQGAP2, NFKBIA, NDRG4, NR4A3, PPP1R15A, RIOK3,* and *ZMAT3* genes were strong candidates since they were mostly downregulated in tumors in at least one breast normal-tumor study, and had CpG islands. *BEX4* gene also was a strong candidate, although its location was on X chromosome, whose one copy is inactivated through DNA methylation in females. However, since MCF12A was also included in our studies, and since this gene was not upregulated upon AZA treatment in this cell line, this gene was included as a candidate as well.

Table 3.6: Combination of all analyses carried out for candidate genes

Gene Symbol	Down in Oncomine	Down in EA	CGI	Methylation shown in any cancer	Methylation in breast
ABCA1	No	No	Yes	No	No
ACVR1C	No	No	Yes	No	No
ADAMTSL4	Yes	Yes	Yes	No	No
AKR1C1	Yes	No	No	No	No
AKR1C2	Yes	No	No	No	No
AXIN2	No	No	Yes	Yes (CRC[155] and Lung Cancer[156])	No
BEX4	No	No	Yes	Yes (Ovarian cancer[238])	No
BMP2	No	Yes	Yes	Yes (Gastric cancer[287])	No
BTG1	No	No	Yes	No	No
CASP9	No	Yes	Yes	No	No
CAST	No	No	Yes	No	No
CDC14B	Yes	Yes	Yes	No	No
CDKN1A	No	No	Yes	Yes (Breast[378])	Yes[378]
CGREF1	No	No	Yes	No	No
CLDN6	No	No	Yes	Yes (ESCC[387], breast[380])	Yes[380]
COL4A6	No	Yes	Yes	Yes (Colon[148])	No
CXCL14	No	No	Yes	No	No
DDIT3	Yes	No	Yes	No	No
DST	Yes	Yes	Yes	No	No
DUSP5	No	Yes	Yes	No	No
EGR2	Yes	No	Yes	No	No

Table 3.6: Combination of all analyses carried out for candidate genes

Gene Symbol	Down in Oncomine	Down in EA	CGI	Methylation shown in any cancer	Methylation in breast
EPB41L2	No	No	Yes	No	No
F11R	No	No	Yes	No	No
GPX1	No	No	Yes	No	No
GSTM1	Yes	No	Yes	Yes (PCa[263])	No
GSTM2	Yes	No	Yes	Yes (BAC[264])	No
HLA-A	Yes	No	Yes	Yes (Gastric cancer[388-389],ESCC[390-391])	No
HLA-B	No	No	Yes	Yes (Gastric cancer[388-389], ESCC[391])	No
HMOX1	No	No	Yes	No	No
IFNGR1	No	Yes	Yes	No	No
IL24	No	Yes	No	No	No
IQGAP2	No	Yes	Yes	Yes (Gastric Cancer[243])	No
ITGA5	No	No	Yes	No	No
ITGA9	Yes	No	Yes	Yes (Kidney, lung, breast, ovarian, cervical cancers, Pca[379])	Yes[379]
LAMA3	Yes	Yes	Yes	Yes (BCC, SCC[392], Pca[393], breast [382])	Yes[382]
NDRG4	No	No	Yes	Yes (CRC[241])	No
NEU1	No	No	Yes	No	No
NFKBIA	No	Yes	Yes	Yes (Osteosarcoma[121])	No
NLRP1	Yes	No	Yes	No	No
NR4A3	Yes	Yes	Yes	No	No
PER1	Yes	Yes	Yes	Yes (Breast)[385-386]	Yes[385-386]
PPP1R15A	Yes	Yes	Yes	No	No
PYY	No	No	Yes	No	No
RIOK3	Yes	Yes	Yes	Yes (Prostate[164])	No
TAP1	No	No	Yes	Yes (SCC, colon, RCC, melanoma[394])	No
TNFRSF10C	No	No	Yes	Yes (PCa[395], Breast [381])	Yes[381]
TNFSF15	No	No	No	No	No
VCL	Yes	Yes	Yes	No	No

Table 3.6: Combination of all analyses carried out for candidate genes

Gene Symbol	Down in Oncomine	Down in EA	CGI	Methylation shown in any cancer	Methylation in breast
WIF1	Yes	Yes	Yes	Yes (Lung[396-397], HCC[398], breast [383, 399-401], BEC[402], NPC[403-404], ESCC[403], GI[405], Mesothelioma[406], Bladder[407-408])	Yes[383, 399-401]
WNT5A	No	Yes	Yes	No	No
ZMAT3	Yes	Yes	Yes	No	No

EA: Expression Atlas; CGI: CpG island; BAC: Barrett's Adenocarcinoma; BCC: Basal Cell Carcinoma; BEC: Barrett's Esophagus Cancer; CRC: Colorectal Cancer; ESCC: Esophageal Squamous Cell Carcinoma; HCC: Hepatocellular carcinoma; NPC: Nasopharyngeal Carcinoma; PCa: Prostate Cancer; RCC: Renal Cell Carcinoma; SCC: Squamous Cell Carcinoma, GI: Gastrointestinal.

3.2. Analyses of selected candidate genes

3.2.1. Validation of the selected genes in microarray set up by qRT-PCR

Relative expressions of the selected genes in treatment and control groups of MCF7, MDA-MB-231 and MCF12A cell lines were determined with qRT-PCR to validate the results obtained via bioinformatics analyses. The genes whose expressions were lower in MCF7 and/or MDA-MB-231 cell lines with respect to MCF12A, and were increased upon treatment with AZA and/or TSA were further selected to be scrutinized among breast cancer and immortalized non-tumorigenic (NT) breast cell lines by qRT-PCR method. Table 3.7 lists the fold-change values (treatment/control) of each gene obtained from the microarray analyses, in comparison with the results obtained from the qRT-PCR analyses. *GSTM1, GSTM2*, and *IQGAP2* were removed from further analyses, since their expressions were increased in cancer cell lines compared to MCF12A NT cell.

Table 3.7: Expression of selected genes in treatment groups of test cell lines

Gene Symbol	Microarray analysis ratios [a] of selected probe-sets [b]						qRT-PCR Analysis ratios [a]					
	231			MCF7			231			MCF7		
	AZA	TSA	A+T	AZA	TSA	A+T	AZA	TSA	A+T	AZA	TSA	A+T
ACVR1C	1.7	2.4	3.5	2.6	1.9	3.3	13.5	15.5	55.7	36.8	6.1	50.2
ADAMTSL4	1.6	3.7	1.9	3.7	**0.8**	2.4	7.2	16.6	8.9	123.6	2.4	87.4
AXIN2	1.2	1.8	3.2	2.8	1.6	5.5	7.7	4.1	23.4	30.9	8.0	26.9
BEX4	10.1	**0.9**	24.5	8.2	4.3	5.9	93.7	20.4	494.6	19.7	7.5	26.0
BMP2	3.1	2.3	5.4	1.8	1.2	6.4	10.9	4.9	64.0	34.3	6.3	861.1
BTG1	2.9	2.4	4.7	1.5	2.7	2.3	N/A	N/A	N/A	2.9	2.5	3.1
CASP9	1.5	1.6	2.9	2.0	2.1	3.3	3.5	1.6	10.6	5.3	2.4	21.1
CDC14B	1.8	3.2	2.5	2.1	4.4	4.9	2.7	3.4	9.5	4.3	1.3	26.0
COL4A6	3.1	1.8	6.5	1.8	1.2	1.5	29.9	4.0	17.8	32.0	5.1	87.4
DST	3.9	1.4	3.8	2.6	1.2	7.3	3.7	1.2	5.5	3.2	**0.5**	1.9
DUSP5	1.6	2.5	2.9	4.9	3.9	8.9	5.3	4.9	9.8	5.5	2.9	326.3
EPB41L2	**0.9**	1.8	1.2	2.6	4.7	8.4	2.1	2.6	3.6	10.6	7.2	36.8
F11R	2.3	4.8	3.3	1.5	2.2	1.7	3.2	2.2	3.6	6.0	5.1	11.9
FOXO1	1.7	7.1	4.2	1.5	3.5	4.0	4.9	5.3	19.0	5.1	4.3	36.8
GSTM1	1.1	1.9	1.3	2.2	1.0	1.2	1.9	**0.6**	1.0	30574	3.1	12417
GSTM2	1.1	2.4	1.5	2.6	1.1	1.4	2.6	24.3	10.2	27.9	11.7	831.7

Table 3.7: Expression of selected genes in treatment groups of test cell lines

Gene Symbol	Microarray analysis ratios [a] of selected probe-sets [b]						qRT-PCR Analysis ratios [a]					
	231			MCF7			231			MCF7		
	AZA	TSA	A+T	AZA	TSA	A+T	AZA	TSA	A+T	AZA	TSA	A+T
IQGAP2	2.7	4.7	6.1	2.0	2.4	5.1	**0.9**	**0.2**	46.9	52.0	39.4	152.2
NDRG4	2.2	5.3	11.7	1.9	4.6	8.1	9.8	21.9	200.9	8.0	8.3	78.8
NFKBIA	1.1	1.2	1.8	2.0	1.4	2.5	2.7	1.9	5.9	3.0	1.3	10.9
NR4A3	1.8	1.6	3.6	1.6	5.4	5.2	52.0	107.6	461.4	38.1	48.5	955.4
PPP1R15A	3.0	**0.5**	3.9	1.7	3.0	3.4	8.3	**0.6**	10.2	4.1	2.7	17.8
RIOK3	1.7	1.8	2.6	1.7	2.6	3.1	2.7	1.8	13.5	3.9	1.5	14.9
ZMAT3	1.6	1.4	1.6	3.8	1.2	2.2	7.5	3.9	10.2	16.0	1.0	3.4

[a] Treatment/control ratios have been presented. [b] Average values were calculated if more than one probe set was present. Bold: inconsistency between microarray and qRT-PCR. GAPDH gene expression was used as a reference gene for calculation of relative expression values.

3.2.2. Analysis of expression in breast cell line panel by qRT-PCR

After the expression of each gene was analyzed by qRT-PCR method in treated test cell lines (MCF12A, MCF7 and MDA-MB-231), the genes whose analyses resulted in accordance with microarray analyses were examined in a panel of breast cancer and non-tumorigenic (NT) breast cell lines. Figure 3.11 shows the relative expression of these genes in breast cell line panel.

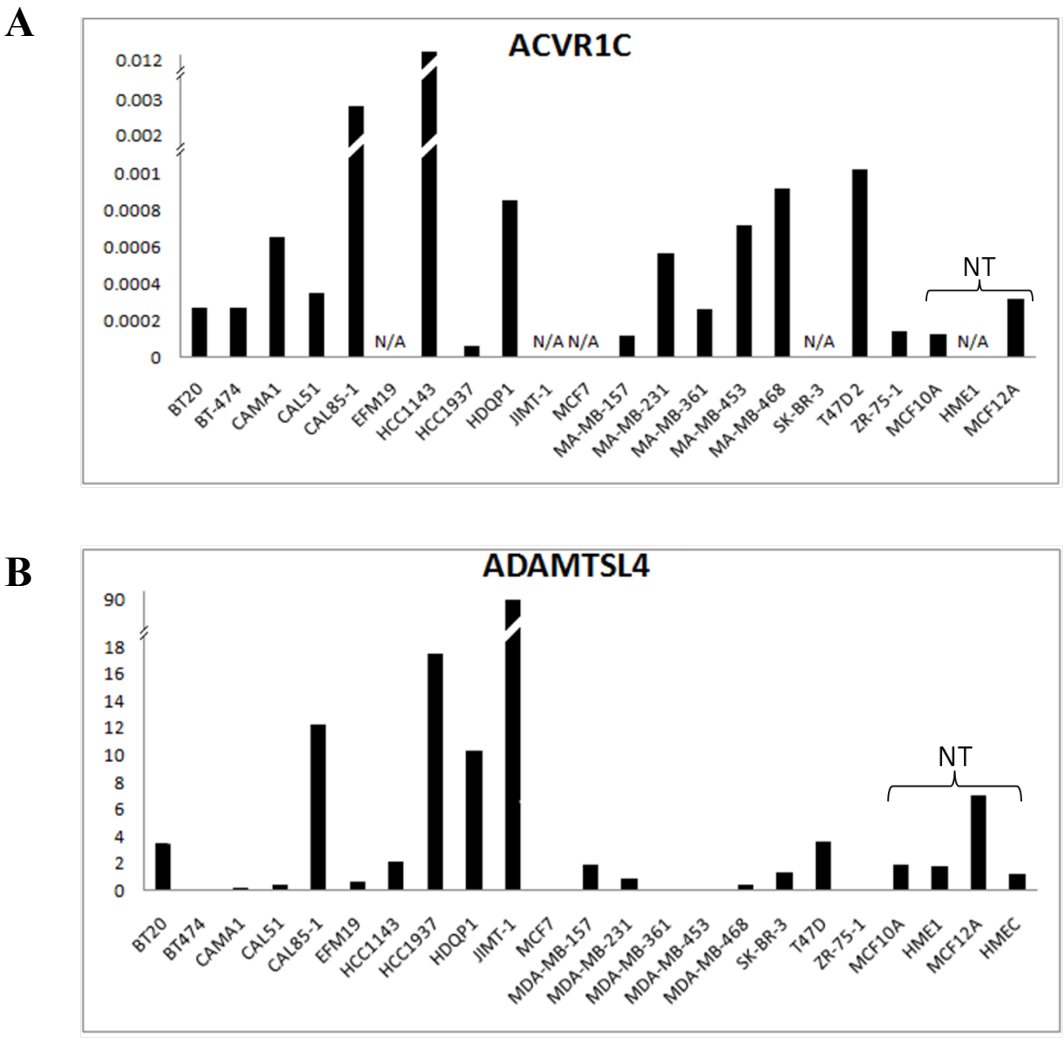

Figure 3.11: Expression of selected genes in a panel of breast cancer and non-tumorigenic breast cell lines.

(A) ACVR1C, (B) ADAMTSL4, (C) AXIN2, (D) RIOK3, (E) PPP1R15A, (F) NR4A3, (G) NFKBIA, (H) NDRG4, (I) INSIG1, (J) HMOX1,(K) FOXO1, (L) F11R, (M) EPB41L2, (N) EGR2, (O) DUSP5, (P) DST, (Q) COL4A6, (R) CDC14B, (S) CASP9, (T)BMP2, (U) BEX4, (V) ZMAT3, and (W) BTG1 expression levels were determined by qRT-PCR in breast cancer and NT breast cells. The relative expression levels were obtained by normalization of the gene expression to the GAPDH gene in each cell line. NT: Non-tumorigenic cell lines, the remaining cell lines are known breast cancer cell lines.

C

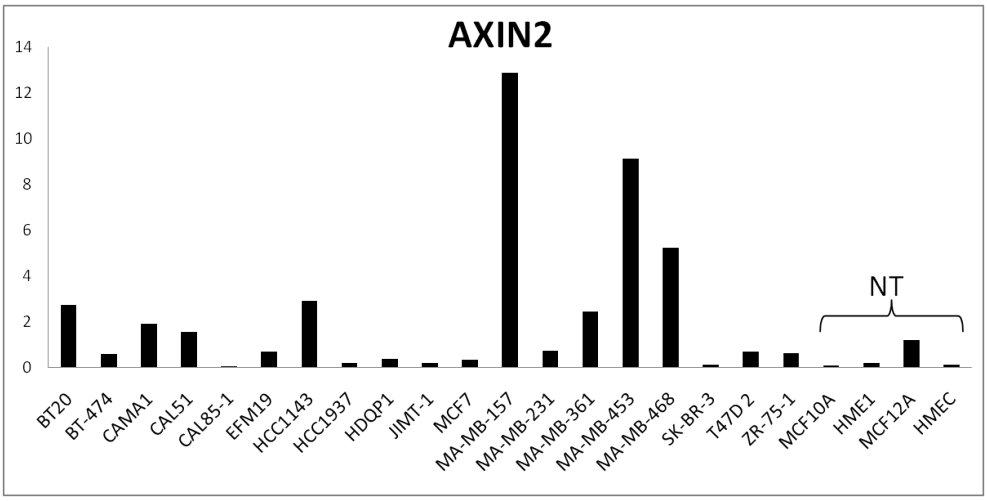

D

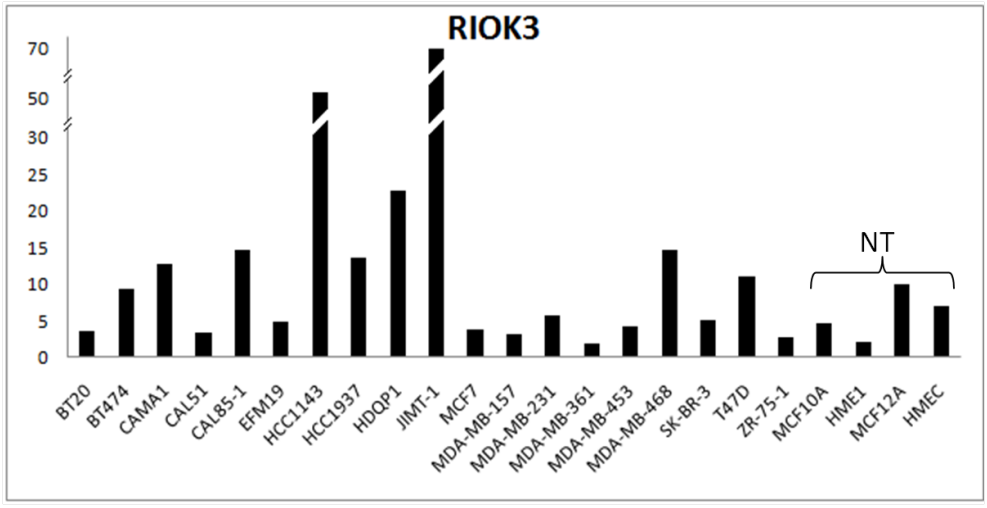

E

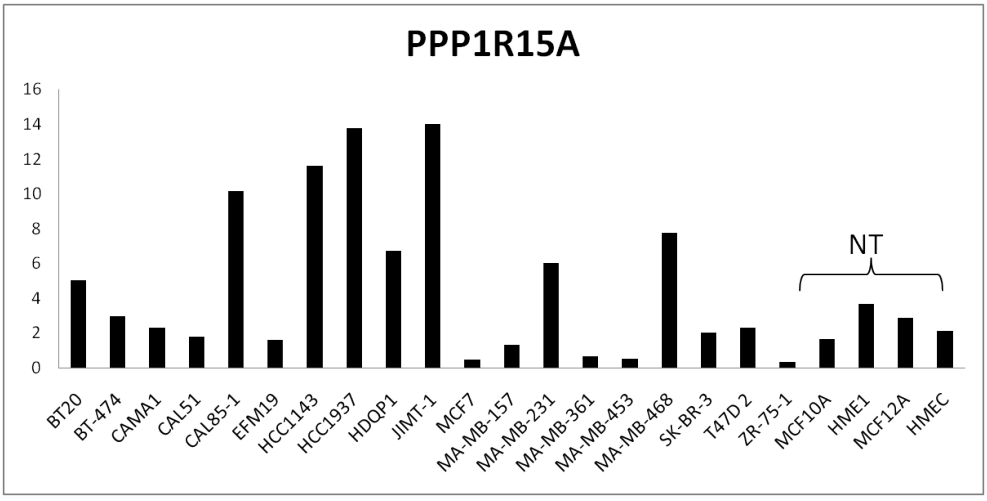

Figure 3.11 Continued

F

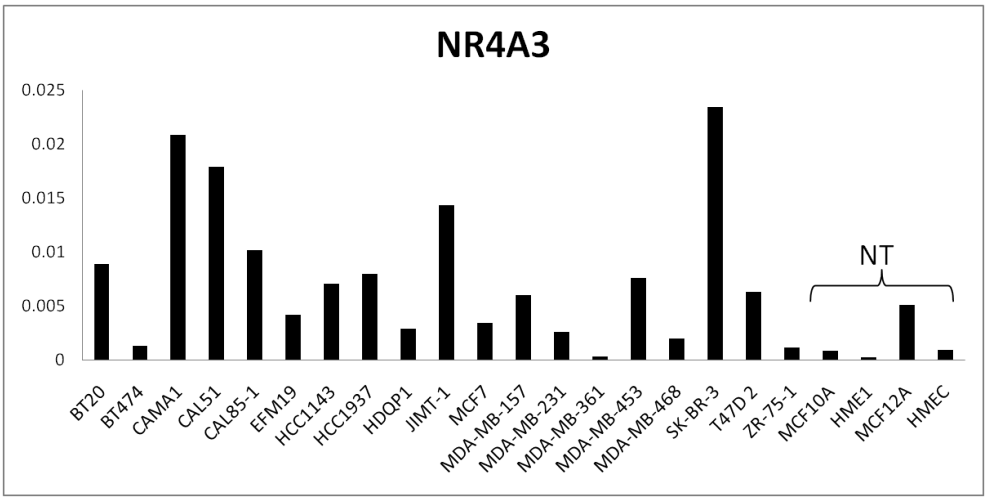

G

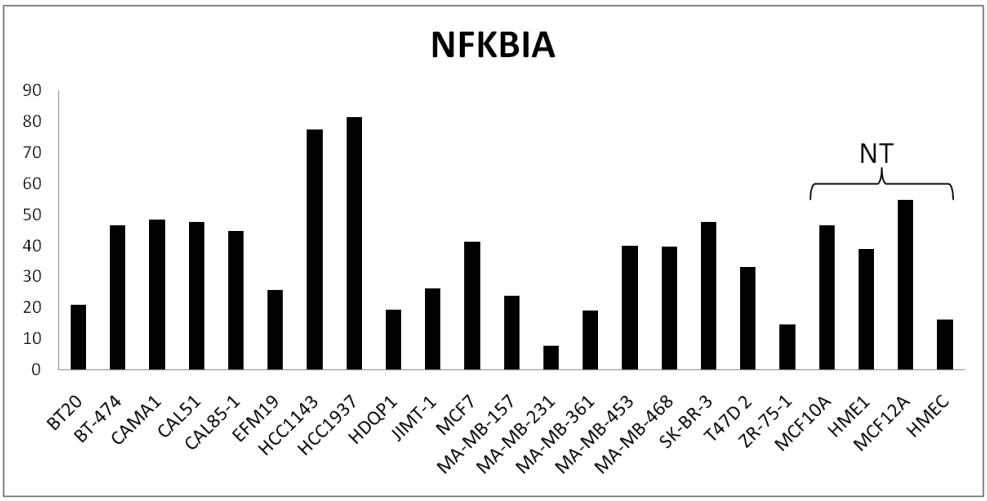

H

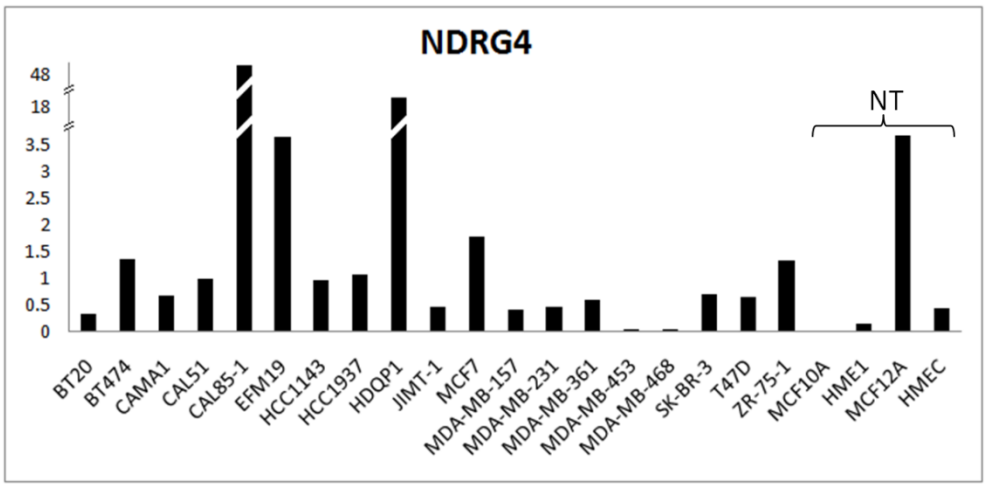

Figure 3.11 Continued

I

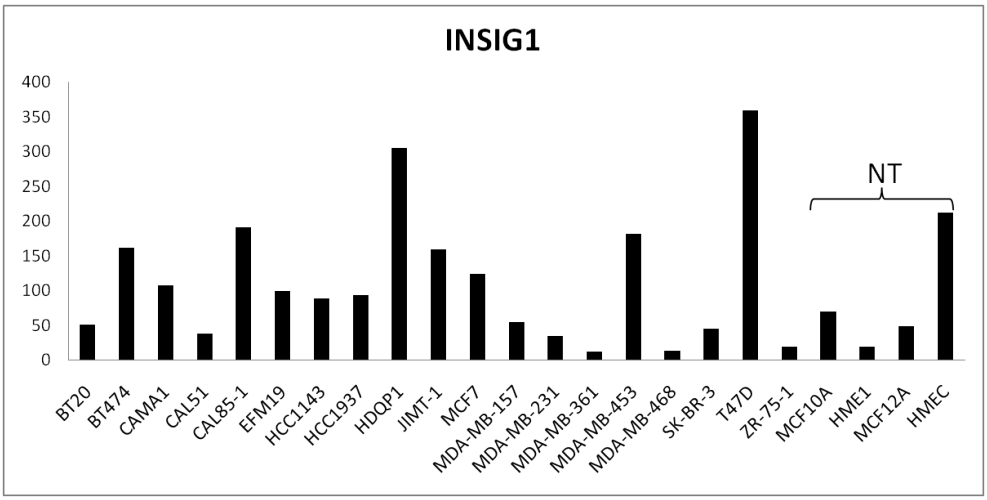

J

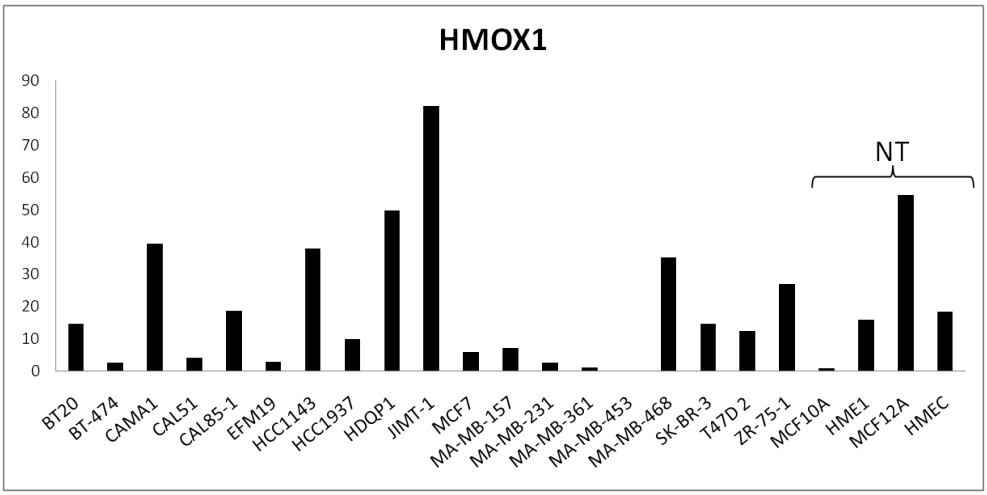

K

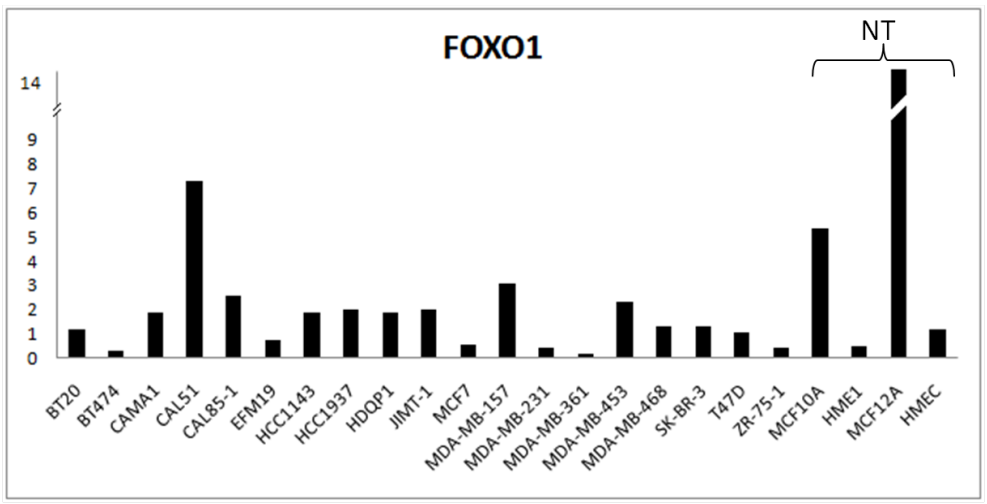

Figure 3.11 Continued

L

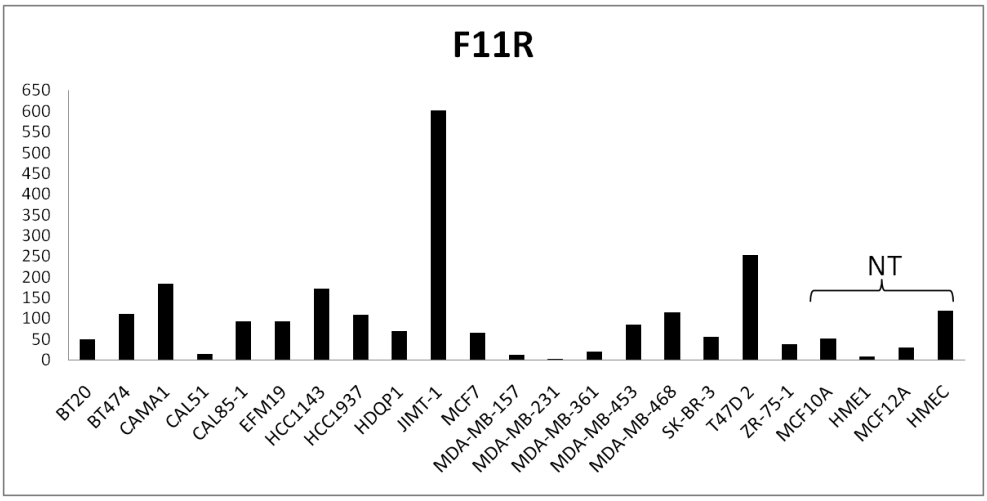

M

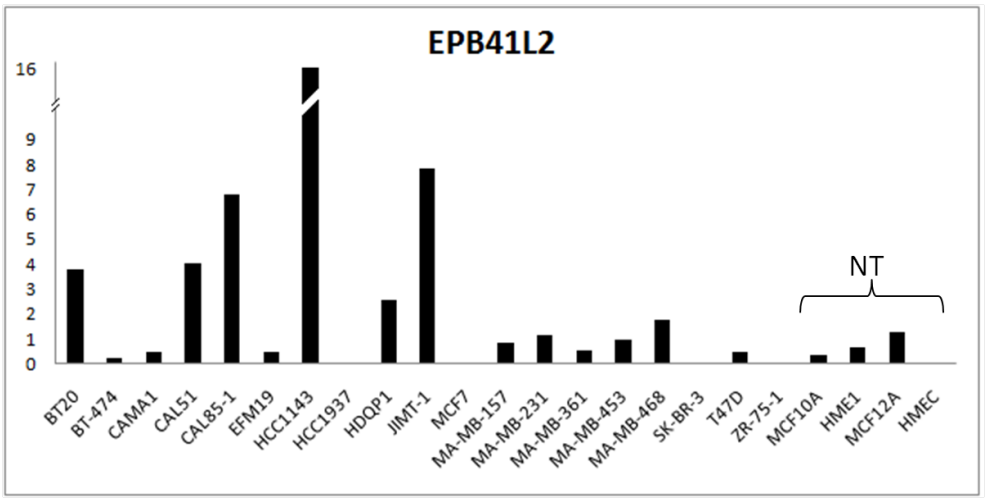

N

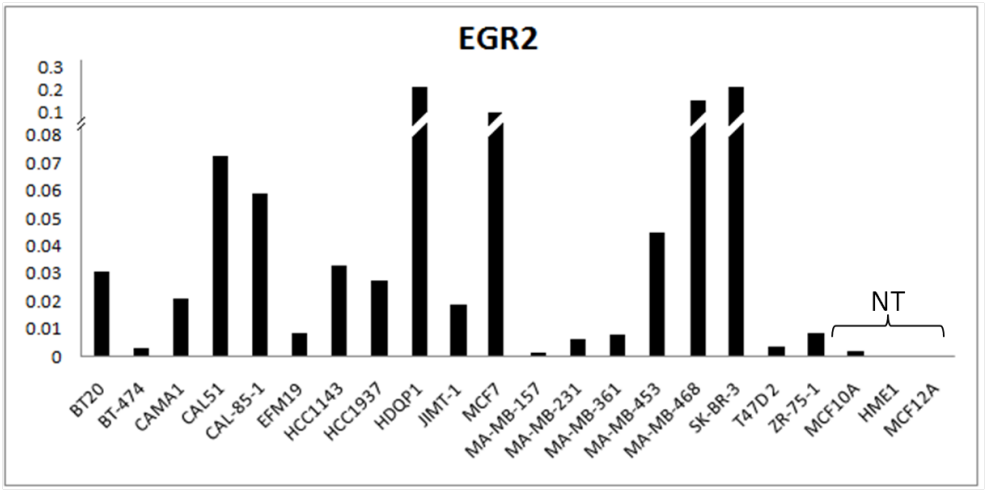

Figure 3.11 Continued

O

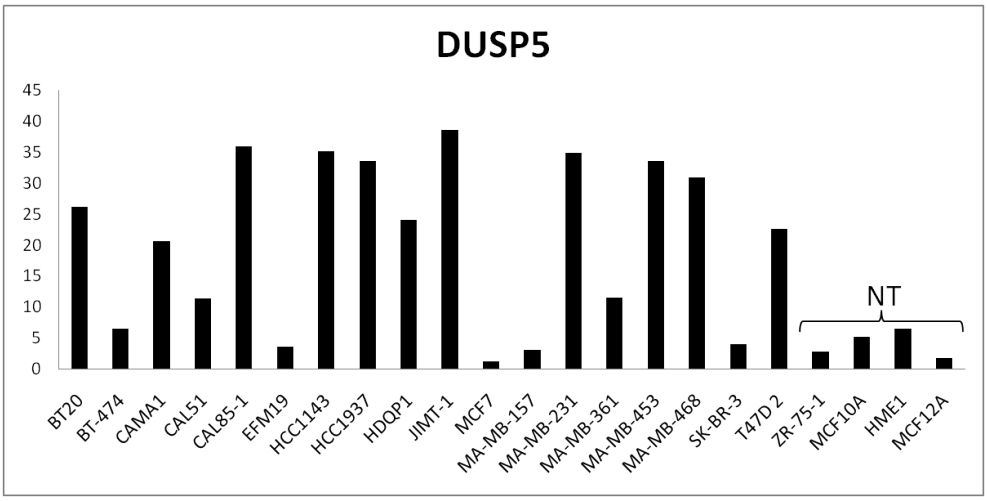

P

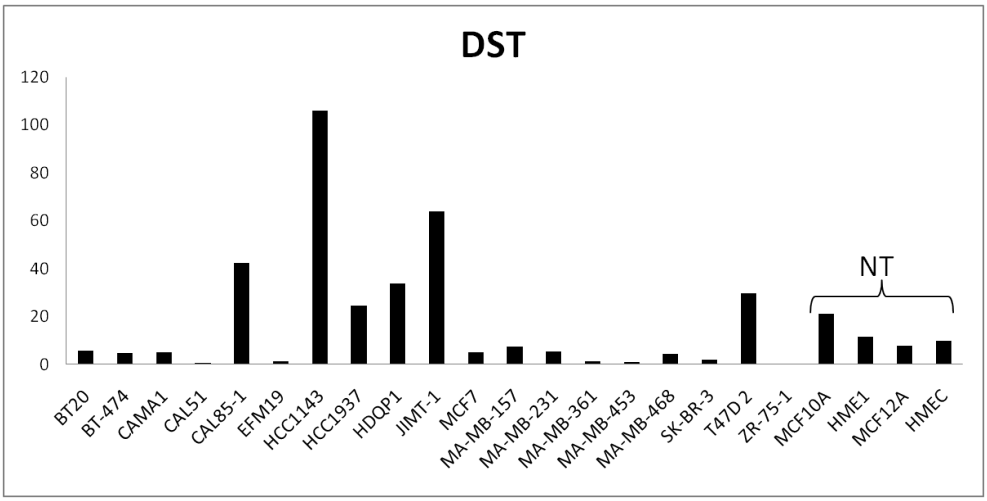

Q

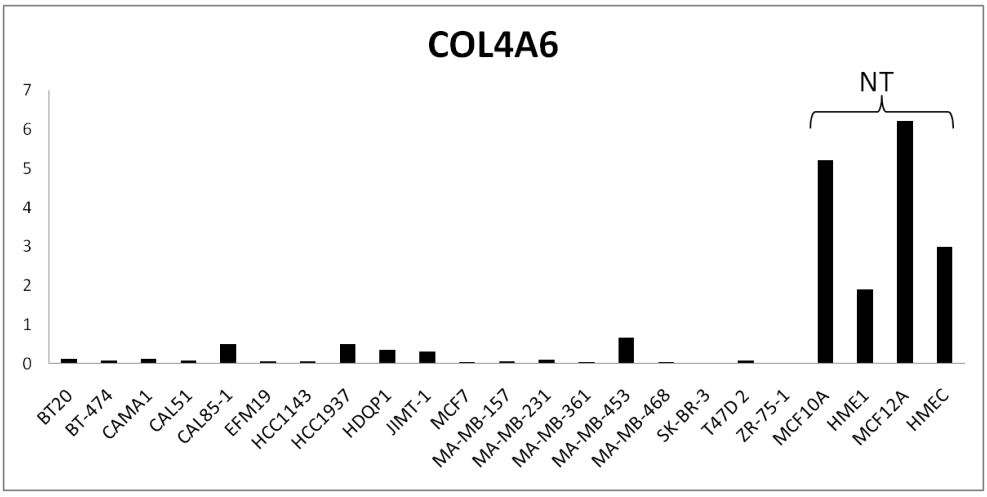

Figure 3.11 Continued

R

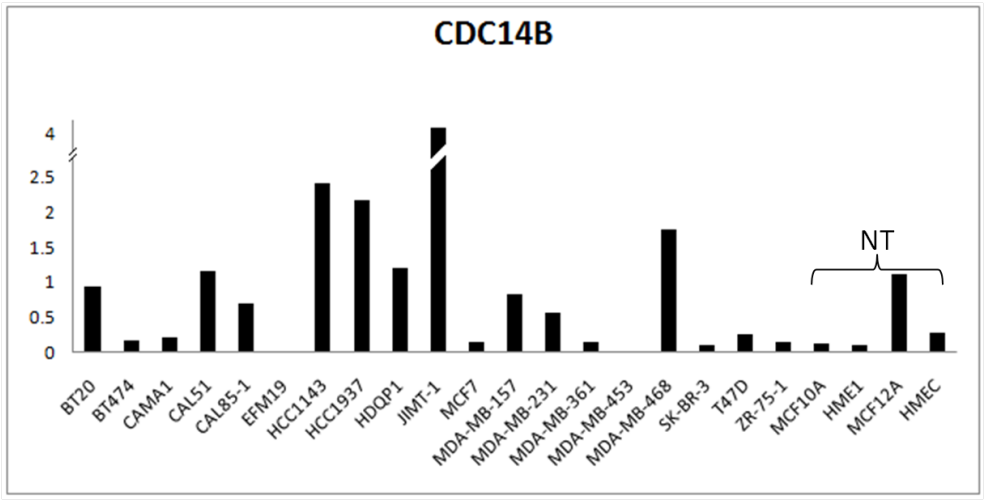

S

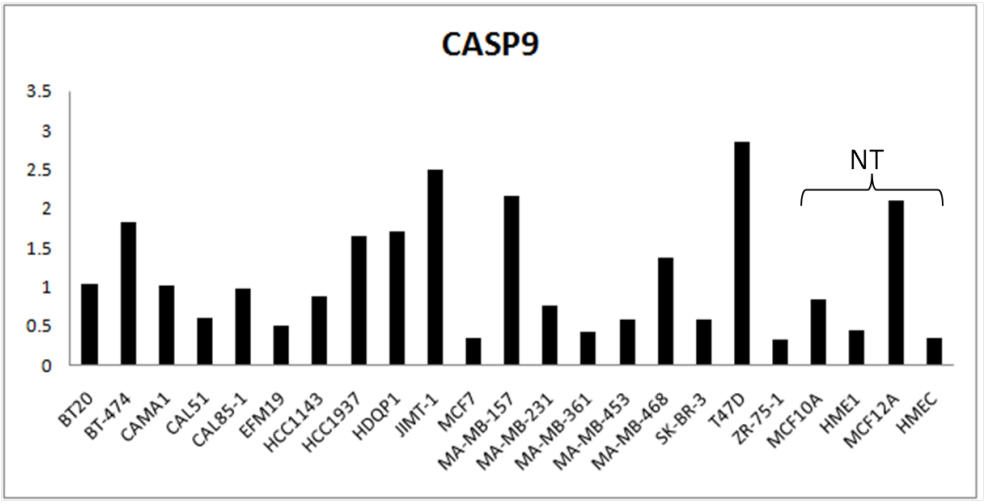

T

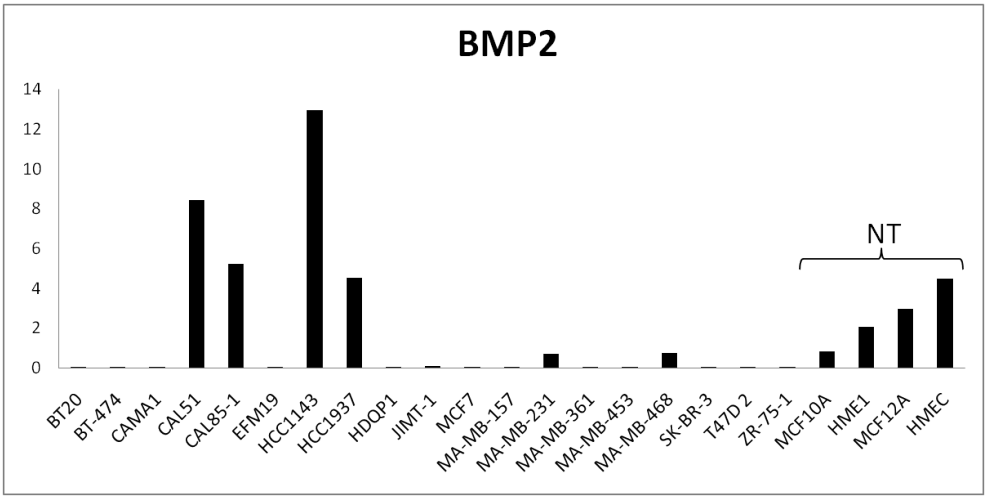

Figure 3.11 Continued

U

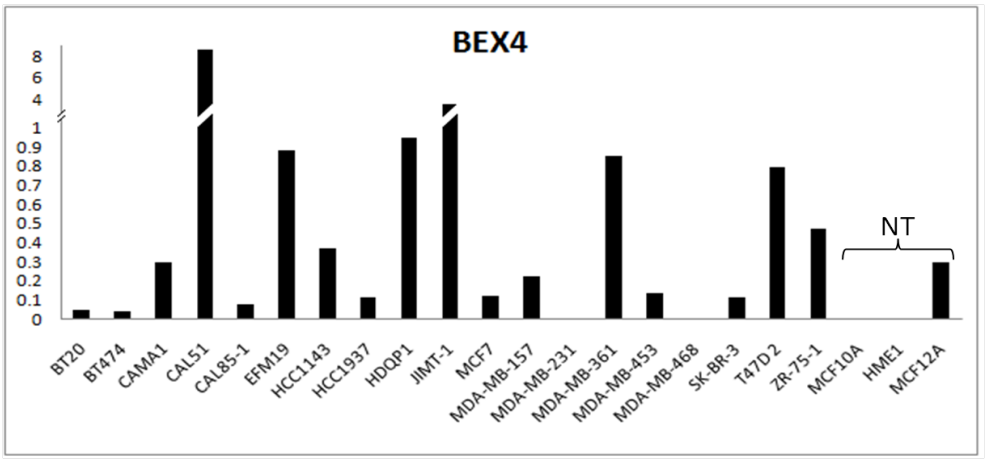

V

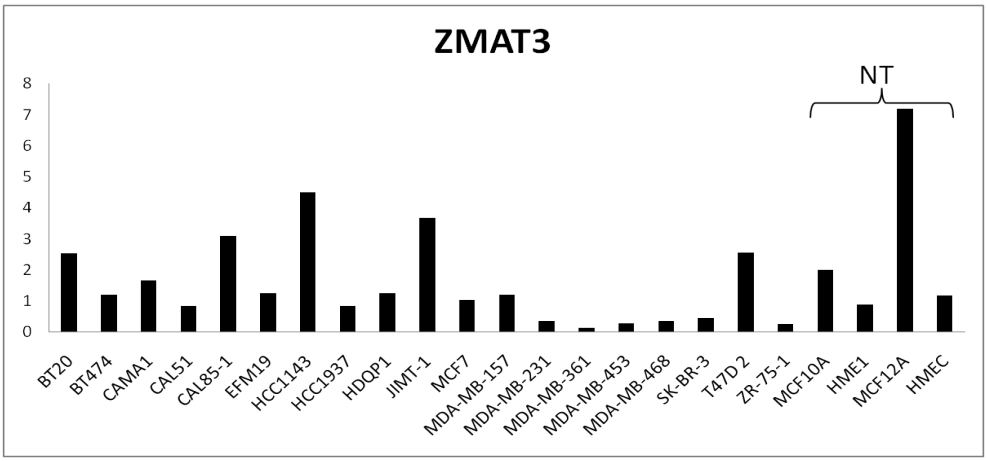

W

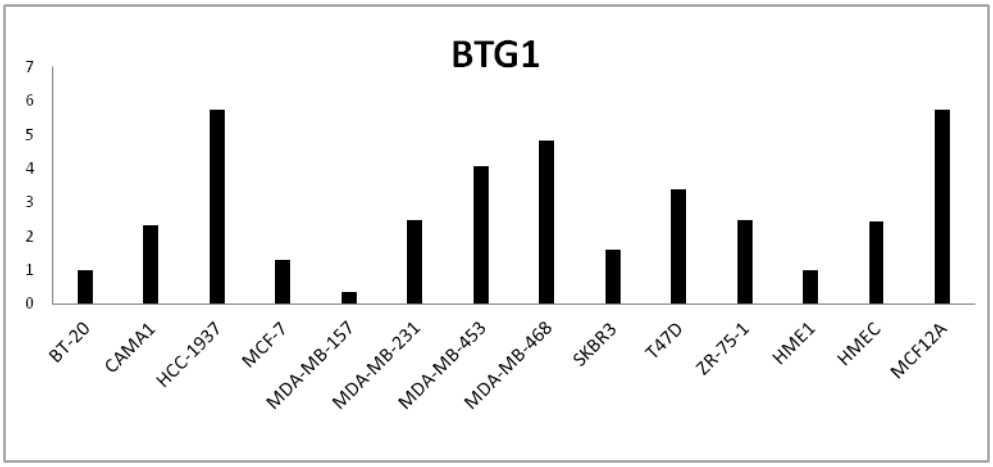

Figure 3.11 Continued

As Figure 3.11 shows, eight of the selected genes (namely *ADAMTSL4* (Figure 3.11-B), *HMOX1* (Figure 3.11-J), *FOXO1* (Figure 3.11-K), *EPB41L2* (Figure 3.11-M), *COL4A6* (Figure 3.11-R, $P < 0.05$, t-test), *DST* (Figure 3.11-P), *BMP2* (Figure 3.11-U), and *ZMAT3* (Figure 3.11-

Y) were expressed at lower levels in at least half of the cancer cell lines compared to the NT cells, while the remaining were either increased or displayed no general trend in the former.

3.2.3. Expression analysis of selected genes in treated breast cell lines

After the expression of selected genes were quantified in breast cell line panel (Figure 3.11), 7 breast cancer cell lines were selected based on the number of genes which were downregulated in these cells with respect to MCF12A and MCF10A NT cell lines. According to this, BT-474, CAL-51, MDA-MB-361, MDA-MB-453, MDA-MB-468, SK-BR-3 and ZR-75-1 cell lines were selected along with the non-tumorigenic cell line MCF-10A, and were treated with 5µM AZA and/or 400nM TSA. Later on, the genes which were found to be downregulated in each cell line by qRT-PCR method were chosen, and were analyzed in the given treatment groups of the cell lines in which they were downregulated, and in MCF10A. Table 3.8 summarizes the fold changes in gene expression levels detected by qRT-PCR method, in indicated cell lines after each treatment. According to this, *ZMAT3* gene was found to be upregulated by AZA, TSA, and A+T treatments in several cell lines; *PPP1R15A* expression increased in response to AZA and/or TSA in MCF7, MDA-MB-231, MDA-MB-361 and MDA-MB-453 cell lines; *FOXO1* expression responded to the treatments in almost every cell line tested. Hence, these genes were regarded as strong candidates for further study. Although could not reach the levels in non-tumorigenic cell lines, expression of *DST* gene was induced upon drug treatments in 6 cell lines, which could be an essential finding to pursue for our study. *COL4A6*, which was found to be downregulated in each and every breast cancer cell line by qRT-PCR method (Figure 3.11), was upregulated in almost all of the cell lines by at least one treatment (Table 3.8); however, none of the experiments (except for AZA and A+T treatment of MDA-MB-231 cell line) could achieve expression levels even close to the levels in non-tumorigenic cell lines, probably meaning that even if methylation has a control over expression of this gene, at least another level of regulation is also in play. Nonetheless, *COL4A6* was still included in our future investigations. *CASP9* gene expression was upregulated in each cell line it was tested by at least one treatment (Table 3.8), so it could be followed as another promising gene, although its expression was not very remarkably downregulated in each cancer cell line (Figure 3.11-T). *ADAMTSL4*, which was induced at least 8 fold in every breast cancer cell line by at least one treatment (Table 3.8) was also selected, given that its expression was also decreased in most of the cancer cell lines compared to NT cells (Figure 3.11-B). *F11R* gene was downregulated in only a small number of breast cancer cell lines (Figure 3.11-L); however, it was induced in response to at least one treatment in each cell line it was tested for (Table 3.8). Therefore, *F11R* gene was also selected for further analyses.

Table 3.8: qRT-PCR analysis of selected genes in treated breast cancer and NT cell lines

Cell Line	Drug	Fold Change (Treatment/Control)													
		1	**2**	**3**	**4**	**5**	**6**	**7**	**8**	**9**	**10**	**11**	**12**	**13**	**14**
	AZA	**8.00**	N/A	1.37	1.57	1.80	0.81	2.16	0.73	2.64	0.44	N/A	N/A	1.57	1.57
BT474	TSA	**16.00**	N/A	2.14	1.00	1.19	**5.10**	1.13	2.73	**42.24**	0.94	N/A	N/A	1.27	2.93
	A+T	**87.43**	N/A	**3.25**	1.52	**3.86**	**6.50**	1.94	**6.96**	**35.19**	**3.42**	N/A	N/A	1.37	2.30
	AZA	**12.13**	**3.03**	N/A	2.22	2.38	N/A	N/A	N/A	1.19	N/A	N/A	1.15	N/A	**4.00**
CAL-51	TSA	**3.14**	2.00	N/A	1.23	1.32	N/A	N/A	N/A	**3.48**	N/A	N/A	0.78	N/A	1.52
	A+T	**8.88**	1.41	N/A	2.22	**6.06**	N/A	N/A	N/A	**4.97**	N/A	N/A	1.15	N/A	1.41
	AZA	**123.64**	**5.28**	**4.29**	**32.00**	**3.25**	**10.56**	**3.19**	**5.10**	**8.57**	1.38	**3.03**	**4.14**	**3.86**	**3.36**
MCF7	TSA	2.38	2.38	1.27	**5.10**	0.28	**7.21**	2.21	**4.29**	**29.00**	**32.77**	1.27	2.73	1.52	1.19
	A+T	**87.43**	**21.11**	**25.99**	**87.43**	1.87	**36.76**	**3.56**	**36.76**	**57.91**	**4.05**	**10.93**	**17.75**	**14.93**	2.30
	AZA	**7.21**	**3.48**	2.73	**29.86**	**3.73**	2.07	**6.03**	**4.92**	0.71	1.32	2.73	**8.28**	2.73	**3.25**
MDA-MB-231	TSA	**16.56**	1.57	**3.36**	**4.00**	2.73	2.64	**5.14**	**5.28**	**4.12**	2.44	1.87	0.62	1.80	1.04
	A+T	**8.88**	**10.56**	**9.51**	**17.75**	**5.46**	**3.61**	**11.85**	**19.03**	**15.88**	**3.05**	**5.86**	**10.20**	**13.45**	1.74

Table 3.8: qRT-PCR analysis of selected genes in treated breast cancer and NT cell lines

Cell Line	Drug	Fold Change (Treatment/Control)													
		1	**2**	**3**	**4**	**5**	**6**	**7**	**8**	**9**	**10**	**11**	**12**	**13**	**14**
	AZA	**16.56**	**5.28**	1.46	0.39	0.84	N/A	1.78	1.46	**5.57**	0.87	0.93	2.14	1.41	**16.00**
MDA-MB-361	TSA	**10.93**	**3.36**	2.64	0.84	2.07	N/A	**3.18**	2.55	**36.77**	**34.66**	0.23	2.22	**3.25**	1.04
	A+T	**100.43**	**3.61**	**3.03**	0.37	**8.28**	N/A	1.31	2.00	**26.92**	**7.59**	0.18	2.55	2.55	**3.36**
	AZA	**93.70**	**4.00**	**16.56**	**3.36**	2.22	N/A	N/A	2.00	**15.60**	N/A	N/A	2.22	2.64	**7.46**
MDA-MB-453	TSA	**50.21**	**4.76**	**29.86**	1.74	0.54	N/A	N/A	2.38	**21.38**	N/A	N/A	2.07	**4.76**	**3.86**
	A+T	**265.03**	**9.51**	**30.91**	1.93	0.66	N/A	N/A	1.93	**51.25**	N/A	N/A	1.32	1.52	10.20
	AZA	2.46	N/A	N/A	2.00	1.07	N/A	N/A	1.07	N/A	1.59	N/A	N/A	N/A	1.19
MDA-MB-468	TSA	**8.28**	N/A	N/A	1.68	1.37	N/A	N/A	0.73	N/A	1.08	N/A	N/A	N/A	**8.57**
	A+T	**10.93**	N/A	N/A	2.93	0.97	N/A	N/A	2.38	N/A	1.07	N/A	N/A	N/A	2.83
	AZA	**11.31**	1.32	2.00	1.52	1.37	**4.29**	N/A	1.46	N/A	1.15	N/A	0.87	N/A	2.55
SK-BR-3	TSA	2.00	2.55	**6.50**	2.38	1.62	**40.79**	N/A	0.93	N/A	**10.19**	N/A	2.00	N/A	0.97
	A+T	**3.48**	**4.14**	**7.73**	**4.29**	1.62	**123.64**	N/A	**4.44**	N/A	**6.64**	N/A	2.22	N/A	**4.44**

Table 3.8: qRT-PCR analysis of selected genes in treated breast cancer and NT cell lines

Cell Line	Drug	Fold Change (Treatment/Control)													
		1	**2**	**3**	**4**	**5**	**6**	**7**	**8**	**9**	**10**	**11**	**12**	**13**	**14**
ZR-75-1	AZA	**32.00**	**3.36**	N/A	**4.76**	**3.61**	2.14	N/A	1.57	N/A	N/A	2.73	**4.59**	1.74	1.32
	TSA	**3.73**	1.80	N/A	0.84	1.27	**3.86**	N/A	2.22	N/A	N/A	0.37	1.27	2.14	1.46
	A+T	**68.59**	**4.00**	N/A	1.00	**6.06**	**6.96**	N/A	2.73	N/A	N/A	1.07	**6.50**	1.87	1.37
MCF10A	AZA	**8.88**	**3.14**	**4.00**	1.68	0.64	0.93	N/A	1.57	**4.38**	2.44	0.87	1.00	1.00	1.32
	TSA	2.22	1.57	**3.25**	1.04	0.35	1.37	0.94	2.14	**8.68**	**7.54**	1.00	0.84	1.41	1.74
	A+T	**21.86**	1.46	**3.14**	**3.03**	1.80	**4.44**	2.67	0.71	**32.11**	1.03	1.19	1.04	1.87	1.57
MCF12A	AZA	2.30	1.32	1.57	0.62	1.32	1.80	1.49	1.57	N/A	1.52	1.52	1.23	1.62	**5.46**
	TSA	**6.06**	1.80	1.07	0.90	2.14	1.52	1.05	1.87	1.01	0.29	**4.00**	1.11	2.07	0.93
	A+T	**5.28**	1.07	0.78	0.66	2.30	1.37	1.57	0.54	2.16	2.37	1.19	**3.36**	1.41	**4.76**

*1: ADAMTSL4; 2: CASP9; 3: CDC14B; 4: COL4A6; 5: DST; 6: EPB41L2; 7: F11R; 8:FOXO1; 9: HMOX1; 10: INSIG1; 11: NFKBIA; 12: PPP1R15A; 13: RIOK3; 14:ZMAT3. Values greater than 3.00 have been marked in **bold**. GAPDH gene expression was used as a reference gene for calculation of relative expression values(Eq (2)).*

3.2.4. Bisulfite sequencing and methylation analysis of selected genes

According to Table 3.8, *ADAMTSL4, CASP9, CDC14B, COL4A6, FOXO1A, PPP1R15A,* and *ZMAT3* genes were analyzed by bisulfite sequencing technique (Figure 3.12). Since all of these genes were downregulated and were induced by AZA in MCF7 cell line, only MCF7 genomic DNA was used initially for most of the analyses. If the analyzed genes were found to be methylated in this cell line, they were also analyzed in the NT cell lines. 5 clones were selected for each gene for bisulfite sequencing. Due to difficulty of the procedure regarding the bisulfite treated DNA, less number of clones were obtained for some genes at the beginning, if there were no methylation in these clones, analysis was not completed (as in *CASP9,*Figure 3.12A).

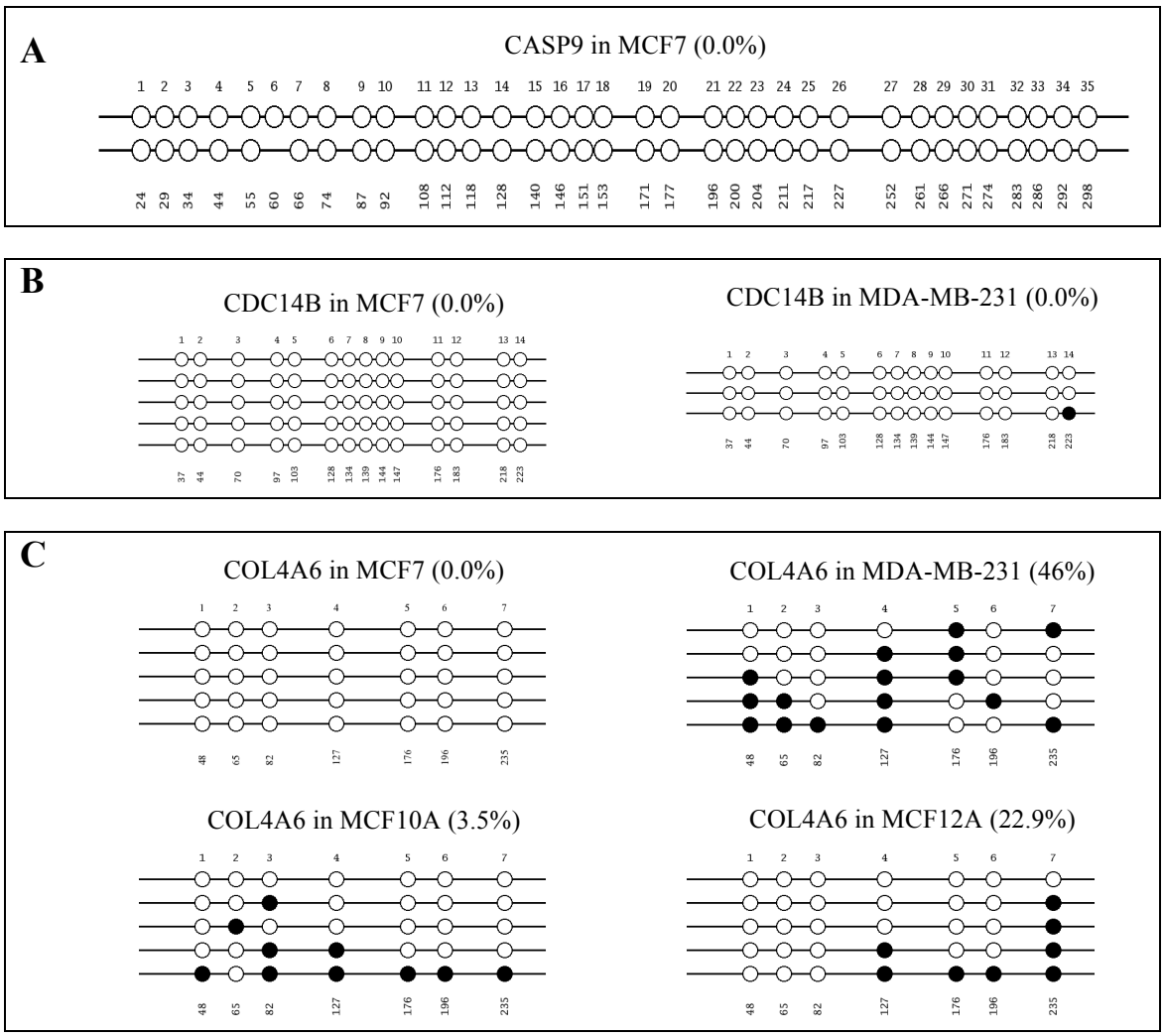

Figure 3.12: Bisulfite sequencing of the genes in test cell lines.

*Average % methylation values of (**A**) CASP9, (**B**) CDC14B, (**C**) COL4A6, (**D**) FOXO1A, (**E**) PPP1R15A, (**F**) ZMAT3, and (**G**) ADAMTSL4 genes. Numbers above each CpG circle denotes the order of the CpG in the sequenced region, while the number below represents the order of the base at which the CpG is present. Empty circles: Unmethylated, Full circles: Methylated.*

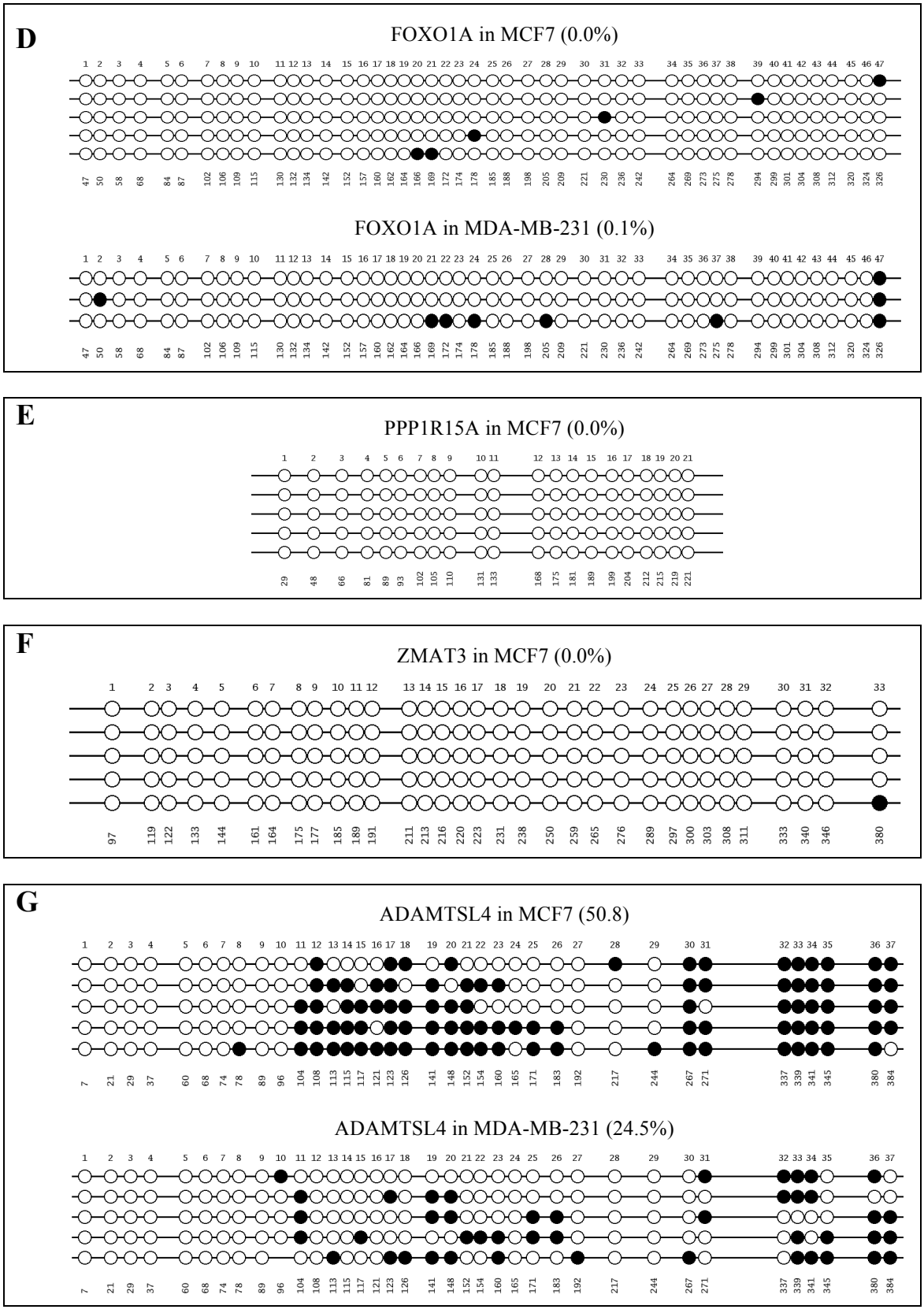

Figure 3.12 Continued

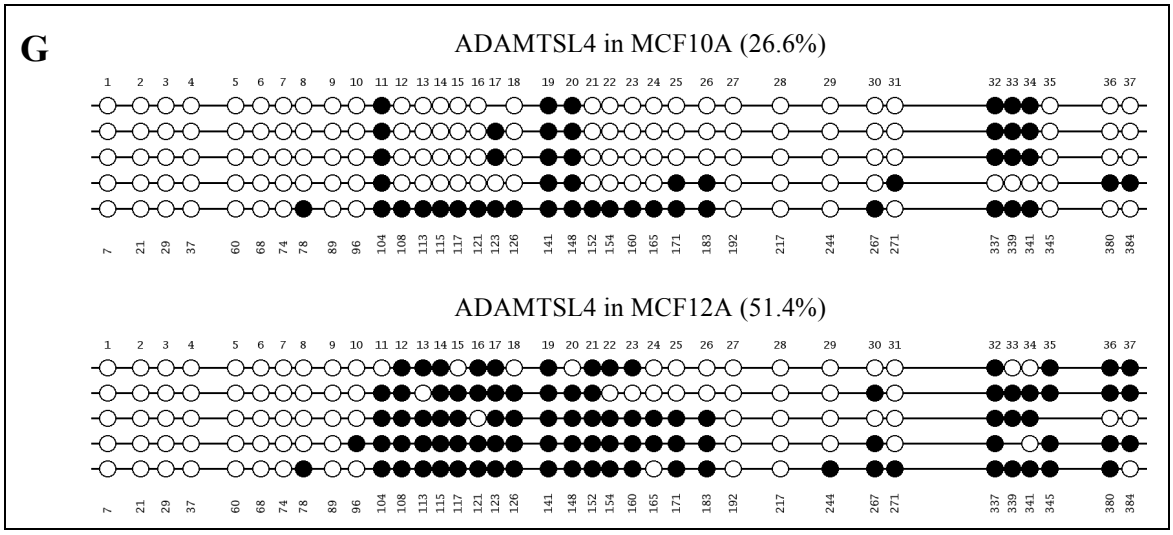

Figure 3.12 Continued

The first results obtained by sequencing bisulfite treated MCF7 and MDA-MB-231 genomic DNAs clearly show that most of the genes were hypomethylated in these cells (Figure 3.12A, B, D, E and F), although they were upregulated by AZA at very significant levels (*ZMAT3* and *COL4A6*, $P < 10^{-7}$; *CDC14B*, $P = 9.3\text{x}10^{-6}$; *PPP1R15A*, $P = 0.0002468$; *CASP9*, $P = 2.12\text{x}10^{-5}$). Only *ADAMTSL4* gene was partially methylated in MCF7 and MDA-MB-231 cell lines, yet it was also methylated in the NT cell lines (Figure 3.12G). Thus, the methylation was not specific to the breast carcinoma cells. Similar situation was evident for the *COL4A6* gene, which was methylated in similar levels in MDA-MB-231 cells, and NT cells (Figure 3.12C). The negative results obtained from the bisulfite sequencing method could be related to the selection of genes based on the *P* value, thus new selection criteria were developed for new candidate genes, based on fold change thresholds.

3.3. Analyses of second phase candidate genes

3.3.1. Selection of new candidate genes based on fold changes

To test the effect of strategy in selection of candidates, the following criteria were used for selection of new candidate genes:

(1) The gene should be upregulated in either MCF7 or MDA-MB-231 cells by AZA, by at least 5 fold, compared to their DMSO controls ($P < 0.01$);

(2) The gene should not be upregulated in MCF12A cell line in response to AZA, by more than 1.5 fold compared to its DMSO control;

(3) The gene should be downregulated in MCF7 and/or MDA-MB-231 mock (untreated) groups by at least 3 fold compared to MCF12A mock group;

(4) The methylation of the gene should not be extensively studied in breast cancer;

(5) The gene function should be related to possible tumor suppressor activities.

Six genes were selected based on these criteria as listed in Table 3.9 and these genes will be referred to as "second phase genes" throughout the text.

Table 3.9: Expression ratios of the second phase candidate genes in microarray data

Probe set	Gene symbol	AZA/Control fold changes			MCF12A/cell line mock fold changes	
		MCF12A	MCF7	MDA-MB-231	MCF7	MDA-MB-231
205547_s_at	*TAGLN*	0.60	**30.98**	1.92	59.61	15.16
1555724_s_at	*TAGLN*	0.60	**23.64**	1.68	40.55	13.03
204268_at	*S100A2*	1.24	**23.47**	1.03	59.35	6.71
210517_s_at	*AKAP12*	1.00	**19.29**	3.36	98.02	4.57
227529_s_at	*AKAP12*	0.70	**8.43**	3.30	25.49	4.59
201506_at	*TGFBI*	0.77	**9.28**	1.66	31.55	13.68
222774_s_at	*NETO2*	1.26	0.94	**14.18**	58.61	11.82
201565_s_at	*ID2*	0.85	1.19	**11.18**	90.58	24.24

3.3.2. Expression of the second phase candidate genes in breast cell lines

The expression levels of the genes in breast cell line panel were analyzed by qRT-PCR method in breast cancer and NT cell line panel. Except for *ID2* (Figure 3.13D), and in most cell lines *NETO2* (Figure 3.13E), all of the genes were revealed to be downregulated in breast cancer cell lines, compared to NT breast cell lines. *S100A2* displayed the greatest downregulation (P <0.01) both in terms of number of cell lines and level of downregulation (Figure 3.13A). *TAGLN* gene was also downregulated in most of the breast cancer cell lines, compared to NT cell lines (Figure 3.13C, P <0.01). Thus, *TAGLN, S100A2, TGFBI* and *AKAP12* genes were selected for further qRT-PCR analysis in AZA and/or TSA treated breast cancer cell lines.

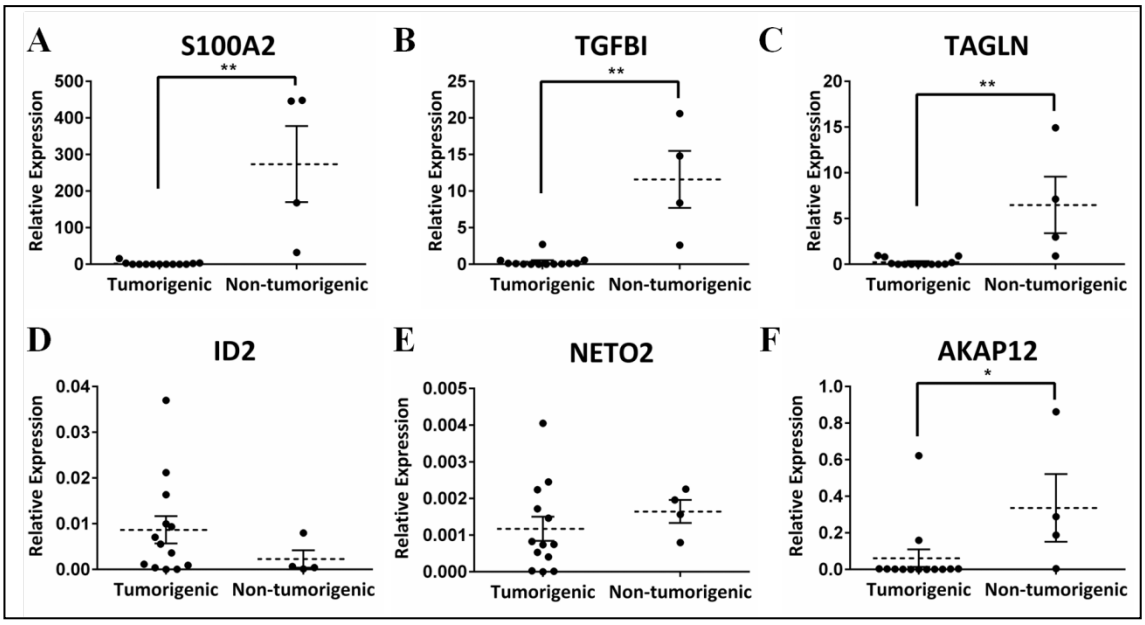

Figure 3.13: Expression of second phase candidate genes in breast cell line panel.

*qRT-PCR analyses of (A) S100A2, (B) TGFBI, (C) TAGLN, (D)ID2, (E)NETO2, and (F) AKAP12 genes in breast cancer and NT breast cells. Values represent the relative expression with respect to GAPDH housekeeping gene. * P <0.05; ** P <0.01, t-test.*

Table 3.10 shows the induction ratios of each gene in each cell line upon drug treatments, according to qRT-PCR analyses. All of the genes, (*TAGLN* is shown as an example in Figure 3.14) were induced by more than 3 fold in most of the cell lines upon AZA and/or TSA treatments, without being induced as much in NT cells. Thus, all of the genes were selected for further analyses by bisulfite sequencing in breast cancer cell lines, MCF7 and MDA-MB-231.

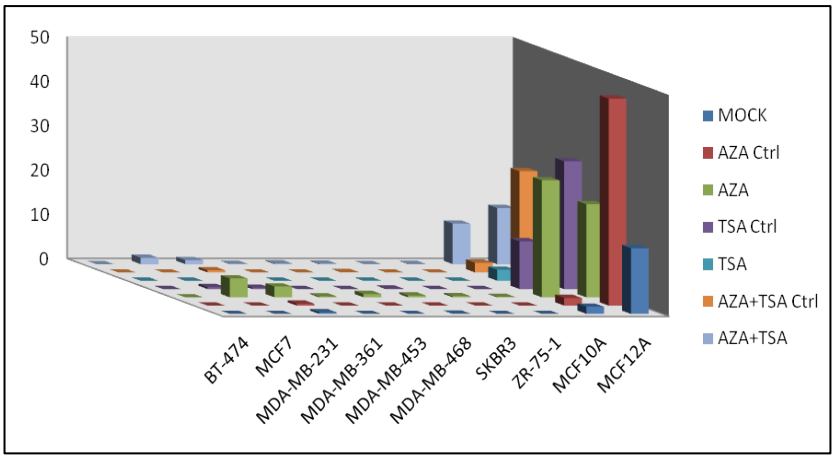

Figure 3.14: Expression of *TAGLN* gene in AZA and/or TSA treated breast cell lines.

Expression of TAGLN was determined by qRT-PCR in AZA and TSA treated breast cancer and NT breast cells. Expression values were normalized by comparing to GAPDH reference gene expressions in each cell line and treatment.

Table 3.10: Expression ratios of the second phase candidate genes in treatment groups

Cell Line	Comparison Group	Fold Change			
		TGFBI	TAGLN	S100A2	AKAP12
MCF10A	**AZA/Ctrl**	1.1	**15.32**	1.11	**4.52**
	TSA/Ctrl	0.5	0.23	0.55	1.03
	A+T/Ctrl	1.05	**4.15**	0.61	19.7
MCF12A	**AZA/Ctrl**	0.49	0.45	1.33	1.62
	TSA/Ctrl	0.49	0.54	0.45	1.33
	A+T/Ctrl	0.7	0.56	2.25	**8.66**
MCF7	**AZA/Ctrl**	**20.59**	**2539.93**	**304.93**	**328.56**
	TSA/Ctrl	0.13	0.02	0.25	0.21
	A+T/Ctrl	**3.96**	**464.41**	**52.53**	**1112.82**
MDA-MB-231	**AZA/Ctrl**	**5.2**	**5.5**	2.47	**28.44**
	TSA/Ctrl	0.87	0.26	2.14	0.95
	A+T/Ctrl	**3.55**	1.85	**3.61**	**121.94**
BT-474	**AZA/Ctrl**	**5**	**52.45**	**9.26**	0.99
	TSA/Ctrl	1.09	0.87	2.24	**65.8**
	A+T/Ctrl	2.71	2.21	**12.24**	**35.75**
CAL-51	**AZA/Ctrl**	1.68	N/A	**6.56**	N/A
	TSA/Ctrl	0.48	N/A	0.32	N/A
	A+T/Ctrl	0.57	N/A	0.81	N/A
MDA-MB-361	**AZA/Ctrl**	1.82	**149.1**	**27.96**	**254.23**
	TSA/Ctrl	1.37	0.66	**11.6**	**17.15**
	A+T/Ctrl	1.08	**49.17**	**10.19**	**341.32**
MDA-MB-453	**AZA/Ctrl**	**7.86**	**393.03**	**90.51**	1.26
	TSA/Ctrl	1.18	0.99	**14.42**	0.6
	A+T/Ctrl	**4.97**	**89.09**	**57.2**	**4.08**
MDA-MB-468	**AZA/Ctrl**	2.15	**9.39**	0.91	**6.57**
	TSA/Ctrl	1.37	0.43	1.23	**15.83**
	A+T/Ctrl	2.27	1.71	0.63	**23.43**
SKBR3	**AZA/Ctrl**	2.51	**19.69**	**6.25**	**6.89**
	TSA/Ctrl	1.06	0.08	**8.39**	**181.02**
	A+T/Ctrl	1.64	0.98	**16.42**	**60.55**

Table 3.10: Expression ratios of the second phase candidate genes in treatment groups

Cell Line	Comparison Group	Fold Change			
		TGFBI	TAGLN	S100A2	AKAP12
ZR-75-1	**AZA/Ctrl**	**6.42**	**442.22**	**15.96**	**7.01**
	TSA/Ctrl	0.78	0.82	1.61	**7.09**
	A+T/Ctrl	**4.58**	**974.22**	**83.86**	**58.89**

*Numbers in **bold** are fold changes >3.0. GAPDH gene expression was used as a reference gene for calculation of relative expression values (Eq (2)).*

3.3.3. Bisulfite sequencing of the second phase genes in breast cancer cell lines

Bisulfite sequencing of the selected genes was performed in MCF7 and MDA-MB-231 cells for the initial analyses. As a first set, 3 clones were selected for each gene in each cell line, and after confirmation of presence of the intended insert, the plasmids were subjected to sequencing. When positivity of methylation was observed, the number of clones was increased to five, and bisulfite treated MCF10A and MCF12A genomic DNAs were also sequenced. Depending on these results, bisulfite treated DNA of other treated cell lines were also sequenced for the selected genes. Figure 3.15A shows that, *TGFBI* gene was not methylated in either of the breast cancer cell lines. *AKAP12* gene promoter was hypermethylated in both MCF7 and MDA-MB-231 cells; however, was also hypermethylated in NT cell lines (Figure 3.15B).

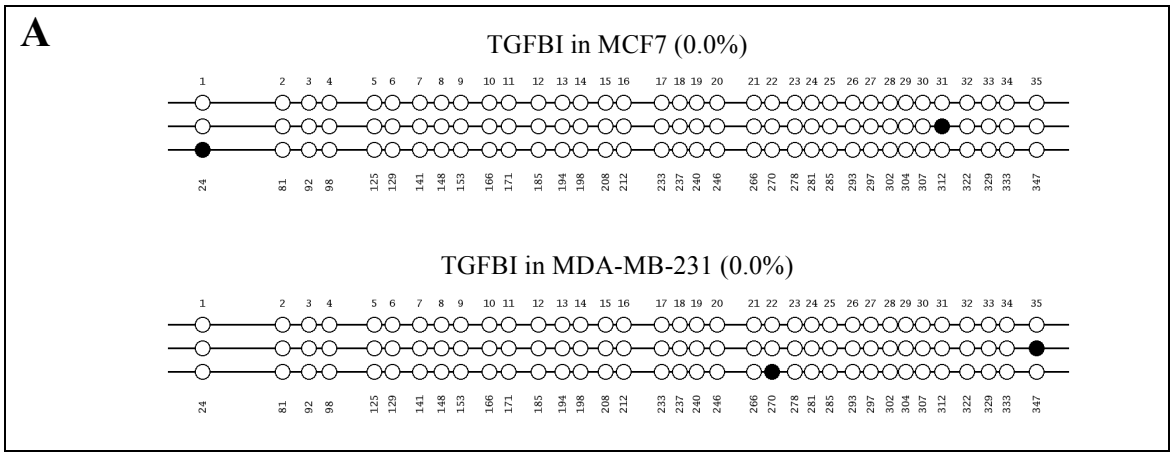

Figure 3.15: Bisulfite sequencing of second phase candidate genes in selected cell lines and tissue samples.

***A.** TGFBI **B.** AKAP12 **C.** S100A2 **D.** TAGLN. Average values of % methylation are presented as (x.x%, analyzed with QUMA). Numbers above each CpG circle denotes the order of the CpG in the sequenced region, while the number below represents the order of the base at which the CpG is present. Empty circles: Unmethylated, Full circles: Methylated.*

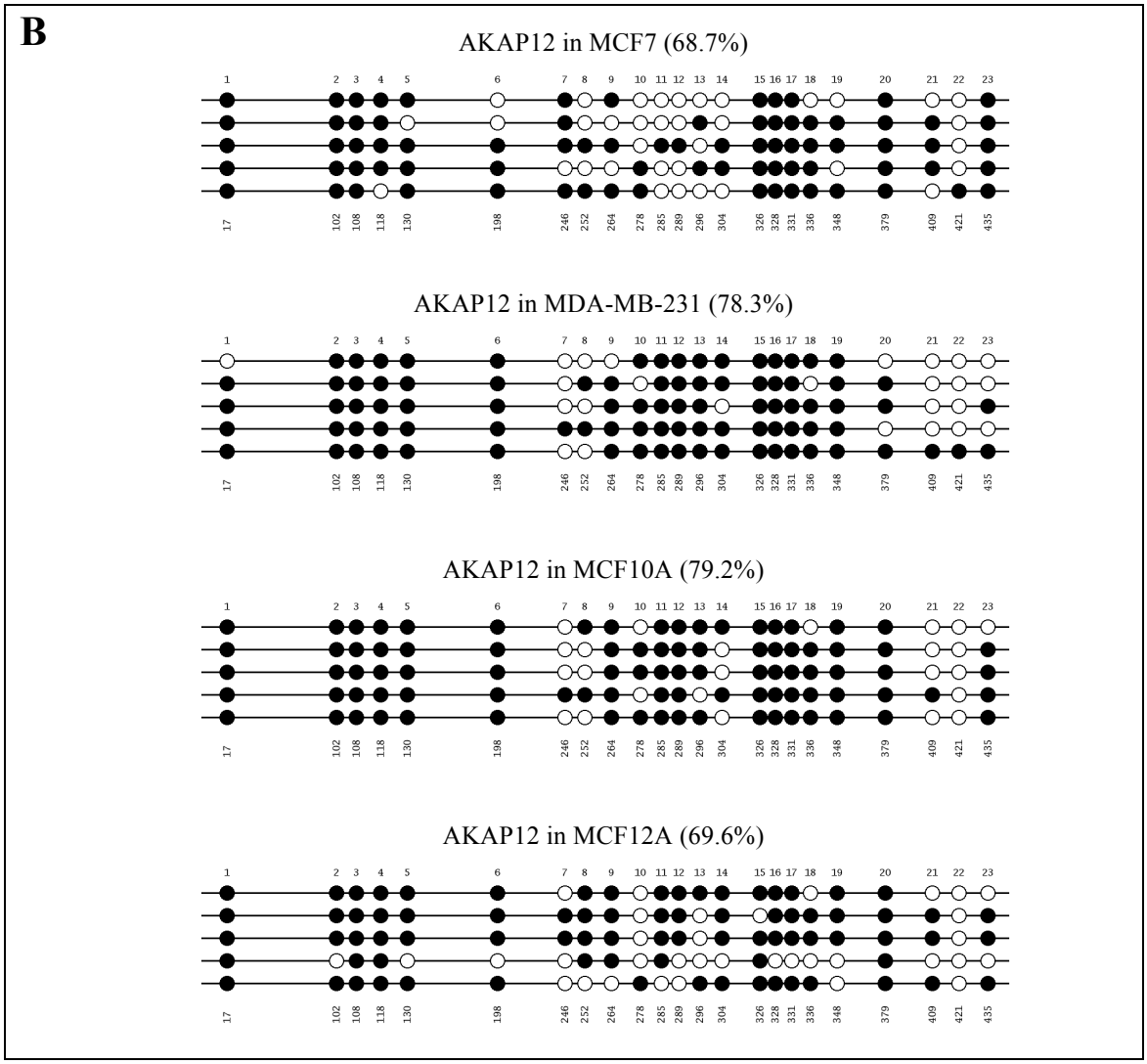

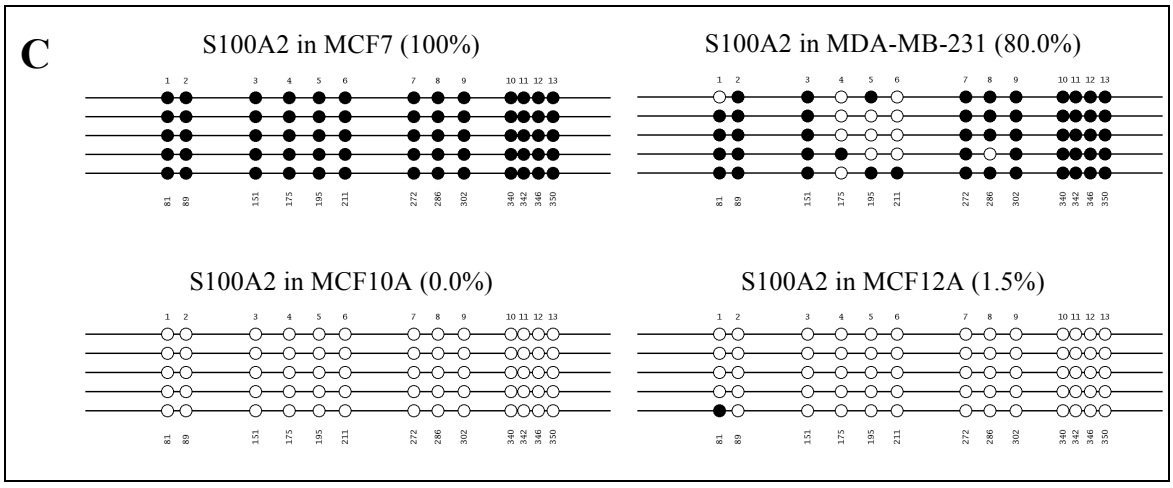

Figure 3.15 continued

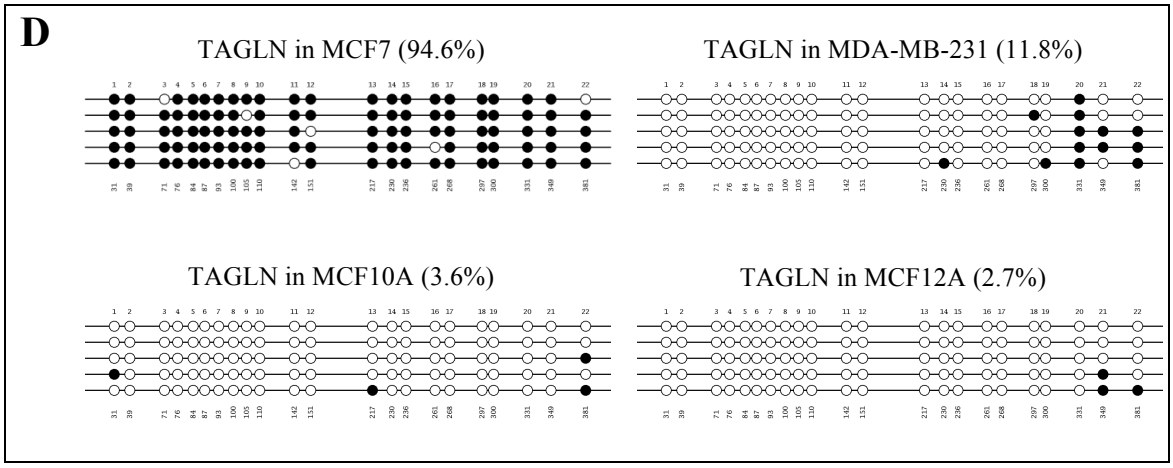

Figure 3.15 continued

S100A2 gene, on the other hand, was hypermethylated in both of the breast cancer cell lines, and was hypomethylated in the NT cell lines, and the difference between NT and breast carcinoma cells was significant (Figure 3.15C, $P < 0.0001$). Similarly, *TAGLN* gene promoter was hypermethylated in MCF7, was partially methylated in MDA-MB-231 cell lines, and was hypomethylated in the NT cells (Figure 3.15D, $P < 0.0001$). Thus, further bisulfite sequencing analyses were performed for these two genes in the other selected breast cancer cell lines which express these genes at lower levels (Figure 3.16). Both of the genes were hypermethylated in breast cancer cell lines analyzed (Figure 3.16A and B), and the differences in the methylation levels of the NT cells and breast carcinoma cells were statistically significant (both $P < 0.0001$, Figure 3.16C and D). Moreover, the expression levels of both *TAGLN* and *S100A2* were significantly and negatively correlated with the methylation percentages of these genes in the analyzed cell lines (Figure 3.16E and F), suggesting that these genes were downregulated via DNA hypermethylation of their promoter regions in breast cancer cell lines. Based on these findings, both of the genes were selected for further analyses in normal-tumor matched breast tissues.

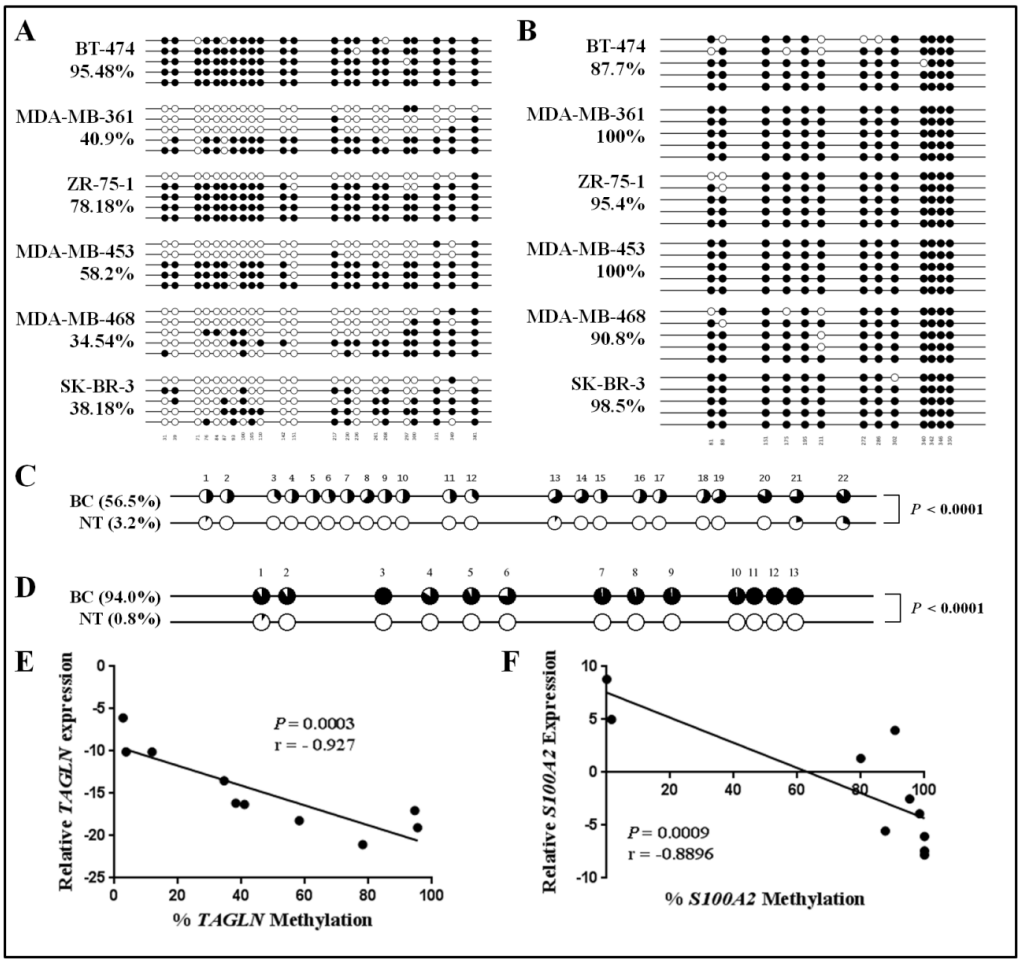

Figure 3.16: Methylation of *S100A2* and *TAGLN* in breast cancer and NT cell lines.

(A) TAGLN and (B) S100A2 promoter regions were hypermethylated in majority of the breast cancer cell lines, but not in NT cells. The differences between the NT and breast cancer (BC) cell lines were statistically significant (Mann-Whitney test) for both TAGLN (C), and S100A2 (D) genes. TAGLN (E), and S100A2 (F) methylation ratios were negatively and significantly correlated with the expression levels (shown in log_2, Spearman correlation). (C-F) Analyses of MCF7, MDA-MB-231, MC10A and MCF12A were also included.

3.3.4. Methylation analysis of *S100A2* in normal breast tissues

Methylation status of the promoter region of *S100A2* gene was analyzed in a set of normal breast tissues via bisulfite sequencing method. It was expected that the methylation ratios would be low in the normal breast tissues, as was the case in the NT breast cell lines. However, the bisulfite sequencing and subsequent QUMA analyses revealed that, *S100A2* gene was also extensively hypermethylated in the analyzed normal breast tissues (Figure 3.17A). Moreover, in a public methylation data (GSE20712) there was no significant difference between normal and breast tumor tissues' methylation scores for *S100A2* (Figure 3.17B). Based on these findings, further analyses on *S100A2* were ceased.

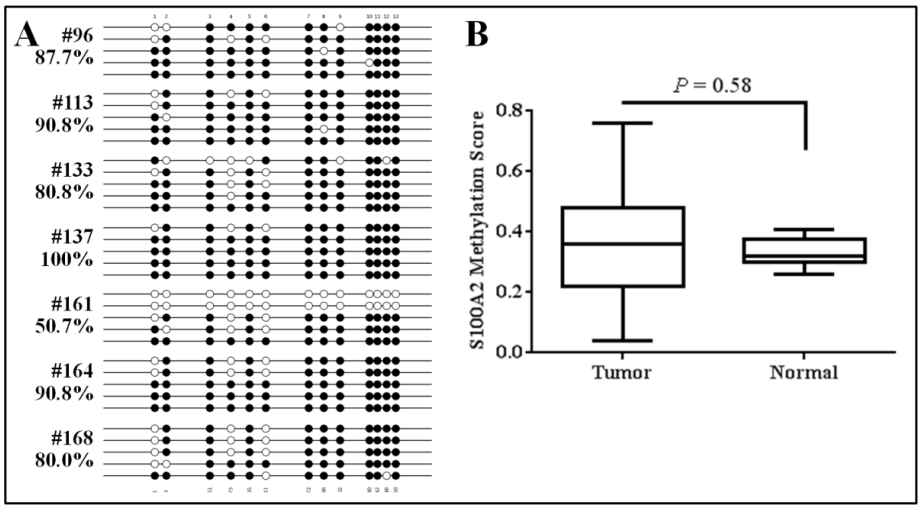

Figure 3.17: *S100A2* methylation in breast tissues.

(A) Bisulfite sequencing of S100A2 gene in normal tissues. The methylation ratios are presented as percentages (x.x%) under the patient codes (#xx).(B) Methylation scores of S100A2in tumor and normal tissues in public methylation array (Mann-Whitney test).

3.4. Methylation and expression analyses of *TAGLN* in breast tumors

3.4.1. Methylation analysis of *TAGLN* gene in breast tumors

Methylation of *TAGLN* was analyzed with bisulfite sequencing method in 21 matched normal-tumor breast tissues, and average *TAGLN* methylation was found to be higher in the tumors (56.3% methylation) compared to the normal tissues (39.4%, $P = 0.026$,Figure 3.18).

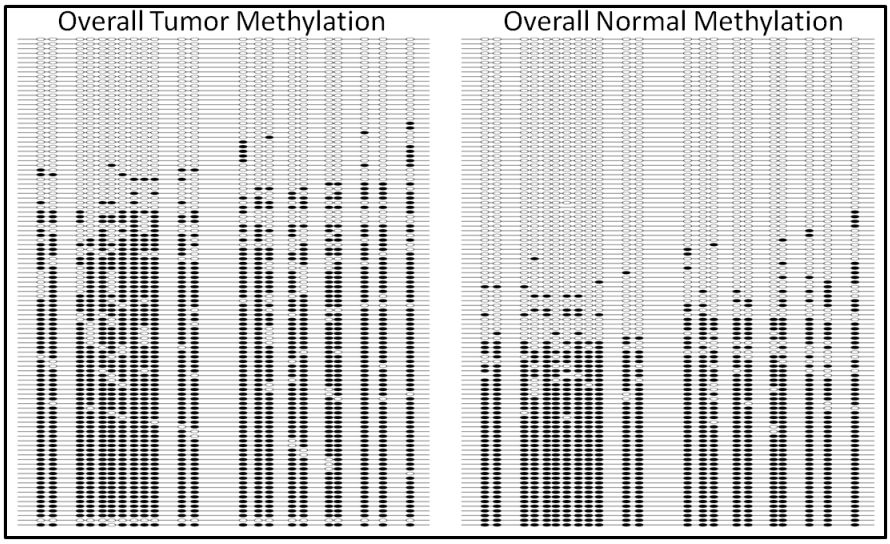

Figure 3.18: Overall *TAGLN* methylation in tumor and normal tissues.

TAGLN was hypermethylated in the tumor tissues compared to the paired normal breast tissues (P =0.026, Wilcoxon signed rank test).

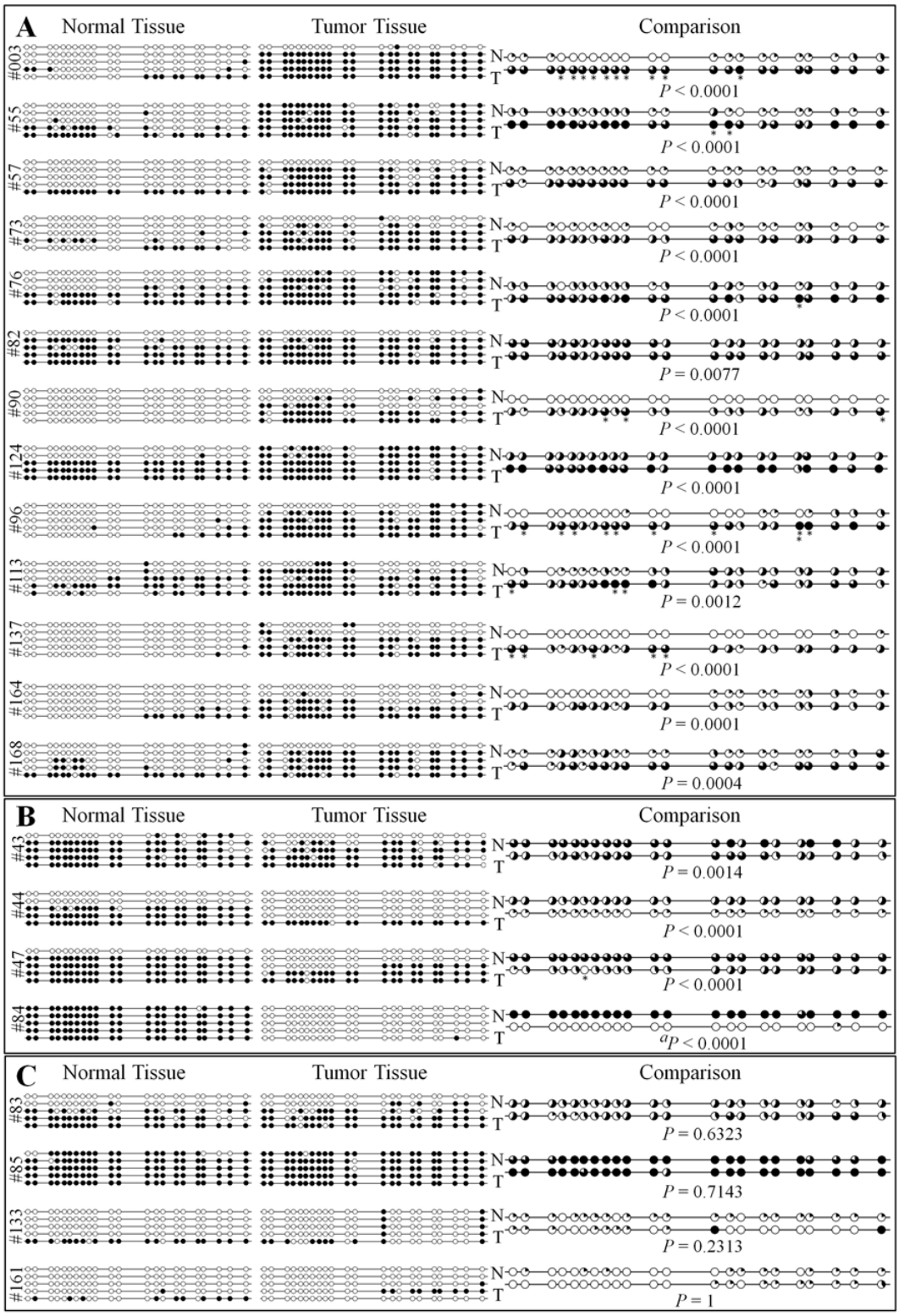

Figure 3.19: *TAGLN* methylation in matched normal-tumor breast tissues.

Paired normal breast and tumor tissues, and Wilcoxon signed rank test comparisons between the pairs are aligned side-by-side, as analyzed with QUMA and GraphPad. Individual significantly altered CpGs are designated with "".[a]All individual CpGs were significantly hypomethylated in the tumors of Patient#84 (P <0.01). (A) Patients with significantly hyper-methylated, and (B) hypomethylated tumors, and (C) with no significant differences between tumor and normal tissues. Empty circles: Unmethylated, Full circles: Methylated.*

When the tumor and normal tissues were analyzed pair-wise, *TAGLN* promoter region was significantly hypermethylated in 13/21 tumors, corresponding to 61.9% of all tumors (Figure 3.19A). *TAGLN* hypermethylation was evident in each grade although percentage of the tumors decreased with increasing grade (P = 0.25, Table 3.11), and there were no significant differences between the pathological or clinical groups analyzed (Figure 3.20B), except for the lymph node (LN) negative tumors, which had significantly higher methylation than the LN positive tumors (Figure 3.20A).

Table 3.11: *TAGLN* hypermethylation in matched tumor and normal breast tissues

Tumors (sample size)	Hypermethylated[a]	Hypomethylated[b]
All Tumors (21)	13 (61.90%)	4 (19.05%)
Grade 1 (5)	5 (100.00%)	0 (0.00%)
Grade 2 (11)	6 (54.55%)	3 (27.27%)
Grade 3 (2)	1 (50.00%)	1 (50.00%)

[a] and [b] numbers of tumors (percentage of tumors in the group), as determined by Wilcoxon signed rank test, P < 0.05. Adapted from Sayar et al.

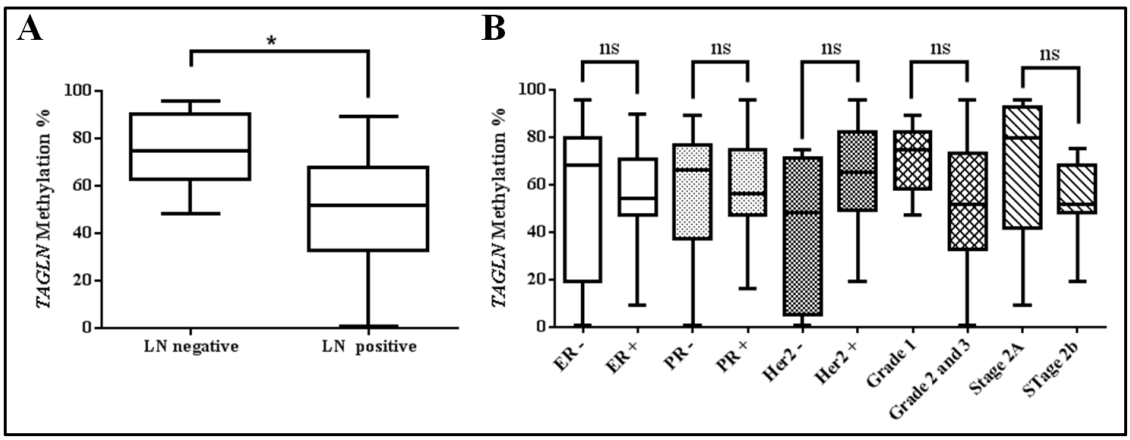

Figure 3.20: *TAGLN* methylation in different clinical and pathological groups.

(A) TAGLN methylation was significantly lower in LN positive tumors (: P <0.05), (B) but did not differ among other clinical and pathological groups (ns: not significant). Mann-Whitney test was used for comparisons.*

3.4.2. Expression analysis of *TAGLN* in matched tumor and normal tissues

TAGLN expression was analyzed in the paired tumor and normal tissues (Table 2.4) with qRT-PCR, using geometric means of *ACTB* and *SDHA* expressions as reference gene controls[367].

TAGLN expression was downregulated in 19 of 21 breast tumors, compared to paired normal tissues (Figure 3.21A). Of these 19 tumors, *TAGLN* was downregulated by more than 2 fold in 15 tumors. When the methylation ratios of *TAGLN* were considered, 9 out of 15, and 12 out of 19 tumors with downregulation displayed hypermethylation of *TAGLN* gene promoter (Figure 3.19A). Only two tumors had higher expression levels of *TAGLN* compared to their paired normal tissues, and one of these (Patient #47) also had hypomethylation of *TAGLN* promoter in the tumor tissue. To evaluate whether *TAGLN* downregulation in the tumors was due to promoter hypermethylation, Spearman correlation was calculated between the expression values and the methylation ratios, and *TAGLN* expression and methylation were found to be significantly and negatively correlated in the breast tissues (Figure 3.21B), implying a role of DNA hypermethylation in the regulation of *TAGLN* gene expression.

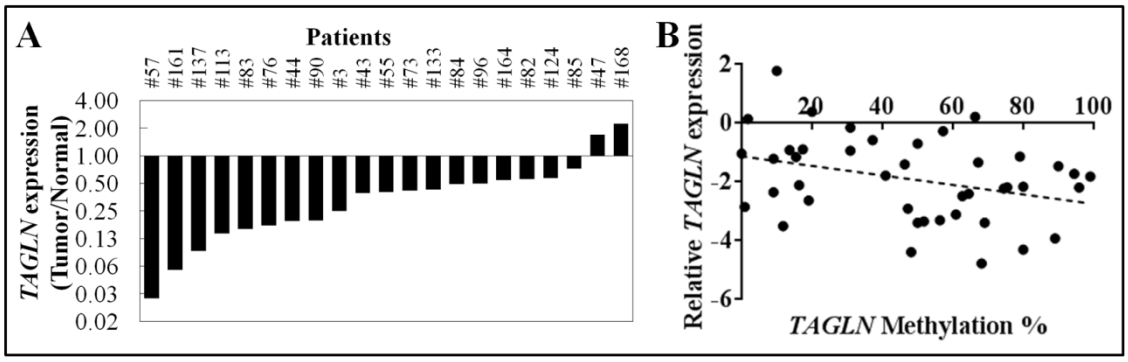

Figure 3.21: *TAGLN* expression in paired normal-tumor breast tissues.

(A) TAGLN expression was determined in matched tumor and normal breast tissues with qRT-PCR, and values were normalized to geometric means of ACTB and SDHA. Tumor-to-normal expression ratios have been depicted with actual values, in log 2 scale. (B) TAGLN methylation and expression in tumor and normal tissues were significantly and negatively correlated (Spearman r= - 0.3130, P = 0.0436). Reproduced from Sayar et al.[366]

Since the sample size of the tumor and normal tissues was small and some of the data regarding the clinical and pathological states of the tumors were missing (Table 2.4), significant associations could not be detected between any clinical parameter and the expression of *TAGLN*. Thus, *ANLN* gene expression was analyzed with qRT-PCR, and used as a determination of high cellular proliferation and worse prognosis in our matched tumor-normal tissues[409]. Its expression was compared with both expression and methylation levels of *TAGLN* gene. The expression of *TAGLN* was negatively (Spearman r = -0.4363, P = 0.0039), and the methylation ratios were positively correlated (Spearman r = 0.4847, P = 0.001) with *ANLN* expression in breast tissues, suggesting that *TAGLN* is hypermethylated and downregulated more in tumors with worse prognosis.

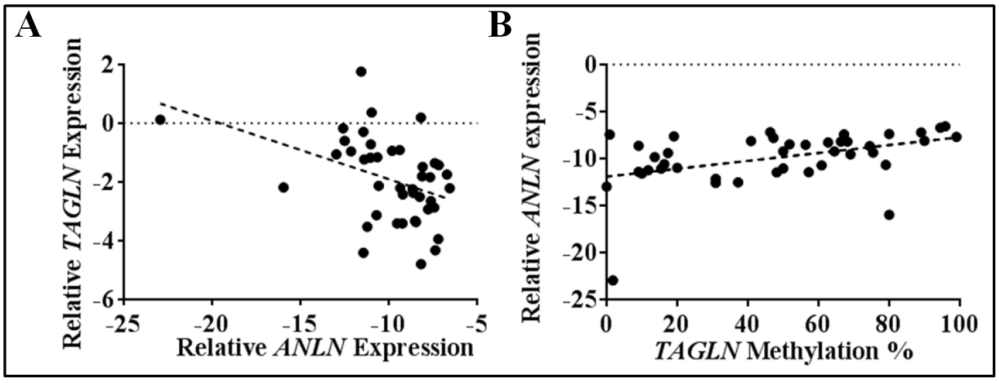

Figure 3.22: Correlation of *TAGLN* expression and methylation with *ANLN* expression in matched tumor-normal breast tissues.

Scatter plots show correlations of ANLN expression with (A) TAGLN expression (Spearman r = -0.4363, P = 0.0039); and (B) TAGLN methylation (Spearman r = 0.4847, P = 0.001) in breast tissues. Adapted from Sayar et al.[366]

3.4.3. Expression and promoter methylation analyses of *TAGLN* in publicly available microarray data

To increase the sample size for the methylation analyses of *TAGLN* gene, publicly available methylation data regarding breast tumors and normal tissues with available clinical data were downloaded from Gene Expression Omnibus (GEO, Super-series: GSE201713[110], n = 247 and GSE31979[375], n = 124). The distributions of the studies were similar, and after normalization using GraphPad Prism 6.0, the data were combined and the normalized average methylation scores (NAMSes) corresponding to the two probes of *TAGLN* gene promoter region were used for the analyses. The CpGs targeted by the probes were covered neither by our bisulfite sequencing primers nor the nearby CpG island (Figure 3.23A). Yet, akin to the results obtained from our matched normal-tumor breast tissues, *TAGLN* probes were also significantly hypermethylated in the tumor tissues compared to the normal tissues in this unpaired tissue set (average $NAMS_{tumors}$ ± SEM = 72.88 ± 0.91, and average $NAMS_{normals}$ ± SEM = 42.49 ± 1.54, $P < 0.0001$, n_{tumors} = 338 and $n_{normals}$ = 33, Figure 3.23B). Moreover, methylation scores of 83% of the tumors were higher than the highest score in the normal tissues. When the difference between the tumor and normal tissues' average NAMSes were considered ($av.NAMS_{tumors} - av.NAMS_{normals}$ = 30.38), tumors with NAMS >72.49 ($av.NAMS_{normals}$ + 30) were analyzed as hypermethylated, and those with NAMS < 22.49 ($av.NAMS_{normals}$ - 30) were analyzed as hypomethylated. Thereupon, 213 tumors (63.02%) were hypermethylated and 3 tumors (0.89%) were hypomethylated, with similar ratios for each grade group (Table 3.12). A subset of the tissues used in the methylation microarrays were also included in the expression microarray analyses (GSE20711; n = 90). When *TAGLN* methylation scores of these tumor were analyzed

with the corresponding *TAGLN* gene expression levels, a significant and negative correlation was evident (Spearman r = -0.5442, $P < 0.0001$), as observed in our matched tumor and normal breast tissues (Figure 3.23C).

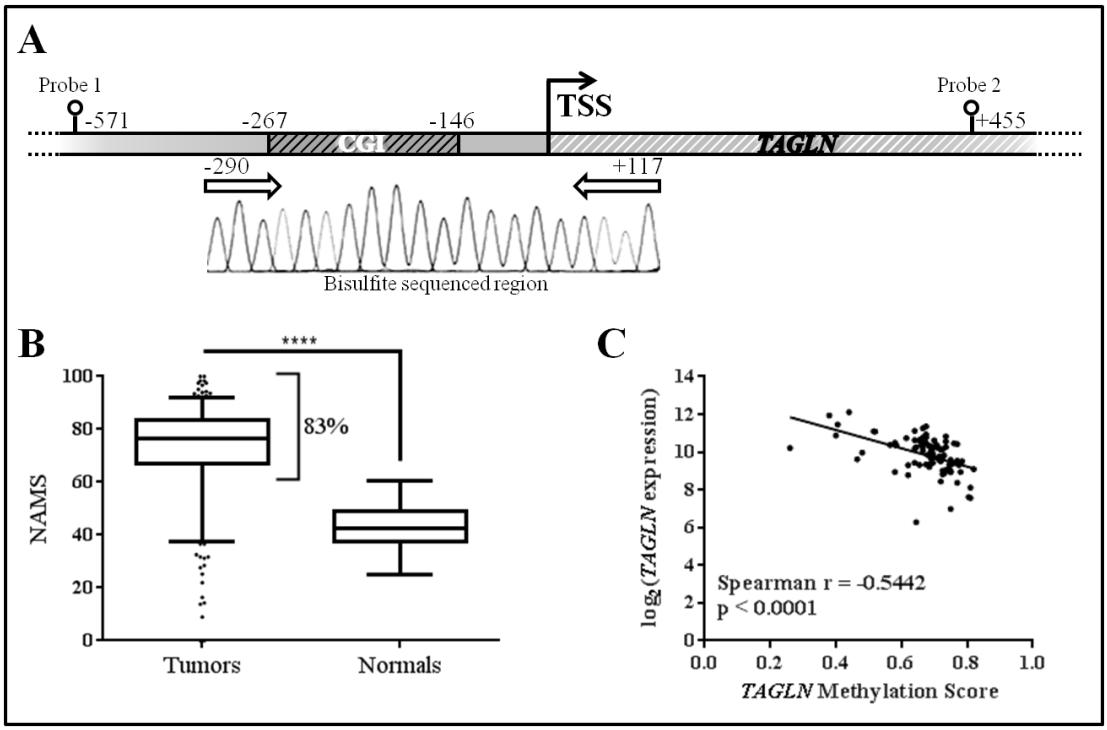

Figure 3.23: Methylation of *TAGLN* probes in public data sets.

*(A) Schematic representation of locations of the CpGs targeted by the probes of the methylation microarray platform GPL8490, and by the bisulfite sequencing primers. TSS: Transcription start site. CGI: CpG island. (B) Box-plots showing hypermethylation of TAGLN in tumor tissues. **** $P < 0.0001$, Mann-Whitney test. Whiskers show 5-95 percentiles. (C) Scatter plot showing correlation of TAGLN methylation scores with log_2 expression levels in dataset GSE20713 (n = 90).*

Table 3.12: *TAGLN* hypermethylation in public tumor and normal breast tissues

Tumors (sample size)	Hypermethylated[a]	Hypomethylated[b]
All Patients (n=338)	213 (63.02%)	3 (0.89%)
Grade 1 (n=64)	41 (64.06%)	0 (0.00%)
Grade 2 (n=57)	35 (61.40%)	1 (1.75%)
Grade 3 (n=215)	135 (62.79%)	2 (0.01%)

[a] Number of tumors (percentage of tumors in the group) with NAMS >72.49; [b] Number of tumors (percentage of tumors in the group) with NAMS < 22.49. Adapted from Sayar et al.

TAGLN methylation levels were compared between different clinical and pathological groups such as grade, stage, ER, PR and Her2 statuses, molecular subtypes, patient age, and tumor size. There were no differences between the groups analyzed, except for the age and the subtypes. *TAGLN* methylation was significantly higher in tumors of older patients (*i.e.* older than 50 years old, Figure 3.24A), and in LumB tumors compared to other subtypes (Figure 3.24B). When relapse free survival (RFS) fractions of patients were analyzed between high and low methylation groups, patients with lower *TAGLN* methylation scores survived better than the patients with higher *TAGLN* methylation in their tumors ($P = 0.0059$, Figure 3.24C). Among the data sets used, only GSE20713 had the overall survival (OS) data available for the patients. Thus, using the methylation scores (MS) of *TAGLN* in this data set, we also performed OS analysis, and similarly found that, patients with lower levels of *TAGLN* methylation scores had significantly higher survival fractions (Figure 3.24D).

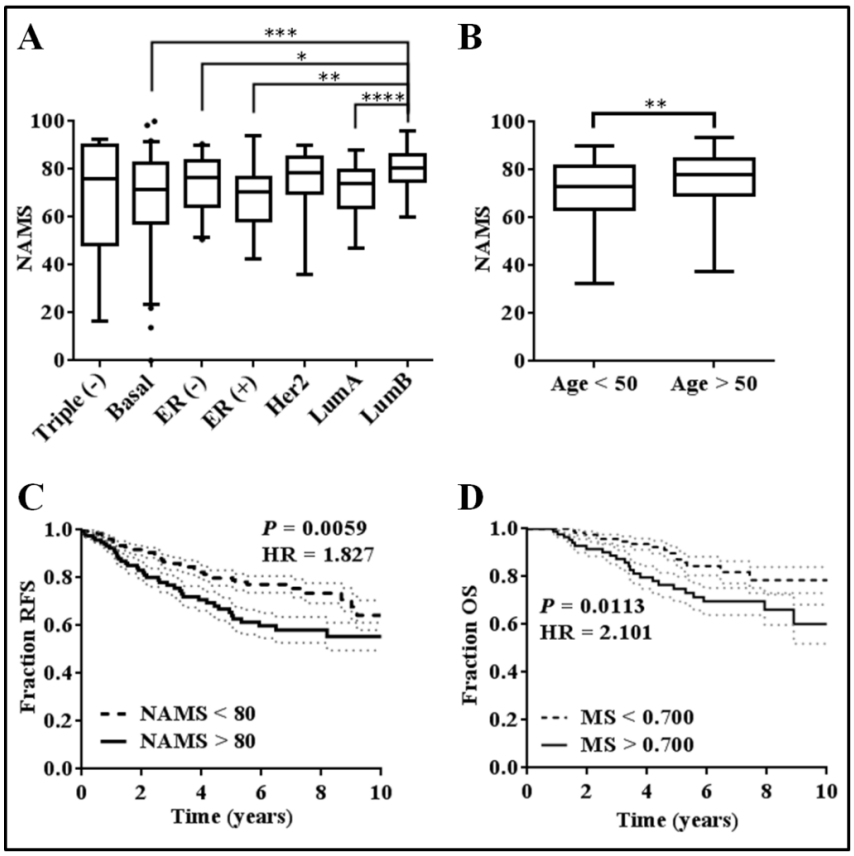

Figure 3.24: Evaluation of *TAGLN* methylation with clinical parameters in public data.

*(A) TAGLN methylation in different molecular subtypes. (B) Comparison of TAGLN methylation in patient age groups. * P < 0.05; ** P < 0.01; *** P < 0.001; **** P < 0.0001, Mann-Whitney test. Whiskers show 5-95 percentiles. (C) RFS of patients with high and low levels of TAGLN methylation (best cut off was used). (D) OS of patients with high and low levels of TAGLN methylation (best cut off was used). HR: hazards ratio. Error bars are represented by gray points.*

3.4.4. *TAGLN* hypermethylation as a breast tumor biomarker

The consistency of higher methylation in the tumor tissues and strikingly stacked and lower methylation levels in the normal tissues (Figure 3.23B) indicated a possible use of *TAGLN* methylation as a tumor biomarker. When receiver-operator characteristics (ROC) analyses were performed with the NAMS values of *TAGLN* to address this issue, NAMS > 60.94 was obtained as the threshold value which could identify breast tumors with 83.14% sensitivity and 100% specificity, among the tumor and normal tissues population. The calculated area under the curve (AUC) was 0.9289, with 95% confidence interval (CI) of 0.9027 to 0.9552, and likelihood ratio > 27.43 ($P < 0.0001$, Figure 3.25A). These results indicated that *TAGLN* promoter methylation could be a promising biomarker in breast cancer. However, it is better to be able to identify the disease by detecting the methylation patterns of the cell free DNA from the blood or serum of patients, for a strong biomarker. To see whether methylation of *TAGLN* could be detected from serum, we have downloaded the breast cancer methylation data sets that were collected from sera samples, namely GSE52621 and GSE5819. Although there were no normal sera samples in GSE52621 data set, *TAGLN* methylation detected from the sera of cancer patients was significantly higher than the methylation levels in the normal tissues (Figure 3.25B). When combined with the healthy sera data from GSE58119, *TAGLN* methylation in the cancer sera was significantly higher than the normal sera samples (Figure 3.25C). However, since the data are from either different tissues or from different studies, it is not possible to make a conclusion. Yet, these data hint that it is possible to detect *TAGLN* methylation from breast cancer patients' serum samples.

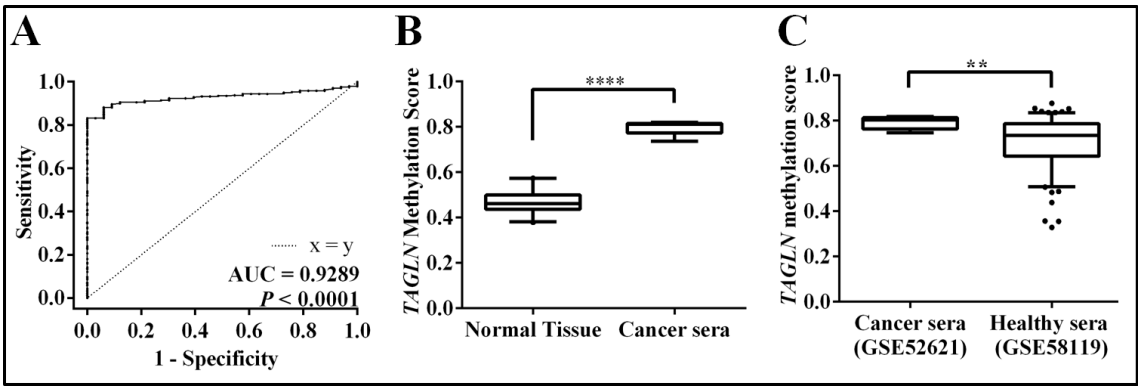

Figure 3.25: *TAGLN* as a serum methylation biomarker for breast tumors.

*(A) TAGLN methylation levels could identify breast tumors among the normal breast tissues with 83.14% sensitivity and 100% specificity, when NAMS > 60.94 threshold was used. Reproduced from Sayar et al[366].(B) TAGLN methylation was higher in the sera from breast cancer patients compared to normal tissues. (C) TAGLN methylation in serum samples from cancer patients was significantly higher than in the healthy individuals' sera. **** P < 0.001; ** P < 0.01, Mann-Whitney test.*

3.4.5. *TAGLN* expression in independent sets of breast tumor tissues

TAGLN expression was analyzed in the breast tumor expression arrays available in Oncomine database[372], and was found to be downregulated by more than two folds (P <0.05) in 62% of the breast cancers compared to the normal tissues (*i.e.,* 8 out of 13 breast cancer vs. normal studies, Table 3.13), similar to our findings in matched tumor-normal breast tissues (Figure 3.21).

Table 3.13: Cancer vs. normal analysis of *TAGLN* mRNA in Oncomine database

Study	Cancerous tissue being compared to normal	*P* value	FC[a]	Gene Rank[b]
Richardson 2 (n = 47)	DBC	$1.03x10^{-12}$	-5.92	0.3
Turashvili (n = 30)	ILC	$8.20x10^{-04}$	-2.26	0.4
	IDC	$1.50x10^{-02}$	-2.95	4.9
Ma 4 (n = 66)	DCIS epitehlia	$2.90x10^{-07}$	-2.78	0.4
	IDC Epithelia	$4.01x10^{-05}$	-2.28	1.2
TCGA (n = 593)	Mucinous BC	$9.64x10^{-07}$	-2.37	1.2
	IDC	$3.48x10^{-38}$	-2.70	1.5
	Invasive BC	$1.69x10^{-19}$	-2.32	3.1
	Mixed LBC and DBC	$8.86x10^{-06}$	-2.35	3.2
	Intraductal Cribriform Breast Adenocarcinoma	$4.10x10^{-02}$	-3.10	21
	IDC and ILC	$4.10x10^{-02}$	-2.55	23.9
Sorlie (n = 85)	LBC	$3.80x10^{-02}$	-2.15	6.8
	DBC	$3.00x10^{-02}$	-2.13	15.4
Perou (n = 65)	DBC	$1.10x10^{-02}$	-2.10	8.6
Curtis (n = 2136)	IDC	$7.15x10^{-50}$	-2.30	4.7
	Medullary BC	$1.29x10^{-09}$	-3.37	7.3
	Mucinous BC	$9.39x10^{-14}$	-2.59	7.5
	ILC	$2.05x10^{-21}$	-2.06	7.8
	BC	$5.77x10^{-05}$	-2.68	8.5
	Invasive BC	$1.68x10^{-04}$	-2.62	12.0
Finak (n = 59)	Invasive BC Stroma	$2.65x10^{-05}$	-3.84	33.4

[a]FC: Fold change; [b]Percent top genes. BC: Breast carcinoma; LBC: Lobular breast carcinoma; DBC: Ductal breast carcinoma.

TAGLN gene expression was downregulated both in the breast cancer cell lines and the tumor tissues compared to the matched normal tissues, yet the sample sizes were not large enough to make conclusions regarding clinical and pathological analyses. Thus, two more completely independent sets of breast tissue arrays with clinical information, one cDNA panel (n = 41 tumors and 7 normal tissues) and one tissue section array (n = 68 tumor tissues and 7 normal tissues), were purchased to analyze *TAGLN* mRNA and protein levels by qRT-PCR and immunohistochemistry (IHC), respectively. Our analyses show that *TAGLN* was significantly downregulated in both mRNA and protein levels in these arrays, compared to the normal tissues included (Table 3.14, Figure 3.26A and B). When the clinical and pathological parameters were considered, both *TAGLN* mRNA and protein expressions were downregulated in grade 3 tumors compared to grade 1 - 2 tumors (P = 0.049 and P = 0.0329, respectively, Figure 3.26C), in progesterone receptor PR $^{(-)}$ tumors compared to PR $^{(+)}$ tumors (P = 0.0031 and P = 0.0043, respectively, Figure 3.26D), and in more aggressive type, triple negative (TN) tumors compared to tumors with any positivity in any of the estrogen or progesterone receptors, or human epidermal growth factor receptor 2 (Her2, P = 0.0063 and P = 0.0489, respectively, Figure 3.26E). There were no differences between the *TAGLN* expression levels in various stages, lymph node groups, or in either estrogen receptor (ER) or Her2 positive or negative tumors.

Table 3.14: Expression of *TAGLN* in independent tumor and normal tissues

Analysis	Tumor value ± SEM (n)	Normal value ± SEM (n)	*P* value[a]
qRT-PCR[b]	0.1858 ± 0.0387 (41)	0.4248 ± 0.0792 (7)	0.0072
IHC (H-score)	169.8 ± 9.773 (67)	243.6 ± 25.35 (7)	0.0116

SEM: standard error of means; n: sample size; [a]P values were calculated according to Mann-Whitney test; [b] Relative expression levels with respect to geometric means of ACTB and SDHA internal control genes. H-score: immunohistochemical score.

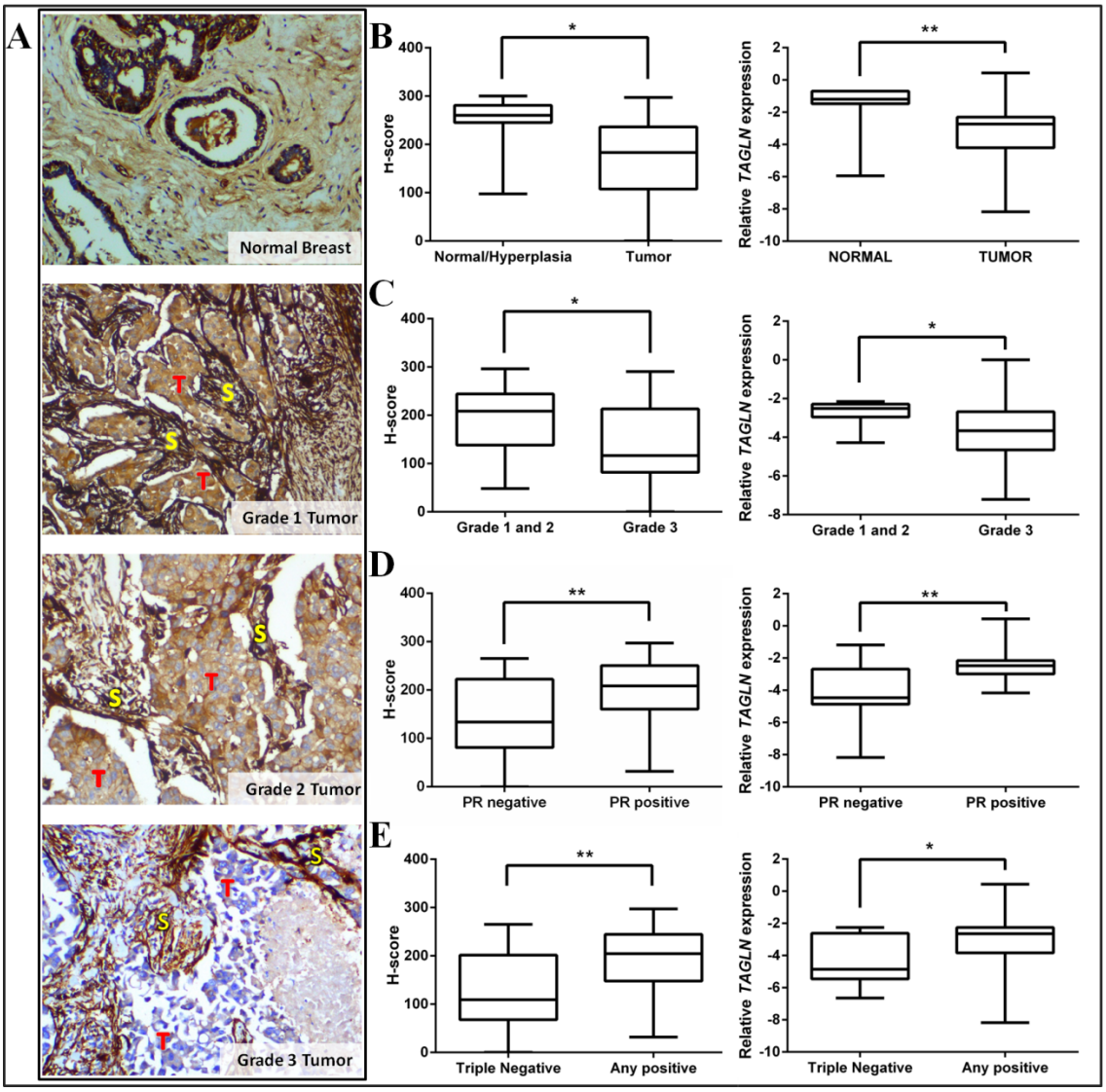

Figure 3.26: *TAGLN* expression in independent sets of breast tumors.

*(A) TAGLN IHC staining in normal tissue, and grade 1, 2 and 3 tumors. TAGLN staining is extensive in stroma (S), and decreased in the tumor tissues (T). (B-E)TAGLN is downregulated in both protein (left) and mRNA (right) levels, respectively: in tumor (n=67 and n=41) compared to normal(n=7 for both) tissues (B); in grade 3 tumors (n=16 and n=20) compared to grade 1-2 tumors(n=39 and n=17) (C); in $PR^{(-)}$ tumors (n=37 and n=14) compared to $PR^{(+)}$ tumors (n=26 and n=15) (D); and in TN tumors (n=17 and n=6) compared to tumors with positivity in any of the ER, PR, or Her2 (n=42 and n=23) (E). * P < 0.05; ** P < 0.01; *** P < 0.001; and **** P < 0.0001. Mann-Whitney test. Adapted from Sayar et al[366].*

Since *TAGLN* expression was consistently downregulated in the tumor tissues and with added significance in more aggressive tumors, we wanted to unveil whether *TAGLN* expression could be used as a determinant for OS or RFS of breast cancer patients. Since none of the tissue panels used in the study offered patient survival data, we used Kaplan-Meier Plotter (KM Plotter [376]) which performs KM analyses using public breast cancer microarray expression and available

survival data to analyze connection of *TAGLN* expression and OS or RFS of breast cancer patients. Neither OS ratios nor RFS ratios differed significantly in low or high *TAGLN* expression groups (Figure 3.27A). However, when the patient cohorts were sub-divided into grade groups, higher *TAGLN* expression was significantly linked with better survival, both OS and RFS, in both grade 1 and grade 2 tumors (Figure 3.27B). There was no significant difference among the grade 3 patients.

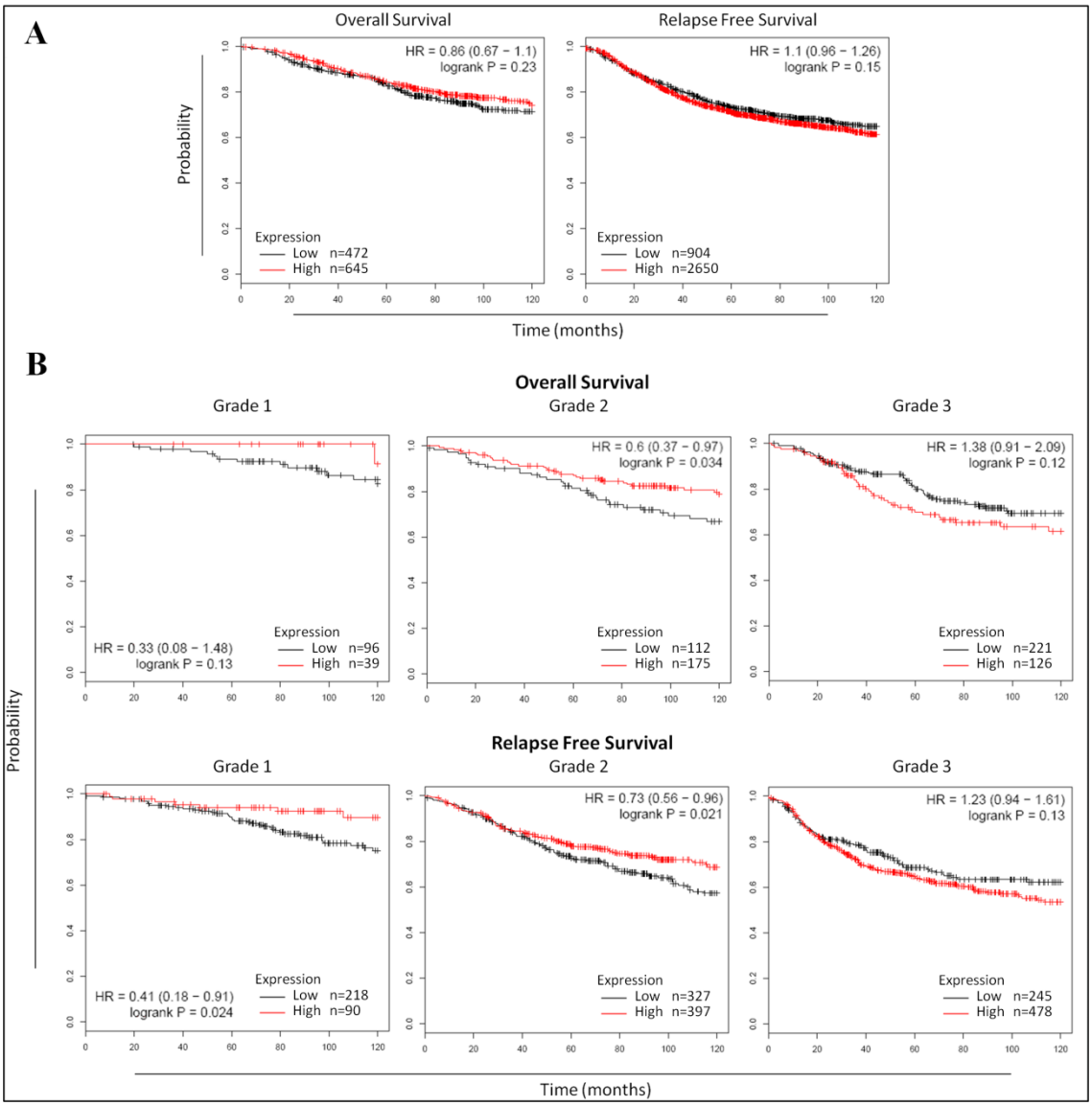

Figure 3.27: Kaplan-Meier analyses with *TAGLN* expression in breast cancer patients.

(A) TAGLN expression levels did not affect survival ratios when all the patients were analyzed together. (B)Patients with grade 1 and grade 2 tumors survived significantly better if TAGLN expression was higher in the tumor tissues (left and middle panels). Neither OS nor RFS were significantly affected by the changes in TAGLN expression levels (right panels).Reproduced from Sayar et al.[366]

3.5. Functional analyses of transgelin

3.5.1. Effect of *TAGLN* expression on colony formation in breast cell lines

Consistent downregulation of *TAGLN* in tumors and its association with survival of patients hint for a tumor suppressor role for this protein in breast cancer. Since *TAGLN* expression was negatively correlated with high proliferation marker *ANLN*'s expression, we studied the effect of changes in *TAGLN* expression levels on colony formation of breast cancer and NT breast cells. MDA-MB-361 cells, which do not express transgelin protein, and MDA-MB-157 cells which express transgelin at intermediate levels, were selected to over-express *TAGLN* gene (Figure 3.28A). The highest expression was observed in NT cells MCF10A and MCF12A cells, as well as the MDA-MB-231 cells. Thus we selected these cell lines and MDA-MB-157 cells to silence *TAGLN* expression with siRNA transfections (Figure 3.28A). siRNA transfections were only successful in MCF10A and MCF12A cells (Figure 3.28B and C), thus the remaining studies were performed with these cell lines. Figure 3.28B and C show that, *TAGLN* silencing in NT breast cell lines resulted in increased colony formation. On the contrary, when *TAGLN* was over-expressed in MDA-MB-361 cells, a decrease in the sizes of colonies, *i.e.* proliferation of the cells, was observed (Figure 3.28D). However, additional *TAGLN* expression in MDA-MB-157 cells, which normally express the gene at intermediate levels, did not affect colony formation potentials of the colonies (Figure 3.28E), suggesting that there is a dose effect in regulation of cellular proliferation and colony formation.

3.5.2. Effect of *TAGLN* over-expression on cell migration and invasion

Transgelin's close association with actin cytoskeleton and stress fibers implies a role of this protein in cellular migration. Thus, we analyzed the effect of *TAGLN* over-expression on migration and invasion of normally motile MDA-MB-157 cells (Figure 3.29). Neither wound closure (Figure 3.29A) nor numbers of cells invading the Matrigel and passing through the basal membrane (Figure 3.29B) were affected by the increase in transgelin protein levels. Wound closure experiments were also performed with non-motile MDA-MB-361 cells, yet there was no difference in the closed area upon increased *TAGLN* expression (Figure 3.29C). Therefore, transgelin over-expression does not affect migration or invasion potentials of these breast cancer cells.

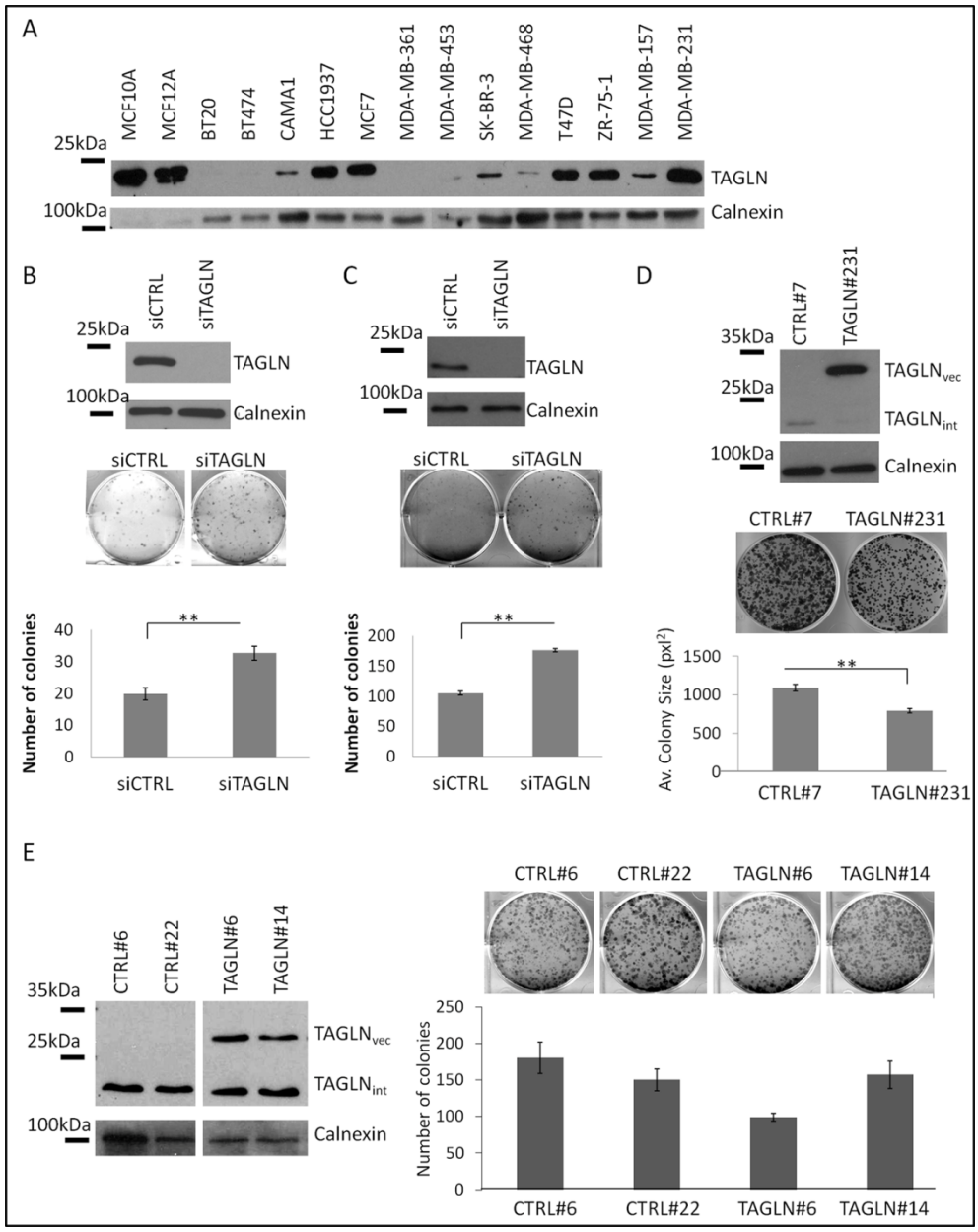

Figure 3.28: Colony formation in cells with altered *TAGLN* expression.

*(A) Transgelin protein expression was determined in cell lines with western blot experiments. (B-C)TAGLN silencing resulted in increased number of colonies in MCF10A cells (B), and MCF12A cells (C). TAGLN overexpression in MDA-MB-361 cells resulted in decreased sizes of colonies (D), while overexpression in MDA-MB-157 cells did not affect colony formation (E) $TAGLN_{vec}$: TAGLN expression from the vector. $TAGLN_{int}$: Intrinsic TAGLN expression. CTRL# and TAGLN# represent control vector and TAGLN overexpressing vector transfected colony numbers, respectively. ** $P < 0.01$, t-test. Reproduced from Sayar et al.*[366]

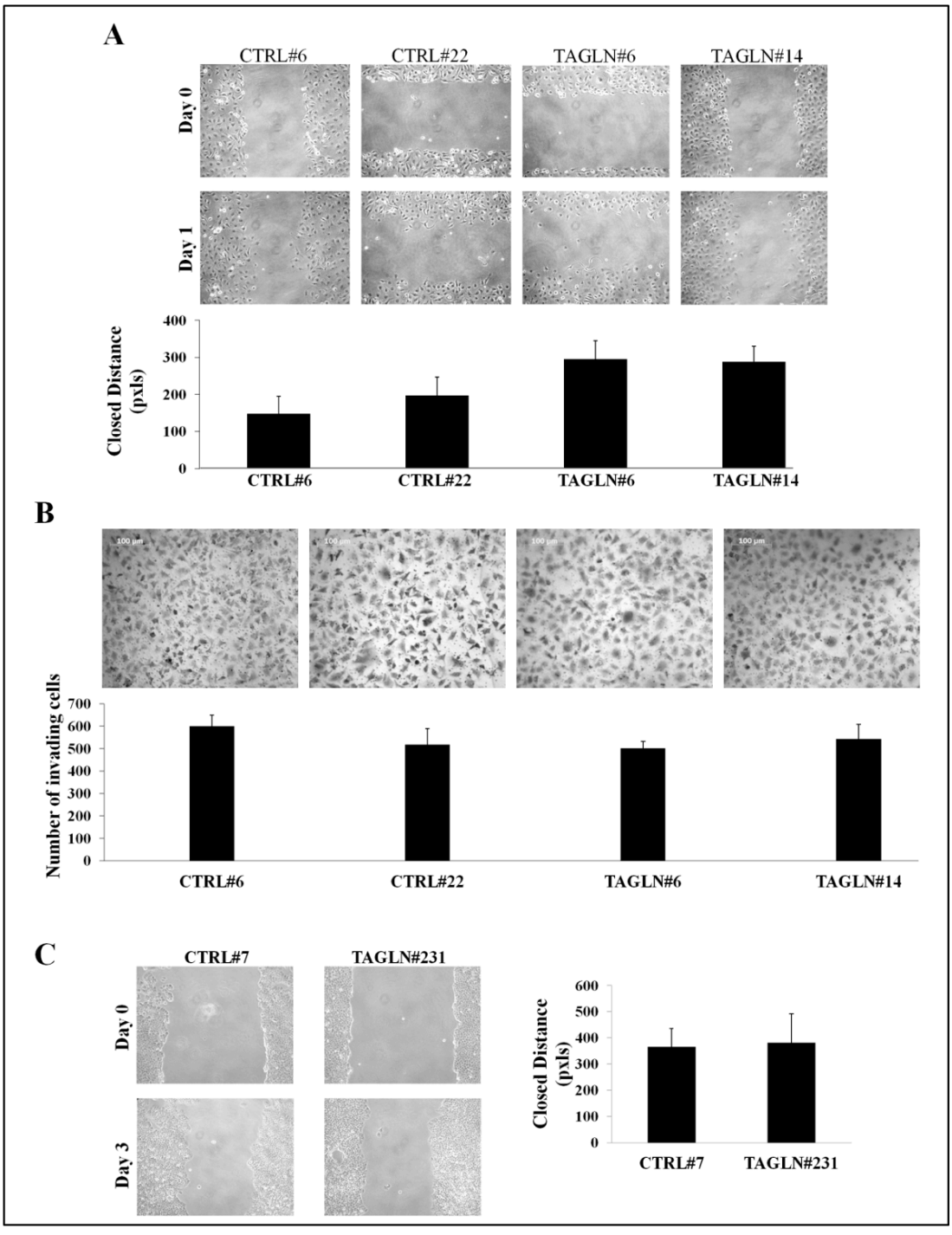

Figure 3.29: Effect of *TAGLN* over-expression on migration and invasion of breast cancer cells.

TAGLN overexpression in MDA-MB-157 cells did not result in a significant difference in either migration (A), or invasion (B) of normally motile MDA-MB-157 cells. CTRL#6 and CTRL#22: MDA-MB-157 cell clones transfected with control vector. TAGLN#6 and TAGLN#14: MDA-MB-157 cell clones transfected with TAGLN over-expression vector. (C)TAGLN over-expression did not affect wound closure in MDA-MB-361 cells. CTRL#7: MDA-MB-361 cell clones transfected with control vector. TAGLN#231: MDA-MB-361cell clones transfected with TAGLN over-expression vector.(A-B) Reproduced from Sayar et al.[366]T-test was performed for comparisons.

3.5.3. Transgelin and epithelial-to-mesenchymal transition (EMT) in breast cancer and NT cell lines

Transgelin is a mesenchymal protein, and its expression increases with EMT[329, 354-355, 410]. Thus, we wanted to explore whether *TAGLN* expression also differs in epithelial and mesenchymal breast cancer cells, and whether it is related to any epithelial or mesenchymal markers. First, we performed immunofluorescent (IF) staining in breast cancer cell lines and NT breast cells; and double-stained the cells either with transgelin and vimentin (mesenchymal marker), or with transgelin and E-cadherin antibodies.

Transgelin staining was positive in NT MCF10A and MCF12A cells (Figure 3.30A and B), with some larger cells having intense staining. All of the transgelin $^{(+)}$ cells were also vimentin $^{(+)}$ (Figure 3.30A and B left panels); however, some cells in MCF10A population showed tendency to be exclusive for transgelin and E-cadherin staining (Figure 3.30A, arrows). Transgelin staining was ubiquitous in the cells, with accumulated levels in nuclei and cell membranes in MCF10A cells (Figure 3.30A). Nuclear expression was lower in MCF12A cells (Figure 3.30B).

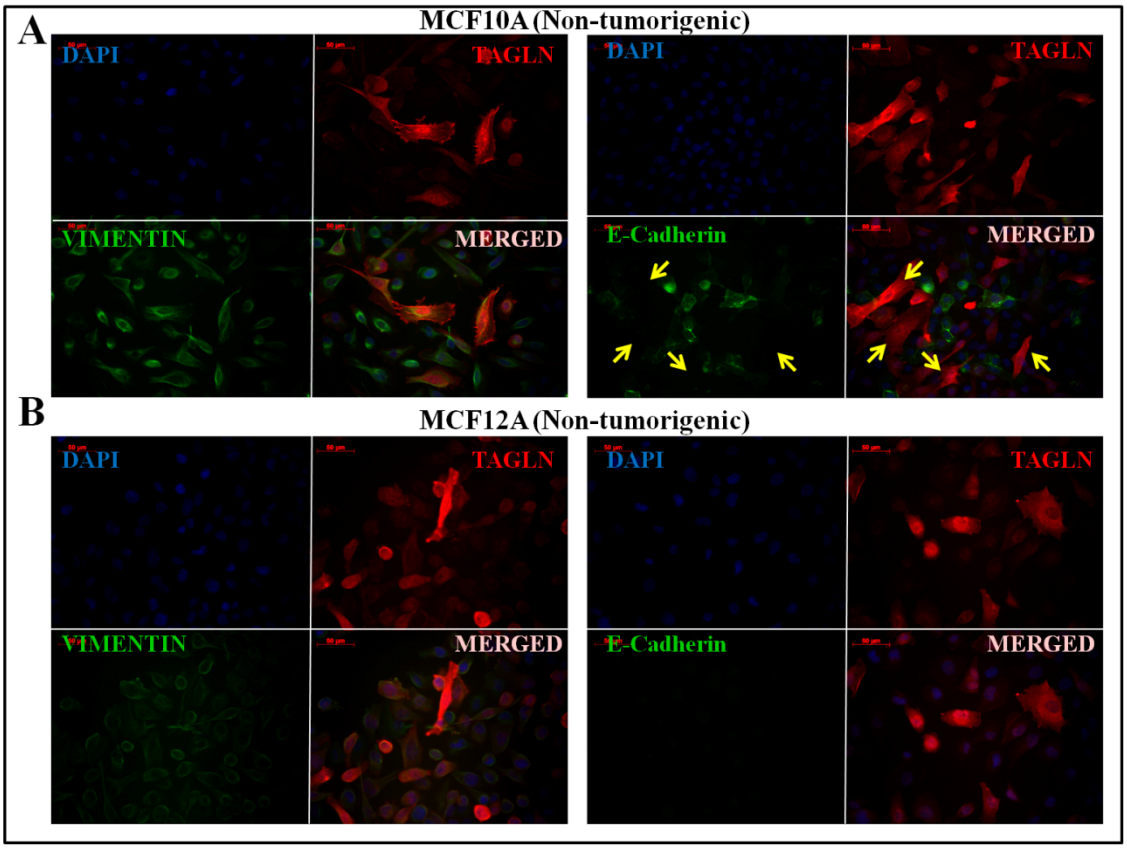

Figure 3.30: Co-staining of transgelin with vimentin or E-cadherin in NT breast cells.

IF co-staining in NT MCF10A (A) and MCF12A (B) cells with transgelin and vimentin (left panel), and transgelin and E-cadherin (right panel) antibodies. Arrows show cells where an exclusion is seen between TAGLN and E-cadherin. 400X images have been shown.

Transgelin staining was much lower in invasive breast cancer cells MDA-MB-231 and MDA-MB-157 (Figure 3.31A and B) compared to NT breast cells (Figure 3.30A and B); however, there was a basal, low level of staining, and some cells had increased staining compared to the others. All of the cells were vimentin $^{(+)}$ (Figure 3.31A and B left panels) and E-cadherin $^{(-)}$ (Figure 3.31A and B right panels), since these are known as mesenchymal cells.

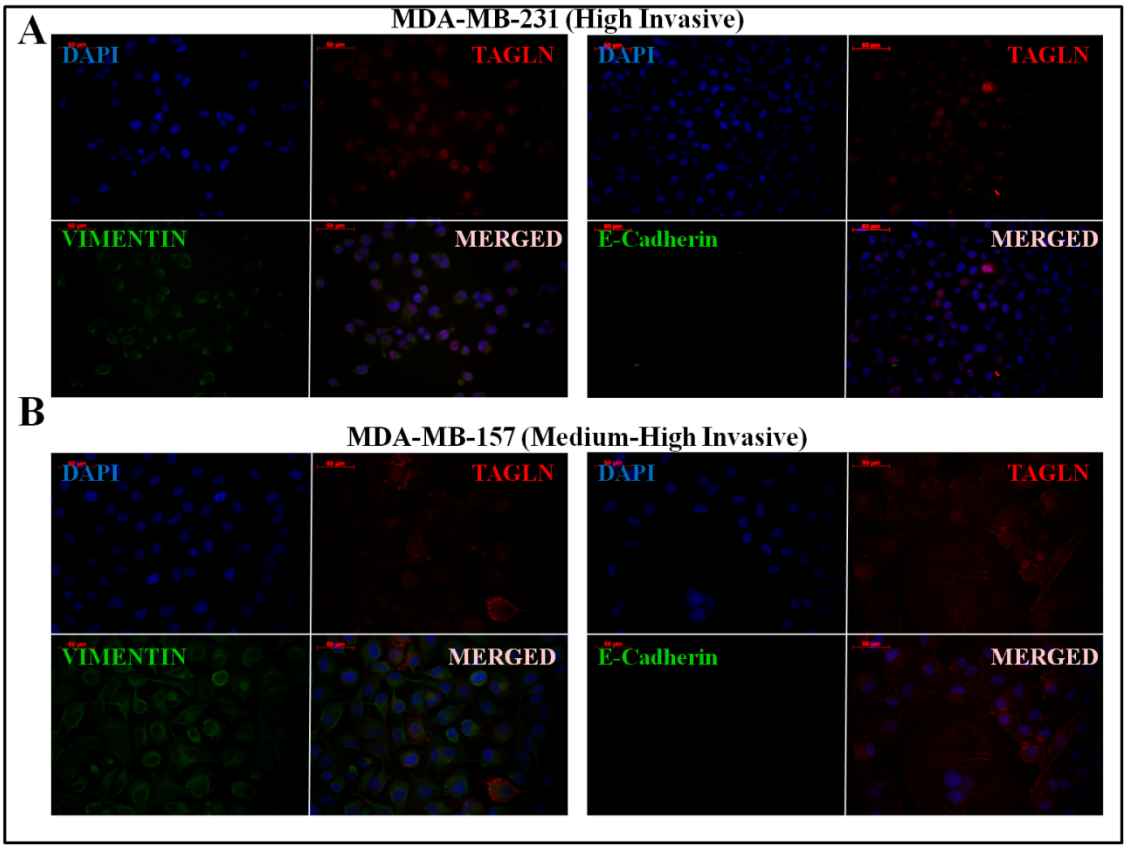

Figure 3.31: Co-staining of transgelin with vimentin or E-cadherin in highly invasive breast cancer cells.

IF co-staining in highly invasive MDA-MB-231 cells (A); and in medium-to-highly invasive MDA-MB-157 cells (B) with transgelin and vimentin (left panel), and transgelin and E-cadherin (right panel) antibodies. 400X images have been shown.

When low-invasive breast cancer cell lines were analyzed, we see that the MDA-MB-468 cells had low levels of transgelin staining, with relative increase in certain cells in the population compared to the others (Figure 3.32A). These cells were neither vimentin $^{(-)}$ nor E-cadherin $^{(-)}$, but expressed both markers at low levels. T47D and ZR-75-1 cells, on the other hand, were highly positive for E-cadherin staining (Figure 3.32B and C, right panels), and expressed transgelin protein at intermediate levels throughout the cells, with minor accumulations at certain points and cell membranes in ZR-75-1 cells (Figure 3.32C). Moreover, the exclusion of E-cadherin and transgelin observed in MCF10A cells was not evident in these cells (Figure

3.32C, right panel) or in T47D cells (Figure 3.32B, right panel). The expression levels of transgelin observed in these cells were similar to the results of the western blot analyses (Figure 3.28A).

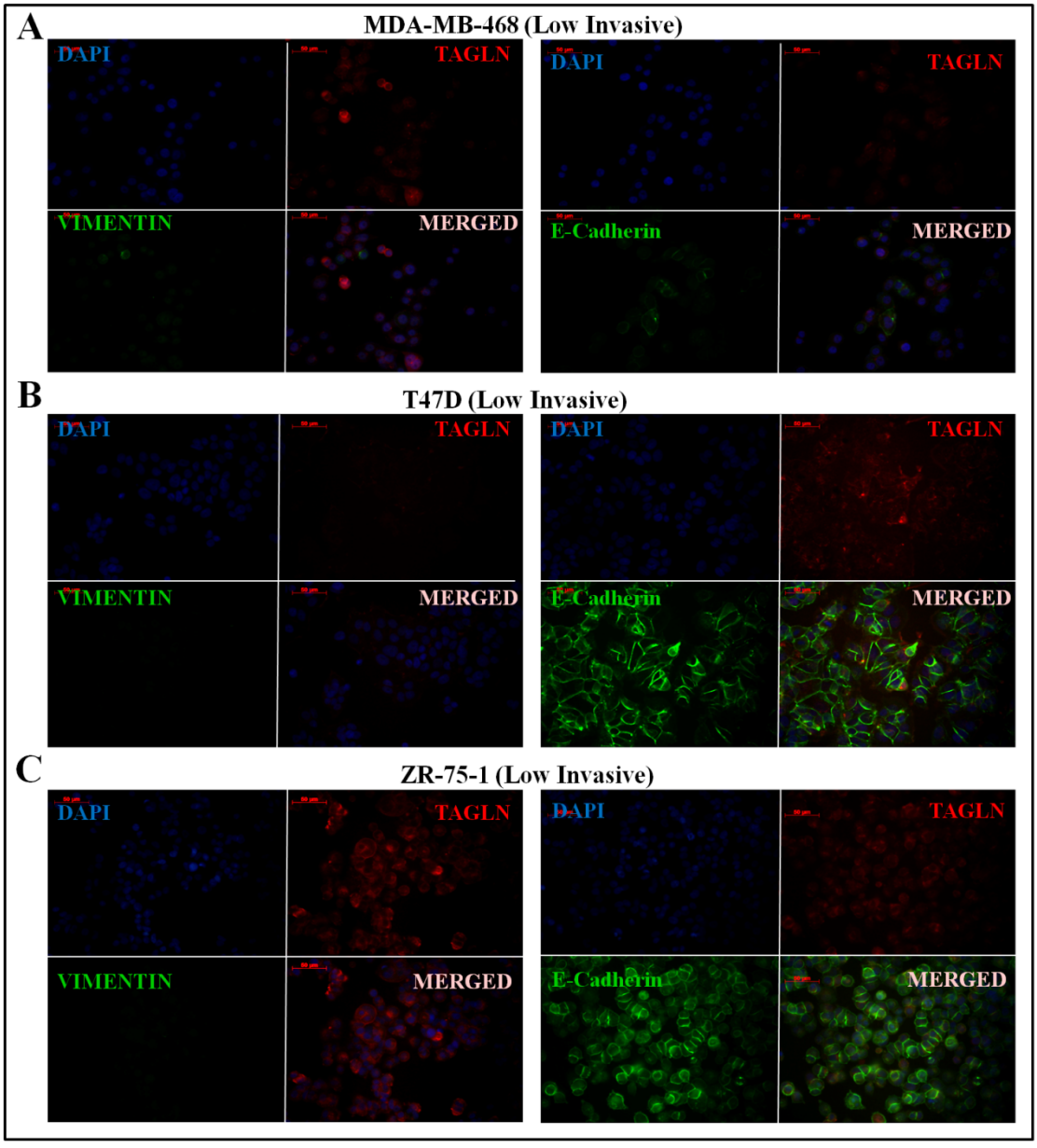

Figure 3.32: Co-staining of transgelin with vimentin or E-cadherin in low invasive breast cancer cells.

IF co-staining in low invasive MDA-MB-468 (A); T47D (B); and ZR-75-1 (C) breast cancer cells with transgelin and vimentin (left panel), and transgelin and E-cadherin (right panel) antibodies. 400X images have been shown.

Next, we analyzed non-invasive breast cancer cells for transgelin, E-cadherin and vimentin staining. Figure 3.33 shows non-invasive breast cancer cells with high E-cadherin expression,

BT-474 and HCC-1937. Transgelin staining was at intermediate levels in these cells and regardless of the E-cadherin staining, each cell expressed transgelin at similar levels in BT-474 cells (Figure 3.33); however, some cells displayed exclusion between E-cadherin and transgelin in HCC-1937 cells (arrows, Figure 3.33B). When localization of the staining was considered, transgelin staining was mostly even throughout the cell body in both BT-474 and HCC-1937 cells.

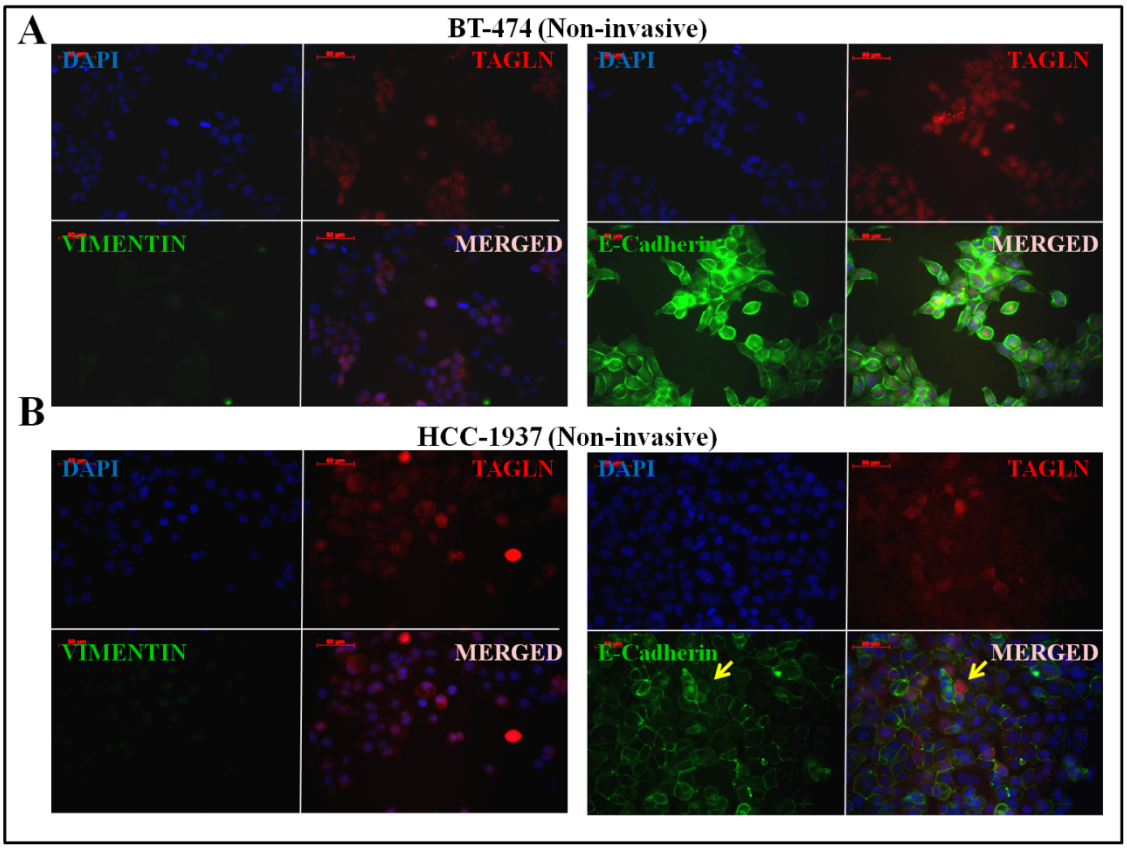

Figure 3.33: Co-staining of transgelin with vimentin or E-cadherin in non-invasive breast cancer cells with high levels of E-cadherin expression.

IF co-staining in non-invasive epithelial BT-474 (A); and HCC-1937 (B) breast cancer cells with transgelin and vimentin (left panel), and transgelin and E-cadherin (right panel) antibodies. Arrows show cells where exclusion is observed between transgelin and E-cadherin staining. 400X images have been shown.

Figure 3.34 shows the non-invasive breast cancer cells MDA-MB-361, BT-20 and MCF7, which have intermediate levels of E-cadherin staining. These cells do not express vimentin, and while MDA-MB-361 and MCF7 cells were negative for transgelin (Figure 3.34A and C), BT-20 cells displayed low-to-intermediate transgelin staining (Figure 3.34B). Transgelin staining was mostly accumulated at the nuclei in the BT-20 cells (Figure 3.34B) with lower levels of staining in the cytoplasm.

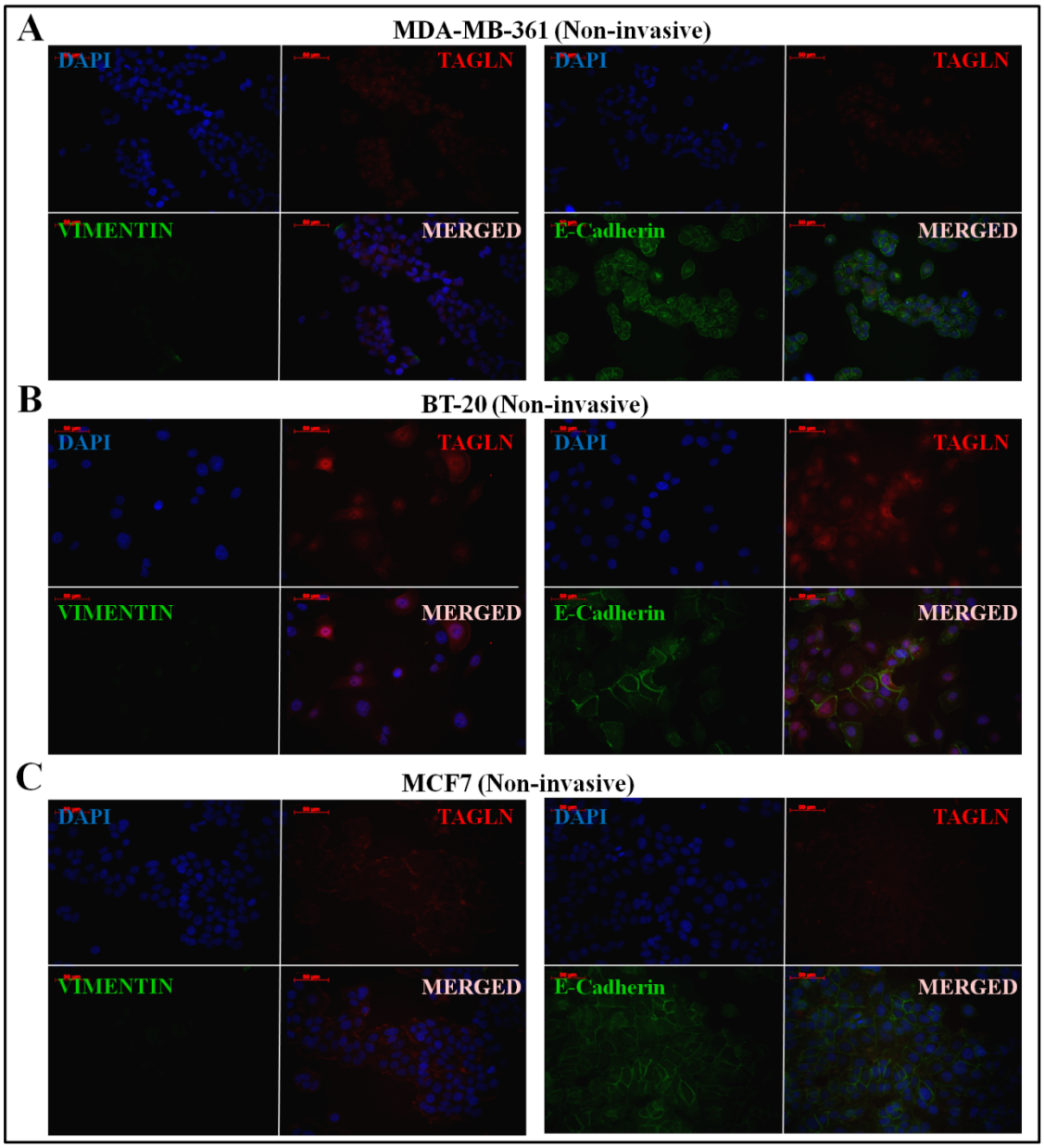

Figure 3.34: Co-staining of transgelin with vimentin or E-cadherin in non-invasive breast cancer cells with medium levels of E-cadherin expression.

IF co-staining in non-invasive epithelial MDA-MB-361(A); BT-20 (B); and MCF7 (C) breast cancer cells with transgelin and vimentin (left panel), and transgelin and E-cadherin (right panel) antibodies. 400X images have been shown.

Figure 3.35 shows the non-invasive breast cancer cell lines MDA-MB-453, CAMA-1 and SK-BR-3, which are both vimentin $^{(-)}$ and E-cadherin $^{(-)}$. While SK-BR-3 cells are mostly negative for transgelin staining with only slight accumulation at cell boundaries (Figure 3.35C), CAMA-1 cells were intensely stained (Figure 3.35B), and there was intermediate staining in the MDA-MB-453 cells (Figure 3.35A). Interestingly in MDA-MB-453 cells, transgelin staining was accumulated near the cell nuclei at single points (Figure 3.35A). A similar case was also

observed in the CAMA-1 cells, with higher levels of staining at the membranes and low levels in the cytoplasm (Figure 3.35B).

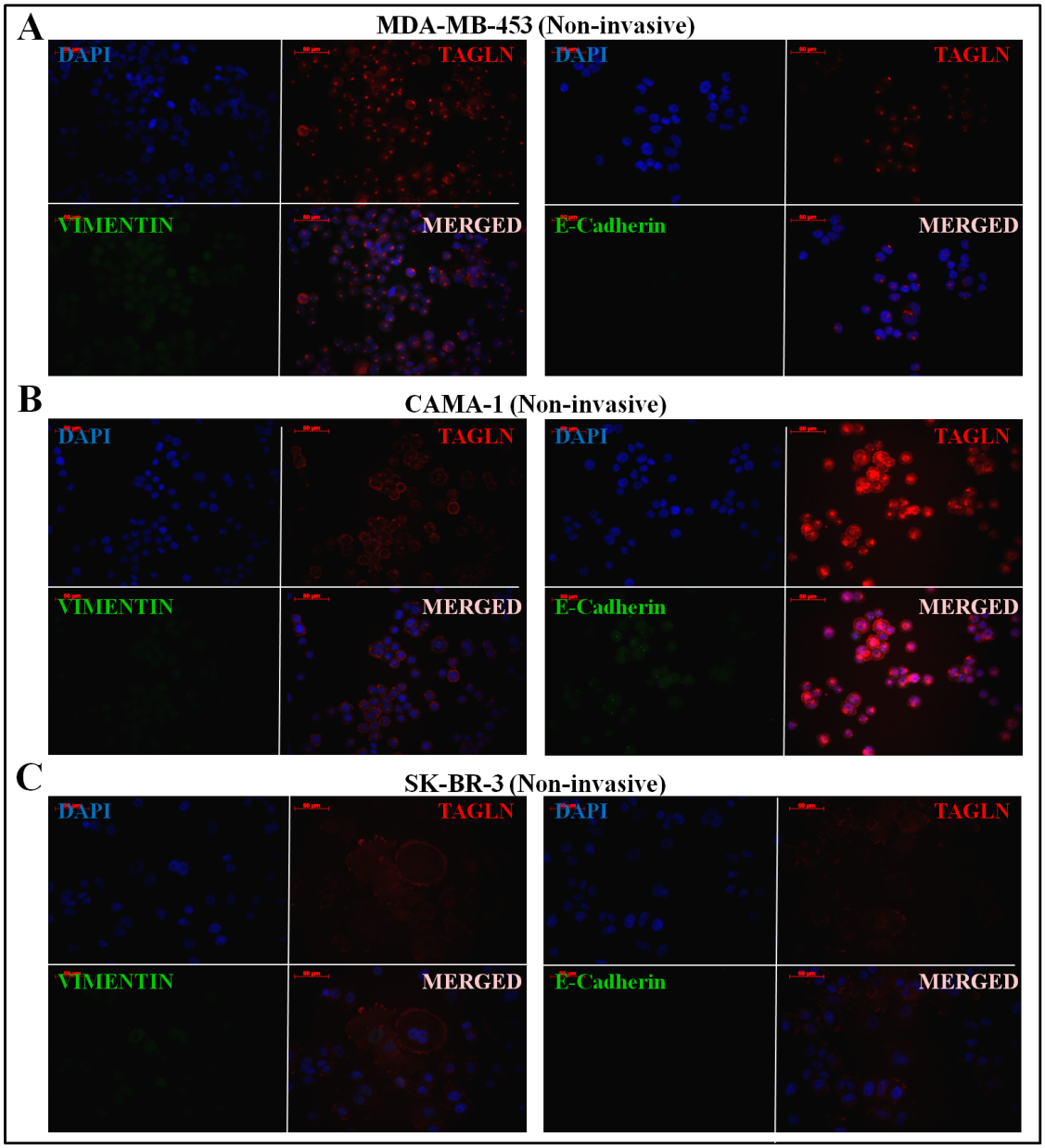

Figure 3.35: Co-staining of transgelin with vimentin or E-cadherin in non-invasive breast cancer cells with low levels of E-cadherin expression.

IF co-staining in non-invasive epithelial MDA-MB-453(A); CAMA-1 (B) and SK-BR-3 (C) breast cancer cells with transgelin and Vimentin (left panel), and transgelin and E-cadherin (right panel) antibodies. 400X images have been shown.

TAGLN expression was also analyzed with the epithelial (*CDH1, KRT18* and *ZO1*) and mesenchymal markers' (*CDH2, FN, MMP9, ZEB1, ZEB2* and *SNAIL*) expressions in epithelial (BT-474, MCF7, T47D, ZR-75-1, MDA-MB-453), undefined (HCC-1937, SK-BR-3, MDA-

MB-468) and mesenchymal (MDA-MB-157, MDA-MB-231, MDA-MB-436) breast cancer cells and mesenchymal NT breast (MCF10A and MCF12A) cells, using qRT-PCR method (Figure 3.36A and B). *TAGLN* expression was higher in mesenchymal cells compared to epithelial cells ($P = 0.0079$), and combination of epithelial and undefined cells ($P = 0.0109$).

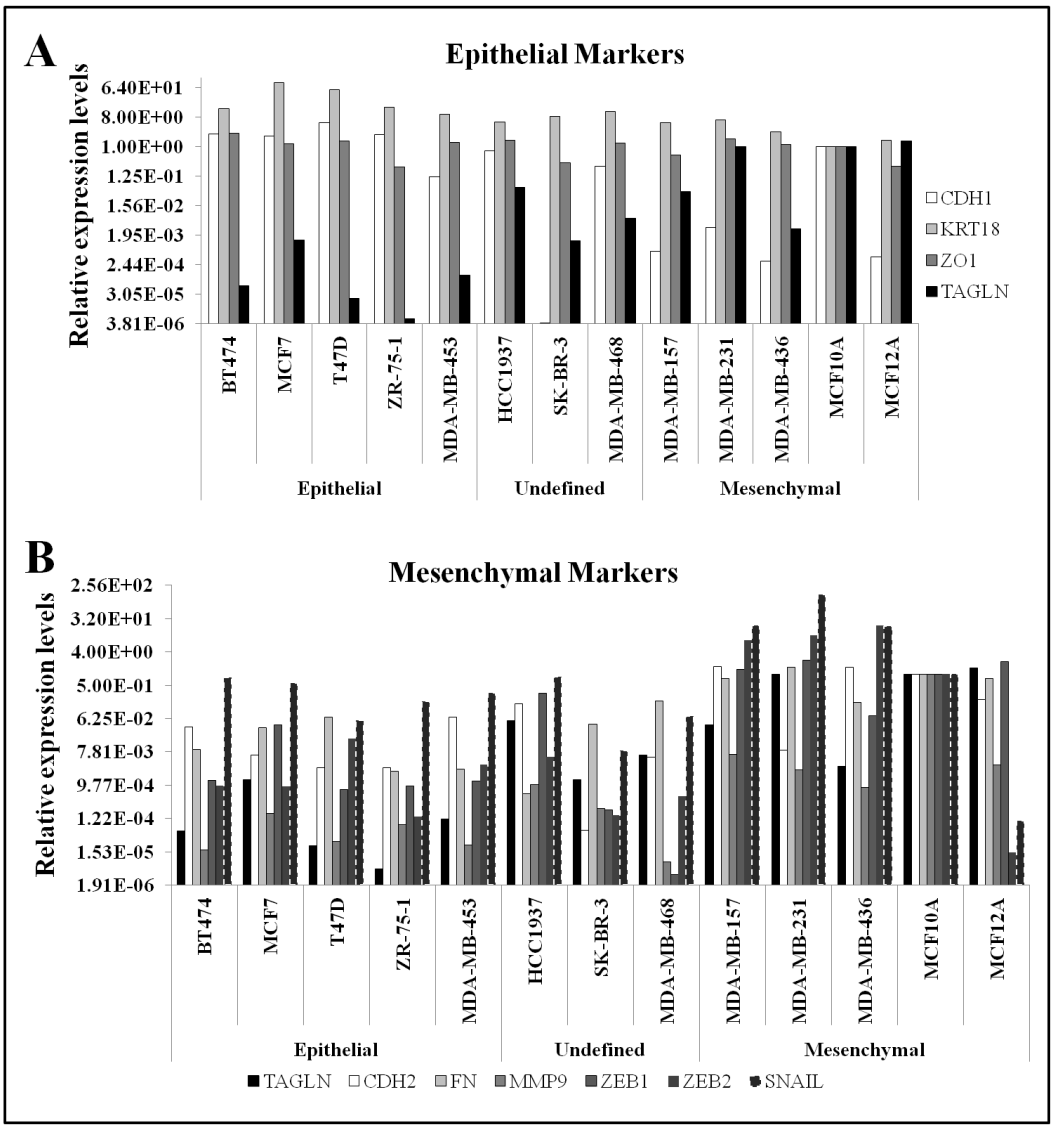

Figure 3.36: qRT-PCR analyses of EMT markers and *TAGLN* in breast cell line panel.

TAGLN expression was analyzed by qRT-PCR with epithelial markers (A), and with mesenchymal markers (B). All the values have been normalized to the expression levels in MCF10A cells, after being normalized with the GAPDH reference gene. Actual relative expressions are represented in Log_2 scales.

TAGLN expression was positively and significantly correlated with the mesenchymal markers *ZEB1, MMP9, FN* and *CDH2,* and was negatively and significantly correlated with the epithelial marker *KRT18* (Table 3.15, bold). Interestingly, not all the epithelial or mesenchymal

markers were significantly correlated with each other. Among the mesenchymal markers, *SNAIL* expression was only correlated to *CDH2*, *ZEB1* and *ZEB2* expressions*; ZEB1* was also correlated to *CDH2* and *MMP9;* and *MMP9* expression was also correlated to *CDH2*. Among the epithelial markers, only *KRT18* and *CDH1* expressions were correlated. The only intergroup correlations were negative correlations of *KRT18* gene expression levels with those of *ZEB1* and *CDH2* genes (Table 3.15).

Table 3.15: Correlations of expressions of epithelial and mesenchymal markers

	SNAIL[a]	ZEB2[a]	ZEB1[a]	MMP9[a]	FN[a]	CDH2[a]	ZO1[b]	KRT18[b]	CDH1[b]	
TAGLN	0.313	0.225	**0.742**	**0.747**	**0.643**	**0.599**	-0.077	**-0.791**	-0.478	Rho
	0.297	0.459	**0.005**	**0.005**	**0.021**	**0.034**	0.806	**0.002**	0.101	*P*
CDH1	-0.060	-0.088	-0.275	-0.429	-0.374	-0.330	0.385	**0.632**	Rho	
	0.849	0.778	0.363	0.146	0.209	0.271	0.196	**0.024**	*P*	
KRT18	-0.335	-0.341	**-0.648**	-0.780	-0.527	**-0.758**	0.275	Rho		
	0.263	0.255	**0.019**	0.002	0.067	**0.004**	0.363	*P*		
ZO1	0.352	0.429	0.022	-0.363	-0.121	-0.060	Rho			
	0.239	0.146	0.949	0.224	0.696	0.849	*P*			
CDH2	**0.593**	0.505	**0.725**	**0.610**	0.330	Rho				
	0.036	0.081	**0.007**	**0.030**	0.271	*P*				
FN	0.302	0.401	0.495	0.549	Rho					
	0.315	0.176	0.089	0.055	*P*					
MMP9	0.429	0.363	**0.813**	Rho						
	0.146	0.224	**0.001**	*P*						
ZEB1	**0.599**	0.434	Rho							
	0.034	0.140	*P*							
ZEB2	**0.830**	Rho								
	0.001	*P*								

[a]*Mesenchymal markers.* [b] *Epithelial markers. Spearman correlation coefficients (Rho) are shown as shaded rows. Significant associations are shown in bold.*

3.5.4.Spontaneous EMT model and *TAGLN* expression in MCF10A NT breast cells

MCF10A cells undergo spontaneous EMT when they are sparsely cultured, and become more mesenchymal; however, they are of epithelial phenotype when crowded[411]. Thus, we used this model to find out changes in transgelin expression upon EMT of MCF10A cells, and cultured cells in various numbers increasing 1,000 to 3 million. As the cell density was increased, there was a minor decrease in total vimentin levels. Yet, transgelin expression was not affected as determined by western blot analyses (Figure 3.37A).

IF analyses also show that vimentin staining increases, while E-cadherin levels decrease, when MCF10A cells were cultured more sparsely (Figure 3.37B). Total amount of transgelin throughout the cells do not change upon this transition from mesenchymal state to the epithelial state. However, in some cells where transgelin staining is very high compared to the other cells, a decrease or total loss in E-cadherin staining was also observed (Figure 3.37B, arrows).

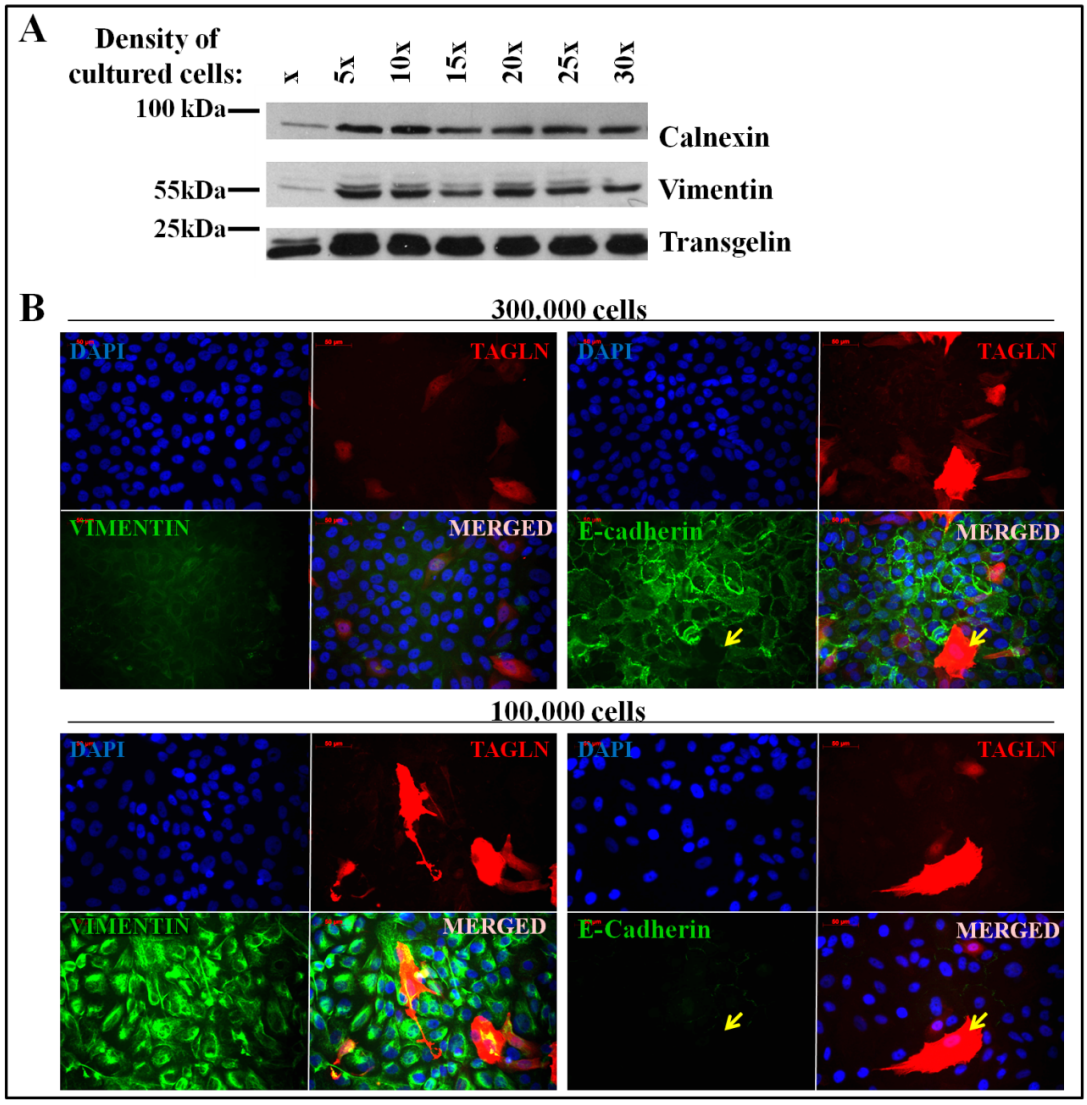

Figure 3.37: Transgelin protein levels in MCF10A spontaneous EMT model.

(A) MCF10A cells were cultured at different densities and transgelin and vimentin levels were determined via Western blot technique.(B)MCF10A cells were cultured at high density (300k/ 24 well plates) and at a lower density (100k/24 wells), and IF staining was performed with transgelin and vimentin (left panel) or transgelin and E-cadherin (right panel). Arrows indicate cells that are negative for E-cadherin but positive for transgelin.

To understand whether TAGLN has an effect on the spontaneous EMT of MCF10A cells, *TAGLN* gene was silenced with siRNAs, and cells were cultured either sparsely, or densely.

When *TAGLN* gene was silenced in MCF10A cells (Figure 3.38A), they transformed into more elongated cells (Figure 3.38B and C) with increased vimentin staining, in both sparsely and densely cultured cells (Figure 3.38C). However, a minor decrease was observed with Western blot in vimentin levels when *TAGLN* was silenced in MCF10A cells (Figure 3.38A).

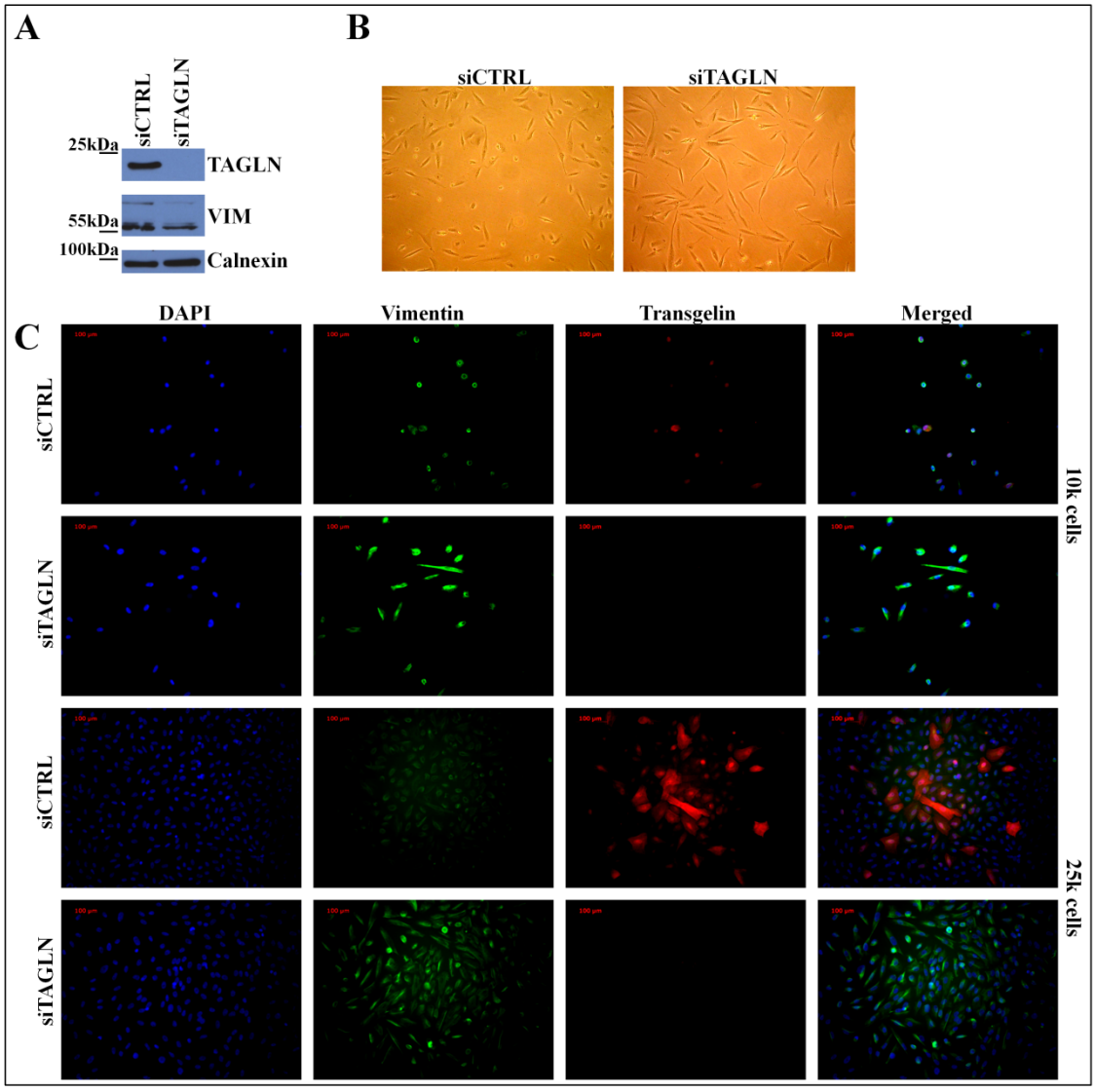

Figure 3.38: Morphologies of MCF10A cells with decreased transgelin protein levels.

(A)Western blot showing decreased levels of TAGLN and vimentin in siTAGLN transfected MCF10A cells. (B)Morphologies of siCTRL and siTAGLN transfected MCF10A cells under light microscope (200x). (C)Transgelin and vimentin staining in sparsely (10k) and densely (100k) cultured MCF10A cells transfected with siCTRL or siTAGLN siRNAs (200x).

3.5.5. EMT markers in transgelin over-expressing cells

We analyzed the vimentin and transgelin protein levels in transgelin over-expressing MDA-MB-157 cells and MDA-MB-361 cells, and E-cadherin levels in MDA-MB-361 cells (Figure 3.39). Unexpectedly, vimentin levels were slightly decreased in *TAGLN* over-expressing MDA-MB-157 cells (Figure 3.39A), but there was a slight increase in vimentin levels and a decrease in E-cadherin staining in MDA-MB-361 cells (Figure 3.39B and C). In MDA-MB-157 cells, the over-expressed transgelin was majorly accumulated in the cell nuclei (Figure 3.39A), whereas in MDA-MB-361 cells, both nuclei and the cytoplasm were occupied by transgelin (Figure 3.39).

Interestingly, MDA-MB-361 cells over-expressing *TAGLN* were larger than the control cells. When the present cell cycle phases of these cells were analyzed, percentage of the cells arrested at G2 phase, where excessive cell growth and protein synthesis occurs, was found to be non-significantly increased in *TAGLN* over-expressing MDA-MB-361 cells ($P > 0.05$, Figure 3.40), which could be the reason for the observed growth of *TAGLN* positive cells.

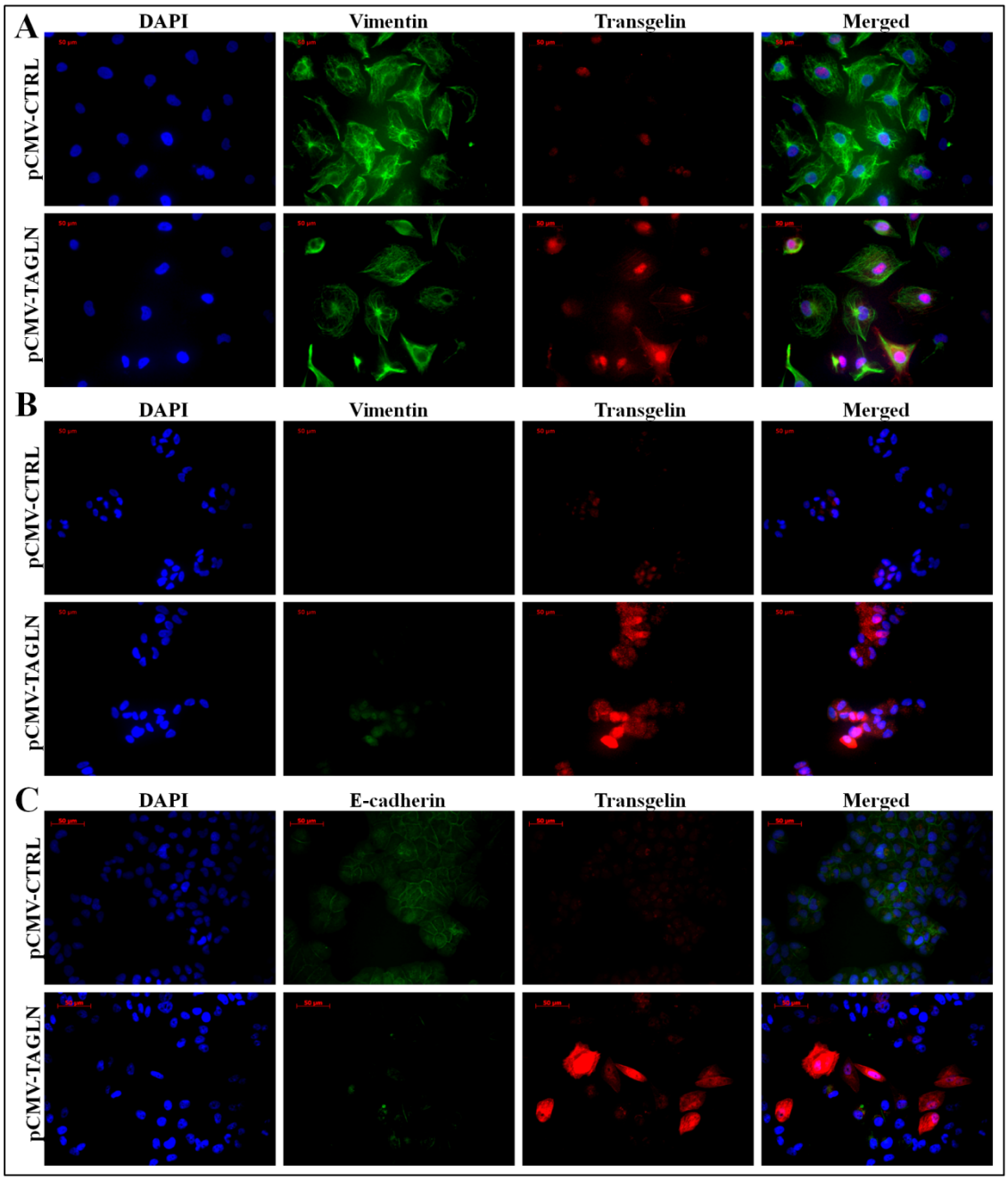

Figure 3.39: EMT markers in *TAGLN* over-expressing breast cancer cells.

(A) TAGLN and vimentin co-staining in control-vector transfected or TAGLN overexpressing MDA-MB-157 cells. (B-C) TAGLN and vimentin (B) or E-cadherin (C) co-staining in control-vector transfected or TAGLN over-expressing MDA-MB-361 cells. 400x images are shown.

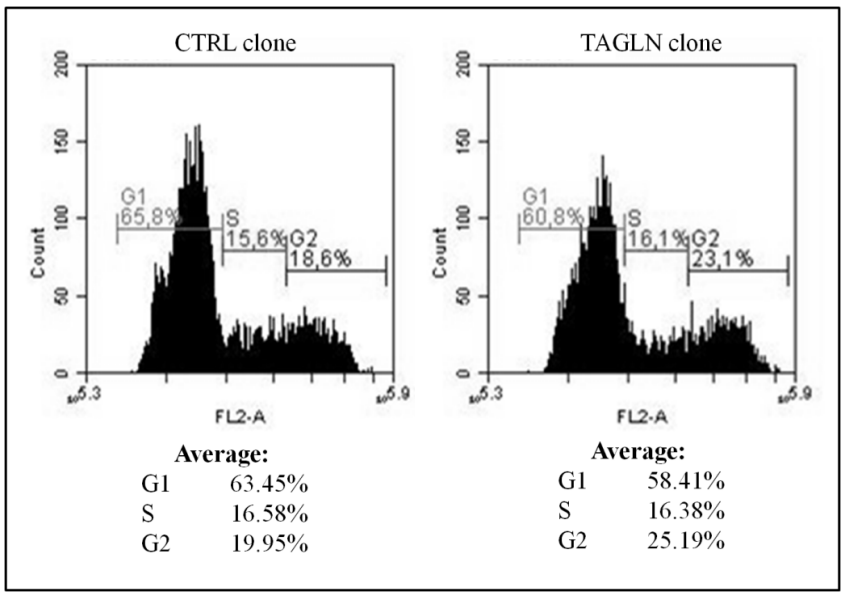

Figure 3.40: Cell cycle analysis using flow cytometry in MDA-MB-361 cells.

Flow cytometry was conducted with PI staining in MDA-MB-361 cells, and the numbers of cells in G1, S and G2 phases of cell cycle have been determined. Each experiment was repeated twice. Differences were non-significant between control and TAGLN clones, according to t-test.

3.5.6. Transgelin and EMT markers in breast tumor and normal tissues

To find out whether transgelin has a correlation with EMT markers in the breast tumor tissues, the tissue arrays that were stained for transgelin were also stained with the epithelial markers E-cadherin and cytokeratin 19 (CK19), and the mesenchymal marker vimentin. When all the tumors were analyzed, transgelin staining was negatively correlated to the E-cadherin staining (Figure 3.41A, left). This correlation was even strengthened when only stage 2, or grade 2-3 tumors were analyzed (Figure 3.41A, middle and right). Transgelin was not correlated to CK19 (Figure 3.41B, left); however, when only ER $^{(+)}$ tumors, or triple negative (TN) breast tumors were analyzed, there was a negative correlation between the H-scores of the two proteins (Figure 3.41, middle and right). Transgelin and vimentin were not correlated in the whole set of tumors, but there was a positive correlation in the ER $^{(+)}$ subset of the tumors (Figure 3.41C).

3.5.7. *TAGLN* and senescence in MDA-MB-361 cells

Since *TAGLN* expression was previously found to be associated with senescence in fibroblasts [334-336], the senescence states of control and transgelin over-expressing MDA-MB-361 cells were analyzed with SA-β-Gal staining. Despite an insignificant minor decrease in *TAGLN* overexpressing cells, there was no significant difference in the percent of SA-β-Gal positive cells than the control cells, implying that *TAGLN* does not affect senescence in these cells.

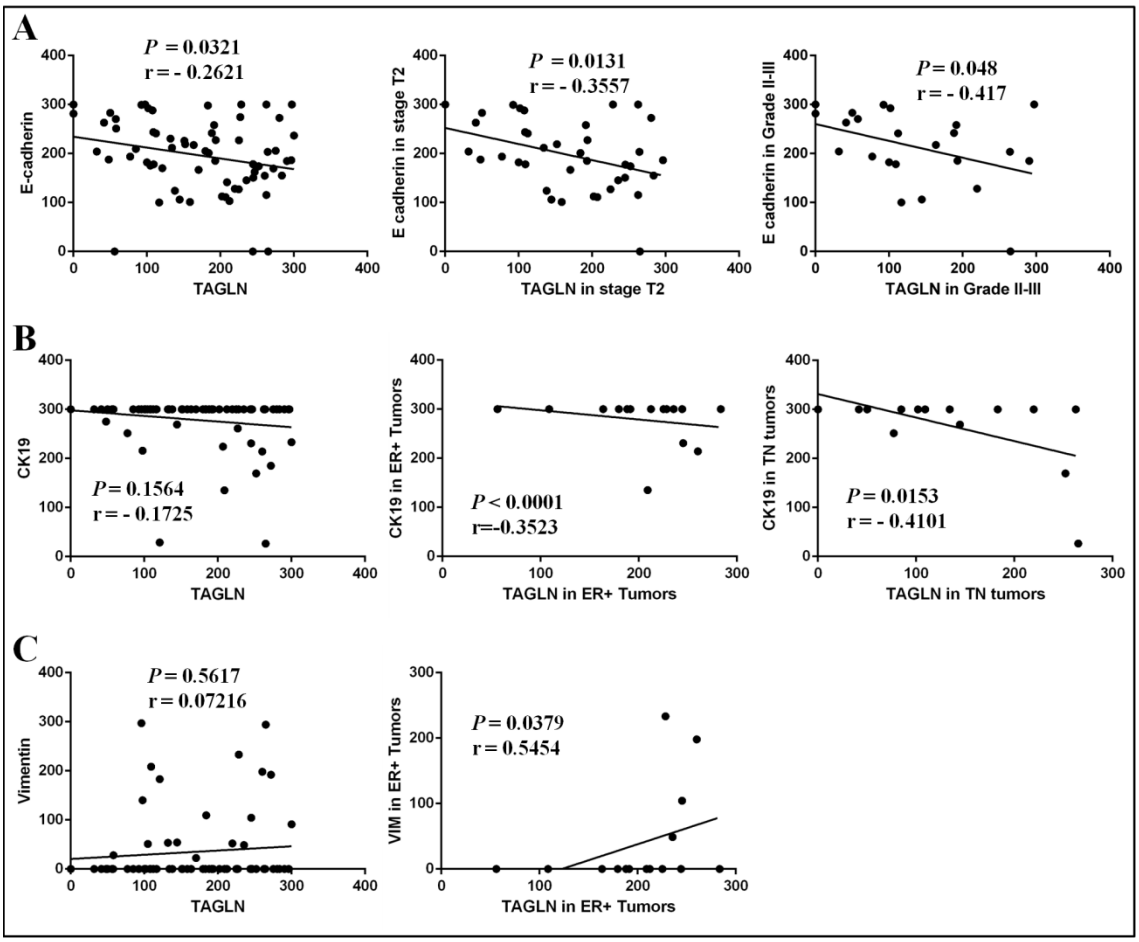

Figure 3.41: Correlation of transgelin with EMT markers in breast tumor tissue array.

Spearman correlations of transgelin and (A) E-cadherin in all tumors (left), in stage 2 (middle) and in Grade 2-3 tumors (right); (B) CK19 in all (left), in ER $^{(+)}$(middle) and in TN tumors, (right); and (C) vimentin in all (left,) and in ER $^{(+)}$ tumors (right). H-scores have been used for correlation. Correlation coefficients (r) and related P values have been shown on each graph.

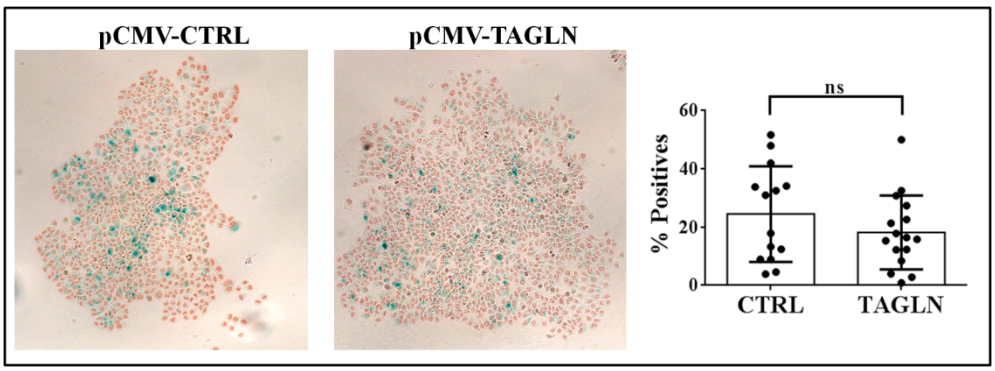

Figure 3.42: SA-β-Gal staining in MDA-MB-361 cells.

Representative figures of SA-β-Gal staining of control or TAGLN over-expressing MDA-MB-361 cells, after 30 days of culturing. Bars show average percent of SA-β-Gal $^{(+)}$ cells (n= 14 CTRL, and 16 TAGLN colonies). Error bars: standard deviations. ns: non-significant, t-test.

Chapter 4. Discussion

In this study, global gene expression profiling (47,000 transcripts) of MCF7 and MDA-MB-231 breast cancer cell lines before and after treatment with AZA and/or TSA was used to identify genes that were significantly up regulated by these treatments. MCF12A, a NT breast cell line, was also included, so that only cancer specific epigenetic alterations would be considered for the future studies. Although secondary effects such as induction of several transcription regulators which may upregulate several other genes may also play a role in the activation of normally suppressed genes in the treated cells, an important number of genes have presumably been inactivated through epigenetic mechanisms. Significant gene lists were generated from the analyses of all three cell lines after each treatment, in order to analyze the groups of genes and select candidate genes for further analyses. Combination of these lists by intersection or exclusion means is useful in terms of identifying significant genes for specific situations, such as commonly regulated genes in cancer cell lines, MCF7 or MDA-MB-231 specific genes, or MCF12A specific genes. Treatment vs. control analyses have demonstrated that, the highest numbers of genes were affected after administration of AZA+TSA or TSA only. It is not surprising that TSA affects far more genes than AZA, since it is documented that global decrease in levels of acetylation of histones is observed in cancers, which would be reversed by TSA, affecting several genomic locations, and hence genes[42]. In agreement with this, TSA treatment caused changes in expression levels of fewer genes in the NT cell line MCF12A, compared to MCF7 or MDA-MB-231. One might think that most of the genes affected by the treatments should be "upregulated" genes as these drugs all relieve the stress on transcription and makes chromatin and promoters available to transcription factors; however, there were as many, or even more, downregulated genes after each treatment. Taking into consideration that there are also secondary effects generated by these drugs, it seems normal to come up with so many downregulated genes. Since silencing of TSGs through epigenetic mechanisms is evident in cancer cells, it is expected to recover those genes after AZA and/or TSA treatments. A significant number of these tumor suppressors will be transcriptional regulators, and in turn, will "suppress" the transcription of their target genes, which are ideally expected to be oncogenes, or genes having oncogene-like activities. Interestingly, analysis of downregulated genes in cancer cell lines after treatments revealed that, the most significantly and consistently enriched pathways after each treatment were related to cell cycle, mitosis, and mRNA metabolism and processing related pathways, which may be related to the previously shown negative effects of AZA and TSA on proliferation of cancer cells, and the activities of induced TSGs[412-414].

Functional analyses of the genes obtained from analyses of the treatment induced genes in cancer cell lines showed that the most prominent pathway which was recovered as significant (P <0.05) from all DAVID analyses was the apoptosis pathway. This finding was also parallel with the previous studies showing that the AZA and TSA treatments result in apoptosis of cancer cells[412, 414-418].The downregulation of some apoptotic genes through epigenetic mechanisms has previously been documented; *CASP8*[419-420] and *DAPK1*[421-423] genes are among the best studied ones. The finding that apoptotic genes were prominent in our analyses could be interpreted to be related to the toxic effects of the drug; however, 5μM (or more) AZA had been widely used for the treatment of breast cancer cell lines[424-428]. Moreover, our study included a NT cell line, which was also treated with the same concentration of AZA ad TSA, yet did not posses remarkable upregulation of some of the apoptosis related genes (*CASP9, F11R, FOXO1, PPP1R15A*) despite their greater sensitivity towards apoptosis compared to the cancer cell lines[429]. Another possibility is that, a master gene which induces apoptosis and is regulated by methylation was upregulated after AZA treatment and induction of apoptosis resulted in increased expression of some of these genes in turn. Indeed, *ACVR1C* and *EGR2* expressions were shown to increase *CASP9* expression, a major initiator of apoptosis[430]. It is possible that activation of *ACVR1C* or *EGR2,* which were induced upon AZA treatment, or any other transcriptional regulator, was the real reason for *CASP9* induction in AZA treated breast cancer cells, as bisulfite sequencing could not identify any methylation in the analyzed promoter region of *CASP9* gene.

In this study, initially 26 candidate genes most of which belong to the enriched pathways were selected: 4 genes (*COL4A6, DST, F11R*, and *IQGAP2*) belong to cell-attachment related pathways, while 8 genes (*AXIN2, ZMAT3, CDC14B, FOXO1, EPB41L2, DUSP5, NDRG4*, and *HMOX1*) function in suppression of cell growth and proliferation. *GSTM1* and *GSTM2* have roles in drug metabolism. *INSIG1* gene function in insulin metabolism and BEX4 gene's function is not clearly identified. The remaining 10 genes in addition to *FOXO1* and *HMOX1* were apoptosis related genes. qRT-PCR analyses of these genes in treated MCF7, MDA-MB-231 and MCF12A cell lines indicated that the microarray experiment results were concordant, and that the high-throughput analyses in deed can reflect the actual expression patterns detected by qRT-PCR method. However, bisulfite sequencing in MCF7 and/or MDA-MB-231 cells revealed that, none of the genes were hypermethylated in these cell lines, although the genes selected were shown to have tumor suppressor activities, or were downregulated in other cancers or in our breast cancer cell lines, and were very significantly upregulated upon AZA treatment ($p<0.00002$ for all) in microarray set. This could have resulted from the selection procedure which was based almost solely on the significance level, and demonstrate the importance of fold change analyses in conjunction with the significance analyses. Thus, 6 more

genes were selected based on their upregulation levels and 4 of them were downregulated in the breast cancer cells to be re-expressed after AZA and/or TSA treatments. It is remarkable that, except for *AKAP12*, none of the genes could be upregulated to the levels similar to the non-tumorigenic cell lines' mock levels, although some of them were induced in orders of 100s. This could be explained by the possibility that other regulatory mechanisms could be acting in concert with DNA methylation, still keeping the expression levels of these genes under the non-tumorigenic levels. A third explanation could be the secondary effects of AZA on regulation of these genes. If AZA treatment resulted in activation of any other epigenetically suppressed gene, which in turn induces our gene of interest, the induction observed could be resulting from the activity of the regulatory gene, but not removal of hypermethylation from the genes promoter. Indeed, this could be the case for *TGFBI* gene, which was almost completely unmethylated in both MCF7 and MDA-MB-231 cells. For other genes, which were methylated in these cells, the first mechanism is more plausible.

Among several candidate genes, this is the first time that significant downregulation of *COL4A6* and *AKAP12* expression was documented in breast cancer cell lines compared to NT cells. *DST*, another selected gene which was previously shown to be downregulated in IDC, was also significantly downregulated in our breast cancer cell lines[139]. Our analyses showed that the expression of *DST* was not robustly induced by AZA in selected breast cancer cell lines, indicating that it may not be regulated by promoter DNA methylation, thus was not analyzed for bisulfite sequencing. *TGFBI* was formerly documented to be downregulated in MDA-MB-231 and MCF7 cells and the ectopic expression of *TGFBI* in these cells suppressed tumorigenesis and metastasis potentials[318, 431]. Nevertheless, promoter hypermethylation was not observed in breast cancer and NT cell lines[432]. We confirm downregulation of this gene in breast cancer cell lines compared to NT cells, and that the promoter region was unmethylated in MDA-MB-231 and MCF7 cells.

S100A2 gene, which was induced by at least 3 fold in eight of nine cancer cell lines by any AZA treatment (AZA or AZA+TSA), and for which no significant induction was observed in NT cell lines was found to be methylated in all cancer cell lines, and to be unmethylated in both of the NT cell lines, as expected. This gene was previously found to methylated in one breast tumor biopsy sample and in T47D breast cancer cell line, and to be unmethylated in HME1 NT breast cell line, by another group[301]. Using the microarray data generated by a recent research studying the effect of AZA on various breast cancer cell lines, this gene was found to be upregulated at least 2 fold in MCF7, T47D, SKBR3, BT-20 and MDA-MB-361 cells by AZA, which was in concordance with our sequencing and AZA treatment results[110]. However, when the normal breast tissues of out matched panel were analyzed for the presence of methylation in the

promoter region of *S100A2* gene, methylation was also evident in these samples. The normal tissues used in this study were acquired from the neighboring tumor tissues during the tumor biopsies. Cancer is a multi step event, and methylation might be the very early signals in the process of cancer development, and might also be affected from the tumor microenvironment. Therefore, methylation observed in the promoter region of *S100A2* gene in normal tissue samples might be result of being too close to the tumor cells, which is usually termed as "field cancerization" [433-436]. The microenvironment generated by the tumor cells might have resulted in hypermethylation of this gene in the neighboring normal tissue, which in turn, might be a very first step of transformation of these cells and gain tumorigenic potential. Further analyses such as morphological examination of these tissues are necessary to validate this hypothesis. Moreover, a study carried out in tumor and adjacent normal tissues found out that, in promoter regions of several TSGs, including *RASSF1A* and *APC*, there was a correlation in the hypermethylation levels in tumors and corresponding adjacent tissues[437]. Another possibility could be the hydroxymethylation in the promoter region of this gene. Hydroxymethylated CpGs (5hmC) are generated during the demethylation process as an intermediate product by DNA demethylating TET enzymes, which hydroxylate the methylated cytosines. Unfortunately, bisulfite sequencing cannot discriminate between methylated cytosines and 5hmC, since 5hmCs also remain as cytosines upon bisulfite treatment[438]. Therefore, it is possible that the methylated CpGs that are highly found in the promoter region of *S100A2* gene in normal breast tissues could be due to presence of 5hmCs. This should be analyzed by methods that discriminate between methylated CpGs and 5hmCpGs, such as MeDIP or oxidative bisulfite sequencing. Since publicly available DNA methylation microarray data of GSE20712 study also hinted that its promoter is not differentially methylated in breast tumors and normal breast tissues[110], further analyses regarding this gene were suspended.

TAGLN, on the other hand, was hypermethylated in almost all of the breast cancer cell lines, 62% of the normal matched tumor tissues and 63% of the unpaired tumor tissues. These percentages were close to the methylation frequencies of previously studied TSGs[439]. Moreover, *TAGLN* expression and methylation levels were always negatively and significantly correlated, which is a strong proof that its expression is regulated by methylation of the promoter region in breast cancer. Indeed, a previous study on smooth muscle cells (SMC) showed that, *in vitro* methylation of *TAGLN* promoter region could regulate the expression of the adjacent luciferase gene in a construct[361]. *TAGLN* promoter was also found to be hypermethylated in colorectal carcinoma[363], yet was found to be hypomethylated in nerve sheath tumors[352]. These findings in addition to our study suggest that *TAGLN* expression is commonly regulated by promoter methylation in different tissues.

TAGLN hypermethylation frequencies in breast tumors was high enough to discriminate between normal and tumor tissues, with 83.14% sensitivity and 100 % specificity, according to ROC analyses of publicly available methylation data. Moreover, its promoter methylation can also be detected from the serum samples of cancer patients as found out by our bioinformatics analyses of another public microarray data. This makes *TAGLN* a good candidate as a biomarker for detection of breast cancer, from easily accessible non-invasive sites like serum. It is possible to obtain cell free DNA (cfDNA) in concentrations as high as 0.1-100ng/ml of serum, which is enough for both bisulfite sequencing and PCR applications[440-441]. Several techniques have been developed for sensitive and quick detection of promoter methylation such as methylation specific PCR (MSP), quantitative MSP (qMSP), and Methylight, which are commonly applied for detection from serum or other body fluids[98-101, 442-443]. For the breast cancer, these could be fine needle aspirates, nipple aspirates, or ductal lavage fluids[444-446]; however, use of serum for diagnosis is less invasive and easier for follow up. In addition to these, diagnosis from DNA is preferred to studying with RNA and protein depending on the following reasons[103]. First, DNA is structurally much more stable than RNA, and it is even possible to study DNA from the archival tissues. Second, it is possible to perform analyses with sensitive techniques such as PCR, with very little amount of DNA. Methylight, for example, can detect tiny concentrations of methylated DNA even in presence of high concentrations of unmethylated DNA[443]. Finally, DNA hypermethylation is usually unique to the tumor tissues, meaning that the detected DNA with use of the selected bio-marker would be specific to the tumor cells. Thus, identification of novel biomarkers for detection of breast cancer from blood based samples is a growing research area[102, 105, 447]. The sensitivity and specificity values obtained using *TAGLN* promoter methylation levels alone is close to the combined values of more than one biomarker for breast cancer diagnosis[105], which may enable one-gene detection, in high risk groups or combined with CT scan or mammography techniques. Even if *TAGLN* promoter methylation cannot be used by its own for detection of breast cancer, it could be incorporated into the present multi-gene panels and combined with other previously identified strong markers, such as widely studied and used *RASSF1A* with 100% specificity and 75% sensitivity [104], or *RARβ* with 94% specificity and 87% sensitivity [448]. Yet, our findings are based on bioinformatics analyses of a microarray data, hence, these hypotheses should be studied in a larger screening study, including serum samples of several breast cancer patients, and healthy individuals, with fast screening methods, accompanied with validation via the gold standard method, bisulfite sequencing, for at least a subset of the samples.

In addition to the diagnosis of breast cancer, *TAGLN* promoter methylation levels could also be useful for determination of prognosis status of breast cancer patients at diagnosis, or during the follow up periods. This conclusion, which should be validated with a study as described above,

is drawn based on our findings that: (1) there was a negative correlation between *TAGLN* methylation scores and expression of worse prognosis marker *ANLN*; and (2) 10-year RFS and OS of patients were higher in patients with lower *TAGLN* methylation in their tumors, independent of grade.

TAGLN expression and regulation seems to be an important event as its expression was found to be persistently downregulated in several types of cancer cells and tumor tissues, including colon, prostate, and although very limited, breast cancer[341, 345, 347, 354, 363, 449-450]. There are also other studies pointing *TAGLN* as an oncogene-like protein and reporting over-expression in various types of tumors including colon, gastric and nerve sheath tumors[351-352, 451-452]. This study shows consistent and significant downregulation of *TAGLN* in three completely independent set of breast tissues, as well as in breast cancer cell lines, both in protein and mRNA levels. Thus, *TAGLN* downregulation seems to be an important player in development and progression of breast cancer. Moreover, our findings imply that *TAGLN* downregulation is augmented in more aggressive or more de-differentiated tumors, such as high grade, *ANLN* $^{(+)}$, and TN tumors, albeit a recent study suggesting *TAGLN* as a biomarker for TN breast tumors[365]. Our findings also show that *TAGLN* expression is also crucial for the survival of the patients, as low grade breast cancer patients' both OS and RFS were better if *TAGLN* expression was higher in their tumors. These results could partly be explained by the results of the functional studies carried out in breast cancer cells over-expressing *TAGLN* or NT breast cells with silenced *TAGLN*. According to the colony formation experiments, *TAGLN* expression was negatively associated with cell proliferation, which is a confirmation of the negative correlation found with *ANLN* expression, a marker of cell proliferation[409]. The negative effect of TAGLN on cellular proliferation could be explained by transgelin's effect on reactive oxygen species (ROS) production. Several studies carried on different systems including melanoma, fibroblasts and yeast cells[354, 453-454] indicate that, increased levels of transgelin results in decreased actin dynamics, which in turn causes mitochondria to be more permeable, and discharge ROS, which are known for their toxic effect on the cancer cells, and even are being used as anti-cancer agents[455]. There could be other mechanisms as well, including other protein partners and signaling pathways, which should be studied in a functional study.

Transgelin is known for its frequent involvement with the actin cytoskeleton, and was first discovered as an actin binding protein, to be given the name based on its actin-"gelling" effects[327, 456]. Afterwards, several studies showed that transgelin can indeed directly affect the actin dynamics[331, 354, 456-457]. Actin cytoskeleton has several effects on a cell, and regulation of cell movement is one of them[458]. Transgelin was shown to direct formation of podosomes, as well as focal adhesions, thereby positively affecting SMC migration[330-332]. However, there are

also other studies in colon cancer, demonstrating that increased levels of transgelin resulted in decreased migration of cells[341, 459]. We observed that transgelin expression was relatively higher in highly invasive cells MDA-MB-231 and MDA-MB-157, yet, over-expression in MDA-MB-157 and MDA-MB-361 cells neither affected cell migration, nor invasion. It is possible that in breast cancer, which is a completely different system than SMCs, transgelin is not involved in cellular migration or invasion. In epithelial and mesenchymal origin of cells, the protein partners might be very different. However, to derive a more reliable conclusion, further studies with stably suppressed expression of *TAGLN* in highly invasive MDA-MB-231 and MDA-MB-157 cells are necessary.

There are also other controversies regarding the association of transgelin with the metastasis status of human cancers. Studies in colon and prostate cancers claim negative association of *TAGLN* expression with lymph node metastasis [341, 460], yet other studies in colorectal cancer and nerve sheath tumors found positive correlations[351-352]. It is hypothesized that, in some of the studies where increased levels of transgelin was found in invasive or metastatic tissues, the observed over-expression was due to the higher expression levels of *TAGLN* in the stroma cells, instead of the cancer tissue itself[350, 461-463]. In agreement with these findings, when the IHC analyses performed in our breast tumor tissue arrays were examined, it is evident that transgelin staining is much higher in the stroma of the tumors at similar levels to the myoepithelial cells of the normal tissues. This is presumably due to the fact that, stroma tissue consists of fibroblasts and myo-fibroblasts, which are known to express *TAGLN* at high levels[464]. Whether *TAGLN* expression in these stromal cells provides a growth or metastatic advantage to the associated cancer cells should be further studied. Moreover, TAGLN staining in the tumor stromal tissues should be evaluated by IHC analyses.

Transgelin protein is accepted as a mesenchymal protein[329]. Moreover, *TAGLN* expression is known to be induced by TGF-β[356-359], which induces EMT in cancer cell lines[360]. Some studies, directly or indirectly, indicate that *TAGLN* expression increases after EMT[354-355]. Thus, its expression may be expected to be re-activated after EMT is achieved in higher grade breast tumors[465-466]. However, our results show that *TAGLN* expression was downregulated even more in grade 3 tumors, compared to grade 1 and 2 tumors. This suggests that, downregulation of *TAGLN* gene is a crucial event not only for the onset, but also for the progression of breast cancer. When analyzed with the epithelial and mesenchymal markers in the breast cancer tissue array, a negative correlation was found between transgelin and E-cadherin in higher grade breast tumors, but not in grade 1 tumors. This result is presumably due to the higher and maximal expression of E-cadherin in all grade 1 tumors, as these tissues are probably still epithelial, and did not start to undergo EMT, given that EMT and the grade status of breast cancer is positively

associated[465-466]. The association of transgelin with the EMT states of the tumor tissues could be studied in a focused study, with special tissue sections encompassing the intersection of tumor and surrounding tissue, with evidence of invasion. Although not with the tissues, we analyzed the expression and localization of transgelin in invasive and non-invasive, and in epithelial and mesenchymal breast cancer and NT cell lines, together with epithelial and mesenchymal markers. The first observation was that transgelin staining was higher in larger cells, which could be explained by the negative effect of transgelin on cellular proliferation. Moreover, preliminary FACS analyses in MDA-MB-361 cells hint that, although not significantly, transgelin over-expression causes a minor increase in the number of cells at G2 phase, where cell growth occurs. The second observation that the localization of transgelin staining differed in between different cells, imply possible protein partners of transgelin which control its localization in the cell. These protein partners should be uncovered with experiments such as yeast-two-hybrid system and co-immunoprecipitation. Third, in some cells, especially MCF10A, a decrease was observed in the canonical E-cadherin staining in cells expressing high levels of transgelin. Here, transgelin might be acting as a mesenchymal marker, with higher staining in mesenchymal cells which have lower levels of E-cadherin. Whether transgelin expression results in the decreased levels of E-cadherin should be studied. Our findings in MDA-MB-361 cells support this idea, as E-cadherin staining was decreased in *TAGLN* over-expressing cells. However, there were still individual cells where transgelin and E-cadherin staining co-existed. Thus, a more comprehensive study, involving more over-expressing clones and cell lines should be carried out in order to find out the effect of transgelin on epithelial and mesenchymal markers. Finally, the last observation was that the morphologies of MCF10A cells were altered when *TAGLN* gene was silenced, such that the cells became more elongated compared to the control siRNA transfected cells. This result is unexpected when compared to the previous result, as the altered morphologies resemble mesenchymal cells rather than epithelial cells. Considering the fact that transgelin staining was not altered in MCF10A cells undergoing spontaneous EMT, it could be interpreted that transgelin may not be related to EMT in breast cancer cells. Yet other findings, including the qRT-PCR analyses, show that *TAGLN* is expressed at higher levels in mesenchymal breast cancer cell lines such as MDA-MB-231, MDA-MB-436, and MD-MB-157, and its exclusion with E-cadherin imply an association of TAGLN with EMT. It is possible that transgelin might have a dual role, like its upstream transcriptional activator TGF-β, which acts as a TSG at the early phases of cancer, but then when the higher stages are achieved, it becomes reactivated and acts like a metastasis enhancer. The activity and function of transgelin may differ in epithelial and mesenchymal cells, or in NT and cancer cells. Extensive studies regarding the effect of changes in expression of *TAGLN* gene

on EMT status of cells, or on EMT induction by TGF-β of cancer cells, as well as effect of EMT induction on *TAGLN* mRNA and protein levels should be identified.

In conclusion, this study identifies molecular pathways in response to AZA and/or TSA treatment of breast cancer and NT cells, and documents significant downregulation of several genes, including *AKAP12*, *COL4A6* and *S100A2* genes in breast cancer cells. This study also identifies *TAGLN* gene to be persistently and significantly downregulated in independent sets of breast tumor tissues compared to matched, or unmatched normal tissues by promoter DNA hypermethylation, for the first time. In addition to these findings, its negative association with poorer prognosis markers and positive association with better survival of breast cancer patients indicate a suppressive role of *TAGLN* on breast carcinogenesis, which could be partly explained by transgelin's negative effect on cellular proliferation capacities of breast cancer cells. High frequency of methylation in breast tumors, and positive association of methylation levels with prognosis of breast cancer points *TAGLN* as a strong bio-marker candidate for both diagnosis and prognosis of breast cancer. Finally, *TAGLN* seems to be related to EMT in breast cancer cells, possibly with a dual role; and whether increased *TAGLN* expression is the reason, or the result of the process should be uncovered with focused and comprehensive functional studies.

Chapter 5. Future Perspectives

The microarray analysis of AZA and TSA treated breast cancer cells uncovered numerous genes that are differentially expressed between treatment and control groups, between breast cancer cells and non-tumorigenic breast cells, and between invasive and non-invasive breast cancer cells. It is important to mine the data for further candidate genes, using the second approach used in this study, by utilizing the fold change values. Selecting significantly altered genes with high fold change values, *i.e.* > 5 folds, would enable identification of more candidate genes, like *TAGLN*, which are regulated by DNA hypermethylation in breast cancer, and could be used as biomarkers for diagnosis, or prognosis. Availability of several microarray methylation data and bisulfite amplicon sequencing would facilitate comparison of expression data to methylation data, and ease determination of new candidate genes[467]. Cell line specific effects of AZA could be studied by comparisons of specifically altered gene sets in either MCF7 or MDA-MB-231 breast cancer cells, which have different origins. Epithelial and mesenchymal phenotype related genes could be revealed by means of these comparisons. Moreover, using the TSA treatment data, potential candidates that are regulated by histone modifications could also be uncovered and studied using techniques like ChIP-seq[468].

Methylation status of *S100A2* gene could be studied in a larger set of breast tumors and normal tissues, together with gene expression analyses. Hydroxymethylation at the promoter region of this gene should also be examined as the observed hypermethylation in the normal tissues could be due to hydroxymethylated CpG residues (5hmC), which are in the process of demethylation. The analysis is possible at single nucleotide resolution by MeDIP using antibodies against 5hmC or combination of bisulfite sequencing and oxidative bisulfite sequencing[438, 469].

TAGLN was identified as a hypermethylated and downregulated gene in breast cancer, and initial analyses showed its negative effect on cellular proliferation. Correlation of TAGLN with EMT markers implies an association of transgelin with EMT status of breast cancer. Whether this association is the cause or result of changes in *TAGLN* expression should be determined with focused and comprehensive analyses, including more stable clones of *TAGLN* over-expressing cells or *TAGLN* silenced invasive and mesenchymal breast cancer cells. Moreover, functional analyses such as soft-agar colony formation, invasion and migration, should be performed with these new stable clones, and if positive results are obtained, the results should be confirmed in *in vivo* systems, such as immune suppressed mice.

An important outcome of this study was that, *TAGLN* promoter was identified as a strong candidate for a breast cancer biomarker. Moreover, its methylation could be detected in sera

collected from breast cancer patients. Yet, the results are based on bioinformatics analyses of public microarray data, and should be validated in large sets of serum and tumor samples, with bisulfite sequencing, and a faster and sensitive technique, such as qMSP or Methylight. If the results can be confirmed, then development of detection kits alone or together with other powerful biomarkers could be considered.

References

1. Ferlay J, Soerjomataram I, Dikshit R, Eser S, Mathers C, Rebelo M, Parkin DM, Forman D, Bray F. Cancer incidence and mortality worldwide: Sources, methods and major patterns in GLOBOCAN 2012. Int J Cancer 2015; 136:E359-86.

2. Polyak K. Heterogeneity in breast cancer. J Clin Invest 2011; 121:3786-8.

3. Hassiotou F, Geddes D. Anatomy of the human mammary gland: Current status of knowledge. Clin Anat 2013; 26:29-48.

4. Yoder BJ, Wilkinson EJ, Massoll NA. Molecular and morphologic distinctions between infiltrating ductal and lobular carcinoma of the breast. Breast J 2007; 13:172-9.

5. Weigelt B, Horlings HM, Kreike B, Hayes MM, Hauptmann M, Wessels LF, de Jong D, Van de Vijver MJ, Van't Veer LJ, Peterse JL. Refinement of breast cancer classification by molecular characterization of histological special types. J Pathol 2008; 216:141-50.

6. Mallon E, Osin P, Nasiri N, Blain I, Howard B, Gusterson B. The basic pathology of human breast cancer. J Mammary Gland Biol Neoplasia 2000; 5:139-63.

7. Ignatiadis M, Sotiriou C. Understanding the molecular basis of histologic grade. Pathobiology 2008; 75:104-11.

8. Baak JP, van Diest PJ, Voorhorst FJ, van der Wall E, Beex LV, Vermorken JB, Janssen EA. Prospective multicenter validation of the independent prognostic value of the mitotic activity index in lymph node-negative breast cancer patients younger than 55 years. J Clin Oncol 2005; 23:5993-6001.

9. Elston CW, Ellis IO. Pathological prognostic factors in breast cancer. I. The value of histological grade in breast cancer: experience from a large study with long-term follow-up. Histopathology 1991; 19:403-10.

10. Perou CM, Sorlie T, Eisen MB, van de Rijn M, Jeffrey SS, Rees CA, Pollack JR, Ross DT, Johnsen H, Akslen LA, et al. Molecular portraits of human breast tumours. Nature 2000; 406:747-52.

11. Cianfrocca M, Gradishar W. New molecular classifications of breast cancer. CA Cancer J Clin 2009; 59:303-13.

12. Gusterson BA, Ross DT, Heath VJ, Stein T. Basal cytokeratins and their relationship to the cellular origin and functional classification of breast cancer. Breast Cancer Res 2005; 7:143-8.

13. Sorlie T, Perou CM, Tibshirani R, Aas T, Geisler S, Johnsen H, Hastie T, Eisen MB, van de Rijn M, Jeffrey SS, et al. Gene expression patterns of breast carcinomas distinguish tumor subclasses with clinical implications. Proc Natl Acad Sci U S A 2001; 98:10869-74.

14. Sotiriou C, Neo SY, McShane LM, Korn EL, Long PM, Jazaeri A, Martiat P, Fox SB, Harris AL, Liu ET. Breast cancer classification and prognosis based on gene expression profiles from a population-based study. Proc Natl Acad Sci U S A 2003; 100:10393-8.

15. van 't Veer LJ, Dai H, van de Vijver MJ, He YD, Hart AA, Mao M, Peterse HL, van der Kooy K, Marton MJ, Witteveen AT, et al. Gene expression profiling predicts clinical outcome of breast cancer. Nature 2002; 415:530-6.

16. Naderi A, Teschendorff AE, Barbosa-Morais NI, Pinder SE, Green AR, Powe DG, Robertson JFR, Aparicio S, Ellis IO, Brenton JD, et al. A gene-expression signature to predict survival in breast cancer across independent data sets. Oncogene 2007; 26:1507-16.

17. Visvader JE. Keeping abreast of the mammary epithelial hierarchy and breast tumorigenesis. Genes Dev 2009; 23:2563-77.

18. Eroles P, Bosch A, Perez-Fidalgo JA, Lluch A. Molecular biology in breast cancer: Intrinsic subtypes and signaling pathways. Cancer Treat Rev 2012; 38:698-707.

19. Sorlie T, Tibshirani R, Parker J, Hastie T, Marron JS, Nobel A, Deng S, Johnsen H, Pesich R, Geisler S, et al. Repeated observation of breast tumor subtypes in independent gene expression data sets. P Natl Acad Sci USA 2003; 100:8418-23.

20. Perou CM. Molecular Stratification of Triple-Negative Breast Cancers. Oncologist 2011; 16:61-70.

21. Ben-Porath I, Thomson MW, Carey VJ, Ge R, Bell GW, Regev A, Weinberg RA. An embryonic stem cell-like gene expression signature in poorly differentiated aggressive human tumors. Nat Genet 2008; 40:499-507.

22. Prat A, Parker JS, Karginova O, Fan C, Livasy C, Herschkowitz JI, He XP, Perou CM. Phenotypic and molecular characterization of the claudin-low intrinsic subtype of breast cancer. Breast Cancer Research 2010; 12.

23. Yersal O, Barutca S. Biological subtypes of breast cancer: Prognostic and therapeutic implications. World J Clin Oncol 2014; 5:412-24.

24. Majdak-Paredes EJ, Fatah F. Hereditary breast cancer syndromes and clinical implications. J Plast Reconstr Aesthet Surg 2009; 62:181-9.

25. Economopoulou P, Dimitriadis G, Psyrri A. Beyond BRCA: New hereditary breast cancer susceptibility genes. Cancer Treat Rev 2015; 41:1-8.

26. Ford D, Easton DF, Stratton M, Narod S, Goldgar D, Devilee P, Bishop DT, Weber B, Lenoir G, Chang-Claude J, et al. Genetic heterogeneity and penetrance analysis of the BRCA1 and BRCA2 genes in breast cancer families. The Breast Cancer Linkage Consortium. Am J Hum Genet 1998; 62:676-89.

27. Welcsh PL, Owens KN, King MC. Insights into the functions of BRCA1 and BRCA2. Trends Genet 2000; 16:69-74.

28. Walsh T, Casadei S, Coats KH, Swisher E, Stray SM, Higgins J, Roach KC, Mandell J, Lee MK, Ciernikova S, et al. Spectrum of mutations in BRCA1, BRCA2, CHEK2, and TP53 in families at high risk of breast cancer. Jama-J Am Med Assoc 2006; 295:1379-88.

29. Starink TM, Vanderveen JPW, Arwert F, Dewaal LP, Delange GG, Gille JJP, Eriksson AW. The Cowden Syndrome - a Clinical and Genetic-Study in 21 Patients. Clin Genet 1986; 29:222-33.

30. Schrager CA, Schneider D, Gruener AC, Tsou HC, Peacocke M. Clinical and pathological features of breast disease in Cowden's syndrome: An underrecognized syndrome with an increased risk of breast cancer. Hum Pathol 1998; 29:47-53.

31. Schrader KA, Masciari S, Boyd N, Salamanca C, Senz J, Saunders DN, Yorida E, Maines-Bandiera S, Kaurah P, Tung N, et al. Germline mutations in CDH1 are infrequent in women with early-onset or familial lobular breast cancers. J Med Genet 2011; 48:64-8.

32. Ahmed M, Rahman N. ATM and breast cancer susceptibility. Oncogene 2006; 25:5906-11.

33. Renwick A, Thompson D, Seal S, Kelly P, Chagtai T, Ahmed M, North B, Jayatilake H, Barfoot R, Spanova K, et al. ATM mutations that cause ataxia-telangiectasia are breast cancer susceptibility alleles. Nature Genetics 2006; 38:873-5.

34. Herman JG, Baylin SB. Gene silencing in cancer in association with promoter hypermethylation. N Engl J Med 2003; 349:2042-54.

35. Hanahan D, Weinberg RA. The hallmarks of cancer. Cell 2000; 100:57-70.

36. Hanahan D, Weinberg RA. Hallmarks of Cancer: The Next Generation. Cell 2011; 144:646-74.

37. Carrer A, Wellen KE. Metabolism and epigenetics: a link cancer cells exploit. Curr Opin Biotechnol 2014; 34:23-9.

38. Esteller M. Epigenetic gene silencing in cancer: the DNA hypermethylome. Hum Mol Genet 2007; 16 Spec No 1:R50-9.

39. Hamidi T, Singh AK, Chen T. Genetic alterations of DNA methylation machinery in human diseases. Epigenomics 2015; 7:247-65.

40. Hon GC, Hawkins RD, Caballero OL, Lo C, Lister R, Pelizzola M, Valsesia A, Ye Z, Kuan S, Edsall LE, et al. Global DNA hypomethylation coupled to repressive chromatin domain formation and gene silencing in breast cancer. Genome Res 2012; 22:246-58.

41. Esteller M. Cancer epigenomics: DNA methylomes and histone-modification maps. Nat Rev Genet 2007; 8:286-98.

42. Lopez-Serra L, Esteller M. Proteins that bind methylated DNA and human cancer: reading the wrong words. Br J Cancer 2008; 98:1881-5.

43. Takai D, Jones PA. Comprehensive analysis of CpG islands in human chromosomes 21 and 22. Proc Natl Acad Sci U S A 2002; 99:3740-5.

44. Gardiner-Garden M, Frommer M. CpG islands in vertebrate genomes. J Mol Biol 1987; 196:261-82.

45. Inbar-Feigenberg M, Choufani S, Butcher DT, Roifman M, Weksberg R. Basic concepts of epigenetics. Fertil Steril 2013; 99:607-15.

46. Esteller M, Herman JG. Cancer as an epigenetic disease: DNA methylation and chromatin alterations in human tumours. J Pathol 2002; 196:1-7.

47. Esteller M. Epigenetics in cancer. N Engl J Med 2008; 358:1148-59.

48. Ballestar E, Esteller M. Epigenetic gene regulation in cancer. Adv Genet 2008; 61:247-67.

49. Miousse IR, Koturbash I. The Fine LINE: Methylation Drawing the Cancer Landscape. Biomed Res Int 2015; 2015:131547.

50. Greger V, Passarge E, Hopping W, Messmer E, Horsthemke B. Epigenetic changes may contribute to the formation and spontaneous regression of retinoblastoma. Hum Genet 1989; 83:155-8.

51. Yoshiura K, Kanai Y, Ochiai A, Shimoyama Y, Sugimura T, Hirohashi S. Silencing of the E-cadherin invasion-suppressor gene by CpG methylation in human carcinomas. Proc Natl Acad Sci U S A 1995; 92:7416-9.

52. Hakkarainen M, Wahlfors J, Myohanen S, Hiltunen MO, Eskelinen M, Johansson R, Janne J. Hypermethylation of calcitonin gene regulatory sequences in human breast cancer as revealed by genomic sequencing. Int J Cancer 1996; 69:471-4.

53. Herman JG, Jen J, Merlo A, Baylin SB. Hypermethylation-associated inactivation indicates a tumor suppressor role for p15INK4B. Cancer Res 1996; 56:722-7.

54. Ottaviano YL, Issa JP, Parl FF, Smith HS, Baylin SB, Davidson NE. Methylation of the estrogen receptor gene CpG island marks loss of estrogen receptor expression in human breast cancer cells. Cancer Res 1994; 54:2552-5.

55. Merlo A, Herman JG, Mao L, Lee DJ, Gabrielson E, Burger PC, Baylin SB, Sidransky D. 5' CpG island methylation is associated with transcriptional silencing of the tumour suppressor p16/CDKN2/MTS1 in human cancers. Nat Med 1995; 1:686-92.

56. Shao L, Cui Y, Li H, Liu Y, Zhao H, Wang Y, Zhang Y, Ng KM, Han W, Ma D, et al. CMTM5 exhibits tumor suppressor activities and is frequently silenced by methylation in carcinoma cell lines. Clin Cancer Res 2007; 13:5756-62.

57. Cui Y, Ying Y, van Hasselt A, Ng KM, Yu J, Zhang Q, Jin J, Liu D, Rhim JS, Rha SY, et al. OPCML is a broad tumor suppressor for multiple carcinomas and lymphomas with frequently epigenetic inactivation. PLoS One 2008; 3:e2990.

58. Kim TY, Lee HJ, Hwang KS, Lee M, Kim JW, Bang YJ, Kang GH. Methylation of RUNX3 in various types of human cancers and premalignant stages of gastric carcinoma. Lab Invest 2004; 84:479-84.

59. Herman JG, Merlo A, Mao L, Lapidus RG, Issa JP, Davidson NE, Sidransky D, Baylin SB. Inactivation of the CDKN2/p16/MTS1 gene is frequently associated with aberrant DNA methylation in all common human cancers. Cancer Res 1995; 55:4525-30.

60. Esteller M, Corn PG, Baylin SB, Herman JG. A gene hypermethylation profile of human cancer. Cancer Res 2001; 61:3225-9.

61. Wang J, Wang B, Chen X, Bi J. The prognostic value of RASSF1A promoter hypermethylation in non-small cell lung carcinoma: a systematic review and meta-analysis. Carcinogenesis 2011; 32:411-6.

62. Zhang W, Jiao H, Zhang X, Zhao R, Wang F, He W, Zong H, Fan Q, Wang L. Correlation between the expression of DNMT1, and GSTP1 and APC, and the methylation status of GSTP1 and APC in association with their clinical significance in prostate cancer. Mol Med Rep 2015; 12:141-6.

63. Balgkouranidou I, Matthaios D, Karayiannakis A, Bolanaki H, Michailidis P, Xenidis N, Amarantidis K, Chelis L, Trypsianis G, Chatzaki E, et al. Prognostic role of APC and RASSF1A promoter methylation status in cell free circulating DNA of operable gastric cancer patients. Mutat Res 2015; 778:46-51.

64. Jones PA, Baylin SB. The fundamental role of epigenetic events in cancer. Nat Rev Genet 2002; 3:415-28.

65. Dobrovic A, Simpfendorfer D. Methylation of the BRCA1 gene in sporadic breast cancer. Cancer Res 1997; 57:3347-50.

66. Li Q, Wei W, Jiang YI, Yang H, Liu J. Promoter methylation and expression changes of in cancerous tissues of patients with sporadic breast cancer. Oncol Lett 2015; 9:1807-13.

67. Li X, Yao X, Wang Y, Hu F, Wang F, Jiang L, Liu Y, Wang D, Sun G, Zhao Y. MLH1 promoter methylation frequency in colorectal cancer patients and related clinicopathological and molecular features. PLoS One 2013; 8:e59064.

68. Choi JD, Lee JS. Interplay between Epigenetics and Genetics in Cancer. Genomics Inform 2013; 11:164-73.

69. Berger AH, Knudson AG, Pandolfi PP. A continuum model for tumour suppression. Nature 2011; 476:163-9.

70. Knudson AG, Jr. Mutation and cancer: statistical study of retinoblastoma. Proc Natl Acad Sci U S A 1971; 68:820-3.

71. Langst G, Manelyte L. Chromatin Remodelers: From Function to Dysfunction. Genes (Basel) 2015; 6:299-324.

72. Hamm CA, Costa FF. Epigenomes as therapeutic targets. Pharmacol Ther 2015; 151:72-86.

73. Zhao Y, Garcia BA. Comprehensive Catalog of Currently Documented Histone Modifications. Cold Spring Harb Perspect Biol 2015; 7.

74. Baxter E, Windloch K, Gannon F, Lee JS. Epigenetic regulation in cancer progression. Cell Biosci 2014; 4:45.

75. Mottamal M, Zheng S, Huang TL, Wang G. Histone deacetylase inhibitors in clinical studies as templates for new anticancer agents. Molecules 2015; 20:3898-941.

76. Yamamura A, Miura K, Karasawa H, Morishita K, Abe K, Mizuguchi Y, Saiki Y, Fukushige S, Kaneko N, Sase T, et al. Suppressed expression of NDRG2 correlates with poor prognosis in pancreatic cancer. Biochem Biophys Res Commun 2013; 441:102-7.

77. Fabian J, Lodrini M, Oehme I, Schier MC, Thole TM, Hielscher T, Kopp-Schneider A, Opitz L, Capper D, von Deimling A, et al. GRHL1 acts as tumor suppressor in neuroblastoma and is negatively regulated by MYCN and HDAC3. Cancer Res 2014; 74:2604-16.

78. Cras A, Darsin-Bettinger D, Balitrand N, Cassinat B, Soulie A, Toubert ME, Delva L, Chomienne C. Epigenetic patterns of the retinoic acid receptor beta2 promoter in retinoic acid-resistant thyroid cancer cells. Oncogene 2007; 26:4018-24.

79. Pasqualucci L, Dominguez-Sola D, Chiarenza A, Fabbri G, Grunn A, Trifonov V, Kasper LH, Lerach S, Tang H, Ma J, et al. Inactivating mutations of acetyltransferase genes in B-cell lymphoma. Nature 2011; 471:189-95.

80. Feng D, Wu J, Tian Y, Zhou H, Zhou Y, Hu W, Zhao W, Wei H, Ling B, Ma C. Targeting of histone deacetylases to reactivate tumour suppressor genes and its therapeutic potential in a human cervical cancer xenograft model. PLoS One 2013; 8:e80657.

81. Szyf M, Pakneshan P, Rabbani SA. DNA methylation and breast cancer. Biochem Pharmacol 2004; 68:1187-97.

82. Dworkin AM, Huang TH, Toland AE. Epigenetic alterations in the breast: Implications for breast cancer detection, prognosis and treatment. Semin Cancer Biol 2009; 19:165-71.

83. Rodenhiser DI, Andrews J, Kennette W, Sadikovic B, Mendlowitz A, Tuck AB, Chambers AF. Epigenetic mapping and functional analysis in a breast cancer metastasis model using whole-genome promoter tiling microarrays. Breast Cancer Res 2008; 10:R62.

84. Feng W, Shen L, Wen S, Rosen DG, Jelinek J, Hu X, Huan S, Huang M, Liu J, Sahin AA, et al. Correlation between CpG methylation profiles and hormone receptor status in breast cancers. Breast Cancer Res 2007; 9:R57.

85. Conway K, Edmiston SN, May R, Kuan PF, Chu H, Bryant C, Tse CK, Swift-Scanlan T, Geradts J, Troester MA, et al. DNA methylation profiling in the Carolina Breast Cancer Study defines cancer subclasses differing in clinicopathologic characteristics and survival. Breast Cancer Res 2014; 16:450.

86. Network CGA. Comprehensive molecular portraits of human breast tumours. Nature 2012; 490:61-70.

87. Byler S, Goldgar S, Heerboth S, Leary M, Housman G, Moulton K, Sarkar S. Genetic and epigenetic aspects of breast cancer progression and therapy. Anticancer Res 2014; 34:1071-7.

88. Soares J, Pinto AE, Cunha CV, Andre S, Barao I, Sousa JM, Cravo M. Global DNA hypomethylation in breast carcinoma: correlation with prognostic factors and tumor progression. Cancer 1999; 85:112-8.

89. Lo PK, Sukumar S. Epigenomics and breast cancer. Pharmacogenomics 2008; 9:1879-902.

90. Park SY, Seo AN, Jung HY, Gwak JM, Jung N, Cho NY, Kang GH. Alu and LINE-1 hypomethylation is associated with HER2 enriched subtype of breast cancer. PLoS One 2014; 9:e100429.

91. Elsheikh SE, Green AR, Rakha EA, Powe DG, Ahmed RA, Collins HM, Soria D, Garibaldi JM, Paish CE, Ammar AA, et al. Global histone modifications in breast cancer correlate with tumor phenotypes, prognostic factors, and patient outcome. Cancer Res 2009; 69:3802-9.

92. Seo J, Min SK, Park HR, Kim DH, Kwon MJ, Kim LS, Ju YS. Expression of Histone Deacetylases HDAC1, HDAC2, HDAC3, and HDAC6 in Invasive Ductal Carcinomas of the Breast. J Breast Cancer 2014; 17:323-31.

93. Kleer CG, Cao Q, Varambally S, Shen R, Ota I, Tomlins SA, Ghosh D, Sewalt RG, Otte AP, Hayes DF, et al. EZH2 is a marker of aggressive breast cancer and promotes neoplastic transformation of breast epithelial cells. Proc Natl Acad Sci U S A 2003; 100:11606-11.

94. Dong C, Wu Y, Yao J, Wang Y, Yu Y, Rychahou PG, Evers BM, Zhou BP. G9a interacts with Snail and is critical for Snail-mediated E-cadherin repression in human breast cancer. J Clin Invest 2012; 122:1469-86.

95. Sirchia SM, Ren M, Pili R, Sironi E, Somenzi G, Ghidoni R, Toma S, Nicolo G, Sacchi N. Endogenous reactivation of the RARbeta2 tumor suppressor gene epigenetically silenced in breast cancer. Cancer Res 2002; 62:2455-61.

96. Yang X, Phillips DL, Ferguson AT, Nelson WG, Herman JG, Davidson NE. Synergistic activation of functional estrogen receptor (ER)-alpha by DNA methyltransferase and histone deacetylase inhibition in human ER-alpha-negative breast cancer cells. Cancer Res 2001; 61:7025-9.

97. Yu Y, Fujii S, Yuan J, Luo RZ, Wang L, Bao J, Kadota M, Oshimura M, Dent SR, Issa JP, et al. Epigenetic regulation of ARHI in breast and ovarian cancer cells. Ann N Y Acad Sci 2003; 983:268-77.

98. Gormally E, Caboux E, Vineis P, Hainaut P. Circulating free DNA in plasma or serum as biomarker of carcinogenesis: practical aspects and biological significance. Mutat Res 2007; 635:105-17.

99. Radpour R, Barekati Z, Kohler C, Lv Q, Burki N, Diesch C, Bitzer J, Zheng H, Schmid S, Zhong XY. Hypermethylation of tumor suppressor genes involved in critical regulatory pathways for developing a blood-based test in breast cancer. PLoS One 2011; 6:e16080.

100. Laird PW. The power and the promise of DNA methylation markers. Nat Rev Cancer 2003; 3:253-66.

101. Sanchez-Cespedes M, Esteller M, Wu L, Nawroz-Danish H, Yoo GH, Koch WM, Jen J, Herman JG, Sidransky D. Gene promoter hypermethylation in tumors and serum of head and neck cancer patients. Cancer Res 2000; 60:892-5.

102. Van De Voorde L, Speeckaert R, Van Gestel D, Bracke M, De Neve W, Delanghe J, Speeckaert M. DNA methylation-based biomarkers in serum of patients with breast cancer. Mutat Res 2012; 751:304-25.

103. Mulero-Navarro S, Esteller M. Epigenetic biomarkers for human cancer: the time is now. Crit Rev Oncol Hematol 2008; 68:1-11.

104. Shukla S, Mirza S, Sharma G, Parshad R, Gupta SD, Ralhan R. Detection of RASSF1A and RARbeta hypermethylation in serum DNA from breast cancer patients. Epigenetics 2006; 1:88-93.

105. Kristiansen S, Jorgensen LM, Guldberg P, Soletormos G. Aberrantly methylated DNA as a biomarker in breast cancer. Int J Biol Markers 2013; 28:141-50.

106. Ordway JM, Budiman MA, Korshunova Y, Maloney RK, Bedell JA, Citek RW, Bacher B, Peterson S, Rohlfing T, Hall J, et al. Identification of novel high-frequency DNA methylation changes in breast cancer. PLoS One 2007; 2:e1314.

107. Patra SK, Bettuzzi S. Epigenetic DNA-(cytosine-5-carbon) modifications: 5-aza-2'-deoxycytidine and DNA-demethylation. Biochemistry (Mosc) 2009; 74:613-9.

108. Finnin MS. Structures of a histone deacetylase homologue bound to the TSA and SAHA inhibitors. Nature 1999; 401:188-93.

109. Suzuki H, Gabrielson E, Chen W, Anbazhagan R, van Engeland M, Weijenberg MP, Herman JG, Baylin SB. A genomic screen for genes upregulated by demethylation and histone deacetylase inhibition in human colorectal cancer. Nat Genet 2002; 31:141-9.

110. Dedeurwaerder S, Desmedt C, Calonne E, Singhal SK, Haibe-Kains B, Defrance M, Michiels S, Volkmar M, Deplus R, Luciani J, et al. DNA methylation profiling reveals a predominant immune component in breast cancers. EMBO Mol Med 2011; 3:726-41.

111. Hinshelwood RA, Huschtscha LI, Melki J, Stirzaker C, Abdipranoto A, Vissel B, Ravasi T, Wells CA, Hume DA, Reddel RR, et al. Concordant epigenetic silencing of transforming growth factor-beta signaling pathway genes occurs early in breast carcinogenesis. Cancer Res 2007; 67:11517-27.

112. Gallagher WM, Bergin OE, Rafferty M, Kelly ZD, Nolan IM, Fox EJ, Culhane AC, McArdle L, Fraga MF, Hughes L, et al. Multiple markers for melanoma progression regulated by DNA methylation: insights from transcriptomic studies. Carcinogenesis 2005; 26:1856-67.

113. Sova P, Feng Q, Geiss G, Wood T, Strauss R, Rudolf V, Lieber A, Kiviat N. Discovery of novel methylation biomarkers in cervical carcinoma by global demethylation and microarray analysis. Cancer Epidemiol Biomarkers Prev 2006; 15:114-23.

114. Kim H, Lapointe J, Kaygusuz G, Ong DE, Li C, van de Rijn M, Brooks JD, Pollack JR. The retinoic acid synthesis gene ALDH1a2 is a candidate tumor suppressor in prostate cancer. Cancer Res 2005; 65:8118-24.

115. Chittur SV, Sangster-Guity N, McCormick PJ. Histone deacetylase inhibitors: a new mode for inhibition of cholesterol metabolism. BMC Genomics 2008; 9:507.

116. Mueller W, Nutt CL, Ehrich M, Riemenschneider MJ, von Deimling A, van den Boom D, Louis DN. Downregulation of RUNX3 and TES by hypermethylation in glioblastoma. Oncogene 2007; 26:583-93.

117. Schuebel KE, Chen W, Cope L, Glockner SC, Suzuki H, Yi JM, Chan TA, Van Neste L, Van Criekinge W, van den Bosch S, et al. Comparing the DNA hypermethylome with gene mutations in human colorectal cancer. PLoS Genet 2007; 3:1709-23.

118. Dannenberg LO, Edenberg HJ. Epigenetics of gene expression in human hepatoma cells: expression profiling the response to inhibition of DNA methylation and histone deacetylation. BMC Genomics 2006; 7:181.

119. Shames DS, Girard L, Gao B, Sato M, Lewis CM, Shivapurkar N, Jiang A, Perou CM, Kim YH, Pollack JR, et al. A genome-wide screen for promoter methylation in lung cancer identifies novel methylation markers for multiple malignancies. PLoS Med 2006; 3:e486.

120. Hellebrekers DM, Melotte V, Vire E, Langenkamp E, Molema G, Fuks F, Herman JG, Van Criekinge W, Griffioen AW, van Engeland M. Identification of epigenetically silenced genes in tumor endothelial cells. Cancer Res 2007; 67:4138-48.

121. Al-Romaih K, Somers GR, Bayani J, Hughes S, Prasad M, Cutz JC, Xue H, Zielenska M, Wang Y, Squire JA. Modulation by decitabine of gene expression and growth of osteosarcoma U2OS cells in vitro and in xenografts: Identification of apoptotic genes as targets for demethylation. Cancer Cell Int 2007; 7:14.

122. Fukutomi S, Seki N, Koda K, Miyazaki M. Identification of methylation-silenced genes in colorectal cancer cell lines: genomic screening using oligonucleotide arrays. Scand J Gastroenterol 2007; 42:1486-94.

123. Ehlers A, Oker E, Bentink S, Lenze D, Stein H, Hummel M. Histone acetylation and DNA demethylation of B cells result in a Hodgkin-like phenotype. Leukemia 2008; 22:835-41.

124. Muthusamy V, Duraisamy S, Bradbury CM, Hobbs C, Curley DP, Nelson B, Bosenberg M. Epigenetic silencing of novel tumor suppressors in malignant melanoma. Cancer Res 2006; 66:11187-93.

125. Mishra PJ, Humeniuk R, Medina DJ, Alexe G, Mesirov JP, Ganesan S, Glod JW, Banerjee D. Carcinoma-associated fibroblast-like differentiation of human mesenchymal stem cells. Cancer Res 2008; 68:4331-9.

126. Toyota M, Suzuki H, Sasaki Y, Maruyama R, Imai K, Shinomura Y, Tokino T. Epigenetic silencing of microRNA-34b/c and B-cell translocation gene 4 is associated with CpG island methylation in colorectal cancer. Cancer Res 2008; 68:4123-32.

127. Jiang X, Tan J, Li J, Kivimae S, Yang X, Zhuang L, Lee PL, Chan MT, Stanton LW, Liu ET, et al. DACT3 is an epigenetic regulator of Wnt/beta-catenin signaling in colorectal cancer and is a therapeutic target of histone modifications. Cancer Cell 2008; 13:529-41.

128. Heller G, Schmidt WM, Ziegler B, Holzer S, Mullauer L, Bilban M, Zielinski CC, Drach J, Zochbauer-Muller S. Genome-wide transcriptional response to 5-aza-2'-deoxycytidine and trichostatin a in multiple myeloma cells. Cancer Res 2008; 68:44-54.

129. Morris MR, Ricketts C, Gentle D, Abdulrahman M, Clarke N, Brown M, Kishida T, Yao M, Latif F, Maher ER. Identification of candidate tumour suppressor genes frequently methylated in renal cell carcinoma. Oncogene 2010; 29:2104-17.

130. Fabiani E, Leone G, Giachelia M, D'Alo F, Greco M, Criscuolo M, Guidi F, Rutella S, Hohaus S, Voso MT. Analysis of genome-wide methylation and gene expression induced by 5-aza-2'-deoxycytidine identifies BCL2L10 as a frequent methylation target in acute myeloid leukemia. Leuk Lymphoma 2010; 51:2275-84.

131. Khamas A, Ishikawa T, Shimokawa K, Mogushi K, Iida S, Ishiguro M, Mizushima H, Tanaka H, Uetake H, Sugihara K. Screening for epigenetically masked genes in colorectal cancer Using 5-Aza-2'-deoxycytidine, microarray and gene expression profile. Cancer Genomics Proteomics 2012; 9:67-75.

132. Heller G, Babinsky VN, Ziegler B, Weinzierl M, Noll C, Altenberger C, Mullauer L, Dekan G, Grin Y, Lang G, et al. Genome-wide CpG island methylation analyses in non-small cell lung cancer patients. Carcinogenesis 2013; 34:513-21.

133. Schayek H, Bentov I, Jacob-Hirsch J, Yeung C, Khanna C, Helman LJ, Plymate SR, Werner H. Global methylation analysis identifies PITX2 as an upstream regulator of the androgen receptor and IGF-I receptor genes in prostate cancer. Horm Metab Res 2012; 44:511-9.

134. Dimitrova L, Seitz V, Hecht J, Lenze D, Hansen P, Szczepanowski M, Ma L, Oker E, Sommerfeld A, Jundt F, et al. PAX5 overexpression is not enough to reestablish the mature B-cell phenotype in classical Hodgkin lymphoma. Leukemia 2014; 28:213-6.

135. Ikegaki N, Shimada H, Fox AM, Regan PL, Jacobs JR, Hicks SL, Rappaport EF, Tang XX. Transient treatment with epigenetic modifiers yields stable neuroblastoma stem cells resembling aggressive large-cell neuroblastomas. Proc Natl Acad Sci U S A 2013; 110:6097-102.

136. Karakoula K, Jacques TS, Phipps KP, Harkness W, Thompson D, Harding BN, Darling JL, Warr TJ. Epigenetic genome-wide analysis identifies BEX1 as a candidate tumour suppressor gene in paediatric intracranial ependymoma. Cancer Lett 2014; 346:34-44.

137. Ruike Y, Imanaka Y, Sato F, Shimizu K, Tsujimoto G. Genome-wide analysis of aberrant methylation in human breast cancer cells using methyl-DNA immunoprecipitation combined with high-throughput sequencing. BMC Genomics 2010; 11:137.

138. Lin IH, Chen DT, Chang YF, Lee YL, Su CH, Cheng C, Tsai YC, Ng SC, Chen HT, Lee MC, et al. Hierarchical clustering of breast cancer methylomes revealed differentially methylated and expressed breast cancer genes. PLoS One 2015; 10:e0118453.

139. Schuetz CS, Bonin M, Clare SE, Nieselt K, Sotlar K, Walter M, Fehm T, Solomayer E, Riess O, Wallwiener D, et al. Progression-specific genes identified by expression profiling of matched ductal carcinomas in situ and invasive breast tumors, combining laser capture microdissection and oligonucleotide microarray analysis. Cancer Res 2006; 66:5278-86.

140. Lo AK, Yuen PW, Liu Y, Wang XH, Cheung AL, Wong YC, Tsao SW. Downregulation of hemidesmosomal proteins in nasopharyngeal carcinoma cells. Cancer Lett 2001; 163:117-23.

141. Chopra A, Maitra B, Korman NJ. Decreased mRNA expression of several basement membrane components in basal cell carcinoma. J Invest Dermatol 1998; 110:52-6.

142. Mundel TM, Yliniemi AM, Maeshima Y, Sugimoto H, Kieran M, Kalluri R. Type IV collagen alpha6 chain-derived noncollagenous domain 1 (alpha6(IV)NC1) inhibits angiogenesis and tumor growth. Int J Cancer 2008; 122:1738-44.

143. Skovbjerg H, Anthonsen D, Lothe IM, Tveit KM, Kure EH, Vogel LK. Collagen mRNA levels changes during colorectal cancer carcinogenesis. BMC Cancer 2009; 9:136.

144. Baba Y, Iyama K, Ikeda K, Ishikawa S, Hayashi N, Miyanari N, Sado Y, Ninomiya Y, Baba H. The expression of type IV collagen alpha6 chain is related to the prognosis in patients with esophageal squamous cell carcinoma. Ann Surg Oncol 2008; 15:555-65.

145. Kadono G, Ishihara T, Yamaguchi T, Kato K, Kondo F, Naito I, Sado Y, Saisho H. Immunohistochemical localization of type IV collagen alpha chains in the basement membrane of the pancreatic duct in human normal pancreas and pancreatic diseases. Pancreas 2004; 29:61-6.

146. Varisli L. Identification of new genes downregulated in prostate cancer and investigation of their effects on prognosis. Genet Test Mol Biomarkers 2013; 17:562-6.

147. Hirashima K, Iyama K, Baba Y, Honda Y, Sado Y, Ninomiya Y, Watanabe M, Takamori H, Beppu T, Baba H. Differential expression of basement membrane type IV collagen alpha2 and alpha6 chains as a prognostic factor in patients with extrahepatic bile duct carcinoma. J Surg Oncol 2013; 107:402-7.

148. Ikeda K, Iyama K, Ishikawa N, Egami H, Nakao M, Sado Y, Ninomiya Y, Baba H. Loss of expression of type IV collagen alpha5 and alpha6 chains in colorectal cancer associated with the hypermethylation of their promoter region. Am J Pathol 2006; 168:856-65.

149. Furuhashi M, Yagi K, Yamamoto H, Furukawa Y, Shimada S, Nakamura Y, Kikuchi A, Miyazono K, Kato M. Axin facilitates Smad3 activation in the transforming growth factor beta signaling pathway. Mol Cell Biol 2001; 21:5132-41.

150. Yook JI, Li XY, Ota I, Hu C, Kim HS, Kim NH, Cha SY, Ryu JK, Choi YJ, Kim J, et al. A Wnt-Axin2-GSK3beta cascade regulates Snail1 activity in breast cancer cells. Nat Cell Biol 2006; 8:1398-406.

151. Hadjihannas MV, Bruckner M, Behrens J. Conductin/axin2 and Wnt signalling regulates centrosome cohesion. EMBO Rep 2010; 11:317-24.

152. Kim MS, Kim SS, Ahn CH, Yoo NJ, Lee SH. Frameshift mutations of Wnt pathway genes AXIN2 and TCF7L2 in gastric carcinomas with high microsatellite instability. Hum Pathol 2009; 40:58-64.

153. Castiglia D, Bernardini S, Alvino E, Pagani E, De Luca N, Falcinelli S, Pacchiarotti A, Bonmassar E, Zambruno G, D'Atri S. Concomitant activation of Wnt pathway and loss of mismatch repair function in human melanoma. Genes Chromosomes Cancer 2008; 47:614-24.

154. Li S, Wang C, Liu X, Hua S. The roles of AXIN2 in tumorigenesis and epigenetic regulation. Fam Cancer 2015; 14:325-31.

155. Koinuma K, Yamashita Y, Liu W, Hatanaka H, Kurashina K, Wada T, Takada S, Kaneda R, Choi YL, Fujiwara SI, et al. Epigenetic silencing of AXIN2 in colorectal carcinoma with microsatellite instability. Oncogene 2006; 25:139-46.

156. Tseng RC, Lin RK, Wen CK, Tseng C, Hsu HS, Hsu WH, Wang YC. Epigenetic silencing of AXIN2/betaTrCP and deregulation of p53-mediated control lead to wild-type beta-catenin nuclear accumulation in lung tumorigenesis. Oncogene 2008; 27:4488-96.

157. Kim JT, Li J, Jang ER, Gulhati P, Rychahou PG, Napier DL, Wang C, Weiss HL, Lee EY, Anthony L, et al. Deregulation of Wnt/beta-catenin signaling through genetic or epigenetic alterations in human neuroendocrine tumors. Carcinogenesis 2013; 34:953-61.

158. Vilborg A, Glahder JA, Wilhelm MT, Bersani C, Corcoran M, Mahmoudi S, Rosenstierne M, Grander D, Farnebo M, Norrild B, et al. The p53 target Wig-1 regulates p53 mRNA stability through an AU-rich element. Proc Natl Acad Sci U S A 2009; 106:15756-61.

159. Mendez Vidal C, Prahl M, Wiman KG. The p53-induced Wig-1 protein binds double-stranded RNAs with structural characteristics of siRNAs and miRNAs. FEBS Lett 2006; 580:4401-8.

160. Bersani C, Xu LD, Vilborg A, Lui WO, Wiman KG. Wig-1 regulates cell cycle arrest and cell death through the p53 targets FAS and 14-3-3sigma. Oncogene 2014; 33:4407-17.

161. Hellborg F, Qian W, Mendez-Vidal C, Asker C, Kost-Alimova M, Wilhelm M, Imreh S, Wiman KG. Human wig-1, a p53 target gene that encodes a growth inhibitory zinc finger protein. Oncogene 2001; 20:5466-74.

162. Shan J, Wang P, Zhou J, Wu D, Shi H, Huo K. RIOK3 interacts with caspase-10 and negatively regulates the NF-kappaB signaling pathway. Mol Cell Biochem 2009; 332:113-20.

163. Roesch A, Vogt T, Stolz W, Dugas M, Landthaler M, Becker B. Discrimination between gene expression patterns in the invasive margin and the tumour core of malignant melanomas. Melanoma Res 2003; 13:503-9.

164. Mishra DK, Chen Z, Wu Y, Sarkissyan M, Koeffler HP, Vadgama JV. Global methylation pattern of genes in androgen-sensitive and androgen-independent prostate cancer cells. Mol Cancer Ther 2010; 9:33-45.

165. Kimmelman AC, Hezel AF, Aguirre AJ, Zheng H, Paik JH, Ying H, Chu GC, Zhang JX, Sahin E, Yeo G, et al. Genomic alterations link Rho family of GTPases to the highly invasive phenotype of pancreas cancer. Proc Natl Acad Sci U S A 2008; 105:19372-7.

166. Singleton DC, Rouhi P, Zois CE, Haider S, Li JL, Kessler BM, Cao Y, Harris AL. Hypoxic regulation of RIOK3 is a major mechanism for cancer cell invasion and metastasis. Oncogene 2015; 34:4713-22.

167. Hollander MC, Kovalsky O, Salvador JM, Kim KE, Patterson AD, Haines DC, Fornace AJ, Jr. Dimethylbenzanthracene carcinogenesis in Gadd45a-null mice is associated with decreased DNA repair and increased mutation frequency. Cancer Res 2001; 61:2487-91.

168. Hollander MC, Sheikh MS, Yu K, Zhan Q, Iglesias M, Woodworth C, Fornace AJ, Jr. Activation of Gadd34 by diverse apoptotic signals and suppression of its growth inhibitory effects by apoptotic inhibitors. Int J Cancer 2001; 96:22-31.

169. Hollander MC, Zhan Q, Bae I, Fornace AJ, Jr. Mammalian GADD34, an apoptosis- and DNA damage-inducible gene. J Biol Chem 1997; 272:13731-7.

170. Hu Y, Sun H, Drake J, Kittrell F, Abba MC, Deng L, Gaddis S, Sahin A, Baggerly K, Medina D, et al. From mice to humans: identification of commonly deregulated genes in mammary cancer via comparative SAGE studies. Cancer Res 2004; 64:7748-55.

171. Minami K, Inoue H, Terashita T, Kawakami T, Watanabe R, Haneda M, Isobe K, Okabe H, Chano T. GADD34 induces p21 expression and cellular senescence. Oncol Rep 2007; 17:1481-5.

172. Tanaka C, Ito S, Nishio N, Kodera Y, Sakurai H, Suzuki H, Nakao A, Isobe K. GADD34 suppresses wound healing by upregulating expression of myosin IIA. Transgenic Res 2010; 19:637-45.

173. Zou H, Li Y, Liu X, Wang X. An APAF-1.cytochrome c multimeric complex is a functional apoptosome that activates procaspase-9. J Biol Chem 1999; 274:11549-56.

174. Soung YH, Lee JW, Kim SY, Park WS, Nam SW, Lee JY, Yoo NJ, Lee SH. Mutational analysis of proapoptotic caspase-9 gene in common human carcinomas. APMIS 2006; 114:292-7.

175. Dajee M, Lazarov M, Zhang JY, Cai T, Green CL, Russell AJ, Marinkovich MP, Tao S, Lin Q, Kubo Y, et al. NF-kappaB blockade and oncogenic Ras trigger invasive human epidermal neoplasia. Nature 2003; 421:639-43.

176. Lake A, Shield LA, Cordano P, Chui DT, Osborne J, Crae S, Wilson KS, Tosi S, Knight SJ, Gesk S, et al. Mutations of NFKBIA, encoding IkappaB alpha, are a recurrent finding in classical Hodgkin lymphoma but are not a unifying feature of non-EBV-associated cases. Int J Cancer 2009; 125:1334-42.

177. Geng P, Ou J, Li J, Liao Y, Wang N, Sa R, Xiang L, Liang H. Genetic Association Between NFKBIA -881A>G Polymorphism and Cancer Susceptibility. Medicine (Baltimore) 2015; 94:e1024.

178. Bassermann F, Frescas D, Guardavaccaro D, Busino L, Peschiaroli A, Pagano M. The Cdc14B-Cdh1-Plk1 axis controls the G2 DNA-damage-response checkpoint. Cell 2008; 134:256-67.

179. Wu J, Cho HP, Rhee DB, Johnson DK, Dunlap J, Liu Y, Wang Y. Cdc14B depletion leads to centriole amplification, and its overexpression prevents unscheduled centriole duplication. J Cell Biol 2008; 181:475-83.

180. Rodier G, Coulombe P, Tanguay PL, Boutonnet C, Meloche S. Phosphorylation of Skp2 regulated by CDK2 and Cdc14B protects it from degradation by APC(Cdh1) in G1 phase. EMBO J 2008; 27:679-91.

181. Guillamot M, Manchado E, Chiesa M, Gomez-Lopez G, Pisano DG, Sacristan MP, Malumbres M. Cdc14b regulates mammalian RNA polymerase II and represses cell cycle transcription. Sci Rep 2011; 1:189.

182. Calvisi DF, Ladu S, Pinna F, Frau M, Tomasi ML, Sini M, Simile MM, Bonelli P, Muroni MR, Seddaiu MA, et al. SKP2 and CKS1 promote degradation of cell cycle regulators and are

associated with hepatocellular carcinoma prognosis. Gastroenterology 2009; 137:1816-26 e1-10.

183. Kim Y, Choi JW, Lee JH, Kim YS. Loss of CDC14B expression in clear cell renal cell carcinoma: meta-analysis of microarray data sets. Am J Clin Pathol 2014; 141:551-8.

184. Karagiannis ED, Popel AS. Peptides derived from type I thrombospondin repeat-containing proteins of the CCN family inhibit proliferation and migration of endothelial cells. Int J Biochem Cell Biol 2007; 39:2314-23.

185. Liu J, Guo Q, Chen B, Yu Y, Lu H, Li YY. Cathepsin B and its interacting proteins, bikunin and TSRC1, correlate with TNF-induced apoptosis of ovarian cancer cells OV-90. FEBS Lett 2006; 580:245-50.

186. Juric D, Lacayo NJ, Ramsey MC, Racevskis J, Wiernik PH, Rowe JM, Goldstone AH, O'Dwyer PJ, Paietta E, Sikic BI. Differential gene expression patterns and interaction networks in BCR-ABL-positive and -negative adult acute lymphoblastic leukemias. J Clin Oncol 2007; 25:1341-9.

187. Crose LE, Galindo KA, Kephart JG, Chen C, Fitamant J, Bardeesy N, Bentley RC, Galindo RL, Chi JT, Linardic CM. Alveolar rhabdomyosarcoma-associated PAX3-FOXO1 promotes tumorigenesis via Hippo pathway suppression. J Clin Invest 2014; 124:285-96.

188. Kikuchi K, Hettmer S, Aslam MI, Michalek JE, Laub W, Wilky BA, Loeb DM, Rubin BP, Wagers AJ, Keller C. Cell-cycle dependent expression of a translocation-mediated fusion oncogene mediates checkpoint adaptation in rhabdomyosarcoma. PLoS Genet 2014; 10:e1004107.

189. Pauta M, Rotllan N, Fernandez-Hernando A, Langhi C, Ribera J, Lu M, Boix L, Bruix J, Jimenez W, Suarez Y, et al. Akt-mediated FoxO1 inhibition is required for liver regeneration. Hepatology 2015.

190. Guttilla IK, White BA. Coordinate regulation of FOXO1 by miR-27a, miR-96, and miR-182 in breast cancer cells. J Biol Chem 2009; 284:23204-16.

191. Yang J, Li T, Gao C, Lv X, Liu K, Song H, Xing Y, Xi T. FOXO1 3'UTR functions as a ceRNA in repressing the metastases of breast cancer cells via regulating miRNA activity. FEBS Lett 2014; 588:3218-24.

192. Mazumdar A, Kumar R. Estrogen regulation of Pak1 and FKHR pathways in breast cancer cells. FEBS Lett 2003; 535:6-10.

193. Silva J, Cavazos DA, Donzis E, Friedrichs WE, Marciniak R, Degraffenried LA. Akt-Induced Tamoxifen Resistance is Associated with Altered FKHR Regulation. Cancer Invest 2007:1-5.

194. Goto T, Takano M, Albergaria A, Briese J, Pomeranz KM, Cloke B, Fusi L, Feroze-Zaidi F, Maywald N, Sajin M, et al. Mechanism and functional consequences of loss of FOXO1 expression in endometrioid endometrial cancer cells. Oncogene 2008; 27:9-19.

195. Dong XY, Chen C, Sun X, Guo P, Vessella RL, Wang RX, Chung LW, Zhou W, Dong JT. FOXO1A is a candidate for the 13q14 tumor suppressor gene inhibiting androgen receptor signaling in prostate cancer. Cancer Res 2006; 66:6998-7006.

196. Maekawa T, Maniwa Y, Doi T, Nishio W, Yoshimura M, Ohbayashi C, Hayashi Y, Okita Y. Expression and localization of FOXO1 in non-small cell lung cancer. Oncol Rep 2009; 22:57-64.

197. Ko YS, Cho SJ, Park J, Kim Y, Choi YJ, Pyo JS, Jang BG, Park JW, Kim WH, Lee BL. Loss of FOXO1 promotes gastric tumour growth and metastasis through upregulation of human epidermal growth factor receptor 2/neu expression. Br J Cancer 2015.

198. Kim SH, Miller FR, Tait L, Zheng J, Novak RF. Proteomic and phosphoproteomic alterations in benign, premalignant and tumor human breast epithelial cells and xenograft lesions: biomarkers of progression. Int J Cancer 2009; 124:2813-28.

199. Han CY, Cho KB, Choi HS, Han HK, Kang KW. Role of FoxO1 activation in MDR1 expression in adriamycin-resistant breast cancer cells. Carcinogenesis 2008; 29:1837-44.

200. Bondestam J, Huotari MA, Moren A, Ustinov J, Kaivo-Oja N, Kallio J, Horelli-Kuitunen N, Aaltonen J, Fujii M, Moustakas A, et al. cDNA cloning, expression studies and chromosome mapping of human type I serine/threonine kinase receptor ALK7 (ACVR1C). Cytogenet Cell Genet 2001; 95:157-62.

201. Kim BC, van Gelder H, Kim TA, Lee HJ, Baik KG, Chun HH, Lee DA, Choi KS, Kim SJ. Activin receptor-like kinase-7 induces apoptosis through activation of MAPKs in a Smad3-dependent mechanism in hepatoma cells. J Biol Chem 2004; 279:28458-65.

202. Xu G, Zhou H, Wang Q, Auersperg N, Peng C. Activin receptor-like kinase 7 induces apoptosis through up-regulation of Bax and down-regulation of Xiap in normal and malignant ovarian epithelial cell lines. Mol Cancer Res 2006; 4:235-46.

203. Xu G, Zhong Y, Munir S, Yang BB, Tsang BK, Peng C. Nodal induces apoptosis and inhibits proliferation in human epithelial ovarian cancer cells via activin receptor-like kinase 7. J Clin Endocrinol Metab 2004; 89:5523-34.

204. Xu G, Bernaudo S, Fu G, Lee DY, Yang BB, Peng C. Cyclin G2 is degraded through the ubiquitin-proteasome pathway and mediates the antiproliferative effect of activin receptor-like kinase 7. Mol Biol Cell 2008; 19:4968-79.

205. Zhang N, Kumar M, Xu G, Ju W, Yoon T, Xu E, Huang X, Gaisano H, Peng C, Wang Q. Activin receptor-like kinase 7 induces apoptosis of pancreatic beta cells and beta cell lines. Diabetologia 2006; 49:506-18.

206. Munir S, Xu G, Wu Y, Yang B, Lala PK, Peng C. Nodal and ALK7 inhibit proliferation and induce apoptosis in human trophoblast cells. J Biol Chem 2004; 279:31277-86.

207. Zeng F, Xu G, Zhou T, Yang C, Wang X, Peng C, Zhou H. Reduced expression of activin receptor-like kinase 7 in breast cancer is associated with tumor progression. Med Oncol 2012; 29:2519-26.

208. Li J, Yang Z, Zou Q, Yuan Y, Liang L, Zeng G, Chen S. PKM2 and ACVR 1C are prognostic markers for poor prognosis of gallbladder cancer. Clin Transl Oncol 2014; 16:200-7.

209. Xiang B, Yi M, Wang L, Liu W, Zhang W, Ouyang J, Peng Y, Li W, Yin D, Zhou M, et al. Preparation of polyclonal antibody specific for NOR1 and detection of its expression pattern in human tissues and nasopharyngeal carcinoma. Acta Biochim Biophys Sin (Shanghai) 2009; 41:754-62.

210. Mullican SE, Zhang S, Konopleva M, Ruvolo V, Andreeff M, Milbrandt J, Conneely OM. Abrogation of nuclear receptors Nr4a3 and Nr4a1 leads to development of acute myeloid leukemia. Nat Med 2007; 13:730-5.

211. Ohkubo T, Ohkura N, Maruyama K, Sasaki K, Nagasaki K, Hanzawa H, Tsukada T, Yamaguchi K. Early induction of the orphan nuclear receptor NOR-1 during cell death of the human breast cancer cell line MCF-7. Mol Cell Endocrinol 2000; 162:151-6.

212. Maruyama K, Tsukada T, Bandoh S, Sasaki K, Ohkura N, Yamaguchi K. Retinoic acids differentially regulate NOR-1 and its closely related orphan nuclear receptor genes in breast cancer cell line MCF-7. Biochem Biophys Res Commun 1997; 231:417-20.

213. Wenzl K, Troppan K, Neumeister P, Deutsch AJ. The nuclear orphan receptor NR4A1 and NR4A3 as tumor suppressors in hematologic neoplasms. Curr Drug Targets 2015; 16:38-46.

214. Hardy K, Mansfield L, Mackay A, Benvenuti S, Ismail S, Arora P, O'Hare MJ, Jat PS. Transcriptional networks and cellular senescence in human mammary fibroblasts. Mol Biol Cell 2005; 16:943-53.

215. Unoki M, Nakamura Y. EGR2 induces apoptosis in various cancer cell lines by direct transactivation of BNIP3L and BAK. Oncogene 2003; 22:2172-85.

216. Wu Q, Jin H, Yang Z, Luo G, Lu Y, Li K, Ren G, Su T, Pan Y, Feng B, et al. MiR-150 promotes gastric cancer proliferation by negatively regulating the pro-apoptotic gene EGR2. Biochem Biophys Res Commun 2010; 392:340-5.

217. Unoki M, Nakamura Y. Methylation at CpG islands in intron 1 of EGR2 confers enhancer-like activity. FEBS Lett 2003; 554:67-72.

218. Suzuki T, Maruno M, Wada K, Kagawa N, Fujimoto Y, Hashimoto N, Izumoto S, Yoshimine T. Genetic analysis of human glioblastomas using a genomic microarray system. Brain Tumor Pathol 2004; 21:27-34.

219. Yeh HY, Cheng SW, Lin YC, Yeh CY, Lin SF, Soo VW. Identifying significant genetic regulatory networks in the prostate cancer from microarray data based on transcription factor analysis and conditional independency. BMC Med Genomics 2009; 2:70.

220. Unoki M, Nakamura Y. Growth-suppressive effects of BPOZ and EGR2, two genes involved in the PTEN signaling pathway. Oncogene 2001; 20:4457-65.

221. Dillon RL, Brown ST, Ling C, Shioda T, Muller WJ. An EGR2/CITED1 transcription factor complex and the 14-3-3sigma tumor suppressor are involved in regulating ErbB2 expression in a transgenic-mouse model of human breast cancer. Mol Cell Biol 2007; 27:8648-57.

222. Vadgama JV, Scuric Z, Chakrabarti R, Marzo E, Shen D, Wu Y. Insulin-like growth factor I differentially regulates the expression of HIRF1/hCAF1 and BTG1 genes in human MCF-7 breast cancer cells. Int J Mol Med 2006; 18:129-39.

223. Rimokh R, Rouault JP, Wahbi K, Gadoux M, Lafage M, Archimbaud E, Charrin C, Gentilhomme O, Germain D, Samarut J, et al. A chromosome 12 coding region is juxtaposed to the MYC protooncogene locus in a t(8;12)(q24;q22) translocation in a case of B-cell chronic lymphocytic leukemia. Genes Chromosomes Cancer 1991; 3:24-36.

224. Li F, Liu J, Park ES, Jo M, Curry TE, Jr. The B cell translocation gene (BTG) family in the rat ovary: hormonal induction, regulation, and impact on cell cycle kinetics. Endocrinology 2009; 150:3894-902.

225. Nahta R, Yuan LX, Fiterman DJ, Zhang L, Symmans WF, Ueno NT, Esteva FJ. B cell translocation gene 1 contributes to antisense Bcl-2-mediated apoptosis in breast cancer cells. Mol Cancer Ther 2006; 5:1593-601.

226. Lee H, Cha S, Lee MS, Cho GJ, Choi WS, Suk K. Role of antiproliferative B cell translocation gene-1 as an apoptotic sensitizer in activation-induced cell death of brain microglia. J Immunol 2003; 171:5802-11.

227. Zhu R, Zou ST, Wan JM, Li W, Li XL, Zhu W. BTG1 inhibits breast cancer cell growth through induction of cell cycle arrest and apoptosis. Oncol Rep 2013; 30:2137-44.

228. Sheng SH, Zhao CM, Sun GG. BTG1 expression correlates with the pathogenesis and progression of breast carcinomas. Tumour Biol 2014; 35:3317-26.

229. Li W, Zou ST, Zhu R, Wan JM, Xu Y, Wu HR. Bcell translocation 1 gene inhibits cellular metastasisassociated behavior in breast cancer. Mol Med Rep 2014; 9:2374-80.

230. Sun CX, Robb VA, Gutmann DH. Protein 4.1 tumor suppressors: getting a FERM grip on growth regulation. J Cell Sci 2002; 115:3991-4000.

231. Zheng XY, Qi YM, Gao YF, Wang XY, Qi MX, Shi XF, An XL. [Expression and significance of membrane skeleton protein 4.1 family in non-small cell lung cancer]. Ai Zheng 2009; 28:679-84.

232. Rajaram V, Gutmann DH, Prasad SK, Mansur DB, Perry A. Alterations of protein 4.1 family members in ependymomas: a study of 84 cases. Mod Pathol 2005; 18:991-7.

233. Mandl M, Slack DN, Keyse SM. Specific inactivation and nuclear anchoring of extracellular signal-regulated kinase 2 by the inducible dual-specificity protein phosphatase DUSP5. Mol Cell Biol 2005; 25:1830-45.

234. Rushworth LK, Kidger AM, Delavaine L, Stewart G, van Schelven S, Davidson J, Bryant CJ, Caddye E, East P, Caunt CJ, et al. Dual-specificity phosphatase 5 regulates nuclear ERK activity and suppresses skin cancer by inhibiting mutant Harvey-Ras (HRasQ61L)-driven SerpinB2 expression. Proc Natl Acad Sci U S A 2014; 111:18267-72.

235. Ueda K, Arakawa H, Nakamura Y. Dual-specificity phosphatase 5 (DUSP5) as a direct transcriptional target of tumor suppressor p53. Oncogene 2003; 22:5586-91.

236. Cai C, Chen JY, Han ZD, He HC, Chen JH, Chen YR, Yang SB, Wu YD, Zeng YR, Zou J, et al. Down-regulation of dual-specificity phosphatase 5 predicts poor prognosis of patients with prostate cancer. Int J Clin Exp Med 2015; 8:4186-94.

237. Shin SH, Park SY, Kang GH. Down-regulation of dual-specificity phosphatase 5 in gastric cancer by promoter CpG island hypermethylation and its potential role in carcinogenesis. Am J Pathol 2013; 182:1275-85.

238. Chien J, Staub J, Avula R, Zhang H, Liu W, Hartmann LC, Kaufmann SH, Smith DI, Shridhar V. Epigenetic silencing of TCEAL7 (Bex4) in ovarian cancer. Oncogene 2005; 24:5089-100.

239. Hongo S, Watanabe T, Takahashi K, Miyazaki A. Ndrg4 enhances NGF-induced ERK activation uncoupled with Elk-1 activation. J Cell Biochem 2006; 98:185-93.

240. Lu H, Huang S, Zhang X, Wang D, Yuan X, Zhang Q, Huang Z. DNA methylation analysis of SFRP2, GATA4/5, NDRG4 and VIM for the detection of colorectal cancer in fecal DNA. Oncol Lett 2014; 8:1751-6.

241. Melotte V, Lentjes MH, van den Bosch SM, Hellebrekers DM, de Hoon JP, Wouters KA, Daenen KL, Partouns-Hendriks IE, Stessels F, Louwagie J, et al. N-Myc downstream-regulated

gene 4 (NDRG4): a candidate tumor suppressor gene and potential biomarker for colorectal cancer. J Natl Cancer Inst 2009; 101:916-27.

242. Kisiel JB, Raimondo M, Taylor WR, Yab TC, Mahoney DW, Sun Z, Middha S, Baheti S, Zou H, Smyrk TC, et al. New DNA Methylation Markers for Pancreatic Cancer: Discovery, Tissue Validation, and Pilot Testing in Pancreatic Juice. Clin Cancer Res 2015; 21:4473-81.

243. Jin SH, Akiyama Y, Fukamachi H, Yanagihara K, Akashi T, Yuasa Y. IQGAP2 inactivation through aberrant promoter methylation and promotion of invasion in gastric cancer cells. Int J Cancer 2008; 122:1040-6.

244. White CD, Brown MD, Sacks DB. IQGAPs in cancer: a family of scaffold proteins underlying tumorigenesis. FEBS Lett 2009; 583:1817-24.

245. Schmidt VA, Chiariello CS, Capilla E, Miller F, Bahou WF. Development of hepatocellular carcinoma in Iqgap2-deficient mice is IQGAP1 dependent. Mol Cell Biol 2008; 28:1489-502.

246. Xia FD, Wang ZL, Chen HX, Huang Y, Li JD, Wang ZM, Li XY. Differential expression of IQGAP1/2 in Hepatocellular carcinoma and its relationship with clinical outcomes. Asian Pac J Cancer Prev 2014; 15:4951-6.

247. Godschalk RW, Dallinga JW, Wikman H, Risch A, Kleinjans JC, Bartsch H, Van Schooten FJ. Modulation of DNA and protein adducts in smokers by genetic polymorphisms in GSTM1,GSTT1, NAT1 and NAT2. Pharmacogenetics 2001; 11:389-98.

248. Godschalk RW, Ostertag JU, Zandsteeg AM, Van Agen B, Neuman HA, Van Straaten H, Van Schooten FJ. Impact of GSTM1 on aromatic-DNA adducts and p53 accumulation in human skin and lymphocytes. Pharmacogenetics 2001; 11:537-43.

249. Strange RC, Matharoo B, Faulder GC, Jones P, Cotton W, Elder JB, Deakin M. The human glutathione S-transferases: a case-control study of the incidence of the GST1 0 phenotype in patients with adenocarcinoma. Carcinogenesis 1991; 12:25-8.

250. van Poppel G, de Vogel N, van Balderen PJ, Kok FJ. Increased cytogenetic damage in smokers deficient in glutathione S-transferase isozyme mu. Carcinogenesis 1992; 13:303-5.

251. Yu KD, Di GH, Fan L, Wu J, Hu Z, Shen ZZ, Huang W, Shao ZM. A functional polymorphism in the promoter region of GSTM1 implies a complex role for GSTM1 in breast cancer. FASEB J 2009; 23:2274-87.

252. Samson M, Swaminathan R, Rama R, Sridevi V, Nancy KN, Rajkumar T. Role of GSTM1 (Null/Present), GSTP1 (Ile105Val) and P53 (Arg72Pro) genetic polymorphisms and the risk of breast cancer: a case control study from South India. Asian Pac J Cancer Prev 2007; 8:253-7.

253. Altinisik J, Balta ZB, Aydin G, Ulutin T, Buyru N. Investigation of glutathione S-transferase M1 and T1 deletions in lung cancer. Mol Biol Rep 2010; 37:263-7.

254. Seidegard J, Pero RW, Miller DG, Beattie EJ. A glutathione transferase in human leukocytes as a marker for the susceptibility to lung cancer. Carcinogenesis 1986; 7:751-3.

255. Seidegard J, Pero RW, Markowitz MM, Roush G, Miller DG, Beattie EJ. Isoenzyme(s) of glutathione transferase (class Mu) as a marker for the susceptibility to lung cancer: a follow up study. Carcinogenesis 1990; 11:33-6.

256. Trizna Z, Clayman GL, Spitz MR, Briggs KL, Goepfert H. Glutathione s-transferase genotypes as risk factors for head and neck cancer. Am J Surg 1995; 170:499-501.

257. Wang H, Zhou Y, Zhuang W, Yin YQ, Liu GJ, Wu TX, Yao X, Du L, Wei ML, Wu XT. Glutathione S-transferase M1 null genotype associated with gastric cancer among Asians. Dig Dis Sci 2010; 55:1824-30.

258. Zhong S, Wyllie AH, Barnes D, Wolf CR, Spurr NK. Relationship between the GSTM1 genetic polymorphism and susceptibility to bladder, breast and colon cancer. Carcinogenesis 1993; 14:1821-4.

259. White DL, Li D, Nurgalieva Z, El-Serag HB. Genetic variants of glutathione S-transferase as possible risk factors for hepatocellular carcinoma: a HuGE systematic review and meta-analysis. Am J Epidemiol 2008; 167:377-89.

260. Li Y, Wan W, Li T, Cao J, Xu G. GSTM1 null genotype may be associated with an increased nasopharyngeal cancer risk in South China: an updated meta-analysis and review. Onco Targets Ther 2015; 8:2479-84.

261. Liu X, Fan Q, Ni L, Liu F, Huang S, Gao J, Chen B. GSTM1 null genotype is a risk factor for laryngeal cancer. Int J Clin Exp Med 2015; 8:7661-6.

262. Mavis CK, Morey Kinney SR, Foster BA, Karpf AR. Expression level and DNA methylation status of glutathione-S-transferase genes in normal murine prostate and TRAMP tumors. Prostate 2009; 69:1312-24.

263. Lodygin D, Epanchintsev A, Menssen A, Diebold J, Hermeking H. Functional epigenomics identifies genes frequently silenced in prostate cancer. Cancer Res 2005; 65:4218-27.

264. Peng DF, Razvi M, Chen H, Washington K, Roessner A, Schneider-Stock R, El-Rifai W. DNA hypermethylation regulates the expression of members of the Mu-class glutathione S-transferases and glutathione peroxidases in Barrett's adenocarcinoma. Gut 2009; 58:5-15.

265. Ebert MN, Klinder A, Peters WH, Schaferhenrich A, Sendt W, Scheele J, Pool-Zobel BL. Expression of glutathione S-transferases (GSTs) in human colon cells and inducibility of GSTM2 by butyrate. Carcinogenesis 2003; 24:1637-44.

266. Hill M, Pereira V, Chauveau C, Zagani R, Remy S, Tesson L, Mazal D, Ubillos L, Brion R, Asghar K, et al. Heme oxygenase-1 inhibits rat and human breast cancer cell proliferation: mutual cross inhibition with indoleamine 2,3-dioxygenase. FASEB J 2005; 19:1957-68.

267. Lin CW, Shen SC, Hou WC, Yang LY, Chen YC. Heme oxygenase-1 inhibits breast cancer invasion via suppressing the expression of matrix metalloproteinase-9. Mol Cancer Ther 2008; 7:1195-206.

268. Becker JC, Fukui H, Imai Y, Sekikawa A, Kimura T, Yamagishi H, Yoshitake N, Pohle T, Domschke W, Fujimori T. Colonic expression of heme oxygenase-1 is associated with a better long-term survival in patients with colorectal cancer. Scand J Gastroenterol 2007; 42:852-8.

269. Noh SJ, Bae JS, Jamiyandorj U, Park HS, Kwon KS, Jung SH, Youn HJ, Lee H, Park BH, Chung MJ, et al. Expression of nerve growth factor and heme oxygenase-1 predict poor survival of breast carcinoma patients. BMC Cancer 2013; 13:516.

270. Kim DH, Kim JH, Kim EH, Na HK, Cha YN, Chung JH, Surh YJ. 15-Deoxy-Delta12,14-prostaglandin J2 upregulates the expression of heme oxygenase-1 and subsequently matrix metalloproteinase-1 in human breast cancer cells: possible roles of iron and ROS. Carcinogenesis 2009; 30:645-54.

271. Kim EH, Na HK, Surh YJ. Upregulation of VEGF by 15-deoxy-Delta12,14-prostaglandin J2 via heme oxygenase-1 and ERK1/2 signaling in MCF-7 cells. Ann N Y Acad Sci 2006; 1090:375-84.

272. Naik MU, Naik TU, Suckow AT, Duncan MK, Naik UP. Attenuation of junctional adhesion molecule-A is a contributing factor for breast cancer cell invasion. Cancer Res 2008; 68:2194-203.

273. Gutwein P, Schramme A, Voss B, Abdel-Bakky MS, Doberstein K, Ludwig A, Altevogt P, Hansmann ML, Moch H, Kristiansen G, et al. Downregulation of junctional adhesion molecule-A is involved in the progression of clear cell renal cell carcinoma. Biochem Biophys Res Commun 2009; 380:387-91.

274. Huang JY, Xu YY, Sun Z, Wang ZN, Zhu Z, Song YX, Luo Y, Zhang X, Xu HM. Low junctional adhesion molecule A expression correlates with poor prognosis in gastric cancer. J Surg Res 2014; 192:494-502.

275. McSherry EA, McGee SF, Jirstrom K, Doyle EM, Brennan DJ, Landberg G, Dervan PA, Hopkins AM, Gallagher WM. JAM-A expression positively correlates with poor prognosis in breast cancer patients. Int J Cancer 2009; 125:1343-51.

276. Brennan K, McSherry EA, Hudson L, Kay EW, Hill AD, Young LS, Hopkins AM. Junctional adhesion molecule-A is co-expressed with HER2 in breast tumors and acts as a novel regulator of HER2 protein degradation and signaling. Oncogene 2013; 32:2799-804.

277. Murakami M, Giampietro C, Giannotta M, Corada M, Torselli I, Orsenigo F, Cocito A, d'Ario G, Mazzarol G, Confalonieri S, et al. Abrogation of junctional adhesion molecule-A expression induces cell apoptosis and reduces breast cancer progression. PLoS One 2011; 6:e21242.

278. Goetsch L, Haeuw JF, Beau-Larvor C, Gonzalez A, Zanna L, Malissard M, Lepecquet AM, Robert A, Bailly C, Broussas M, et al. A novel role for junctional adhesion molecule-A in tumor proliferation: modulation by an anti-JAM-A monoclonal antibody. Int J Cancer 2013; 132:1463-74.

279. Gotte M, Mohr C, Koo CY, Stock C, Vaske AK, Viola M, Ibrahim SA, Peddibhotla S, Teng YH, Low JY, et al. miR-145-dependent targeting of junctional adhesion molecule A and modulation of fascin expression are associated with reduced breast cancer cell motility and invasiveness. Oncogene 2010; 29:6569-80.

280. McSherry EA, Brennan K, Hudson L, Hill AD, Hopkins AM. Breast cancer cell migration is regulated through junctional adhesion molecule-A-mediated activation of Rap1 GTPase. Breast Cancer Res 2011; 13:R31.

281. Hardwick JC, Van Den Brink GR, Bleuming SA, Ballester I, Van Den Brande JM, Keller JJ, Offerhaus GJ, Van Deventer SJ, Peppelenbosch MP. Bone morphogenetic protein 2 is expressed by, and acts upon, mature epithelial cells in the colon. Gastroenterology 2004; 126:111-21.

282. Kodach LL, Bleuming SA, Peppelenbosch MP, Hommes DW, van den Brink GR, Hardwick JC. The effect of statins in colorectal cancer is mediated through the bone morphogenetic protein pathway. Gastroenterology 2007; 133:1272-81.

283. Nakashima K, Yanagisawa M, Arakawa H, Taga T. Astrocyte differentiation mediated by LIF in cooperation with BMP2. FEBS Lett 1999; 457:43-6.

284. Waite KA, Eng C. BMP2 exposure results in decreased PTEN protein degradation and increased PTEN levels. Hum Mol Genet 2003; 12:679-84.

285. Takahashi M, Otsuka F, Miyoshi T, Otani H, Goto J, Yamashita M, Ogura T, Makino H, Doihara H. Bone morphogenetic protein 6 (BMP6) and BMP7 inhibit estrogen-induced proliferation of breast cancer cells by suppressing p38 mitogen-activated protein kinase activation. J Endocrinol 2008; 199:445-55.

286. Pouliot F, Labrie C. Role of Smad1 and Smad4 proteins in the induction of p21WAF1,Cip1 during bone morphogenetic protein-induced growth arrest in human breast cancer cells. J Endocrinol 2002; 172:187-98.

287. Wen XZ, Akiyama Y, Baylin SB, Yuasa Y. Frequent epigenetic silencing of the bone morphogenetic protein 2 gene through methylation in gastric carcinomas. Oncogene 2006; 25:2666-73.

288. Ma Y, Ma L, Guo Q, Zhang S. Expression of bone morphogenetic protein-2 and its receptors in epithelial ovarian cancer and their influence on the prognosis of ovarian cancer patients. J Exp Clin Cancer Res 2010; 29:85.

289. Raida M, Clement JH, Leek RD, Ameri K, Bicknell R, Niederwieser D, Harris AL. Bone morphogenetic protein 2 (BMP-2) and induction of tumor angiogenesis. J Cancer Res Clin Oncol 2005; 131:741-50.

290. Clement JH, Raida M, Sanger J, Bicknell R, Liu J, Naumann A, Geyer A, Waldau A, Hortschansky P, Schmidt A, et al. Bone morphogenetic protein 2 (BMP-2) induces in vitro invasion and in vivo hormone independent growth of breast carcinoma cells. Int J Oncol 2005; 27:401-7.

291. Raida M, Clement JH, Ameri K, Han C, Leek RD, Harris AL. Expression of bone morphogenetic protein 2 in breast cancer cells inhibits hypoxic cell death. Int J Oncol 2005; 26:1465-70.

292. Kaneda A, Kaminishi M, Nakanishi Y, Sugimura T, Ushijima T. Reduced expression of the insulin-induced protein 1 and p41 Arp2/3 complex genes in human gastric cancers. Int J Cancer 2002; 100:57-62.

293. Horak CE, Lee JH, Elkahloun AG, Boissan M, Dumont S, Maga TK, Arnaud-Dabernat S, Palmieri D, Stetler-Stevenson WG, Lacombe ML, et al. Nm23-H1 suppresses tumor cell motility by down-regulating the lysophosphatidic acid receptor EDG2. Cancer Res 2007; 67:7238-46.

294. Appaiah H, Bhat-Nakshatri P, Mehta R, Thorat M, Badve S, Nakshatri H. ITF2 is a target of CXCR4 in MDA-MB-231 breast cancer cells and is associated with reduced survival in estrogen receptor-negative breast cancer. Cancer Biol Ther 2010; 10:600-14.

295. Itahana Y, Singh J, Sumida T, Coppe JP, Parrinello S, Bennington JL, Desprez PY. Role of Id-2 in the maintenance of a differentiated and noninvasive phenotype in breast cancer cells. Cancer Res 2003; 63:7098-105.

296. Stighall M, Manetopoulos C, Axelson H, Landberg G. High ID2 protein expression correlates with a favourable prognosis in patients with primary breast cancer and reduces cellular invasiveness of breast cancer cells. Int J Cancer 2005; 115:403-11.

297. Meng Y, Gu C, Wu Z, Zhao Y, Si Y, Fu X, Han W. Id2 promotes the invasive growth of MCF-7 and SKOV-3 cells by a novel mechanism independent of dimerization to basic helix-loop-helix factors. BMC Cancer 2009; 9:75.

298. Zhang X, Lv C, Du B, Ma X, Guan J, Gao S, Li X, Zheng L, Lei L. Upregulation of ID2 antagonizes arsenic trioxide-induced antitumor effects in cancer cells. Tumori 2014; 100:352-7.

299. Li K, Yao L, Chen L, Cao ZG, Yu SJ, Kuang XY, Hu X, Shao ZM. ID2 predicts poor prognosis in breast cancer, especially in triple-negative breast cancer, and inhibits E-cadherin expression. Onco Targets Ther 2014; 7:1083-94.

300. Liu D, Rudland PS, Sibson DR, Platt-Higgins A, Barraclough R. Expression of calcium-binding protein S100A2 in breast lesions. Br J Cancer 2000; 83:1473-9.

301. Wicki R, Franz C, Scholl FA, Heizmann CW, Schafer BW. Repression of the candidate tumor suppressor gene S100A2 in breast cancer is mediated by site-specific hypermethylation. Cell Calcium 1997; 22:243-54.

302. Feng G, Xu X, Youssef EM, Lotan R. Diminished expression of S100A2, a putative tumor suppressor, at early stage of human lung carcinogenesis. Cancer Res 2001; 61:7999-8004.

303. Lee J, Wysocki PT, Topaloglu O, Maldonado L, Brait M, Begum S, Moon D, Kim MS, Califano JA, Sidransky D, et al. Epigenetic silencing of S100A2 in bladder and head and neck cancers. Oncoscience 2015; 2:410-8.

304. Buckley NE, D'Costa Z, Kaminska M, Mullan PB. S100A2 is a BRCA1/p63 coregulated tumour suppressor gene with roles in the regulation of mutant p53 stability. Cell Death Dis 2014; 5:e1070.

305. Liu YF, Liu QQ, Wang X, Luo CH. Clinical significance of S100A2 expression in gastric cancer. Tumour Biol 2014; 35:3731-41.

306. Naba A, Clauser KR, Lamar JM, Carr SA, Hynes RO. Extracellular matrix signatures of human mammary carcinoma identify novel metastasis promoters. Elife 2014; 3:e01308.

307. McKiernan E, McDermott EW, Evoy D, Crown J, Duffy MJ. The role of S100 genes in breast cancer progression. Tumour Biol 2011; 32:441-50.

308. Lee SW, Jung KH, Jeong CH, Seo JH, Yoon DK, Suh JK, Kim KW, Kim WJ. Inhibition of endothelial cell migration through the downregulation of MMP-9 by A-kinase anchoring protein 12. Mol Med Report 2011; 4:145-9.

309. Su B, Bu Y, Engelberg D, Gelman IH. SSeCKS/Gravin/AKAP12 inhibits cancer cell invasiveness and chemotaxis by suppressing a protein kinase C- Raf/MEK/ERK pathway. J Biol Chem 2010; 285:4578-86.

310. Liu W, Guan M, Hu T, Gu X, Lu Y. Re-expression of AKAP12 inhibits progression and metastasis potential of colorectal carcinoma in vivo and in vitro. PLoS One 2011; 6:e24015.

311. Mardin WA, Petrov KO, Enns A, Senninger N, Haier J, Mees ST. SERPINB5 and AKAP12 - expression and promoter methylation of metastasis suppressor genes in pancreatic ductal adenocarcinoma. BMC Cancer 2010; 10:549.

312. Akakura S, Bouchard R, Bshara W, Morrison C, Gelman IH. Carcinogen-induced squamous papillomas and oncogenic progression in the absence of the SSeCKS/AKAP12 metastasis suppressor correlates with FAK upregulation. Int J Cancer 2010.

313. Hayashi M, Nomoto S, Kanda M, Okamura Y, Nishikawa Y, Yamada S, Fujii T, Sugimoto H, Takeda S, Kodera Y. Identification of the a kinase anchor protein 12 (AKAP12) gene as a candidate tumor suppressor of hepatocellular carcinoma. J Surg Oncol 2011.

314. Liu W, Gong J, Hu J, Hu T, Sun Y, Du J, Sun C, Guan M, Jiang H, Lu Y. Quantitative assessment of AKAP12 promoter methylation in human prostate cancer using methylation-sensitive high-resolution melting: correlation with Gleason score. Urology 2011; 77:1006 e1-7.

315. Jo UH, Whang YM, Sung JS, Kim YH. Methylation of AKAP12{alpha} promoter in lung cancer. Anticancer Res 2010; 30:4595-600.

316. Liu W, Guan M, Su B, Ye C, Li J, Zhang X, Liu C, Li M, Lin Y, Lu Y. Quantitative assessment of AKAP12 promoter methylation in colorectal cancer using methylation-sensitive high resolution melting: Correlation with Duke's stage. Cancer Biol Ther 2010; 9:862-71.

317. Flotho C, Paulun A, Batz C, Niemeyer CM. AKAP12, a gene with tumour suppressor properties, is a target of promoter DNA methylation in childhood myeloid malignancies. Br J Haematol 2007; 138:644-50.

318. Wen G, Partridge MA, Li B, Hong M, Liao W, Cheng SK, Zhao Y, Calaf GM, Liu T, Zhou J, et al. TGFBI expression reduces in vitro and in vivo metastatic potential of lung and breast tumor cells. Cancer Lett 2011; 308:23-32.

319. Rudra-Ganguly N, Lowe C, Mattie M, Chang MS, Satpayev D, Verlinsky A, An Z, Hu L, Yang P, Challita-Eid P, et al. Discoidin domain receptor 1 contributes to tumorigenesis through modulation of TGFBI expression. PLoS One 2014; 9:e111515.

320. Irigoyen M, Pajares MJ, Agorreta J, Ponz-Sarvise M, Salvo E, Lozano MD, Pio R, Gil-Bazo I, Rouzaut A. TGFBI expression is associated with a better response to chemotherapy in NSCLC. Mol Cancer 2010; 9:130.

321. Lee JJ, Park K, Shin MH, Yang WJ, Song MJ, Park JH, Yong TS, Kim EK, Kim HP. Accessible chromatin structure permits factors Sp1 and Sp3 to regulate human TGFBI gene expression. Biochem Biophys Res Commun 2011; 409:222-8.

322. Kang S, Dong SM, Park NH. Frequent promoter hypermethylation of TGFBI in epithelial ovarian cancer. Gynecol Oncol 2010; 118:58-63.

323. Shah JN, Shao G, Hei TK, Zhao Y. Methylation screening of the TGFBI promoter in human lung and prostate cancer by methylation-specific PCR. BMC Cancer 2008; 8:284.

324. Caren H, Djos A, Nethander M, Sjoberg RM, Kogner P, Enstrom C, Nilsson S, Martinsson T. Identification of epigenetically regulated genes that predict patient outcome in neuroblastoma. BMC Cancer 2011; 11:66.

325. Zhang Y, Wen G, Shao G, Wang C, Lin C, Fang H, Balajee AS, Bhagat G, Hei TK, Zhao Y. TGFBI deficiency predisposes mice to spontaneous tumor development. Cancer Res 2009; 69:37-44.

326. Prinjha RK, Shapland CE, Hsuan JJ, Totty NF, Mason IJ, Lawson D. Cloning and sequencing of cDNAs encoding the actin cross-linking protein transgelin defines a new family of actin-associated proteins. Cell Motil Cytoskeleton 1994; 28:243-55.

327. Shapland C, Lowings P, Lawson D. Identification of new actin-associated polypeptides that are modified by viral transformation and changes in cell shape. J Cell Biol 1988; 107:153-61.

328. Camoretti-Mercado B, Forsythe SM, LeBeau MM, Espinosa R, 3rd, Vieira JE, Halayko AJ, Willadsen S, Kurtz B, Ober C, Evans GA, et al. Expression and cytogenetic localization of the human SM22 gene (TAGLN). Genomics 1998; 49:452-7.

329. Lees-Miller JP, Heeley DH, Smillie LB. An abundant and novel protein of 22 kDa (SM22) is widely distributed in smooth muscles. Purification from bovine aorta. Biochem J 1987; 244:705-9.

330. Zhang R, Zhou L, Li Q, Liu J, Yao W, Wan H. Up-regulation of two actin-associated proteins prompts pulmonary artery smooth muscle cell migration under hypoxia. Am J Respir Cell Mol Biol 2009; 41:467-75.

331. Gimona M, Kaverina I, Resch GP, Vignal E, Burgstaller G. Calponin repeats regulate actin filament stability and formation of podosomes in smooth muscle cells. Mol Biol Cell 2003; 14:2482-91.

332. Kaverina I, Stradal TE, Gimona M. Podosome formation in cultured A7r5 vascular smooth muscle cells requires Arp2/3-dependent de-novo actin polymerization at discrete microdomains. J Cell Sci 2003; 116:4915-24.

333. Chen R, Zhang F, Song L, Shu Y, Lin Y, Dong L, Nie X, Zhang D, Chen P, Han M. Transcriptome profiling reveals that the SM22alpha-regulated molecular pathways contribute to vascular pathology. J Mol Cell Cardiol 2014; 72:263-72.

334. Thweatt R, Lumpkin CK, Jr., Goldstein S. A novel gene encoding a smooth muscle protein is overexpressed in senescent human fibroblasts. Biochem Biophys Res Commun 1992; 187:1-7.

335. Gonos ES, Derventzi A, Kveiborg M, Agiostratidou G, Kassem M, Clark BF, Jat PS, Rattan SI. Cloning and identification of genes that associate with mammalian replicative senescence. Exp Cell Res 1998; 240:66-74.

336. Dumont P, Burton M, Chen QM, Gonos ES, Frippiat C, Mazarati JB, Eliaers F, Remacle J, Toussaint O. Induction of replicative senescence biomarkers by sublethal oxidative stresses in normal human fibroblast. Free Radic Biol Med 2000; 28:361-73.

337. Marshall CB, Krofft RD, Blonski MJ, Kowalewska J, Logar CM, Pippin JW, Kim F, Feil R, Alpers CE, Shankland SJ. Role of smooth muscle protein SM22alpha in glomerular epithelial cell injury. Am J Physiol Renal Physiol 2011; 300:F1026-42.

338. Zhang ZW, Yang ZM, Zheng YC, Chen ZD. Transgelin induces apoptosis of human prostate LNCaP cells through its interaction with p53. Asian J Androl 2010; 12:186-95.

339. Nair RR, Solway J, Boyd DD. Expression cloning identifies transgelin (SM22) as a novel repressor of 92-kDa type IV collagenase (MMP-9) expression. J Biol Chem 2006; 281:26424-36.

340. Kalhori V, Tornquist K. MMP2 and MMP9 participate in S1P-induced invasion of follicular ML-1 thyroid cancer cells. Mol Cell Endocrinol 2015; 404:113-22.

341. Yeo M, Park HJ, Kim DK, Kim YB, Cheong JY, Lee KJ, Cho SW. Loss of SM22 is a characteristic signature of colon carcinogenesis and its restoration suppresses colon tumorigenicity in vivo and in vitro. Cancer 2010; 116:2581-9.

342. Almendral JM, Santaren JF, Perera J, Zerial M, Bravo R. Expression, cloning and cDNA sequence of a fibroblast serum-regulated gene encoding a putative actin-associated protein (p27). Exp Cell Res 1989; 181:518-30.

343. Schenker T, Trueb B. Down-regulated proteins of mesenchymal tumor cells. Exp Cell Res 1998; 239:161-8.

344. Xie XL, Liu YB, Liu YP, Du BL, Li Y, Han M, Li BH. Reduced expression of SM22 is correlated with low autophagy activity in human colorectal cancer. Pathol Res Pract 2013; 209:237-43.

345. Shields JM, Rogers-Graham K, Der CJ. Loss of transgelin in breast and colon tumors and in RIE-1 cells by Ras deregulation of gene expression through Raf-independent pathways. J Biol Chem 2002; 277:9790-9.

346. Prasad PD, Stanton JA, Assinder SJ. Expression of the actin-associated protein transgelin (SM22) is decreased in prostate cancer. Cell Tissue Res 2010; 339:337-47.

347. Wulfkuhle JD, Sgroi DC, Krutzsch H, McLean K, McGarvey K, Knowlton M, Chen S, Shu H, Sahin A, Kurek R, et al. Proteomics of human breast ductal carcinoma in situ. Cancer Res 2002; 62:6740-9.

348. Sahasrabuddhe NA, Barbhuiya MA, Bhunia S, Subbannayya T, Gowda H, Advani J, Shrivastav BR, Navani S, Leal P, Roa JC, et al. Identification of prosaposin and transgelin as potential biomarkers for gallbladder cancer using quantitative proteomics. Biochem Biophys Res Commun 2014; 446:863-9.

349. Zhou L, Zhang R, Zhang L, Sun Y, Yao W, Zhao A, Li J, Yuan Y. Upregulation of transgelin is an independent factor predictive of poor prognosis in patients with advanced pancreatic cancer. Cancer Sci 2013; 104:423-30.

350. Li N, Zhang J, Liang Y, Shao J, Peng F, Sun M, Xu N, Li X, Wang R, Liu S, et al. A controversial tumor marker: is SM22 a proper biomarker for gastric cancer cells? J Proteome Res 2007; 6:3304-12.

351. Lin Y, Buckhaults PJ, Lee JR, Xiong H, Farrell C, Podolsky RH, Schade RR, Dynan WS. Association of the actin-binding protein transgelin with lymph node metastasis in human colorectal cancer. Neoplasia 2009; 11:864-73.

352. Park GH, Lee SJ, Yim H, Han JH, Kim HJ, Sohn YB, Ko JM, Jeong SY. TAGLN expression is upregulated in NF1-associated malignant peripheral nerve sheath tumors by hypomethylation in its promoter and subpromoter regions. Oncol Rep 2014; 32:1347-54.

353. Bu J, Bu X, Liu B, Chen F, Chen P. Increased Expression of Tissue/Salivary Transgelin mRNA Predicts Poor Prognosis in Patients with Oral Squamous Cell Carcinoma (OSCC). Med Sci Monit 2015; 21:2275-81.

354. Thompson O, Moghraby JS, Ayscough KR, Winder SJ. Depletion of the actin bundling protein SM22/transgelin increases actin dynamics and enhances the tumourigenic phenotypes of cells. BMC Cell Biol 2012; 13:1.

355. Groger CJ, Grubinger M, Waldhor T, Vierlinger K, Mikulits W. Meta-analysis of gene expression signatures defining the epithelial to mesenchymal transition during cancer progression. PLoS One 2012; 7:e51136.

356. Adam PJ, Regan CP, Hautmann MB, Owens GK. Positive- and negative-acting Kruppel-like transcription factors bind a transforming growth factor beta control element required for expression of the smooth muscle cell differentiation marker SM22alpha in vivo. J Biol Chem 2000; 275:37798-806.

357. Chen S, Kulik M, Lechleider RJ. Smad proteins regulate transcriptional induction of the SM22alpha gene by TGF-beta. Nucleic Acids Res 2003; 31:1302-10.

358. Qiu P, Ritchie RP, Fu Z, Cao D, Cumming J, Miano JM, Wang DZ, Li HJ, Li L. Myocardin enhances Smad3-mediated transforming growth factor-beta1 signaling in a CArG box-independent manner: Smad-binding element is an important cis element for SM22alpha transcription in vivo. Circ Res 2005; 97:983-91.

359. Deaton RA, Su C, Valencia TG, Grant SR. Transforming growth factor-beta1-induced expression of smooth muscle marker genes involves activation of PKN and p38 MAPK. J Biol Chem 2005; 280:31172-81.

360. Oft M, Peli J, Rudaz C, Schwarz H, Beug H, Reichmann E. TGF-beta1 and Ha-Ras collaborate in modulating the phenotypic plasticity and invasiveness of epithelial tumor cells. Genes Dev 1996; 10:2462-77.

361. Yamamura H, Masuda H, Ikeda W, Tokuyama T, Takagi M, Shibata N, Tatsuta M, Takahashi K. Structure and expression of the human SM22alpha gene, assignment of the gene to chromosome 11, and repression of the promoter activity by cytosine DNA methylation. J Biochem 1997; 122:157-67.

362. Hirasawa Y, Arai M, Imazeki F, Tada M, Mikata R, Fukai K, Miyazaki M, Ochiai T, Saisho H, Yokosuka O. Methylation status of genes upregulated by demethylating agent 5-aza-2'-deoxycytidine in hepatocellular carcinoma. Oncology 2006; 71:77-85.

363. Zhao L, Wang H, Deng YJ, Wang S, Liu C, Jin H, Ding YQ. Transgelin as a suppressor is associated with poor prognosis in colorectal carcinoma patients. Mod Pathol 2009; 22:786-96.

364. Maleszewska M, Gjaltema RA, Krenning G, Harmsen MC. Enhancer of zeste homolog-2 (EZH2) methyltransferase regulates transgelin/smooth muscle-22alpha expression in endothelial cells in response to interleukin-1beta and transforming growth factor-beta2. Cell Signal 2015; 27:1589-96.

365. Rao D, Kimler BF, Nothnick WB, Davis MK, Fan F, Tawfik O. Transgelin: a potentially useful diagnostic marker differentially expressed in triple-negative and non-triple-negative breast cancers. Hum Pathol 2015; 46:876-83.

366. Sayar N, Karahan G, Konu O, Bozkurt B, Bozdogan O, Yulug IG. Transgelin gene is frequently downregulated by promoter DNA hypermethylation in breast cancer. Clin Epigenetics 2015; 7:104.

367. Gur-Dedeoglu B, Konu O, Bozkurt B, Ergul G, Seckin S, Yulug IG. Identification of endogenous reference genes for qRT-PCR analysis in normal matched breast tumor tissues. Oncol Res 2009; 17:353-65.

368. Huang da W, Sherman BT, Lempicki RA. Systematic and integrative analysis of large gene lists using DAVID bioinformatics resources. Nat Protoc 2009; 4:44-57.

369. Huang da W, Sherman BT, Lempicki RA. Bioinformatics enrichment tools: paths toward the comprehensive functional analysis of large gene lists. Nucleic Acids Res 2009; 37:1-13.

370. Li LC, Dahiya R. MethPrimer: designing primers for methylation PCRs. Bioinformatics 2002; 18:1427-31.

371. Takai D, Jones PA. The CpG island searcher: a new WWW resource. In Silico Biol 2003; 3:235-40.

372. Rhodes DR, Yu J, Shanker K, Deshpande N, Varambally R, Ghosh D, Barrette T, Pandey A, Chinnaiyan AM. ONCOMINE: a cancer microarray database and integrated data-mining platform. Neoplasia 2004; 6:1-6.

373. Kumaki Y, Oda M, Okano M. QUMA: quantification tool for methylation analysis. Nucleic Acids Res 2008; 36:W170-5.

374. Mihaly Z, Kormos M, Lanczky A, Dank M, Budczies J, Szasz MA, Gyorffy B. A meta-analysis of gene expression-based biomarkers predicting outcome after tamoxifen treatment in breast cancer. Breast Cancer Res Treat 2013; 140:219-32.

375. Fackler MJ, Umbricht CB, Williams D, Argani P, Cruz LA, Merino VF, Teo WW, Zhang Z, Huang P, Visvananthan K, et al. Genome-wide methylation analysis identifies genes specific to breast cancer hormone receptor status and risk of recurrence. Cancer Res 2011; 71:6195-207.

376. Gyorffy B, Lanczky A, Eklund AC, Denkert C, Budczies J, Li Q, Szallasi Z. An online survival analysis tool to rapidly assess the effect of 22,277 genes on breast cancer prognosis using microarray data of 1,809 patients. Breast Cancer Res Treat 2010; 123:725-31.

377. McCarty KS, Jr., Szabo E, Flowers JL, Cox EB, Leight GS, Miller L, Konrath J, Soper JT, Budwit DA, Creasman WT, et al. Use of a monoclonal anti-estrogen receptor antibody in the immunohistochemical evaluation of human tumors. Cancer Res 1986; 46:4244s-8s.

378. Radpour R, Kohler C, Haghighi MM, Fan AX, Holzgreve W, Zhong XY. Methylation profiles of 22 candidate genes in breast cancer using high-throughput MALDI-TOF mass array. Oncogene 2009; 28:2969-78.

379. Pavlova TV, Kashuba VI, Muravenko OV, Yenamandra SP, Ivanova TA, Zabarovskaia VI, Rakhmanaliev ER, Petrenko LA, Pronina IV, Loginov VI, et al. [Technology of analysis of epigenetic and structural changes of epithelial tumors genome with NotI-microarrays by the example of human chromosome]. Mol Biol (Mosk) 2009; 43:339-47.

380. Osanai M, Murata M, Chiba H, Kojima T, Sawada N. Epigenetic silencing of claudin-6 promotes anchorage-independent growth of breast carcinoma cells. Cancer Sci 2007; 98:1557-62.

381. Shivapurkar N, Toyooka S, Toyooka KO, Reddy J, Miyajima K, Suzuki M, Shigematsu H, Takahashi T, Parikh G, Pass HI, et al. Aberrant methylation of trail decoy receptor genes is frequent in multiple tumor types. Int J Cancer 2004; 109:786-92.

382. Sathyanarayana UG, Padar A, Huang CX, Suzuki M, Shigematsu H, Bekele BN, Gazdar AF. Aberrant promoter methylation and silencing of laminin-5-encoding genes in breast carcinoma. Clin Cancer Res 2003; 9:6389-94.

383. Liu J, Lam JB, Chow KH, Xu A, Lam KS, Moon RT, Wang Y. Adiponectin stimulates Wnt inhibitory factor-1 expression through epigenetic regulations involving the transcription factor specificity protein 1. Carcinogenesis 2008; 29:2195-202.

384. Kolesnikov N, Hastings E, Keays M, Melnichuk O, Tang YA, Williams E, Dylag M, Kurbatova N, Brandizi M, Burdett T, et al. ArrayExpress update--simplifying data submissions. Nucleic Acids Res 2015; 43:D1113-6.

385. Chen ST, Choo KB, Hou MF, Yeh KT, Kuo SJ, Chang JG. Deregulated expression of the PER1, PER2 and PER3 genes in breast cancers. Carcinogenesis 2005; 26:1241-6.

386. Kuo SJ, Chen ST, Yeh KT, Hou MF, Chang YS, Hsu NC, Chang JG. Disturbance of circadian gene expression in breast cancer. Virchows Arch 2009; 454:467-74.

387. Tsunoda S, Smith E, De Young NJ, Wang X, Tian ZQ, Liu JF, Jamieson GG, Drew PA. Methylation of CLDN6, FBN2, RBP1, RBP4, TFPI2, and TMEFF2 in esophageal squamous cell carcinoma. Oncol Rep 2009; 21:1067-73.

388. Ye Q, Shen Y, Wang X, Yang J, Miao F, Shen C, Zhang J. Hypermethylation of HLA class I gene is associated with HLA class I down-regulation in human gastric cancer. Tissue Antigens 2009.

389. Hirata T, Yamamoto H, Taniguchi H, Horiuchi S, Oki M, Adachi Y, Imai K, Shinomura Y. Characterization of the immune escape phenotype of human gastric cancers with and without high-frequency microsatellite instability. J Pathol 2007; 211:516-23.

390. Nie Y, Liao J, Zhao X, Song Y, Yang GY, Wang LD, Yang CS. Detection of multiple gene hypermethylation in the development of esophageal squamous cell carcinoma. Carcinogenesis 2002; 23:1713-20.

391. Nie Y, Yang G, Song Y, Zhao X, So C, Liao J, Wang LD, Yang CS. DNA hypermethylation is a mechanism for loss of expression of the HLA class I genes in human esophageal squamous cell carcinomas. Carcinogenesis 2001; 22:1615-23.

392. Sathyanarayana UG, Moore AY, Li L, Padar A, Majmudar K, Stastny V, Makarla P, Suzuki M, Minna JD, Feng Z, et al. Sun exposure related methylation in malignant and non-malignant skin lesions. Cancer Lett 2007; 245:112-20.

393. Sathyanarayana UG, Padar A, Suzuki M, Maruyama R, Shigematsu H, Hsieh JT, Frenkel EP, Gazdar AF. Aberrant promoter methylation of laminin-5-encoding genes in prostate cancers and its relationship to clinicopathological features. Clin Cancer Res 2003; 9:6395-400.

394. Seliger B. Molecular mechanisms of MHC class I abnormalities and APM components in human tumors. Cancer Immunol Immunother 2008; 57:1719-26.

395. Cheng Y, Kim JW, Liu W, Dunn TA, Luo J, Loza MJ, Kim ST, Zheng SL, Xu J, Isaacs WB, et al. Genetic and epigenetic inactivation of TNFRSF10C in human prostate cancer. Prostate 2009; 69:327-35.

396. Gao Z, Xu Z, Hung MS, Lin YC, Wang T, Gong M, Zhi X, Jablon DM, You L. Promoter demethylation of WIF-1 by epigallocatechin-3-gallate in lung cancer cells. Anticancer Res 2009; 29:2025-30.

397. Reguart N, He B, Xu Z, You L, Lee AY, Mazieres J, Mikami I, Batra S, Rosell R, McCormick F, et al. Cloning and characterization of the promoter of human Wnt inhibitory factor-1. Biochem Biophys Res Commun 2004; 323:229-34.

398. Ding Z, Qian YB, Zhu LX, Xiong QR. Promoter methylation and mRNA expression of DKK-3 and WIF-1 in hepatocellular carcinoma. World J Gastroenterol 2009; 15:2595-601.

399. Veeck J, Wild PJ, Fuchs T, Schuffler PJ, Hartmann A, Knuchel R, Dahl E. Prognostic relevance of Wnt-inhibitory factor-1 (WIF1) and Dickkopf-3 (DKK3) promoter methylation in human breast cancer. BMC Cancer 2009; 9:217.

400. Demircan B, Dyer LM, Gerace M, Lobenhofer EK, Robertson KD, Brown KD. Comparative epigenomics of human and mouse mammary tumors. Genes Chromosomes Cancer 2009; 48:83-97.

401. CDC releases recommendations on diagnosis and management of PID. Am Fam Physician 1991; 44:673, 5-6.

402. Clement G, Guilleret I, He B, Yagui-Beltran A, Lin YC, You L, Xu Z, Shi Y, Okamoto J, Benhattar J, et al. Epigenetic alteration of the Wnt inhibitory factor-1 promoter occurs early in the carcinogenesis of Barrett's esophagus. Cancer Sci 2008; 99:46-53.

403. Chan SL, Cui Y, van Hasselt A, Li H, Srivastava G, Jin H, Ng KM, Wang Y, Lee KY, Tsao GS, et al. The tumor suppressor Wnt inhibitory factor 1 is frequently methylated in nasopharyngeal and esophageal carcinomas. Lab Invest 2007; 87:644-50.

404. Lin YC, You L, Xu Z, He B, Mikami I, Thung E, Chou J, Kuchenbecker K, Kim J, Raz D, et al. Wnt signaling activation and WIF-1 silencing in nasopharyngeal cancer cell lines. Biochem Biophys Res Commun 2006; 341:635-40.

405. Taniguchi H, Yamamoto H, Hirata T, Miyamoto N, Oki M, Nosho K, Adachi Y, Endo T, Imai K, Shinomura Y. Frequent epigenetic inactivation of Wnt inhibitory factor-1 in human gastrointestinal cancers. Oncogene 2005; 24:7946-52.

406. Batra S, Shi Y, Kuchenbecker KM, He B, Reguart N, Mikami I, You L, Xu Z, Lin YC, Clement G, et al. Wnt inhibitory factor-1, a Wnt antagonist, is silenced by promoter hypermethylation in malignant pleural mesothelioma. Biochem Biophys Res Commun 2006; 342:1228-32.

407. Urakami S, Shiina H, Enokida H, Kawakami T, Kawamoto K, Hirata H, Tanaka Y, Kikuno N, Nakagawa M, Igawa M, et al. Combination analysis of hypermethylated Wnt-antagonist family genes as a novel epigenetic biomarker panel for bladder cancer detection. Clin Cancer Res 2006; 12:2109-16.

408. Urakami S, Shiina H, Enokida H, Kawakami T, Tokizane T, Ogishima T, Tanaka Y, Li LC, Ribeiro-Filho LA, Terashima M, et al. Epigenetic inactivation of Wnt inhibitory factor-1 plays an important role in bladder cancer through aberrant canonical Wnt/beta-catenin signaling pathway. Clin Cancer Res 2006; 12:383-91.

409. O. Leary P, Penny SA, Dolan RT, Kelly CM, Madden SF, Rexhepaj E, Brennan DJ, McCann AH, Ponten F, Uhlen M, et al. Systematic antibody generation and validation via tissue microarray technology leading to identification of a novel protein prognostic panel in breast cancer. BMC Cancer 2013; 13:175.

410. Naito S, Pippin JW, Shankland SJ. The glomerular parietal epithelial cell's responses are influenced by SM22 alpha levels. BMC Nephrol 2014; 15:174.

411. Sarrio D, Rodriguez-Pinilla SM, Hardisson D, Cano A, Moreno-Bueno G, Palacios J. Epithelial-mesenchymal transition in breast cancer relates to the basal-like phenotype. Cancer Res 2008; 68:989-97.

412. Ma J, Guo X, Zhang S, Liu H, Lu J, Dong Z, Liu K, Ming L. Trichostatin A, a histone deacetylase inhibitor, suppresses proliferation and promotes apoptosis of esophageal squamous cell lines. Mol Med Rep 2015; 11:4525-31.

413. Zhu WG, Hileman T, Ke Y, Wang P, Lu S, Duan W, Dai Z, Tong T, Villalona-Calero MA, Plass C, et al. 5-aza-2'-deoxycytidine activates the p53/p21Waf1/Cip1 pathway to inhibit cell proliferation. J Biol Chem 2004; 279:15161-6.

414. Yao TT, Mo SM, Liu LY, Lu HW, Huang ML, Lin ZQ. 5-Aza-2'-deoxycytidine may influence the proliferation and apoptosis of cervical cancer cells via demethylation in a dose- and time-dependent manner. Genet Mol Res 2013; 12:312-8.

415. Gomyo Y, Sasaki J, Branch C, Roth JA, Mukhopadhyay T. 5-aza-2'-deoxycytidine upregulates caspase-9 expression cooperating with p53-induced apoptosis in human lung cancer cells. Oncogene 2004; 23:6779-87.

416. Hackanson B, Daskalakis M. Decitabine. Recent Results Cancer Res 2014; 201:269-97.

417. Sun S, Han Y, Liu J, Fang Y, Tian Y, Zhou J, Ma D, Wu P. Trichostatin A targets the mitochondrial respiratory chain, increasing mitochondrial reactive oxygen species production to trigger apoptosis in human breast cancer cells. PLoS One 2014; 9:e91610.

418. Peiffer L, Poll-Wolbeck SJ, Flamme H, Gehrke I, Hallek M, Kreuzer KA. Trichostatin A effectively induces apoptosis in chronic lymphocytic leukemia cells via inhibition of Wnt signaling and histone deacetylation. J Cancer Res Clin Oncol 2014; 140:1283-93.

419. Lazcoz P, Munoz J, Nistal M, Pestana A, Encio I, Castresana JS. Frequent promoter hypermethylation of RASSF1A and CASP8 in neuroblastoma. BMC Cancer 2006; 6:254.

420. Martinez R, Setien F, Voelter C, Casado S, Quesada MP, Schackert G, Esteller M. CpG island promoter hypermethylation of the pro-apoptotic gene caspase-8 is a common hallmark of relapsed glioblastoma multiforme. Carcinogenesis 2007; 28:1264-8.

421. Qian J, Yao DM, Lin J, Wang YL, Han LX, Xu WR, Wu CY. Methylation of DAPK1 promoter: frequent but not an adverse prognostic factor in myelodysplastic syndrome. Int J Lab Hematol 2009.

422. Stephen JK, Chen KM, Raitanen M, Grenman S, Worsham MJ. DNA hypermethylation profiles in squamous cell carcinoma of the vulva. Int J Gynecol Pathol 2009; 28:63-75.

423. Garcia P, Manterola C, Araya JC, Villaseca M, Guzman P, Sanhueza A, Thomas M, Alvarez H, Roa JC. Promoter methylation profile in preneoplastic and neoplastic gallbladder lesions. Mol Carcinog 2009; 48:79-89.

424. Phuong NT, Kim SK, Lim SC, Kim HS, Kim TH, Lee KY, Ahn SG, Yoon JH, Kang KW. Role of PTEN promoter methylation in tamoxifen-resistant breast cancer cells. Breast Cancer Res Treat 2010.

425. Mirza S, Sharma G, Pandya P, Ralhan R. Demethylating agent 5-aza-2-deoxycytidine enhances susceptibility of breast cancer cells to anticancer agents. Mol Cell Biochem 2010; 342:101-9.

426. Zhao LY, Niu Y, Santiago A, Liu J, Albert SH, Robertson KD, Liao D. An EBF3-mediated transcriptional program that induces cell cycle arrest and apoptosis. Cancer Res 2006; 66:9445-52.

427. Zhang M, Wang Q, Yuan W, Yang S, Wang X, Yan JD, Du J, Yin J, Gao SY, Sun BC, et al. Epigenetic regulation of bone morphogenetic protein-6 gene expression in breast cancer cells. J Steroid Biochem Mol Biol 2007; 105:91-7.

428. Hines WC, Bazarov AV, Mukhopadhyay R, Yaswen P. BORIS (CTCFL) is not expressed in most human breast cell lines and high grade breast carcinomas. PLoS One 2010; 5:e9738.

429. Starcevic SL, Elferink C, Novak RF. Progressive resistance to apoptosis in a cell lineage model of human proliferative breast disease. J Natl Cancer Inst 2001; 93:776-82.

430. Li P, Nijhawan D, Budihardjo I, Srinivasula SM, Ahmad M, Alnemri ES, Wang X. Cytochrome c and dATP-dependent formation of Apaf-1/caspase-9 complex initiates an apoptotic protease cascade. Cell 1997; 91:479-89.

431. Li B, Wen G, Zhao Y, Tong J, Hei TK. The role of TGFBI in mesothelioma and breast cancer: association with tumor suppression. BMC Cancer 2012; 12:239.

432. Shao G, Berenguer J, Borczuk AC, Powell CA, Hei TK, Zhao Y. Epigenetic inactivation of Betaig-h3 gene in human cancer cells. Cancer Res 2006; 66:4566-73.

433. Cheng AS, Culhane AC, Chan MW, Venkataramu CR, Ehrich M, Nasir A, Rodriguez BA, Liu J, Yan PS, Quackenbush J, et al. Epithelial progeny of estrogen-exposed breast progenitor cells display a cancer-like methylome. Cancer Res 2008; 68:1786-96.

434. Ramirez N, Bandres E, Navarro A, Pons A, Jansa S, Moreno I, Martinez-Rodenas F, Zarate R, Bitarte N, Monzo M, et al. Epigenetic events in normal colonic mucosa surrounding colorectal cancer lesions. Eur J Cancer 2008; 44:2689-95.

435. Ushijima T. Epigenetic field for cancerization. J Biochem Mol Biol 2007; 40:142-50.

436. Ramachandran K, Singal R. DNA methylation and field cancerization. Epigenomics 2012; 4:243-5.

437. Cho YH, Yazici H, Wu HC, Terry MB, Gonzalez K, Qu M, Dalay N, Santella RM. Aberrant promoter hypermethylation and genomic hypomethylation in tumor, adjacent normal tissues and blood from breast cancer patients. Anticancer Res 2010; 30:2489-96.

438. Booth MJ, Branco MR, Ficz G, Oxley D, Krueger F, Reik W, Balasubramanian S. Quantitative sequencing of 5-methylcytosine and 5-hydroxymethylcytosine at single-base resolution. Science 2012; 336:934-7.

439. Murria R, Palanca S, de Juan I, Egoavil C, Alenda C, Garcia-Casado Z, Juan MJ, Sanchez AB, Santaballa A, Chirivella I, et al. Methylation of tumor suppressor genes is related with copy number aberrations in breast cancer. Am J Cancer Res 2015; 5:375-85.

440. Schmidt B, Weickmann S, Witt C, Fleischhacker M. Improved method for isolating cell-free DNA. Clin Chem 2005; 51:1561-3.

441. Chun FK, Muller I, Lange I, Friedrich MG, Erbersdobler A, Karakiewicz PI, Graefen M, Pantel K, Huland H, Schwarzenbach H. Circulating tumour-associated plasma DNA represents an independent and informative predictor of prostate cancer. BJU Int 2006; 98:544-8.

442. Kim Y, Kim DH. CpG island hypermethylation as a biomarker for the early detection of lung cancer. Methods Mol Biol 2015; 1238:141-71.

443. Eads CA, Danenberg KD, Kawakami K, Saltz LB, Blake C, Shibata D, Danenberg PV, Laird PW. MethyLight: a high-throughput assay to measure DNA methylation. Nucleic Acids Res 2000; 28:E32.

444. Jeronimo C, Costa I, Martins MC, Monteiro P, Lisboa S, Palmeira C, Henrique R, Teixeira MR, Lopes C. Detection of gene promoter hypermethylation in fine needle washings from breast lesions. Clin Cancer Res 2003; 9:3413-7.

445. Krassenstein R, Sauter E, Dulaimi E, Battagli C, Ehya H, Klein-Szanto A, Cairns P. Detection of breast cancer in nipple aspirate fluid by CpG island hypermethylation. Clin Cancer Res 2004; 10:28-32.

446. Antill YC, Mitchell G, Johnson SA, Devereux L, Milner A, Di Iulio J, Lindeman GJ, Kirk J, Phillips KA, Campbell IG. Gene methylation in breast ductal fluid from BRCA1 and BRCA2 mutation carriers. Cancer Epidemiol Biomarkers Prev 2010; 19:265-74.

447. Schwarzenbach H, Pantel K. Circulating DNA as biomarker in breast cancer. Breast Cancer Res 2015; 17:136.

448. Kim JH, Shin MH, Kweon SS, Park MH, Yoon JH, Lee JS, Choi C, Fackler MJ, Sukumar S. Evaluation of promoter hypermethylation detection in serum as a diagnostic tool for breast carcinoma in Korean women. Gynecol Oncol 2010; 118:176-81.

449. Assinder SJ, Stanton JA, Prasad PD. Transgelin: an actin-binding protein and tumour suppressor. Int J Biochem Cell Biol 2009; 41:482-6.

450. Yang Z, Chang YJ, Miyamoto H, Ni J, Niu Y, Chen Z, Chen YL, Yao JL, di Sant'Agnese PA, Chang C. Transgelin functions as a suppressor via inhibition of ARA54-enhanced androgen receptor transactivation and prostate cancer cell growth. Mol Endocrinol 2007; 21:343-58.

451. Ryu JW, Kim HJ, Lee YS, Myong NH, Hwang CH, Lee GS, Yom HC. The proteomics approach to find biomarkers in gastric cancer. J Korean Med Sci 2003; 18:505-9.

452. Yu B, Chen X, Li J, Qu Y, Su L, Peng Y, Huang J, Yan J, Yu Y, Gu Q, et al. Stromal fibroblasts in the microenvironment of gastric carcinomas promote tumor metastasis via upregulating TAGLN expression. BMC Cell Biol 2013; 14:17.

453. Gourlay CW, Carpp LN, Timpson P, Winder SJ, Ayscough KR. A role for the actin cytoskeleton in cell death and aging in yeast. J Cell Biol 2004; 164:803-9.

454. Kato Y, Salumbides BC, Wang XF, Qian DZ, Williams S, Wei Y, Sanni TB, Atadja P, Pili R. Antitumor effect of the histone deacetylase inhibitor LAQ824 in combination with 13-cis-retinoic acid in human malignant melanoma. Mol Cancer Ther 2007; 6:70-81.

455. Liu J, Guo W, Li J, Li X, Geng J, Chen Q, Gao J. Tumor-targeting novel manganese complex induces ROS-mediated apoptotic and autophagic cancer cell death. Int J Mol Med 2015; 35:607-16.

456. Shapland C, Hsuan JJ, Totty NF, Lawson D. Purification and properties of transgelin: a transformation and shape change sensitive actin-gelling protein. J Cell Biol 1993; 121:1065-73.

457. Shen J, Yang M, Ju D, Jiang H, Zheng JP, Xu Z, Li L. Disruption of SM22 promotes inflammation after artery injury via nuclear factor kappaB activation. Circ Res 2010; 106:1351-62.

458. Hall A. The cytoskeleton and cancer. Cancer Metastasis Rev 2009; 28:5-14.

459. Chunhua L, Donglan L, Xiuqiong F, Lihua Z, Qin F, Yawei L, Liang Z, Ge W, Linlin J, Ping Z, et al. Apigenin up-regulates transgelin and inhibits invasion and migration of colorectal cancer through decreased phosphorylation of AKT. J Nutr Biochem 2013; 24:1766-75.

460. Pang J, Liu WP, Liu XP, Li LY, Fang YQ, Sun QP, Liu SJ, Li MT, Su ZL, Gao X. Profiling protein markers associated with lymph node metastasis in prostate cancer by DIGE-based proteomics analysis. J Proteome Res 2010; 9:216-26.

461. Mikuriya K, Kuramitsu Y, Ryozawa S, Fujimoto M, Mori S, Oka M, Hamano K, Okita K, Sakaida I, Nakamura K. Expression of glycolytic enzymes is increased in pancreatic cancerous tissues as evidenced by proteomic profiling by two-dimensional electrophoresis and liquid chromatography-mass spectrometry/mass spectrometry. Int J Oncol 2007; 30:849-55.

462. Klade CS, Voss T, Krystek E, Ahorn H, Zatloukal K, Pummer K, Adolf GR. Identification of tumor antigens in renal cell carcinoma by serological proteome analysis. Proteomics 2001; 1:890-8.

463. Rho JH, Roehrl MH, Wang JY. Tissue proteomics reveals differential and compartment-specific expression of the homologs transgelin and transgelin-2 in lung adenocarcinoma and its stroma. J Proteome Res 2009; 8:5610-8.

464. Zang C, Eucker J, Habbel P, Neumann C, Schulz CO, Bangemann N, Kissner L, Riess H, Liu H. Targeting multiple tyrosine kinase receptors with Dovitinib blocks invasion and the

interaction between tumor cells and cancer-associated fibroblasts in breast cancer. Cell Cycle 2015; 14:1291-9.

465. Rismanchi S, Yadegar O, Muhammadnejad S, Amanpour S, Taghizadeh-Jahed M, Muhammadnejad A. Expression of vimentin filaments in canine malignant mammary gland tumors: A simulation of clinicopathological features of human breast cancer. Biomed Rep 2014; 2:725-8.

466. Aleskandarany MA, Negm OH, Green AR, Ahmed MA, Nolan CC, Tighe PJ, Ellis IO, Rakha EA. Epithelial mesenchymal transition in early invasive breast cancer: an immunohistochemical and reverse phase protein array study. Breast Cancer Res Treat 2014; 145:339-48.

467. Masser DR, Stanford DR, Freeman WM. Targeted DNA methylation analysis by next-generation sequencing. J Vis Exp 2015.

468. O'Geen H, Echipare L, Farnham PJ. Using ChIP-seq technology to generate high-resolution profiles of histone modifications. Methods Mol Biol 2011; 791:265-86.

469. Ficz G, Branco MR, Seisenberger S, Santos F, Krueger F, Hore TA, Marques CJ, Andrews S, Reik W. Dynamic regulation of 5-hydroxymethylcytosine in mouse ES cells and during differentiation. Nature 2011; 473:398-402.

Appendices

Appendix A – Gene lists

Appendix Table 1: Top 50 probe sets commonly induced by AZA according to MCF7 fold change ratios [a]

				Fold Change [b]			Mocks	
#	Probe set	Gene symbol	p-value	MCF7	231	MCF12A	12A/MCF7	12A /231
1	1552487_a_at	BNC1	< 1e-07	2.59	5.72	1.46	14.25	13.90
2	1552703_s_at	CARD16	< 1e-07	4.76	5.01	0.98	34.90	3.06
3	1555724_s_at	TAGLN	< 1e-07	23.64	1.68	0.60	40.55	13.03
4	201060_x_at	STOM	< 1e-07	2.03	5.90	1.03	3.60	50.08
5	201061_s_at	STOM	< 1e-07	1.98	5.54	0.92	4.61	49.36
6	201141_at	GPNMB	< 1e-07	8.59	3.55	0.71	8.55	29.85
7	201506_at	TGFBI	< 1e-07	9.28	1.66	0.77	31.55	13.68
8	202948_at	IL1R1	< 1e-07	4.65	2.32	0.21	62.99	49.54
9	203407_at	PPL	< 1e-07	3.28	1.50	1.03	2.72	38.38
10	203434_s_at	MME	< 1e-07	3.94	1.68	0.54	319.41	502.92
11	204083_s_at	TPM2	< 1e-07	4.15	5.18	0.62	57.10	36.21
12	205547_s_at	TAGLN	< 1e-07	30.98	1.92	0.60	59.61	15.16
13	205627_at	CDA	< 1e-07	4.02	2.12	0.74	28.20	6.03
14	205792_at	WISP2	< 1e-07	4.19	1.59	0.34	18.27	79.82
15	209576_at	GNAI1	< 1e-07	2.23	1.55	1.17	97.23	4.36
16	210517_s_at	AKAP12	< 1e-07	19.29	3.36	1.00	98.02	4.57
17	213436_at	CNR1	< 1e-07	3.78	1.62	0.28	79.92	84.02
18	213992_at	COL4A6	< 1e-07	5.63	8.71	0.98	43.45	29.06
19	214651_s_at	HOXA9	< 1e-07	2.70	1.97	0.91	90.38	78.20
20	215446_s_at	LOX	< 1e-07	16.61	2.59	0.44	299.49	7.30
21	223204_at	C4orf18	< 1e-07	1.78	5.09	0.67	22.88	50.36
22	224463_s_at	C11orf70	< 1e-07	1.68	2.28	0.74	29.53	23.73
23	224588_at	XIST	< 1e-07	29.44	6.96	0.72	134.15	101.33
24	225803_at	FBXO32	< 1e-07	2.70	1.68	0.28	66.84	32.74
25	226545_at	CD109	< 1e-07	2.17	3.11	0.67	111.27	292.69
26	227399_at	VGLL3	< 1e-07	1.78	3.97	0.54	116.89	4.20
27	227529_s_at	AKAP12	< 1e-07	8.43	3.30	0.70	25.49	4.59
28	228824_s_at	PTGR1	< 1e-07	3.20	1.63	0.68	38.23	11.49
29	231897_at	PTGR1	< 1e-07	3.42	1.61	0.69	52.17	17.48
30	204298_s_at	LOX	< 1e-07	5.36	2.55	0.51	79.77	5.73
31	209283_at	CRYAB	< 1e-07	3.08	2.38	1.00	19.02	17.41
32	221728_x_at	XIST	< 1e-07	25.96	4.90	0.72	106.21	92.14

Appendix Table 1: Top 50 probe sets commonly induced by AZA according to MCF7 fold change ratios [a]

				Fold Change [b]			Mocks	
#	Probe set	Gene symbol	p-value	MCF7	231	MCF12A	12A/MCF7	12A /231
33	226325_at	ADSSL1	< 1e-07	1.62	1.72	0.49	9.65	54.66
34	228293_at	DEPDC7	< 1e-07	13.89	5.89	1.47	40.25	8.87
35	207826_s_at	ID3	< 1e-07	1.71	2.50	0.54	2.17	22.12
36	212992_at	AHNAK2	< 1e-07	2.71	2.37	0.58	11.38	25.00
37	215501_s_at	DUSP10	< 1e-07	1.96	1.56	0.38	11.92	3.87
38	224589_at	XIST	< 1e-07	19.22	3.40	0.58	68.89	66.98
39	228776_at	GJC1	< 1e-07	1.75	2.68	0.90	20.30	19.88
40	213711_at	KRT81	< 1e-07	11.32	2.06	0.82	6.55	7.24
41	241763_s_at	FBXO32	< 1e-07	3.83	3.13	0.57	31.25	13.05
42	221563_at	DUSP10	< 1e-07	3.08	1.53	0.41	19.90	3.73
43	225373_at	C10orf54	< 1e-07	2.74	2.23	0.69	29.13	14.97
44	1556190_s_at	PRNP	< 1e-07	2.07	1.56	0.63	19.59	3.45
45	218162_at	OLFML3	< 1e-07	16.53	1.53	0.37	7.30	8.76
46	213640_s_at	LOX	< 1e-07	1.59	2.41	0.43	17.92	6.21
47	202967_at	GSTA4	< 1e-07	1.82	1.58	0.36	10.58	5.83
48	202504_at	TRIM29	< 1e-07	8.56	1.77	0.62	14.55	26.06
49	227461_at	STON2	< 1e-07	3.00	2.84	0.84	2.04	9.20
50	227530_at	AKAP12	< 1e-07	5.38	3.06	0.74	23.54	4.35

a Genes upregulated by $P < 0.05$ in both MCF7 and MDA-MB-231 cells, but not in MCF12A >1.5 fold are listed. b AZA/CTRL. 12A: MCF12A; 231: MDA-MB-231

Appendix Table 2: Top 50 probe sets commonly induced by TSA according to MCF7 fold change ratios [a]

				Fold Change [b]			Mocks	
#	Probe set	Gene symbol	p-value	MCF7	231	MCF12A	12A/MCF7	12A /231
1	219534_x_at	CDKN1C	< 1e-07	29.93	7.66	0.60	6.04	3.35
2	213348_at	CDKN1C	< 1e-07	25.87	7.95	0.53	6.55	3.23
3	227062_at	NCRNA00084	< 1e-07	20.47	9.35	1.28	6.44	3.87
4	211781_x_at	NA	< 1e-07	19.85	2.63	0.79	3.02	2.06
5	213182_x_at	CDKN1C	< 1e-07	19.54	7.54	0.62	3.97	2.69
6	203665_at	HMOX1	< 1e-07	19.42	1.65	1.45	2.43	3.11
7	201427_s_at	SEPP1	< 1e-07	18.22	6.54	1.21	84.78	534.46
8	208747_s_at	C1S	< 1e-07	17.43	1.53	0.98	6.45	7.18
9	216894_x_at	CDKN1C	< 1e-07	13.52	4.01	0.54	2.71	2.32
10	1555229_a_at	C1S	< 1e-07	11.55	1.51	0.82	9.29	8.05
11	212276_at	LPIN1	< 1e-07	10.16	2.14	0.94	2.24	2.65
12	236656_s_at	LOC100130506	< 1e-07	10.06	5.34	1.46	5.26	2.07
13	238320_at	NCRNA00084	< 1e-07	9.78	4.87	1.08	6.97	4.62
14	209160_at	AKR1C3	< 1e-07	9.49	5.29	1.01	598.00	23.17
15	212274_at	LPIN1	< 1e-07	8.63	1.70	1.14	2.56	3.19
16	223854_at	PCDHB10	< 1e-07	7.72	3.36	1.24	3.01	2.70
17	234513_at	ELOVL3	< 1e-07	7.71	6.59	0.95	5.36	4.32
18	219928_s_at	CABYR	< 1e-07	7.71	3.38	1.16	3.55	4.32
19	212706_at	RASA4	< 1e-07	7.31	4.54	1.14	2.15	5.94
20	226051_at	SELM	< 1e-07	6.92	3.01	1.41	5.15	4.88
21	209576_at	GNAI1	< 1e-07	6.85	2.30	1.39	97.23	4.36
22	202388_at	RGS2	< 1e-07	6.48	2.68	0.65	18.51	4.79
23	1561690_at	NA	1.00E-07	5.95	2.05	0.88	2.09	5.41
24	224568_x_at	MALAT1	< 1e-07	5.93	9.38	1.42	2.51	2.95
25	226675_s_at	MALAT1	2.00E-07	5.87	10.63	1.29	2.58	5.03
26	200696_s_at	GSN	< 1e-07	5.56	4.16	1.46	3.43	3.37
27	203650_at	PROCR	< 1e-07	5.56	1.51	0.74	19.24	2.08
28	224567_x_at	MALAT1	< 1e-07	5.45	11.14	1.38	2.21	4.11
29	225123_at	NA	< 1e-07	5.40	5.17	0.80	22.19	7.61
30	225025_at	IGSF8	< 1e-07	5.39	2.93	0.78	2.45	6.03
31	225239_at	NA	< 1e-07	5.28	4.41	1.05	4.50	8.55
32	236657_at	LOC100130506	< 1e-07	5.14	4.59	1.36	3.99	2.09
33	239058_at	NA	< 1e-07	5.11	1.66	0.80	4.14	4.77
34	223940_x_at	MALAT1	< 1e-07	4.95	8.46	1.37	2.12	2.70
35	223340_at	ATL1	< 1e-07	4.87	3.01	0.95	7.34	2.19
36	226158_at	KLHL24	< 1e-07	4.73	5.35	1.05	4.65	15.01
37	202887_s_at	DDIT4	< 1e-07	4.60	6.54	0.95	2.73	4.64
38	209183_s_at	C10orf10	< 1e-07	4.60	3.92	1.21	2.48	2.11
39	221563_at	DUSP10	< 1e-07	4.43	2.32	0.87	19.90	3.73

Appendix Table 2: Top 50 probe sets commonly induced by TSA according to MCF7 fold change ratios [a]

				Fold Change [b]			Mocks	
#	Probe set	Gene symbol	p-value	MCF7	231	MCF12A	12A/MCF7	12A /231
40	200878_at	EPAS1	< 1e-07	4.41	5.66	1.32	21.95	5.24
41	201041_s_at	DUSP1	< 1e-07	4.39	4.90	1.30	4.28	2.28
42	201531_at	ZFP36	< 1e-07	4.26	2.37	1.45	2.28	3.43
43	202075_s_at	PLTP	< 1e-07	4.18	1.82	1.07	26.02	18.92
44	225207_at	PDK4	< 1e-07	4.13	3.57	1.31	335.57	36.56
45	218217_at	SCPEP1	< 1e-07	4.03	3.78	1.40	6.92	6.45
46	213156_at	NA	< 1e-07	4.01	1.53	1.07	34.71	6.10
47	202967_at	GSTA4	< 1e-07	3.98	3.96	1.30	10.58	5.83
48	240440_at	NPL	< 1e-07	3.92	1.68	1.13	2.27	2.00
49	234989_at	NCRNA00084	< 1e-07	3.87	4.44	1.01	3.18	3.61
50	241198_s_at	C11orf70	< 1e-07	3.85	2.81	1.22	16.67	18.59

a Genes upregulated by P < 0.05 in both MCF7 and MDA-MB-231 cells, but not in MCF12A >1.5 fold are listed. b TSA/CTRL. 12A: MCF12A; 231: MDA-MB-231

Appendix Table 3: Top 50 probe sets commonly induced by A+T according to MCF7 fold change ratios [a]

#	Probe set	Gene symbol	p-value	Fold Change [b]			Mocks	
				MCF7	231	MCF12A	12A/MCF7	12A /231
1	242907_at	NA	< 1e-07	49.15	6.86	0.37	22.52	4.28
2	228293_at	DEPDC7	< 1e-07	45.90	16.97	1.09	40.25	8.87
3	208747_s_at	C1S	< 1e-07	37.49	6.43	0.85	6.45	7.18
4	221690_s_at	NLRP2	< 1e-07	30.46	2.45	0.94	3.01	3.27
5	211781_x_at	NA	< 1e-07	27.71	3.66	1.48	3.02	2.06
6	202748_at	GBP2	< 1e-07	23.31	3.72	0.47	9.77	4.09
7	209392_at	ENPP2	< 1e-07	22.11	27.04	0.90	43.08	37.61
8	203665_at	HMOX1	< 1e-07	21.31	1.65	1.15	2.43	3.11
9	202388_at	RGS2	< 1e-07	18.63	15.24	1.22	18.51	4.79
10	226905_at	FAM101B	< 1e-07	16.47	15.58	0.88	16.06	49.66
11	213348_at	CDKN1C	< 1e-07	16.47	9.10	0.85	6.55	3.23
12	219534_x_at	CDKN1C	< 1e-07	14.36	11.46	0.96	6.04	3.35
13	234513_at	ELOVL3	< 1e-07	14.22	9.57	0.94	5.36	4.32
14	227862_at	TRNP1	< 1e-07	12.58	8.63	1.18	3.38	3.02
15	201564_s_at	FSCN1	< 1e-07	12.54	2.56	1.47	3.80	2.96
16	231897_at	PTGR1	< 1e-07	12.50	2.08	0.69	52.17	17.48
17	214651_s_at	HOXA9	< 1e-07	11.79	6.38	0.71	90.38	78.20
18	214247_s_at	DKK3	< 1e-07	10.85	4.56	0.99	18.98	7.18
19	212992_at	AHNAK2	< 1e-07	10.82	9.43	0.64	11.38	25.00
20	209692_at	EYA2	< 1e-07	10.42	3.74	0.52	3.40	9.25
21	201272_at	AKR1B1	< 1e-07	10.22	1.62	1.11	170.13	5.08
22	228776_at	GJC1	< 1e-07	9.31	3.22	1.15	20.30	19.88
23	227530_at	AKAP12	< 1e-07	9.03	11.68	1.44	23.54	4.35
24	216894_x_at	CDKN1C	< 1e-07	8.92	9.32	0.98	2.71	2.32
25	213182_x_at	CDKN1C	< 1e-07	8.72	12.06	0.88	3.97	2.69
26	210933_s_at	FSCN1	< 1e-07	8.57	2.55	1.46	3.91	3.00
27	235683_at	SESN3	< 1e-07	8.48	10.20	0.80	7.67	3.98
28	206785_s_at	KLRC2	< 1e-07	8.32	13.96	1.11	48.51	27.75
29	228824_s_at	PTGR1	< 1e-07	8.20	2.27	0.78	38.23	11.49
30	221728_x_at	XIST	< 1e-07	8.08	5.74	0.79	106.21	92.14
31	214218_s_at	XIST	< 1e-07	7.36	4.20	0.96	43.44	57.69
32	210839_s_at	ENPP2	< 1e-07	7.06	6.14	0.80	11.25	12.96
33	211828_s_at	TNIK	< 1e-07	6.86	3.79	0.68	9.59	3.87
34	226657_at	MGC33894	< 1e-07	6.83	8.55	1.47	2.05	2.17
35	202075_s_at	PLTP	< 1e-07	6.79	2.54	1.13	26.02	18.92
36	221504_s_at	ATP6V1H	< 1e-07	6.77	1.65	0.97	4.11	2.84
37	201141_at	GPNMB	< 1e-07	6.75	7.82	1.11	8.55	29.85
38	224588_at	XIST	< 1e-07	6.57	6.81	0.84	134.15	101.33
39	205505_at	GCNT1	< 1e-07	6.28	2.28	0.93	9.01	2.18

Appendix Table 3: Top 50 probe sets commonly induced by A+T according to MCF7 fold change ratios [a]

				Fold Change [b]			Mocks	
#	Probe set	Gene symbol	p-value	MCF7	231	MCF12A	12A/MCF7	12A /231
40	214657_s_at	NCRNA00084	< 1e-07	6.26	7.38	0.91	2.98	5.54
41	200824_at	GSTP1	< 1e-07	6.20	1.62	0.94	20.56	3.57
42	205027_s_at	MAP3K8	< 1e-07	6.10	3.53	1.02	3.06	4.59
43	223340_at	ATL1	< 1e-07	5.99	4.66	0.58	7.34	2.19
44	241763_s_at	FBXO32	< 1e-07	5.92	3.97	0.65	31.25	13.05
45	221986_s_at	KLHL24	< 1e-07	5.91	5.52	1.05	4.12	6.89
46	217767_at	C3	< 1e-07	5.78	2.19	1.19	74.34	90.79
47	231067_s_at	NA	< 1e-07	5.43	11.13	1.34	10.16	3.45
48	209160_at	AKR1C3	< 1e-07	5.32	1.65	0.22	598.00	23.17
49	209822_s_at	VLDLR	< 1e-07	5.24	2.21	0.61	34.51	11.50
50	218217_at	SCPEP1	< 1e-07	5.17	2.15	0.49	6.92	6.45

[a] Genes upregulated by P < 0.05 in both MCF7 and MDA-MB-231 cells, but not in MCF12A >1.5 fold are listed. [b] A+T/CTRL. 12A: MCF12A; 231: MDA-MB-231

Appendix Table 4: Top 50 probe sets commonly suppressed by AZA according to MCF7 fold change ratios [a]

#	Probe set	Gene symbol	p-value	Fold Change [b]			Mocks	
				MCF7	231	MCF12A	MCF7/12A	231/12A
1	230836_at	ST8SIA4	< 1e-07	8.32	2.41	0.96	75.14	6.27
2	221703_at	BRIP1	< 1e-07	3.98	1.70	0.95	41.30	11.18
3	239253_at	NA	< 1e-07	3.93	2.20	1.01	3.22	4.65
4	236302_at	PPM1E	< 1e-07	3.87	2.29	0.97	18.34	4.46
5	231121_at	HPS3	< 1e-07	3.86	3.20	1.05	7.01	3.11
6	203685_at	BCL2	< 1e-07	3.69	3.78	1.41	17.19	3.56
7	219306_at	KIF15	< 1e-07	3.36	2.25	1.37	4.13	7.03
8	232278_s_at	DEPDC1	< 1e-07	3.14	2.37	1.21	3.36	10.68
9	239744_at	NA	< 1e-07	3.13	3.45	0.94	5.19	2.87
10	235545_at	DEPDC1	< 1e-07	3.11	2.66	1.37	2.87	11.19
11	236641_at	KIF14	< 1e-07	3.07	2.10	1.05	5.10	5.63
12	222958_s_at	DEPDC1	< 1e-07	3.03	2.54	1.20	3.20	10.45
13	226016_at	CD47	< 1e-07	2.95	2.34	1.14	4.98	2.54
14	238748_at	NA	< 1e-07	2.87	2.29	0.79	2.68	4.96
15	205967_at	HIST1H4C	1.00E-07	2.85	1.55	1.27	4.02	6.25
16	213745_at	ATRNL1	1.00E-07	2.84	1.75	0.99	3.68	3.10
17	220295_x_at	DEPDC1	< 1e-07	2.81	2.18	1.27	2.83	10.68
18	239999_at	C21orf34	1.62E-05	2.75	1.74	1.13	3.23	3.25
19	1558750_a_at	NA	< 1e-07	2.74	2.34	1.10	3.34	4.26
20	203755_at	BUB1B	< 1e-07	2.65	2.45	1.33	3.29	4.56
21	243927_x_at	KIAA1429	< 1e-07	2.64	1.84	0.91	6.83	2.60
22	223381_at	NUF2	< 1e-07	2.63	1.76	1.08	2.59	6.75
23	206364_at	KIF14	< 1e-07	2.61	2.27	1.00	4.75	8.25
24	227928_at	C12orf48	< 1e-07	2.58	1.91	1.28	5.85	4.12
25	213054_at	KIAA0841	1.00E-07	2.56	1.63	1.10	2.41	2.87
26	230165_at	SGOL2	< 1e-07	2.50	2.61	1.14	3.13	5.02
27	229075_at	SPATA5	< 1e-07	2.49	3.56	1.19	2.18	3.87
28	206102_at	GINS1	< 1e-07	2.43	1.57	0.80	7.24	5.88
29	235046_at	NA	< 1e-07	2.42	2.27	0.71	5.16	2.80
30	1568951_at	ZNF280D	< 1e-07	2.40	1.85	1.11	2.63	3.60
31	212949_at	NCAPH	< 1e-07	2.39	2.03	1.02	3.37	6.85
32	226980_at	DEPDC1B	< 1e-07	2.39	2.64	1.49	6.46	6.01
33	215509_s_at	BUB1	< 1e-07	2.38	2.36	1.29	2.59	8.49
34	214764_at	RRP15	< 1e-07	2.38	2.70	1.40	2.21	2.06
35	208931_s_at	ILF3	< 1e-07	2.37	2.38	1.39	2.05	4.72
36	232238_at	ASPM	3.04E-05	2.37	1.56	1.48	2.10	5.88
37	210220_at	FZD2	< 1e-07	2.35	2.20	1.22	2.37	6.81
38	38158_at	ESPL1	< 1e-07	2.34	2.15	1.21	3.52	3.06

Appendix Table 4: Top 50 probe sets commonly suppressed by AZA according to MCF7 fold change ratios [a]

#	Probe set	Gene symbol	p-value	Fold Change [b]			Mocks	
				MCF7	231	MCF12A	MCF7/12A	231/12A
39	223785_at	FANCI	< 1e-07	2.31	1.76	1.02	2.80	7.03
40	229129_at	NA	< 1e-07	2.31	1.75	0.96	2.84	6.64
41	204817_at	ESPL1	< 1e-07	2.30	2.33	1.29	3.64	3.06
42	238719_at	NA	< 1e-07	2.30	1.55	1.02	2.34	3.57
43	211088_s_at	PLK4	< 1e-07	2.29	1.62	0.99	6.07	13.16
44	211450_s_at	MSH6	< 1e-07	2.28	1.59	0.65	2.48	4.20
45	221685_s_at	CCDC99	< 1e-07	2.26	1.55	1.03	2.25	4.62
46	213226_at	CCNA2	< 1e-07	2.25	2.07	1.36	5.68	8.24
47	209773_s_at	RRM2	< 1e-07	2.22	1.73	1.11	4.65	4.09
48	235611_at	NA	< 1e-07	2.22	2.61	1.23	2.74	2.36
49	209642_at	BUB1	< 1e-07	2.22	2.36	1.23	2.96	8.91
50	204162_at	NDC80	< 1e-07	2.21	1.73	1.00	3.42	9.18

[a] Genes downregulated by $P < 0.05$ in both MCF7 and MDA-MB-231 cells, but not in MCF12A >1.5 fold are listed. [b] CTRL/AZA. 12A: MCF12A; 231: MDA-MB-231

Appendix Table 5: Top 50 probe sets commonly suppressed by TSA according to MCF7 fold change ratios [a]

#	Probe set	Gene symbol	p-value	Fold Change [b]			Mocks	
				MCF7	231	MCF12A	MCF7/12A	231/12A
1	235046_at	NA	< 1e-07	22.83	1.60	0.67	5.16	2.80
2	208712_at	CCND1	< 1e-07	18.47	1.97	0.56	7.95	8.56
3	209369_at	ANXA3	< 1e-07	11.63	4.32	0.82	10.54	40.45
4	218513_at	C4orf43	< 1e-07	9.27	3.04	1.00	3.57	2.22
5	213511_s_at	MTMR1	< 1e-07	7.29	2.15	1.43	2.02	3.92
6	210059_s_at	MAPK13	< 1e-07	7.23	1.71	0.91	14.15	9.28
7	214975_s_at	MTMR1	< 1e-07	7.11	2.48	1.40	2.10	5.65
8	227211_at	PHF19	< 1e-07	6.74	5.00	1.14	2.15	2.43
9	1555225_at	C1orf43	< 1e-07	6.48	2.93	1.00	4.79	3.95
10	232278_s_at	DEPDC1	< 1e-07	6.40	4.91	1.14	3.36	10.68
11	227212_s_at	PHF19	< 1e-07	6.37	6.21	1.36	2.28	2.40
12	222958_s_at	DEPDC1	< 1e-07	6.31	4.53	1.19	3.20	10.45
13	230207_s_at	DOCK5	< 1e-07	6.23	2.51	1.02	3.13	4.99
14	218755_at	KIF20A	< 1e-07	6.10	6.34	1.46	4.00	4.94
15	204352_at	TRAF5	< 1e-07	5.99	1.90	1.10	3.89	2.78
16	226517_at	BCAT1	< 1e-07	5.97	2.66	0.89	8.34	149.27
17	235957_at	NA	< 1e-07	5.94	3.22	1.37	9.77	3.72
18	230263_s_at	DOCK5	< 1e-07	5.89	2.13	0.97	3.46	2.88
19	230206_at	DOCK5	< 1e-07	5.78	2.16	0.91	2.87	4.27
20	204317_at	GTSE1	< 1e-07	5.74	6.68	1.32	5.73	7.55
21	225342_at	AK3L1	< 1e-07	5.47	1.78	1.02	6.13	9.19
22	221618_s_at	TAF9B	< 1e-07	5.08	2.93	1.47	3.14	7.14
23	228357_at	UNK	< 1e-07	4.87	3.17	1.37	15.52	4.30
24	236451_at	NA	< 1e-07	4.86	1.61	0.80	14.09	21.74
25	231851_at	RAVER2	< 1e-07	4.83	2.99	1.48	4.29	5.82
26	201125_s_at	ITGB5	< 1e-07	4.78	2.22	1.18	5.12	2.48
27	204932_at	TNFRSF11B	< 1e-07	4.77	1.95	1.02	6.24	21.01
28	204962_s_at	CENPA	< 1e-07	4.75	5.02	1.26	6.05	6.34
29	210058_at	MAPK13	< 1e-07	4.75	1.74	1.14	5.90	4.21
30	202330_s_at	UNG	< 1e-07	4.75	5.19	1.47	7.02	5.89
31	209515_s_at	RAB27A	< 1e-07	4.59	2.67	1.39	5.02	7.19
32	228729_at	CCNB1	< 1e-07	4.54	7.43	1.31	4.34	4.58
33	202240_at	PLK1	< 1e-07	4.40	5.22	1.26	2.99	3.01
34	209679_s_at	LOC57228	< 1e-07	4.35	3.59	1.41	4.62	5.14
35	242045_at	ANKRD18A	< 1e-07	4.33	1.62	1.19	6.63	4.46
36	208079_s_at	AURKA	< 1e-07	4.32	4.47	1.23	3.67	6.76
37	237291_at	NCRNA00117	< 1e-07	4.15	1.55	0.97	5.15	2.42
38	225836_s_at	C12orf32	< 1e-07	4.13	3.48	1.36	4.34	3.17
39	204347_at	AK3L1	< 1e-07	4.11	1.72	1.06	5.10	11.11

Appendix Table 5: Top 50 probe sets commonly suppressed by TSA according to MCF7 fold change ratios [a]

				Fold Change [b]			Mocks	
#	Probe set	Gene symbol	p-value	MCF7	231	MCF12A	MCF7/12A	231/12A
40	219347_at	NUDT15	< 1e-07	4.08	2.41	1.26	2.98	4.88
41	239744_at	NA	< 1e-07	4.08	2.56	1.26	5.19	2.87
42	235545_at	DEPDC1	< 1e-07	4.06	4.31	1.20	2.87	11.19
43	232067_at	C6orf168	< 1e-07	4.06	1.58	0.89	9.49	4.01
44	226037_s_at	TAF9B	< 1e-07	4.03	2.52	1.38	2.73	5.36
45	227379_at	MBOAT1	< 1e-07	4.03	1.79	1.38	8.86	2.98
46	210278_s_at	AP4S1	< 1e-07	4.02	3.03	1.22	3.78	2.26
47	220295_x_at	DEPDC1	< 1e-07	4.01	4.47	0.99	2.83	10.68
48	210277_at	AP4S1	< 1e-07	4.00	2.65	1.23	4.06	2.55
49	223808_s_at	PTPMT1	< 1e-07	3.93	2.08	1.37	3.73	2.49
50	212646_at	RFTN1	< 1e-07	3.90	1.76	1.19	8.36	24.30

[a] Genes downregulated by P < 0.05 in both MCF7 and MDA-MB-231 cells, but not in MCF12A >1.5 fold are listed. [b] TSA/CTRL. 12A: MCF12A; 231: MDA-MB-231

Appendix Table 6: Top 50 probe sets commonly suppressed by A+T according to MCF7 fold change ratios [a]

				Fold Change [b]			Mocks	
#	Probe set	Gene symbol	p-value	MCF7	231	MCF12A	MCF7/12A	231/12A
1	235046_at	NA	< 1e-07	19.78	5.12	0.45	5.16	2.80
2	230836_at	ST8SIA4	< 1e-07	18.00	2.81	1.42	75.14	6.27
3	230261_at	ST8SIA4	< 1e-07	11.12	1.68	1.16	34.34	3.56
4	1554696_s_at	TYMS	< 1e-07	10.44	5.05	1.42	2.17	5.88
5	202589_at	TYMS	< 1e-07	9.56	4.39	1.36	2.54	5.32
6	218513_at	C4orf43	< 1e-07	9.28	1.95	0.99	3.57	2.22
7	1555225_at	C1orf43	< 1e-07	8.18	3.01	1.02	4.79	3.95
8	226016_at	CD47	< 1e-07	6.99	3.06	1.49	4.98	2.54
9	239253_at	NA	< 1e-07	6.77	4.54	1.17	3.22	4.65
10	209696_at	FBP1	< 1e-07	6.52	5.11	0.52	52.24	24.37
11	231851_at	RAVER2	< 1e-07	6.43	3.70	0.99	4.29	5.82
12	242979_at	IRS1	< 1e-07	5.46	3.00	0.89	5.64	2.87
13	208712_at	CCND1	< 1e-07	5.46	3.89	0.22	7.95	8.56
14	222424_s_at	NUCKS1	< 1e-07	5.33	2.59	1.46	4.28	2.81
15	242890_at	NA	< 1e-07	5.29	1.85	0.70	4.78	4.20
16	230263_s_at	DOCK5	< 1e-07	5.29	2.18	0.69	3.46	2.88
17	236451_at	NA	< 1e-07	5.17	2.91	0.89	14.09	21.74
18	213222_at	PLCB1	< 1e-07	5.12	2.78	0.98	21.36	10.74
19	223808_s_at	PTPMT1	< 1e-07	4.98	3.22	1.46	3.73	2.49
20	209754_s_at	TMPO	< 1e-07	4.98	2.58	1.21	8.53	14.12
21	229353_s_at	NUCKS1	< 1e-07	4.97	3.05	1.39	3.04	2.33
22	225447_at	GPD2	< 1e-07	4.96	2.08	1.13	2.43	2.70
23	214975_s_at	MTMR1	< 1e-07	4.94	2.00	1.20	2.10	5.65
24	209369_at	ANXA3	< 1e-07	4.91	2.65	0.29	10.54	40.45
25	208711_s_at	CCND1	< 1e-07	4.79	3.48	0.20	6.08	7.78
26	1555461_at	NA	< 1e-07	4.72	2.42	0.96	3.67	3.46
27	235611_at	NA	< 1e-07	4.39	3.53	1.08	2.74	2.36
28	206061_s_at	DICER1	< 1e-07	4.33	1.98	0.72	3.75	4.99
29	213511_s_at	MTMR1	< 1e-07	4.27	1.77	1.15	2.02	3.92
30	201125_s_at	ITGB5	< 1e-07	4.22	2.40	0.49	5.12	2.48
31	225768_at	NR1D2	< 1e-07	4.17	1.86	0.98	2.50	2.38
32	205909_at	POLE2	< 1e-07	4.15	2.64	0.74	4.88	8.33
33	235957_at	NA	< 1e-07	4.10	1.69	1.00	9.77	3.72
34	219262_at	SUV39H2	< 1e-07	4.05	1.83	0.53	3.61	4.74
35	228026_at	RP5-1000E10.4	< 1e-07	4.02	2.75	1.41	5.73	2.08
36	204887_s_at	PLK4	< 1e-07	3.97	2.01	0.95	4.77	8.27
37	225928_at	RDH11	< 1e-07	3.97	2.87	1.20	2.53	2.06
38	218741_at	CENPM	< 1e-07	3.96	2.30	1.43	2.98	3.44
39	223824_at	C10orf59	< 1e-07	3.95	1.87	0.42	4.61	2.97

Appendix Table 6: Top 50 probe sets commonly suppressed by A+T according to MCF7 fold change ratios [a]

				Fold Change [b]			Mocks	
#	Probe set	Gene symbol	p-value	MCF7	231	MCF12A	MCF7/12A	231/12A
40	227350_at	HELLS	< 1e-07	3.90	2.29	0.89	3.88	3.19
41	202330_s_at	UNG	< 1e-07	3.89	2.32	0.45	7.02	5.89
42	209053_s_at	WHSC1	< 1e-07	3.89	3.34	1.09	7.02	9.81
43	209052_s_at	WHSC1	< 1e-07	3.82	3.03	1.21	4.84	8.19
44	228654_at	SPIN4	< 1e-07	3.79	1.55	0.82	2.54	6.87
45	213308_at	SHANK2	< 1e-07	3.79	2.48	0.73	21.03	6.65
46	205036_at	LSM6	< 1e-07	3.77	2.18	1.29	2.51	3.58
47	209531_at	GSTZ1	< 1e-07	3.75	2.33	1.01	3.94	2.73
48	213229_at	DICER1	< 1e-07	3.73	2.04	0.79	3.08	3.75
49	209054_s_at	WHSC1	< 1e-07	3.69	3.67	1.28	4.17	8.06
50	226421_at	AMMECR1	< 1e-07	3.68	2.54	1.20	2.79	3.44

[a] Genes downregulated by P < 0.05 in both MCF7 and MDA-MB-231 cells, but not in MCF12A >1.5 fold are listed. [b] A+T/CTRL. 12A: MCF12A; 231: MDA-MB-231

Appendix B – Copyright Permissions

No copyright permissions were required for Figure 1.4A and B.

Skeletal formula of decitabine (**5-aza-2'-deoxycytidine**). Created using ACD/ChemSketch 10.0 and Inkscape.

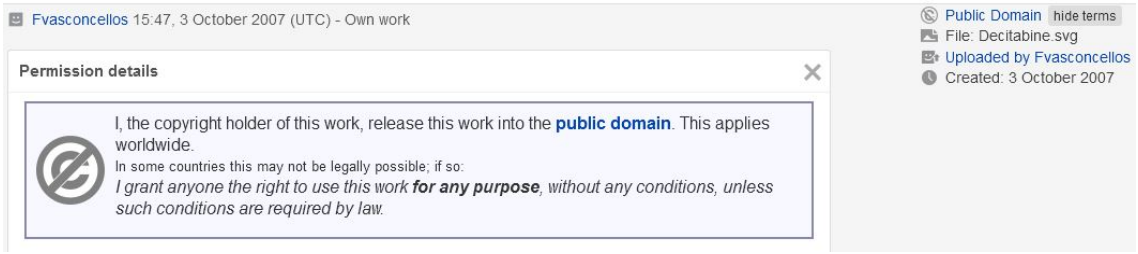

Structural formula of trichostatin A

Copyright permissions for figures and tables taken or reproduced from Sayar *et al.*[366] (Tables Table 2.4, Table 3.11, Table 3.12, and figures Figure 3.21, Figure 3.22, Figure 3.25, Figure 3.26, Figure 3.27, Figure 3.28, Figure 3.29). License: Creative Commons Attribution 4.0 International. URL: http://creativecommons.org/licenses/by/4.0/.

Transgelin gene is frequently downregulated by promoter DNA hypermethylation in breast cancer

Nilufer Sayar, Gurbet Karahan, Ozlen Konu, Betul Bozkurt, Onder Bozdogan, and Isik G. Yulug

Author information ▶ Article notes ▶ Copyright and License information ▼

Copyright © Sayar et al. 2015

Open Access This article is distributed under the terms of the Creative Commons Attribution 4.0 International License (http://creativecommons.org/licenses/by/4.0/), which permits unrestricted use, distribution, and reproduction in any medium, provided you give appropriate credit to the original author(s) and the source, provide a link to the Creative Commons license, and indicate if changes were made. The Creative Commons Public Domain Dedication waiver (http://creativecommons.org/publicdomain/zero/1.0/) applies to the data made available in this article, unless otherwise stated.

Attribution 4.0 International (CC BY 4.0)

This is a human-readable summary of (and not a substitute for) the license.

Disclaimer

You are free to:

Share — copy and redistribute the material in any medium or format

Adapt — remix, transform, and build upon the material

for any purpose, even commercially.

The licensor cannot revoke these freedoms as long as you follow the license terms.

Under the following terms:

Attribution — You must give **appropriate credit**, provide a link to the license, and **indicate if changes were made**. You may do so in any reasonable manner, but not in any way that suggests the licensor endorses you or your use.

No additional restrictions — You may not apply legal terms or **technological measures** that legally restrict others from doing anything the license permits.

Notices:

You do not have to comply with the license for elements of the material in the public domain or where your use is permitted by an applicable **exception or limitation**.

No warranties are given. The license may not give you all of the permissions necessary for your intended use. For example, other rights such as **publicity, privacy, or moral rights** may limit how you use the material.

Copyright permissions for Figure 1.3, taken from Esteller *et al.,* 2007[38].

OXFORD UNIVERSITY PRESS LICENSE TERMS AND CONDITIONS

Oct 25, 2015

This is a License Agreement between Nilufer Sayar ("You") and Oxford University Press ("Oxford University Press") provided by Copyright Clearance Center ("CCC"). The license consists of your order details, the terms and conditions provided by Oxford University Press, and the payment terms and conditions.

All payments must be made in full to CCC. For payment instructions, please see information listed at the bottom of this form.

License Number	3735880575071
License date	Oct 25, 2015
Licensed content publisher	Oxford University Press
Licensed content publication	Human Molecular Genetics
Licensed content title	Epigenetic gene silencing in cancer: the DNA hypermethylome:
Licensed content author	Manel Esteller
Licensed content date	04/15/2007
Type of Use	Thesis/Dissertation
Institution name	None
Title of your work	UNMASKING OF EPIGENETICALLY SILENCED GENES AND IDENTIFICATION OF TRANSGELIN AS A POTENTIAL METHYLATION BIOMARKER IN BREAST CANCER
Publisher of your work	n/a
Expected publication date	Nov 2015
Permissions cost	0.00 USD
Value added tax	0.00 USD
Total	0.00 USD
Total	0.00 USD
Terms and Conditions	

Sayar et al. Clinical Epigenetics (2015) 7:104
DOI 10.1186/s13148-015-0138-5

CLINICAL EPIGENETICS

RESEARCH Open Access

Transgelin gene is frequently downregulated by promoter DNA hypermethylation in breast cancer

Nilufer Sayar[1], Gurbet Karahan[1], Ozlen Konu[1], Betul Bozkurt[2], Onder Bozdogan[3] and Isik G. Yulug[1*]

Abstract

Background: CpG hypermethylation in gene promoters is a frequent mechanism of tumor suppressor gene silencing in various types of cancers. It usually occurs at early steps of cancer progression and can be detected easily, giving rise to development of promising biomarkers for both detection and progression of cancer, including breast cancer. 5-aza-2′-deoxycytidine (AZA) is a DNA demethylating and anti-cancer agent resulting in induction of genes suppressed via DNA hypermethylation.

Results: Using microarray expression profiling of AZA- or DMSO-treated breast cancer and non-tumorigenic breast (NTB) cells, we identified for the first time *TAGLN* gene as a target of DNA hypermethylation in breast cancer. *TAGLN* expression was significantly and frequently downregulated via promoter DNA hypermethylation in breast cancer cells compared to NTB cells, and also in 13/21 (61.9 %) of breast tumors compared to matched normal tissues. Analyses of public microarray methylation data showed that *TAGLN* was also hypermethylated in 63.02 % of tumors compared to normal tissues; relapse-free survival of patients was worse with higher *TAGLN* methylation; and methylation levels could discriminate between tumors and healthy tissues with 83.14 % sensitivity and 100 % specificity. Additionally, qRT-PCR and immunohistochemistry experiments showed that *TAGLN* expression was significantly downregulated in two more independent sets of breast tumors compared to normal tissues and was lower in tumors with poor prognosis. Colony formation was increased in *TAGLN* silenced NTB cells, while decreased in overexpressing BC cells.

Conclusions: *TAGLN* gene is frequently downregulated by DNA hypermethylation, and *TAGLN* promoter methylation profiles could serve as a future diagnostic biomarker, with possible clinical impact regarding the prognosis in breast cancer.

Keywords: DNA methylation, Hypermethylation, Breast cancer, TAGLN, SM22 alpha, Prognosis, Diagnosis

Background

Breast cancer is the most common cancer in women, constituting 29 % of new cancer cases estimated for 2015 in US. Breast cancer can be classified according to molecular and histological subtypes with the most aggressive behavior usually being attributed to the triple negative (TN) subtypes, characterized with loss of estrogen, progesterone, and Her2 receptor expressions [1–3].

Epigenetic changes are heritable changes in gene expression patterns that do not involve alterations in the nucleotide sequence of DNA [4]. DNA methylation is a well-known mechanism for epigenetic gene silencing in mammals. CpG islands are CpG-rich regions around the promoters; 5′ untranslated regions and first exons of many genes and are usually unmethylated in normal cells [5]. The methylated state of a CpG island usually refers to transcriptionally repressed promoters [5]. Tumor suppressor genes (TSG) may become inactivated during tumorigenesis through hypermethylation of associated CpG islands, providing several survival advantages [5–8].

5-aza-2′-deoxycytidine (Decitabine, AZA), a cytosine analogue that causes covalent arrest of DNA methyltransferases (DNMT) upon binding, is one of the most commonly used DNMT inhibitors in cultured cells and to treat cancer patients [9, 10]. Use of demethylating agents together with expression microarrays enables the analysis of genes that may be regulated by hypermethylation of their promoter regions [11]. Discovering these genes is essential not only for therapeutic achievements but can also serve diagnostic, prognostic, and monitoring purposes [12].

* Correspondence: yulug@fen.bilkent.edu.tr
[1]Department of Molecular Biology and Genetics, Bilkent University, Faculty of Science, TR-06800 Ankara, Turkey
Full list of author information is available at the end of the article

BioMed Central

© 2015 Sayar et al. **Open Access** This article is distributed under the terms of the Creative Commons Attribution 4.0 International License (http://creativecommons.org/licenses/by/4.0/), which permits unrestricted use, distribution, and reproduction in any medium, provided you give appropriate credit to the original author(s) and the source, provide a link to the Creative Commons license, and indicate if changes were made. The Creative Commons Public Domain Dedication waiver (http://creativecommons.org/publicdomain/zero/1.0/) applies to the data made available in this article, unless otherwise stated.

Detection of hypermethylated DNA as cancer biomarkers is advantageous regarding the stable nature of DNA, ease of detection, and specificity of DNA hypermethylation for tumor cells [13]. Many known cancer-related genes like *RASSF1A*, *APC*, *BRCA1*, *GSTP1*, and *DAPK1* can be detected from serum or blood of breast cancer patients [14, 15]. Yet, there is still demand for novel diagnosis markers for detection of early breast cancer. In this study, we utilized microarray expression profiling of AZA-treated breast cancer (BC) and non-tumorigenic breast (NTB) cell lines, and identified *TAGLN* gene to be a frequently hypermethylated gene and a potential future biomarker in breast cancer.

Transgelin (TAGLN, SM22α) is an actin-binding protein that is abundantly expressed in smooth muscle cells (SMC) [16–19]. It is downregulated in transformed fibroblasts and several cancer cell lines and tissues [20–24]. *TAGLN* gene function has been associated with increased senescence in fibroblasts [25–27], and with increased apoptosis in glomerular epithelial cells and prostate cancer cells [28, 29]. TAGLN suppresses MMP9 [30], a known element of invasion [31], and therefore prevents the migration of colon and prostate cancer cells [32]. Controversially, it has also been found to be increased in gastric cancer and in lymph node (LN) metastasis of colon cancer [33, 34].

Here, we show that *TAGLN* is an epigenetically suppressed candidate epigenetic biomarker for diagnosis in breast cancer, by presenting its consistent downregulation of expression and frequent hypermethylation in breast carcinoma cell lines as well as in three independent breast tumor tissue cohorts. We also provide evidence that TAGLN decreases the proliferation potentials of BC and NTB cells. Better survival of breast cancer patients with higher expression or lower promoter methylation of *TAGLN*, in addition to competence of its promoter methylation levels to discriminate cancer from healthy tissue, emphasize a possible clinical impact for this gene in breast cancer.

Results

Changes in the transcriptome of breast cell lines upon AZA treatment

We treated the MCF7 and MDA-MB-231 BC cells and a NTB cell line MCF12A with AZA or corresponding DMSO controls before subjecting them to microarray analysis to identify new TSG targets for promoter DNA hypermethylation in breast cancer. Quality control analyses proved our data to be of high quality, and replicates of each experiment correlated well with each other (data not shown). Expressions of large groups of genes were altered upon AZA treatment by 1.5-fold and above, even at very stringent significance thresholds (Additional file 1 and Additional file 4: Table S1). A selection procedure was applied to identify the genes that are altered upon AZA treatment in MCF7 and MDA-MB-231 cells, but not in MCF 12A cells (Additional file 2 and Fig. 1a). Gene lists, generated using this procedure, were used for further analyses (Additional file 3). Probe sets commonly or differentially altered in MCF7 and MDA-MB-231 cell lines were also determined (Fig. 1b). We found that 17 and 22 % of the probe sets induced in MCF7 or MDA-MB-231 cells, respectively, were induced in common while the remaining genes were cell-line specific.

Functional annotation and clustering of significantly altered genes in either the MCF7 or MDA-MB-231 cell lines were analyzed using the DAVID Functional Analysis Tool (Fig. 1c, d) [35, 36]. Pathways mainly involved in mitosis and cell cycle were significantly enriched among the downregulated genes in both of the cell lines. Pathways related to cell communication and motility, signal transduction, cell proliferation, and apoptosis regulation were significantly enriched among the AZA-induced genes in MCF7 (Fig. 1c) while regulation of gene expression was highlighted in addition to these pathways in MDA-MB-231 cells (Fig. 1d).

Paired *t* tests between seven AZA-treated and untreated BC cell lines of a publicly available independent dataset (GSE20713 [37]) revealed that 53.5 % of the probe sets that were significantly upregulated upon AZA treatment in both MCF7 and MDA-MB-231 cells in our experimental setup were also significantly upregulated in the AZA-treated BC cell lines of this independent study ($P < 0.05$, Additional file 4: Table S2).

Probe set lists were screened for the presence of CpG islands in the proximity of their promoter regions, and the induction in expression levels of several genes were validated by qRT-PCR among the genes with proximal CpG islands. *TAGLN* emerged as a strong candidate gene among a large number of genes, as it was commonly and significantly upregulated upon AZA treatment in both MCF7 (by 27.3-fold) and MDA-MB-231 (by 1.77-fold) cell lines (Additional file 3), and our bioinformatics analyses showed that *TAGLN* expression was significantly downregulated (>2-fold, $P < 0.05$) in breast tumor tissues of 8 out of 13 (62 %) breast cancer datasets included in Oncomine database [38] (Additional file 4: Table S3). Moreover, *TAGLN* promoter region was previously shown to be responsive to hypermethylation in smooth muscle cells [39]. Based on these findings, we selected this gene for further analyses.

TAGLN gene expression and promoter methylation analyses in breast carcinoma cell lines

TAGLN gene expression was analyzed with qRT-PCR and found to be significantly downregulated in 15 different breast carcinoma cell lines compared to the non-tumorigenic cell lines ($P = 0.0034$, Fig. 2a). The expression

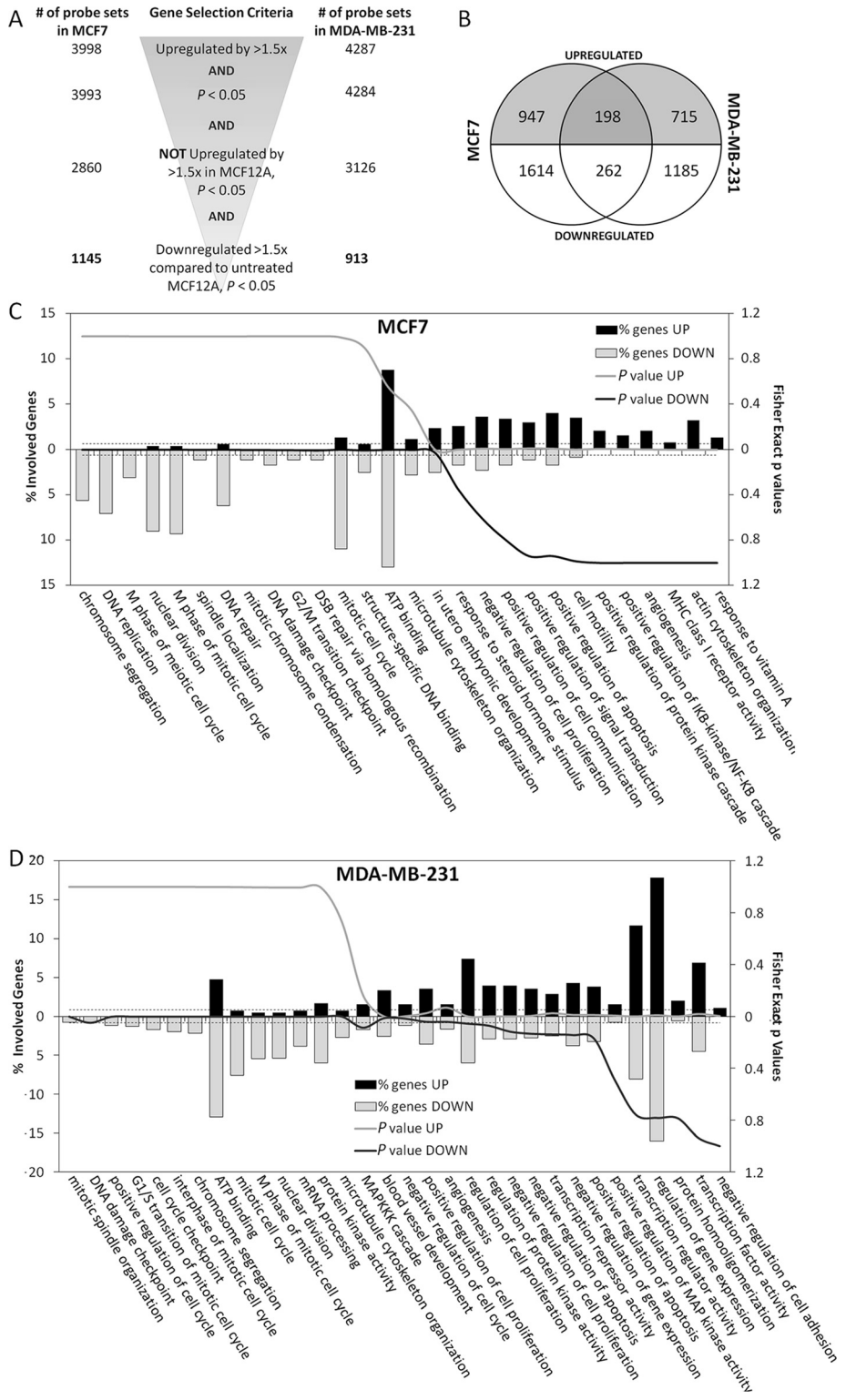

Fig. 1 Analyses of AZA affected genes in BC cell lines. **a** The outline of the gene selection process. The numbers on the *left* and *right* represent the probe sets obtained after the filtering process for gene selection in MCF7 and MDA-MB-231 cell lines, respectively. **b** Number of probe sets significantly up/downregulated by AZA treatment, determined by the selection process given in (**a**). **c**, **d** DAVID analyses of Pathways affected upon AZA treatment in MCF7 cells (**c**) and MDA-MB 231 cells (**d**). *Bars* represent the percentage of up- and downregulated genes involved in the indicated pathways while the lines represent the *P* values for enrichment. *Dashed lines* indicate $P = 0.05$ thresholds

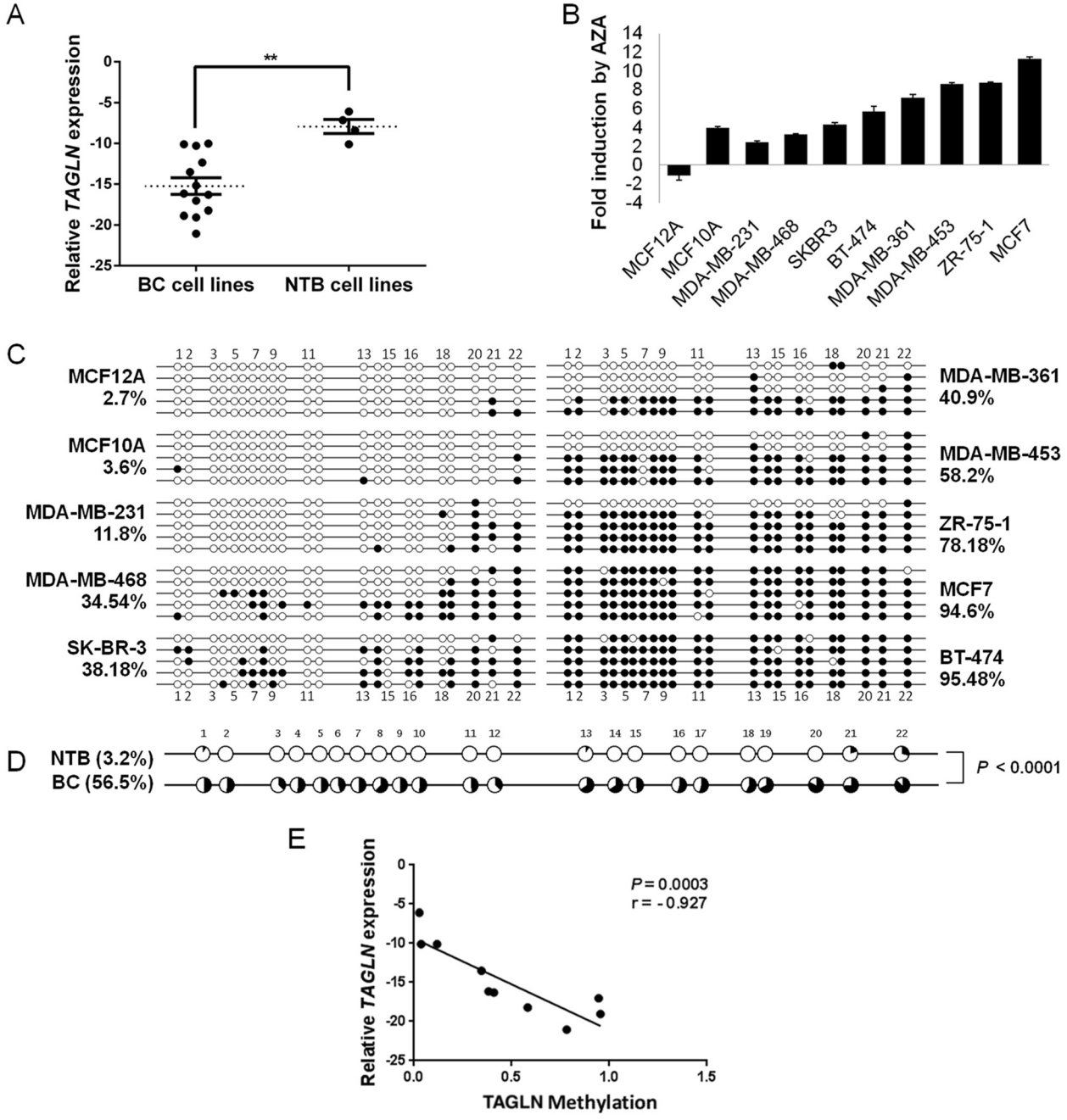

Fig. 2 Expression and promoter methylation analyses of *TAGLN* gene in BC cell lines. **a** Box-plot analysis based on qRT-PCR results showing strong downregulation of *TAGLN* expression in BC cell lines compared to NTB cell lines. Log_2 expression levels relative to *GAPDH* reference gene are shown. *Horizontal dashed lines* represent median values. *Error bars*: standard error of means (SEM). $^{**}P < 0.01$; Mann–Whitney Test. **b** qRT-PCR analysis of AZA-treated BC and NTB cell lines indicating high levels of induction in *TAGLN* expression levels. Values represent the log_2 ratios of expression levels in AZA-treated cell lines to those in their DMSO-treated cells. **c** QUMA software analyses based on bisulfite sequencing of BC and NTB cell lines showing hypermethylation in *TAGLN* promoter in BC cells. Percent values represent the average methylation of 5 clones for each cell line. *Full circles*: methylated; *Empty circles*: unmethylated. Sequence numbers of CpGs are shown *above circles*. **d** QUMA analysis showing significantly higher methylation in BC cells compared to NTB; Mann–Whitney test. Methylated DNA ratio: *black area*; unmethylated ratio: *white area* in the pie chart. **e** Scatter plot showing the spearman correlation of *TAGLN* methylation status with log_2(expression) levels in BC and NTB cell lines

of *TAGLN* was restored in all analyzed cell lines upon AZA treatment, except for NTB cell line MCF12A (Fig. 2b). Expression levels of *TAGLN* were concordant in microarray and qRT-PCR experiments, when fold induction levels upon AZA treatment were compared in MCF7, MDA-MB-231, and MCF12A cell lines.

Bisulfite sequencing of *TAGLN* promoter region was used to characterize *TAGLN* methylation status in eight BC and two NTB cell lines (Fig. 2c). The analyzed promoter region was significantly hypermethylated in majority of BC cell lines (with an average of 56.5 % methylation) compared to the NTB cell lines (with an average of 3.2 % methylation; $P < 0.0001$, Fig. 2d). Moreover, mRNA expression and methylation levels of *TAGLN* were significantly and negatively correlated (Spearman $r = -0.927$, $P = 0.0003$, Fig. 2e) suggesting that the expression of *TAGLN* was downregulated by promoter DNA methylation in BC cell lines.

TAGLN is downregulated by promoter hypermethylation in human breast tumor tissues

To profile the expression and methylation status of *TAGLN* in breast tumor tissues, *TAGLN* mRNA expression and promoter methylation levels were determined in 21 breast tumor samples and their pair-matched normal tissues (Table 1). The expression of *TAGLN* was found to be significantly downregulated in tumors compared to matched normal breast tissues by qRT-PCR (19/21 tumors, 90.5 %, $P < 0.0001$, Fig. 3a). The average relative expression (ARE) ± standard error of means (SEM) was 0.476 ± 0.1520 for normal tissues while it was 0.146 ± 0.0511 for tumor tissues, with an average decrease in *TAGLN* expression of 3.255-fold in breast tumor tissues.

Table 1 Pathological features of normal matched breast tumor tissues

Patient code	Lymph node	Grade	Stage	ER status	PR status	Her2 status
#003	1	1	N/A	1	1	0
#043	0	2	N/A	1	1	1
#044	1	2	2B	0	1	1
#047	1	2	4	1	0	1
#055	0	2	N/A	1	1	1
#057	0	N/A	2B	0	0	0
#073	1	2	N/A	1	0	1
#076	1	3	2A	0	0	1
#082	0	1	2B	1	0	1
#083	1	2	2B	1	0	1
#084	1	3	N/A	0	0	0
#085	0	2	2A	0	1	1
#090	1	2	2B	1	1	1
#096	0	1	2A	0	1	0
#113	1	1	3B	1	0	1
#124	1	1	2A	1	0	1
#137	1	N/A	3A	1	1	N/A
#133	N/A	N/A	N/A	N/A	N/A	N/A
#161	1	2	2A	1	0	0
#164	0	2	2B	1	1	0
#168	1	2	2B	0	1	1

ER estrogen receptor, *PR* progesterone receptor, *Her2* Erbb2 receptor amplification, *N/A* information regarding the pathological feature is missing, *1* positive for the given condition, *0* negative for the given condition

The promoter methylation status of *TAGLN* was analyzed via the bisulfite sequencing method, and the examined region was found to be significantly hypermethylated in 13 (61.9 %) tumors ($P < 0.05$, Fig. 3b, Table 2) compared to matched normal tissues; hypermethylation was consistent across all grades (Table 2). The overall methylation levels were also significantly higher in tumor tissues in comparison with normals ($P = 0.0263$, Fig. 3c). *TAGLN* mRNA expression and the promoter methylation ratios were significantly and negatively correlated in breast tissues (Spearman $r = -0.31$, $P = 0.044$, Fig. 3d) as in BC cell lines, suggesting that *TAGLN* transcription could be regulated by DNA methylation. We used *ANLN* (Anillin) gene expression, a poor prognosis and high cellular proliferation marker in breast cancer patients [40], to better infer proliferative capacity and prognostic status of the tumors. Expression of *TAGLN* was negatively (Spearman $r = -0.44$, $P = 0.0039$) and the promoter methylation of *TAGLN* was positively (Spearman $r = 0.48$, $P = 0.0011$) correlated with mRNA expression of *ANLN* gene (Fig. 3e, f). This shows that *TAGLN* is likely to be downregulated more by promoter DNA hypermethylation in breast tumors with worse prognosis. When the tumors' pathological features were analyzed, promoter methylation, but not expression, of *TAGLN* was significantly decreased in LN negative tumors when compared with LN positives ($P = 0.0476$, Additional file 5: Figure S1A-B) while both expression and methylation levels did not exhibit any significant difference between grades, stages, and hormone statuses in our tumor-normal matched breast tissue panel.

To increase our sample size and extend our DNA methylation analyses to a larger panel with clinical and long-term outcome data, we downloaded the publicly available methylation data of two independent microarray datasets (Super-series: GSE201713 [37], $n = 247$ and GSE31979 [41], $n = 124$), whose distributions for methylation scores were similar, and used the normalized average methylation scores (NAMS) of two probes corresponding to *TAGLN* gene. In support of our results, *TAGLN* probes were significantly hypermethylated in breast tumors (NAMS ± SEM = 72.88 ± 0.9137, $n = 338$) compared to normal tissues (NAMS ± SEM = 42.49 ± 1.541, $n = 33$, $P < 0.0001$, Fig. 4a), even though the CpG dinucleotides corresponding to the probes were not covered by our bisulfite primers. 83 % of the tumors displayed higher methylation scores than the highest score observed in the normal cohort. The average

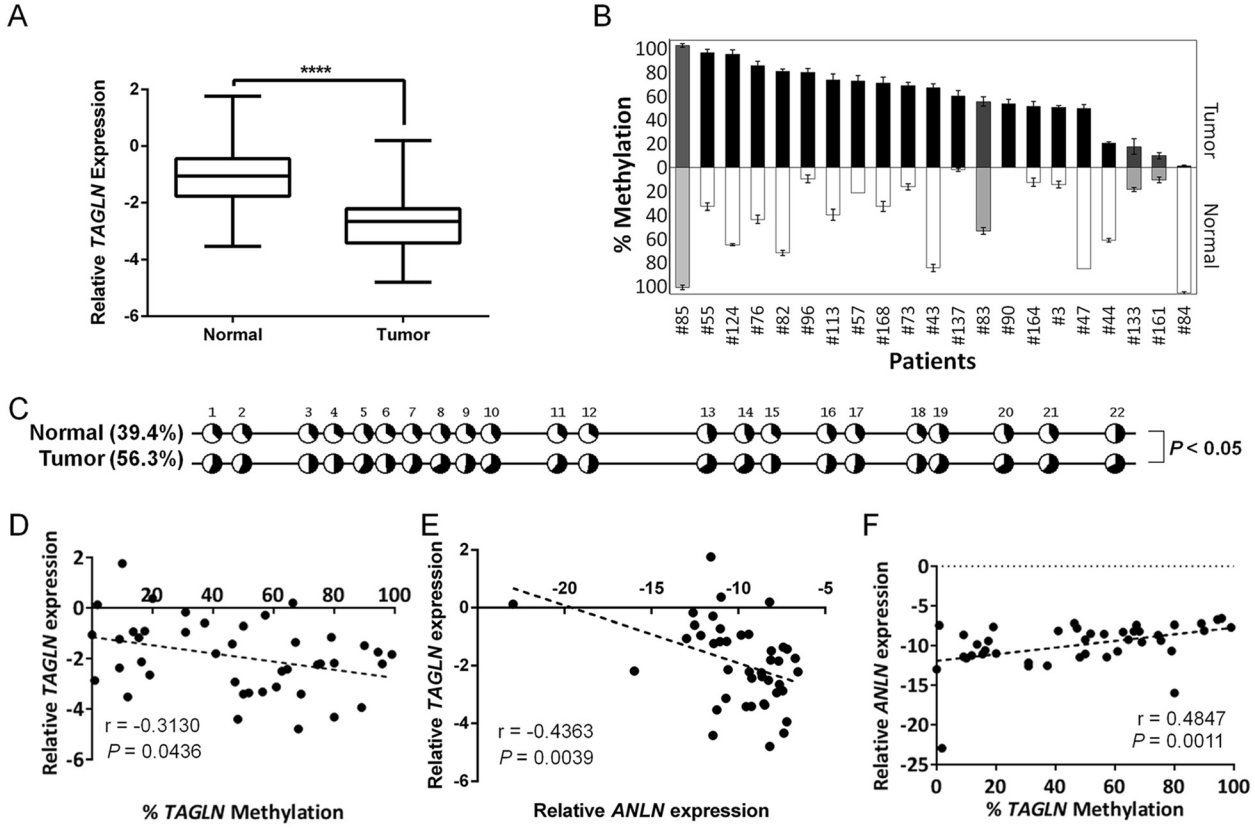

Fig. 3 Expression and promoter methylation analyses of *TAGLN* gene in normal matched tumor tissues. **a** Box-plot analysis showing strong downregulation in average *TAGLN* expression in tumor tissues compared to matched normal tissues. Log_2 expression levels relative to geometric means of *ACTB* and *SDHA* reference genes were determined by qRT-PCR. ****$P < 0.0001$, Wilcoxon signed rank test. **b** Comparative bar charts of bisulfite sequencing based percent methylation scores of matched tumor and normal pairs showing significance hypermethylation in majority of tumors. Methylation percentages represent the average of five clones for each tissue. *Black-white bar* pairs represent significant ($P < 0.05$) differences between tumor and normal tissues (Wilcoxon signed rank test). *Error bars* represent SEM values. **c** Overall average methylation levels based on QUMA were significantly higher in breast tumors compared to normal tissues; Wilcoxon signed rank test. Methylated DNA ratio; *black area* and unmethylated; *white area* in the pie chart. **d–f** Scatter plots show correlations between relative *TAGLN* expression levels and methylation status of *TAGLN* promoter in tumor and normal tissues; Spearman $r = -0.3130$, $P = 0.0436$ **d**; relative *TAGLN* and *ANLN* expressions; Spearman $r = -0.4363$; $P = 0.0039$ **e**; and relative *ANLN* expression and *TAGLN* methylation; Spearman $r = 0.4847$, $P = 0.0011$ **f**. All expression values are log_2. The correlations were robust to outliers

Table 2 Frequency of *TAGLN* hypermethylation in tumor and normal breast tissues

Study	Analyzed CpGs	Cohort	Hypermethylated[c]	Hypomethylated[d]
Matched tumor tissue panel (bisulfite sequencing)[a]	−290 to +117	All patients ($n = 21$)	13 (61.90 %)	4 (19.05 %)
	22 CpGs	Grade 1 ($n = 5$)	5 (100.00 %)	0 (0.00 %)
		Grade 2 ($n = 11$)	6 (54.55 %)	3 (27.27 %)
		Grade 3 ($n = 2$)	1 (50.00 %)	1 (50.00 %)
GSE20713 Methylation data (microarray analysis)[b]	−571 and 455	All patients ($n = 338$)	213 (63.02 %)	3 (0.89 %)
	2 CpGs	Grade 1 ($n = 64$)	41 (64.06 %)	0 (0.00 %)
		Grade 2 ($n = 57$)	35 (61.40 %)	1 (1.75 %)
		Grade 3 ($n = 215$)	135 (62.79 %)	2 (0.01 %)

[a]Number of tumors were calculated based on average methylation ratio of 22 CpGs in our normal matched tumor tissues
[b]Number of tumors were calculated based on average methylation scores of two probes corresponding to two CpGs at given locations
[c]Number of tumors that are significantly hypermethylated in normal matched tumor tissue panel ($P < 0.05$, Wilcoxon signed rank test). In microarray methylation data, tumors with normalized average methylation score (NAMS) >30 higher than the average normal tissue NAMS were considered hypermethylated
[d]Number of tumors that are significantly hypomethylated in normal matched tumor tissue panel ($P < 0.05$, Wilcoxon signed rank test). In microarray methylation data, tumors with NAMS >30 lower than the average normal tissue NAMS were considered hypomethylated

difference between the methylation scores of the tumor and normal tissues was 30.38; thus, the tumors with methylation scores that were >30 higher than the average value for normal tissues were considered as hypermethylated. Accordingly, 63.02 % of the tumors displayed hypermethylation of *TAGLN* probes in this data set (Table 2). When grouped into tumor grades, these ratios were at least 61.40 % for each group (Table 2). Available expression data (GSE20711; $n = 90$) of the same patients were significantly and negatively correlated with *TAGLN* methylation scores (Spearman $r = -0.5442$, $P < 0.0001$, Fig. 4b). This correlation was preserved in each grade and pathological subtype tested except for Luminal B (LumB) tumors, which are known for their hypermethylator phenotypes [42] (data not shown). Receiver-operator characteristics (ROC) analyses of *TAGLN* promoter methylation showed that a threshold of NAMS >60.94, which was derived from the ROC analysis itself, could discriminate healthy individuals from breast cancer patients, with 83.14 % sensitivity and 100 % specificity (area under the curve (AUC) = 0.9289, and 95 % confidence interval (CI): 0.9027 to 0.9552, $P < 0.0001$, Fig. 4c). Moreover, 10-year relapse-free survival (RFS) of patients was significantly decreased with higher tumor methylation of the *TAGLN* probes compared to the patients with lower levels of methylation ($P = 0.0059$, Fig. 4d). NAMSs of the *TAGLN* probes were compared for different pathological features of breast cancer, and *TAGLN* methylation states were similar, independent of grade, Her2, and ER states, and sizes of the tumors.

TAGLN mRNA and protein is downregulated in independent sets of breast tumor tissues

To confirm downregulation of *TAGLN* in both protein and mRNA levels in other independent breast tumor tissue panels of larger sample sizes with pathological information, expression of *TAGLN* was examined in a breast cancer tissue array by IHC staining (BioChain, Cat.No:Z7020005), and in an independent cDNA panel by qRT-PCR (OriGene, Cat.No:BCRT101). Both protein ($P = 0.0116$) and mRNA expression levels ($P = 0.0072$) of *TAGLN* were significantly downregulated in breast tumors in comparison to non-tumor tissues (Fig. 5a, b). Average of relative mRNA expression, $ARE_{(mRNA)} \pm SEM$ was 0.4248 ± 0.0792 in normal tissues ($n = 7$) and 0.1858 ± 0.0387 in tumor tissues ($n = 41$). Average histochemical score H-score ± SEM was 243.6 ± 25.35 in normal tissues ($n = 7$), with extensive staining in myoepithelial cells (Fig. 5a), and was 169.8 ± 9.773 in tumor tissues ($n = 67$). In both the tissue and cDNA arrays, *TAGLN* expression was downregulated in grade 3 tumors when compared to grade 1 and 2 tumors

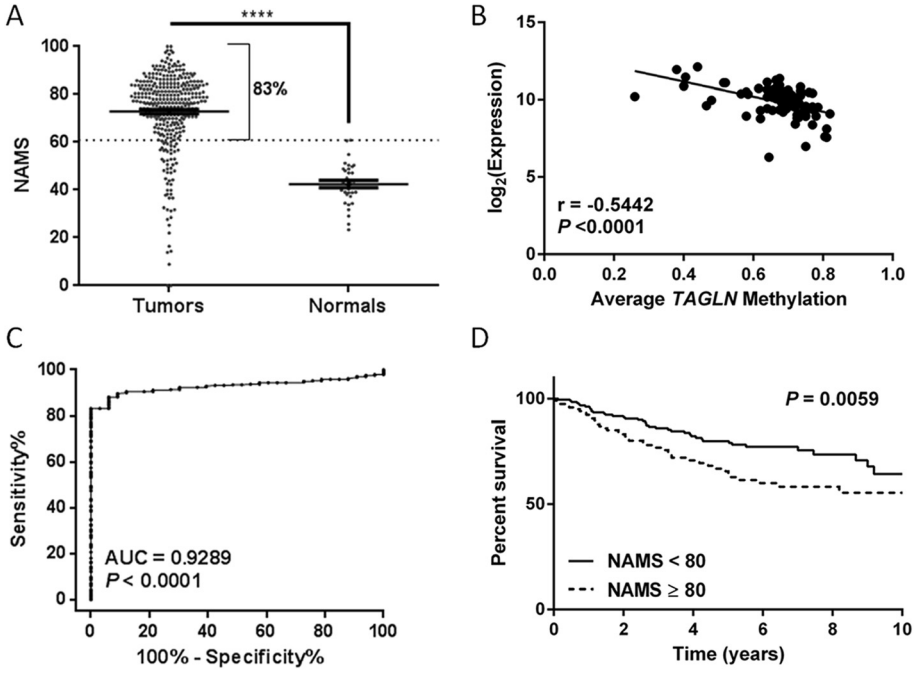

Fig. 4 Methylation status of *TAGLN* in public datasets GSE20713 and GSE31979. **a** Graphs showing higher normalized average methylation scores (NAMS) for two probes of *TAGLN* in tumor tissues Mann–Whitney test, ****$P < 0.0001$. *Horizontal lines*: mean ± SEM. **b** Scatter plot showing correlation of average methylation scores of *TAGLN* probes (GSE20713) to average expression (log_2) of *TAGLN* probe sets (GSE20711); Spearman $r = -0.5442$, $P < 0.0001$. **c** ROC analyses for discrimination between healthy individuals and breast cancer patients, using *TAGLN* NAMSs. **d** Kaplan-Meier (KM) survival analysis showing higher RFS percentages for patients with tumor *TAGLN* NAMSs ≤80 (best cutoff among tested)

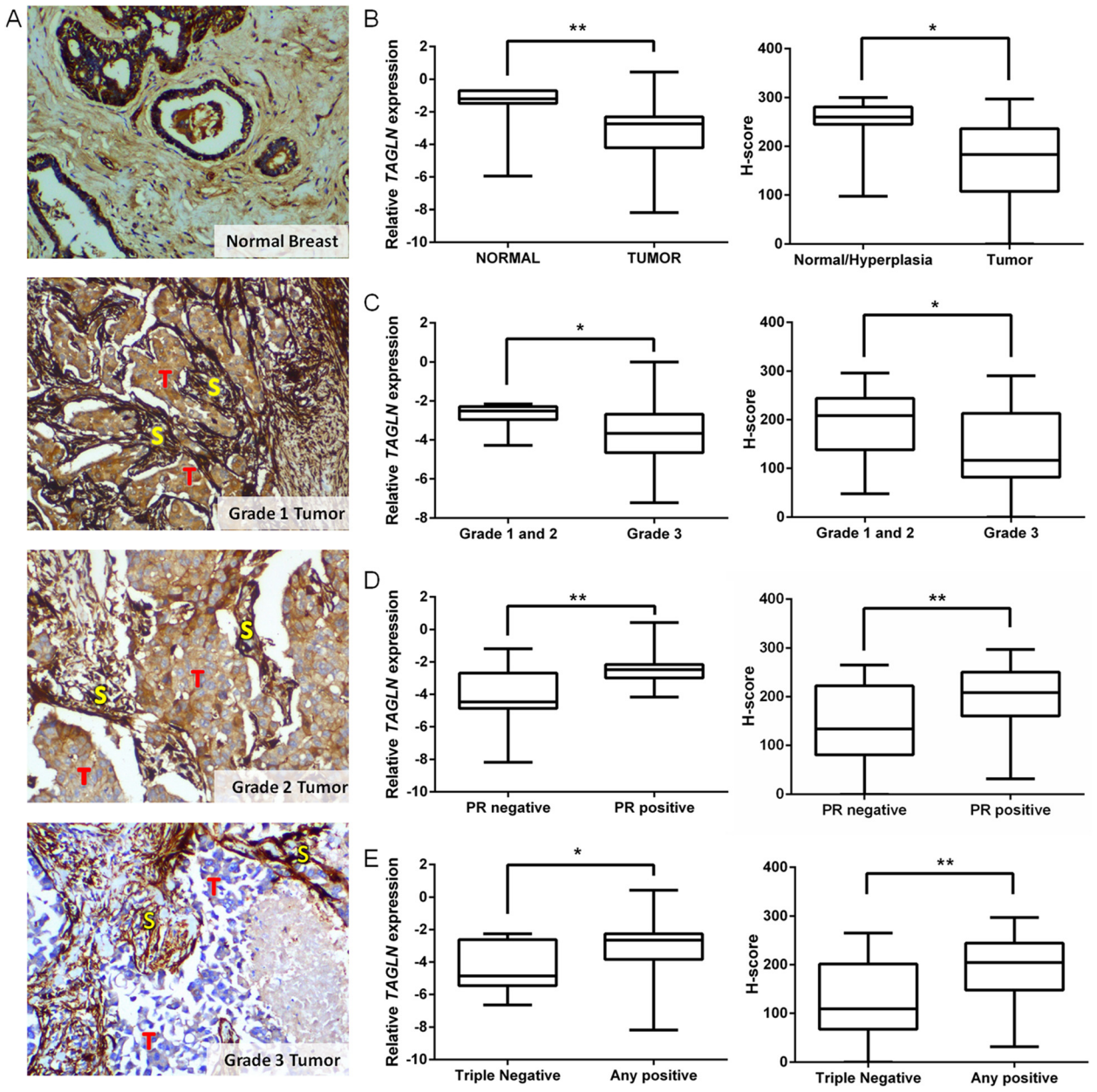

Fig. 5 *TAGLN* expression in independent sets of tumor and normal breast tissues. **a** Examples of IHC staining of TAGLN in normal and tumor tissues. T (*red*), tumor tissue; S (*yellow*), stroma, ×100 magnification. **b–e** Box-plot analyses showing significant downregulation of *TAGLN* mRNA (*left*) and protein (*right*) expression levels in tumors compared to normal breast tissues (**b**); in grade 3 compared to grade 1 and 2 tumors (**c**); progesterone receptor (PR) negative compared to positive subtypes (**d**); and in triple negative compared to any hormone receptor positive (ER and/or PR and/or Her2 positive, Any positive) tumors (**e**). *Horizontal lines*: maximum, median, and minimum values. *Left panels*: qRT-PCR analysis of *TAGLN* mRNA expression levels (log_2 transformed) in a cDNA array ($n = 7$ normal, $n = 41$ tumor tissues) relative to geometric means of *ACTB* and *SDHA* mRNA reference genes. *Right panels*: IHC staining of TAGLN protein in a tissue array ($n = 67$ tumor, $n = 7$ normal tissues). H-score method was used for staining intensity calculation. *$P < 0.05$, **$P < 0.01$, Mann–Whitney Test

($P = 0.049$ and $P = 0.0329$, respectively, Fig. 5c), upregulated in progesterone receptor PR (+) tumors ($P = 0.0031$ and $P = 0.0043$, respectively, Fig. 5d) and in any hormone receptor positive tumors with respect to triple negative tumor types ($P = 0.0063$ and $P = 0.0489$, respectively, Fig. 5e). *TAGLN* expression levels were not significantly different in estrogen receptor (ER) or human epidermal growth factor receptor 2 (Her2) positive or negative tumors or in different stage groups.

The tissue panels used in this study did not have enough information about patient survival data. KM plotter [43], which uses public microarray expression data for survival

analyses, was used to test the effect of *TAGLN* expression on OS or RFS of breast cancer patients (Additional file 5: Figure S2). There was no significant difference between either OS or RFS of the patients based on their tumor expression levels of *TAGLN* when all patient cohorts were analyzed (Additional file 5: Figure S2A). However, when the patients were grouped for tumor grades, higher expression of *TAGLN* was associated with increased OS and RFS probabilities in patients with grade 1 and 2 tumors (Additional file 5: Figure S2B). In grade 3 tumors, the differences were not significant.

TAGLN decreases colony formation potentials of breast carcinoma cell lines

Since *TAGLN* was frequently hypermethylated and consistently downregulated in both the BC cell lines and three independent panels of tumor tissues, we analyzed the functional role of TAGLN in BC and NTB cells. *TAGLN* gene was silenced in MCF10A and MCF12A cells with abundant expression (Fig. 6a–c), and was overexpressed it in MDA-MB-361 and MDA-MB-157 BC cell lines (Fig. 6d, e) that expressed *TAGLN* at zero to intermediate levels, respectively (Fig. 6a). 2D colony formation assays were performed to test the effect of TAGLN on proliferation potentials of these cells. Compared to control siRNA (siCTRL), si*TAGLN* transfected MCF10A and MCF12A cells formed significantly ($P = 0.0013$ and $P = 0.0016$, respectively) higher number of colonies (Fig. 6b, c, middle and lower panels). Colony formation capabilities of MDA-MB-361 cells, but not MDA-MB-157 cells, were significantly impaired when they overexpressed TAGLN protein (Fig. 6d, middle and lower panels and Fig. 6e, right panel). To examine possible effects of TAGLN on migration and invasion potentials of BC cells, we performed *in vitro* wound healing and Matrigel invasion assays in normally motile MDA-MB-157 cells; however, *TAGLN* overexpression in these cells did not affect either wound closure or Matrigel invasion capacities of these cells (Additional file 5: Figure S3).

Discussion

The combination of high-throughput expression profiling technology and treatment of cells with various DNA methylation inhibitors has been widely used to discover genome-wide effects of these drugs or to identify specific genes involved in the related pathways. Here, we used the same technology and identified *TAGLN* as an important candidate biomarker, frequently downregulated by promoter hypermethylation in breast cancer. A recent study (GEO ID: GSE22250) also used this method in breast cancer [37], in which multiple breast cancer cell lines without biological replicates were exposed to 1 μM AZA. About half of the probe sets commonly upregulated in BC cells by AZA treatment in our setup were also upregulated ($P < 0.05$) in the AZA-treated BC cell lines in the aforementioned study, although they used a lower dose (1 μM) of AZA. This indicates a potential dose dependency of AZA treatment such that some of the genes may require higher concentration of AZA to be induced. However, we determined *TAGLN* to be upregulated by 2.38-fold (average of two probe sets, $P < 0.05$, paired t test) also in GSE22250 study, yet this was not reported by the authors.

The pathway analyses of 5 μM AZA-induced genes revealed that the most significantly enriched pathways in MCF7 cells were the cell motility, angiogenesis, cytoskeleton, and cell communication pathways, which could have been suppressed in these non-motile cells under normal conditions by DNA methylation. Yet, motility-associated genes in invasive and motile MDA-MB-231 cells might have already been active even before the AZA treatment, so only gene expression and protein kinase regulation pathways were enriched upon AZA treatment. Commonly induced pathways in both cell lines were those relatively known as characteristics of the AZA effect on cancer cell lines [44–47], while commonly downregulated pathways mostly consisted of the cell cycle, cell division and metabolism-related pathways, potentially resulting in cessation of cell growth and proliferation when deactivated, enabling AZA's anti-cancer effect. Yet, most of these downregulated genes could be possibly repressed due to secondary effects of AZA treatment, as it caused induction of several transcription regulatory genes.

The promoter region of *TAGLN*, one of the strongest candidate genes among many probe sets, was previously found to be methylated in hepatocellular carcinoma and normal hepatocytes [48] and was hypermethylated in colorectal carcinoma [49]. Using a luciferase reporter gene construct containing the 5′-flanking region of *TAGLN* promoter, and *in vitro* methylation of the CpG dinucleotides within this region, Yamamura et al. [39] showed that the transcriptional activity of *TAGLN* promoter could indeed be controlled by DNA methylation in smooth muscle cells. However, transcriptional regulation of this gene in breast cancer has never been studied before.

Our study is the first to document the regulation of *TAGLN* gene expression by promoter hypermethylation in both breast carcinoma cell lines and normal matched tumor breast tissues, as well as in tumor tissues of large set of publicly available data by means of bioinformatics analyses. Frequent hypermethylation of the *TAGLN* promoter region, in breast cancer even at low-grade tumors, is comparable to the hypermethylation frequencies of known TSGs in breast and other types of tumors [50]. High frequency of DNA hypermethylation of certain

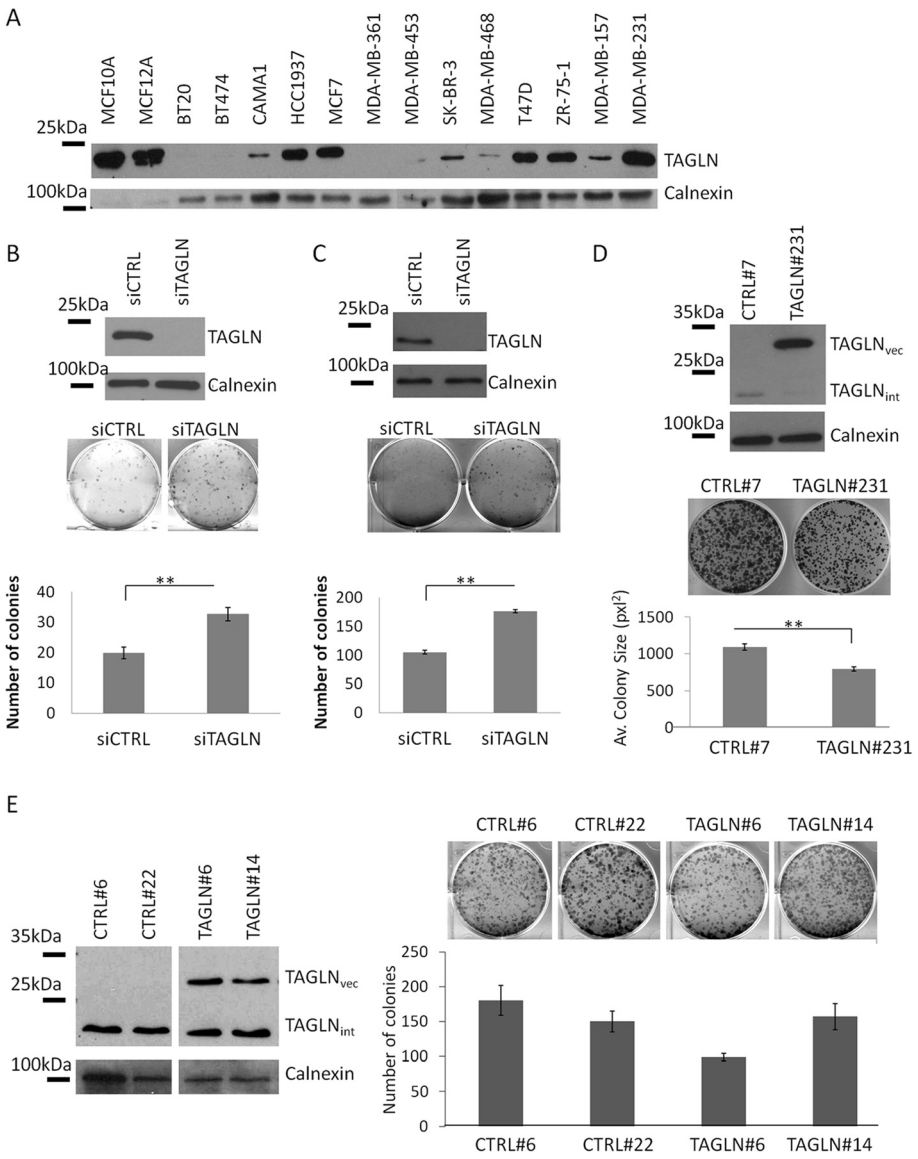

Fig. 6 Effect of *TAGLN* overexpression and silencing on breast cell lines. **a** Western blot analysis of TAGLN in breast carcinoma and non-tumorigenic breast cell lines. **b–c** Western blot shows *TAGLN* silencing in MCF10A (**b**) and MCF12A (**c**) cells (*upper panels*). 2D colony formation assays (*middle* and *lower panels*) show increased colony formation in *TAGLN* silenced (si*TAGLN*) MCF10A (**b**) and MCF12A (**c**) cells compared to controls (siCTRL). **d–e** Western blot analyses of *TAGLN* overexpression and subsequent colony formation assays in MDA-MB-361 (**d**, *upper panel*), and MDA-MB-157 (**e**, *left panel*) cell clones. Overexpression of ectopic TAGLN ($TAGLN_{vec}$) and levels of endogenous TAGLN ($TAGLN_{int}$) were determined with TAGLN specific antibody in clones. *TAGLN* overexpression caused higher cell proliferation in MDA-MB-361 cells (**e**), while did not affect MDA-MB-157 cells (**f**). Each assay was conducted at least in quadruplicates. Two sample *t* test was used for comparisons. *Error bars* represent standard errors. $^{**}P < 0.01$

genes enables detection of circulating cell-free tumor DNA from easily accessible and noninvasive sites, like serum or plasma, of cancer patients, with quick and sensitive techniques such as methylation-specific PCR (MSP) [14, 15, 51]. Even though it is possible to detect and analyze hypermethylated genes from the fine needle aspirates, nipple aspirates, and ductal lavage for breast cancer patients [52–54], diagnosis from serum or plasma is more patient friendly and noninvasive and can be easily repeated during the follow-up period. Thus, pursuit for blood-based tests for diagnosis of breast cancer has been an ever expanding research area [12, 55]. The most common biomarker candidates for detection of breast cancer from serum is *RASSF1A* gene, with 100 % specificity and 75 % sensitivity [56], and *RARβ* with 94 % specificity and 87 % sensitivity [57]. Based on the high frequency of hypermethylation in breast cancer patients compared to healthy tissues, *TAGLN* promoter methylation levels can be used as an epigenetic based biomarker for diagnosis, either alone or together with other frequent

markers. Indeed, the results of our ROC analyses with high sensitivity and specificity values, point out *TAGLN* gene methylation as a good candidate for a tumor marker, with 83.14 % sensitivity and 100 % specificity. These ratios are similar to the ones obtained by combining the scores of more than one gene for detection of breast cancer (reviewed in Kristiansen 2013 [12]), and could increase their competence when included in these panels. The power of *TAGLN* promoter hypermethylation as an epigenetic diagnosis biomarker seems promising and should be validated for detection of tumor DNA from serum, plasma, or nipple and ductal fluids in a large, prospective screening study.

TAGLN methylation states also relate to the prognosis of breast cancer, as *TAGLN* promoter methylation levels were negatively correlated with cellular proliferation and worse prognosis marker *ANLN* expression in our tumor-normal matched tissue panel [40]. Moreover, the probability of 10-year RFS of patients was greater with lower *TAGLN* methylation scores, independent of grade, stage, and other prognostic factors. These outcomes indicate that hypermethylation of *TAGLN* promoter can also be used as a prognostic marker. Larger cohorts of patients with matched breast cancer and adjacent normal tissues, and available survival information should be used to validate these findings with bisulfite sequencing or other sensitive techniques like MSP.

TAGLN expression was previously found to be downregulated in several types of cancer and transformed cells [18, 20–22, 24]. However, studies on breast cancer were limited to a small number of cell lines and tissues, all of which were ductal carcinoma in situ. In this study, we showed strong and consistent downregulation of *TAGLN* mRNA and protein expression in three independent sets of breast tumor tissues compared to non-tumor tissues (total number of samples $n = 130$ tumors and $n = 35$ normal tissues). Furthermore, this is the first time an association between *TAGLN* expression and breast cancer prognosis is suggested by independent findings: (1) negative correlation of *TAGLN* expression with poor prognosis marker *ANLN* [40]; (2) decreased *TAGLN* expression particularly in triple negative breast cancer in addition to all molecular subtypes of breast cancer tissues; and (3) longer 10-year OS and RFS of low-grade breast cancer patients with higher *TAGLN* expression.

TAGLN is usually known as a mesenchymal protein [19], whose expression increases with epithelial to mesenchymal transition (EMT) [58–60]. In this study, we found that the expression of *TAGLN* was higher in grade 1 and 2 tumors compared to grade 3, suggesting that *TAGLN* expression could be decreased even more when the tumor progresses into a more undifferentiated state in breast cancer. This suggests that downregulation of *TAGLN* expression may not be related to the EMT state of breast tumors while its downregulation can be an important marker in breast tumor progression. Future studies with higher numbers of grade 2 and grade 3 tumor samples will help increase confidence in this regard.

Previous data on association of *TAGLN* with metastatic states of other tumor types are also controversial. While some studies negatively correlated *TAGLN* expression with lymph node status in colon [32] and prostate cancers [61], others found positive correlation in colorectal cancer [34]. Increased expression of *TAGLN* in metastatic nerve sheath tumors was also shown [62]. At least part of the discrepancies in the expression levels of *TAGLN* in different studies has been explained as a result of higher *TAGLN* expression in the tumor stroma of invasive tumors rather than the tumor tissue itself, which is revealed by subsequent IHC staining analyses [33, 63–65]. Accordingly, extensive staining of TAGLN in the tumor stroma was also found in our panel of breast tissues stained by IHC, while *TAGLN* gene expression was specifically downregulated in tumor tissues of all grades and pathological types, when compared to normal tissues.

While some studies suggest a TSG function for *TAGLN* due to downregulation in different types of tumors [22, 24, 32, 49, 60, 66, 67], others define tumor-promoting activities or overexpression in cancer [34, 68, 69]. Despite these contradictory functions suggested in different types of tumors, our findings support a possible tumor suppressive role of this protein in breast cancer. The observed anti-proliferative effect exerted by TAGLN on breast cells in our study can be caused by its close association with the actin cytoskeleton [17, 70], which has essential roles in several pathways in a cell (reviewed in Hall, 2009 [71]). *TAGLN* expression is known to directly affect actin cytoskeleton dynamics [60, 70, 72, 73]. In yeast, higher expression of *TAGLN* homolog Scp1 decreases actin dynamics, leading to increased permeability of mitochondria and release of reactive oxygen species (ROS), which in turn results in cell death [74]. Similar results have been reported in melanoma cells [75]. Likewise, *TAGLN* depletion in fibroblasts resulted in disrupted actin organization and lower levels of ROS [60]. Thus, lower *TAGLN* expression observed in breast tumors and cell lines can support tumor development or cell proliferation by means of decreased ROS production resulting in longevity, or other mechanisms and pathways involved, which should be further tested in a comprehensive and focused functional study.

TAGLN is known to be involved in SMC migration via formation of podosomes and focal adhesions [73, 76, 77], as well as in lung fibrosis [78]. Controversially, its overexpression results in decreased cellular migration in colon cancer [32, 79]. We found that overexpression of *TAGLN*

in MDA-MB-157 cells did not cause any significant change in both the migration and invasion capabilities of these BC cells. It is possible that TAGLN acts differently in mesenchymal SMCs and in epithelial origin of cancer cells, as protein profiles might differ among different cell types, affecting the functions of individual proteins. Further studies are required to unravel possible protein partners of TAGLN in cells with different origins to explain the contradictory outcomes observed in different studies.

Conclusions

Our novel findings support the essential role of *TAGLN* gene in breast cancer pathogenesis, regarding its negative effect on cellular proliferation and its consistent downregulation in tumors. Based on substantially high methylation frequencies in breast cancer, further studies focusing on *TAGLN* promoter methylation as a diagnostic marker, combined with other biomarkers, should seriously be considered. These further studies with expanded breast cancer patient cohorts and bisulfite sequencing accompanied with expression analyses will determine whether *TAGLN* expression and/or methylation could also be used as a prognostic marker as well.

Methods

Cell culture and AZA treatment of breast cell lines

MCF7, MDA-MB-231, MDA-MB-453, MDA-MB-468, BT-20, BT-474, ZR-75-1, HCC1937, MDA-MB-361, MDA-MB-157, and MCF12A cell lines were purchased from American Type Culture Collection (ATCC). MCF10A cell line was kindly provided by Elif Erson Bensan, (METU, Ankara, Turkey). All cell lines were grown as recommended by ATCC. AZA (5 μM, Sigma-Aldrich, A3656) dissolved in DMSO (Applichem, A1584.0100) was used to treat cells for 96 h, and equivalent amount of DMSO was used as control treatment. Media was changed at every 24th hour, and cells were harvested at 96^{th} hour.

RNA isolation, determination of RNA quality and hybridization to microchips

RNA was isolated from the cell lines with Nucleospin RNA kit (Macherey-Nagel (MN), 740955.5), quantified with NanoDrop ND-1000 spectrophotometer (Thermo Scientific, USA) and the RNA integrity was determined with Agilent 2100 Bioanalyzer (Agilent Technologies, Germany) and all RNA samples had RNA integrity number (RIN) between 9.8–10. Hybridization of the processed RNA samples to the gene chips (HGU-133-Plus 2.0, Affymetrix, USA) were done following the standard Affymetrix protocol, in the Microarray Hybridization Facility, at Bilkent University (Ankara, Turkey).

Quality control and analysis of the microarray expression data

Data were scanned from the microchips with GCOS software (Affymetrix, USA). Raw data were normalized with justRMA method using BRB-ArrayTools 3.8.0-beta, developed by Dr. Richard Simon and the BRB-ArrayTools Development Team (NCI, USA). Quality control and further analyses were performed using BrB-ArrayTools. RNA degradation plots and 3′ to 5′ signal ratios for probe sets corresponding to *ACTB* and *GAPDH* mRNAs were calculated for quality control assessments. Class comparison tool, which uses random variance model of *t* test for small size samples, was used to find differentially expressed genes between treatment groups. Functional annotations were done using "Functional Annotation Chart" tool of DAVID Bioinformatics Resources 6.7 (NIH, USA).

CDNA synthesis and quantitative RT-PCR

cDNA was synthesized from 1 μg total RNA, using oligo-dT primers and RevertAid First Strand cDNA Synthesis Kit (Thermo Scientific, K1622) according to user's protocol. Specific primers for PCR amplification (available upon request) were designed using PrimerBlast of NCBI [80]. qRT-PCR experiments were performed in duplicates, using DyNAmo™ HS SYBR® Green qPCR Kit (Thermo Scientific, F-410 L). *GAPDH* as a reference gene was tested by calculating the significance of the $\log_2$ fold change of multiple probe sets represented in the array. Our results suggested that *GAPDH* was a reliable and stable reference gene in response to AZA treatment in MCF7, MDA-231, and MCF12A cell lines since no probe set exhibited fold change greater than 1.2 fold ($\log_2$ fold change: −0.28, FDR >0.1). Thus, *GAPDH* was used as an internal control gene in cell lines, and *ACTB* and *SDHA* geometric means were used [81] for internal control genes in tissue samples. Delta Ct method [82] was used for relative quantification of mRNAs, using the calculated efficiency values of each primer pair. Statistical significance of differences between groups was tested with Mann–Whitney test or Wilcoxon signed rank test (for paired data), using the $\log_2$ transformed expression values, using GraphPad Prism 6.0 (GraphPad Software Inc., USA).

DNA isolation, bisulfite treatment and sequencing

DNA was obtained using Nucleospin Tissue kit (Macherey-Nagel, 740952.5) as described in the user protocol. Bilsulfite treatment was carried out with 1 μg DNA, using Epitect Bisulfite Kit (Qiagen, 59104). CpG islands were detected and bisulfite sequencing primers for *TAGLN* gene were designed using the Methyl Primer Express® software (Applied Biosystems, USA). The primers amplified the region between −290 to +117 bp with respect to TSS (GenBank: NM_003186.3) (Left primer: 5′-GGGGTTAGAGAATAGTGAAGTAGGAGTA-3′; Right primer: 5′-

ACACTCACAAAACTTCCTCAAAACT-3′). Gel extraction was carried out with the QIAquick Gel extraction kit (Qiagen, 28704). Specific PCR products were cloned into pGEM-T-easy cloning vector (Promega, A1360) after which plasmid isolation of selected colonies (5 for each sample) was performed with the PureLink Quick Plasmid Miniprep Kit (Invitrogen, K210011) and sent for sequencing. Sequencing of the bisulfite-treated DNA inserts was performed with SP6 primers using the dideoxy chain termination method (by Iontek, Istanbul, Turkey). Bisulfite sequencing results were analyzed using QUMA software [83]. Statistical differences between breast cancer and NTB cell lines were tested with Mann–Whitney test. Statistical differences between methylation percentages of paired tissues were tested with Wilcoxon signed rank test, in GraphPad Prism 6.0.

Breast tumors and normal tissue samples

TAGLN expression in publicly available datasets was analyzed using Oncomine™ (Compendia Bioscience, USA). Primary breast tumors and their matched normal tissues (Table 1) were surgically removed from patients ($n = 21$), at Numune Training and Research Hospital, Ankara, Turkey. The use of the tissue material in this project was approved by the Ethics Committee and consents were obtained in accordance with the Helsinki Declaration of 1975. Tumor samples used in the study were composed >90 % of tumor cells, according to hematoxylin and eosin staining. RNA isolation from tissues was performed with Trizol (Life Technologies, 15596–026). Breast tumor cDNA array (OriGene, BCRT101) was composed of 41 tumor and 7 normal tissues. Breast tumor tissue array (BioChain, Z7020005) was composed of 7 non-tumor and 68 tumor tissues of breast.

IHC staining and scoring

Immunohistochemical studies were performed automatically in the Bond Max equipment (Leica Microsystems Inc.). Antigen retrieval steps were performed in Bond-Epitope Retrieval Solution 1 (Leica Microsystems, Germany) with TAGLN antibody (1:500, Abcam ab1416) at 100 °C. Detection was carried out with Bond Polymer Refine Red Detection kit (Leica Microsystems, DS9390). Stained slides were dehydrated and covered with mounting medium (Dako, CS70330) and cover-slips. Digital images of the slides were evaluated using the H-score method [84]. Statistical differences between groups were calculated with Mann–Whitney test while correlations were tested with Spearman correlation, in GraphPad Prism 6.0.

Survival analysis and analysis of publicly available methylation data

Survival analyses regarding the expression of *TAGLN* were performed using Kaplan-Meier (KM) plotter, breast cancer cohort [43]. Gene expression information of 205547_s_at probe set corresponding to *TAGLN* was used. Auto cutoff was used to generate the best performing KM curves. To perform methylation analyses, all the methylation data published under super-series GSE20713 (GSE20712 and GSE22249) and a separate dataset (GSE31979), whose data distributions were similar, were downloaded from GEO2R. Both of the studies were performed on GPL8490 Illumina HumanMethylation27 BeadChip arrays. One probe (cg24619694) corresponded to a CpG at +445 position from TSS of *TAGLN*, and the other probe (cg06950730) corresponded to a CpG at −561 position. Methylation scores of two probes were correlated (Spearman coefficient = 0.714, $P < 0.0001$). Thus, average methylation scores of the two probes were used for the calculations. The data were normalized by assigning 0 for the lowest average methylation scores for two probes of *TAGLN* gene, and assigning the value 100 for the highest scores for each dataset, and the scores in between are fit into a sigmoidal curve. Normalized methylation scores (NAMS) were used for the further studies. Mann–Whitney test was used to compare two groups. For correlation analyses, expression data (GSE20711) corresponding to 88 breast cancer patients and 2 healthy individuals included in the methylation study (GSE20713) was downloaded from GEO2R, and the Spearman's rank correlation between expression and methylation scores was calculated. For survival analyses using the NAMS values, a range of values greater than or equal to the diagnostic cutoff (i.e., 60, 65, 70, 75, 80, 85, and 90) was tested, and the best performing cutoff was determined to be NAMS >80 [85]. Patients were divided into NAMS ≥80 and NAMS <80 groups, and 10-year RFS were calculated for each group. *P* values were calculated using Gehan-Breslow-Wilocoxon test in GraphPad Prism 6.0.

Western blotting

Protein lysates (20–50 mg) from cell lines were separated under reducing conditions (5 % β-mercaptoethanol), in 12 % Tris-glycine gels and SDS-Tris-glycine running buffer and were blotted on nitrocellulose membranes. Membranes were incubated overnight at 4 °C, with primary antibodies (α-TAGLN, Abcam ab1416, 1:2,000; α-Calnexin, Abcam, 1:20,000), followed by washing with Tris buffered saline – Tween-20 (0.25 %, TBS-T) and secondary antibody (horse radish peroxidase-conjugated anti-rabbit IgG, Abcam 1:5,000) incubations for 1 h at room temperature. Signal detection was performed with ECL prime system (Amersham Life Science, RPN2232).

siRNA transfections and overexpression of *TAGLN* in breast cancer cells

siGENOME Human *TAGLN* siRNA (SMARTpool, Thermo Scientific, M-003714-02-0020) and siGENOME

Non-Targeting siRNA #2 (Thermo Scientific, D-001210-02-20) control siRNA transfections were performed with RNAi-max (Invitrogen, 13778150), using the reverse transcription protocol supplied by the producer. *TAGLN* overexpression, TrueORF-Gold pCMV6-Entry-*TAGLN* (Origene, RC215789), and control pCMV6-Entry vectors (Origene, PS100001) were transfected to MDA-MB-361 and MDA-MB-157 cells using Lipofectamine 2000 reagent (Invitrogen, 11668019). Stable clones were generated with Geneticin (Gibco-Life Technologies, 10131–035) selection.

2D colony formation assays

Cells were seeded to be 2.000/well in 6-well plates and were grown for 2 weeks (MDA-MB-157, MCF10A, and MCF12A) or for 4 weeks (MDA-MB-361). Colonies were then stained with 0.5 % crystal violet and counted using Image J (NIH). Colony sizes of MDA-MB-361 were calculated using Image J. Colony sizes of other cell lines could not be determined due to more scattered nature of colonies of these mesenchymal types of cells. Statistical differences were calculated with two sample *t* test in GraphPad Prism 6.0.

In vitro wound healing and Matrigel invasion assays

For *in vitro* wound healing assays, cells were plated to be confluent in 24-well plates. Next day, media was changed to low serum media (0.5 % FBS) and at least 6 independent scratches/sample were made with 200-μl pipette tips, and photos were taken after 24 h. Statistical differences between groups were tested with the Mann–Whitney test in GraphPad Prism 6.0. For Matrigel invasion assays, Growth Factor Reduced Matrigel Matrix Basement Membrane (BD, 356230) was diluted (1:5) and added to Transwell Permeable Support invasion chambers (Corning, 3422) in 24 wells to form a thin layer. Cells (150,000) per chamber were added to the upper chamber with 0.5 % serum containing media and the lower chamber was supplied with 10 % serum containing medium. Cells on the lower side of the chamber were stained with Giemsa and counted at the 48th hour.

Availability of supporting data

The data set supporting the results of this article is available in the Gene Expression Omnibus (GEO) repository, [GSE71363, http://www.ncbi.nlm.nih.gov/geo/query/acc.cgi?acc=GSE71363].

Additional files

Additional file 1: Expression changes upon AZA treatments. Probe IDs, gene names, and fold change ratios of the genes altered upon AZA treatment in each cell line at 1.5 fold and $P < 0.05$ have been listed. (XLSX 2886 kb)

Additional file 2: Expression in untreated breast cancer cell lines in comparison to MCF12A. Probe IDs, gene names, and relative expressions in breast cancer cell lines with respect to untreated MCF12A at 1.5 fold and $P < 0.05$ have been listed. (XLSX 11397 kb)

Additional file 3: Final gene lists altered upon AZA treatments only in breast cancer cell lines. Probe IDs, gene names, accession numbers and fold change ratios of the genes altered upon AZA treatment, in each breast cancer cell line at 1.5 fold and $P < 0.05$, and filtered as shown in Fig. 1A have been listed. (XLSX 387 kb)

Additional file 4: Tables not included in the main manuscript have been listed. Table S1. Number of probe sets affected by AZA treatment; **Table S2.** Comparison of significantly altered probe sets with the independent study GSE20713 Dataset; **Table S3.** Cancer vs. normal analysis of *TAGLN* mRNA in Oncomine database. (PDF 18 kb)

Additional file 5: Figure S1. *TAGLN* expression and methylation status, and lymph node metastasis of breast cancer; **Figure S2.** Univariate survival analysis of *TAGLN* microarray expression levels; **Figure S3.** Effect of *TAGLN* over-expression on migration and invasion of MDA-MB-157 cells. (PDF 1151 kb)

Abbreviations

ANLN: Anillin; ARE: average relative expression; AZA: 5-aza-2′-deoxycytidine, Decitabine; BC: breast carcinoma; DMSO: dimethyl sulfoxide; LN: lymph node; NAMS: normalized average methylation score; NTB: non-tumorigenic breast; ROC: receiver-operator characteristics; SEM: standard error of means; TAGLN: transgelin; TN: triple negative; TSG: tumor suppressor gene.

Competing interests

The authors declare that they have no competing interests.

Authors' contributions

NS performed laboratory experiments and statistical analyses at all steps, interpreted the results, and wrote and revised the manuscript. GK performed initial laboratory experiments and revised the manuscript. OK mentored statistical analyses and revised the manuscript. BB provided tissue samples, conducted pathology review and revised the manuscript. OB performed tissue array IHC experiments, conducted pathology review and revised the manuscript. IGY designed the approach, interpreted the results, and wrote and revised the manuscript. All authors have read and approved the final manuscript.

Authors' information

Not applicable

Availability of data and materials

Not applicable

Acknowledgements

This study has been supported by grants from The Scientific and Technological Research Council of Turkey (TÜBİTAK-107T181). and Bilkent University.

Author details

[1]Department of Molecular Biology and Genetics, Bilkent University, Faculty of Science, TR-06800 Ankara, Turkey. [2]Department of General Surgery, Ankara Numune Training and Research Hospital, 06100 Ankara, Turkey. [3]Department of Pathology, Ankara Numune Training and Research Hospital, 06100 Ankara, Turkey.

Received: 26 July 2015 Accepted: 18 September 2015
Published online: 28 September 2015

References

1. Dent R, Trudeau M, Pritchard KI, Hanna WM, Kahn HK, Sawka CA, et al. Triple-negative breast cancer: clinical features and patterns of recurrence. Clin Cancer Res. 2007;13(15 Pt 1):4429–34. doi:10.1158/1078-0432.CCR-06-3045.
2. Perou CM, Sorlie T, Eisen MB, van de Rijn M, Jeffrey SS, Rees CA, et al. Molecular portraits of human breast tumours. Nature. 2000;406(6797):747–52. doi:10.1038/35021093.

3. Sorlie T, Perou CM, Tibshirani R, Aas T, Geisler S, Johnsen H, et al. Gene expression patterns of breast carcinomas distinguish tumor subclasses with clinical implications. Proc Natl Acad Sci USA. 2001;98(19):10869–74. doi:10.1073/pnas.191367098.
4. Herman JG, Baylin SB. Gene silencing in cancer in association with promoter hypermethylation. N Engl J Med. 2003;349(21):2042–54. doi:10.1056/NEJMra023075.
5. Esteller M. Cancer epigenomics: DNA methylomes and histone-modification maps. Nat Rev Genet. 2007;8(4):286–98. doi:10.1038/nrg2005.
6. Hanahan D, Weinberg RA. The hallmarks of cancer. Cell. 2000;100(1):57–70.
7. Baylin SB, Esteller M, Rountree MR, Bachman KE, Schuebel K, Herman JG. Aberrant patterns of DNA methylation, chromatin formation and gene expression in cancer. Hum Mol Genet. 2001;10(7):687–92.
8. Dworkin AM, Huang TH, Toland AE. Epigenetic alterations in the breast: implications for breast cancer detection, prognosis and treatment. Semin Cancer Biol. 2009;19(3):165–71. doi:10.1016/j.semcancer.2009.02.007.
9. Qiu X, Hother C, Ralfkiaer UM, Sogaard A, Lu Q, Workman CT, et al. Equitoxic doses of 5-azacytidine and 5-aza-2'deoxycytidine induce diverse immediate and overlapping heritable changes in the transcriptome. PLoS One. 2010;5:9. doi:10.1371/journal.pone.0012994.
10. Momparler RL, Cote S, Momparler LF, Idaghdour Y. Epigenetic therapy of acute myeloid leukemia using 5-aza-2'-deoxycytidine (decitabine) in combination with inhibitors of histone methylation and deacetylation. Clin Epigenetics. 2014;6(1):19. doi:10.1186/1868-7083-6-19.
11. Suzuki H, Gabrielson E, Chen W, Anbazhagan R, van Engeland M, Weijenberg MP, et al. A genomic screen for genes upregulated by demethylation and histone deacetylase inhibition in human colorectal cancer. Nat Genet. 2002;31(2):141–9. doi:10.1038/ng892.
12. Kristiansen S, Jorgensen LM, Guldberg P, Soletormos G. Aberrantly methylated DNA as a biomarker in breast cancer. Int J Biol Markers. 2013;28(2):141–50. doi:10.5301/jbm.5000009.
13. Mulero-Navarro S, Esteller M. Epigenetic biomarkers for human cancer: the time is now. Crit Rev Oncol Hematol. 2008;68(1):1–11. doi:10.1016/j.critrevonc.2008.03.001.
14. Radpour R, Barekati Z, Kohler C, Lv Q, Burki N, Diesch C, et al. Hypermethylation of tumor suppressor genes involved in critical regulatory pathways for developing a blood-based test in breast cancer. PLoS One. 2011;6(1), e16080. doi:10.1371/journal.pone.0016080.
15. Laird PW. The power and the promise of DNA methylation markers. Nat Rev Cancer. 2003;3(4):253–66. doi:10.1038/nrc1045.
16. Prinjha RK, Shapland CE, Hsuan JJ, Totty NF, Mason IJ, Lawson D. Cloning and sequencing of cDNAs encoding the actin cross-linking protein transgelin defines a new family of actin-associated proteins. Cell Motil Cytoskeleton. 1994;28(3):243–55. doi:10.1002/cm.970280307.
17. Shapland C, Lowings P, Lawson D. Identification of new actin-associated polypeptides that are modified by viral transformation and changes in cell shape. J Cell Biol. 1988;107(1):153–61.
18. Camoretti-Mercado B, Forsythe SM, LeBeau MM, Espinosa 3rd R, Vieira JE, Halayko AJ, et al. Expression and cytogenetic localization of the human SM22 gene (TAGLN). Genomics. 1998;49(3):452–7. doi:10.1006/geno.1998.5267.
19. Lees-Miller JP, Heeley DH, Smillie LB. An abundant and novel protein of 22 kDa (SM22) is widely distributed in smooth muscles. Purification from bovine aorta. Biochem J. 1987;244(3):705–9.
20. Almendral JM, Santaren JF, Perera J, Zerial M, Bravo R. Expression, cloning and cDNA sequence of a fibroblast serum-regulated gene encoding a putative actin-associated protein (p27). Exp Cell Res. 1989;181(2):518–30.
21. Schenker T, Trueb B. Down-regulated proteins of mesenchymal tumor cells. Exp Cell Res. 1998;239(1):161–8. doi:10.1006/excr.1997.3896.
22. Shields JM, Rogers-Graham K, Der CJ. Loss of transgelin in breast and colon tumors and in RIE-1 cells by Ras deregulation of gene expression through Raf-independent pathways. J Biol Chem. 2002;277(12):9790–9. doi:10.1074/jbc.M110086200.
23. Prasad PD, Stanton JA, Assinder SJ. Expression of the actin-associated protein transgelin (SM22) is decreased in prostate cancer. Cell Tissue Res. 2010;339(2):337–47. doi:10.1007/s00441-009-0902-y.
24. Wulfkuhle JD, Sgroi DC, Krutzsch H, McLean K, McGarvey K, Knowlton M, et al. Proteomics of human breast ductal carcinoma in situ. Cancer Res. 2002;62(22):6740–9.
25. Thweatt R, Lumpkin Jr CK, Goldstein S. A novel gene encoding a smooth muscle protein is overexpressed in senescent human fibroblasts. Biochem Biophys Res Commun. 1992;187(1):1–7.
26. Gonos ES, Derventzi A, Kveiborg M, Agiostratidou G, Kassem M, Clark BF, et al. Cloning and identification of genes that associate with mammalian replicative senescence. Exp Cell Res. 1998;240(1):66–74. doi:10.1006/excr.1998.3948.
27. Dumont P, Burton M, Chen QM, Gonos ES, Frippiat C, Mazarati JB, et al. Induction of replicative senescence biomarkers by sublethal oxidative stresses in normal human fibroblast. Free Radic Biol Med. 2000;28(3):361–73.
28. Marshall CB, Krofft RD, Blonski MJ, Kowalewska J, Logar CM, Pippin JW, et al. Role of smooth muscle protein SM22alpha in glomerular epithelial cell injury. Am J Physiol Renal Physiol. 2011;300(4):F1026–42. doi:10.1152/ajprenal.00187.2010.
29. Zhang ZW, Yang ZM, Zheng YC, Chen ZD. Transgelin induces apoptosis of human prostate LNCaP cells through its interaction with p53. Asian J Androl. 2010;12(2):186–95. doi:10.1038/aja.2009.76.
30. Nair RR, Solway J, Boyd DD. Expression cloning identifies transgelin (SM22) as a novel repressor of 92-kDa type IV collagenase (MMP-9) expression. J Biol Chem. 2006;281(36):26424–36. doi:10.1074/jbc.M602703200.
31. Kalhori V, Tornquist K. MMP2 and MMP9 participate in S1P-induced invasion of follicular ML-1 thyroid cancer cells. Mol Cell Endocrinol. 2015;404:113–22. doi:10.1016/j.mce.2015.01.037.
32. Yeo M, Park HJ, Kim DK, Kim YB, Cheong JY, Lee KJ, et al. Loss of SM22 is a characteristic signature of colon carcinogenesis and its restoration suppresses colon tumorigenicity in vivo and in vitro. Cancer. 2010;116(11):2581–9. doi:10.1002/cncr.25003.
33. Li N, Zhang J, Liang Y, Shao J, Peng F, Sun M, et al. A controversial tumor marker: is SM22 a proper biomarker for gastric cancer cells? J Proteome Res. 2007;6(8):3304–12. doi:10.1021/pr0702363.
34. Lin Y, Buckhaults PJ, Lee JR, Xiong H, Farrell C, Podolsky RH, et al. Association of the actin-binding protein transgelin with lymph node metastasis in human colorectal cancer. Neoplasia. 2009;11(9):864–73.
35. da Huang W, Sherman BT, Lempicki RA. Systematic and integrative analysis of large gene lists using DAVID bioinformatics resources. Nat Protoc. 2009;4(1):44–57. doi:10.1038/nprot.2008.211.
36. da Huang W, Sherman BT, Lempicki RA. Bioinformatics enrichment tools: paths toward the comprehensive functional analysis of large gene lists. Nucleic Acids Res. 2009;37(1):1–13. doi:10.1093/nar/gkn923.
37. Dedeurwaerder S, Desmedt C, Calonne E, Singhal SK, Haibe-Kains B, Defrance M, et al. DNA methylation profiling reveals a predominant immune component in breast cancers. EMBO Mol Med. 2011;3(12):726–41. doi:10.1002/emmm.201100801.
38. Rhodes DR, Yu J, Shanker K, Deshpande N, Varambally R, Ghosh D, et al. ONCOMINE: a cancer microarray database and integrated data-mining platform. Neoplasia. 2004;6(1):1–6.
39. Yamamura H, Masuda H, Ikeda W, Tokuyama T, Takagi M, Shibata N, et al. Structure and expression of the human SM22alpha gene, assignment of the gene to chromosome 11, and repression of the promoter activity by cytosine DNA methylation. J Biochem. 1997;122(1):157–67.
40. O'Leary P, Penny SA, Dolan RT, Kelly CM, Madden SF, Rexhepaj E, et al. Systematic antibody generation and validation via tissue microarray technology leading to identification of a novel protein prognostic panel in breast cancer. BMC Cancer. 2013;13:175. doi:10.1186/1471-2407-13-175.
41. Fackler MJ, Umbricht CB, Williams D, Argani P, Cruz LA, Merino VF, et al. Genome-wide methylation analysis identifies genes specific to breast cancer hormone receptor status and risk of recurrence. Cancer Res. 2011;71(19):6195–207. doi:10.1158/0008-5472.CAN-11-1630.
42. Network CGA. Comprehensive molecular portraits of human breast tumours. Nature. 2012;490(7418):61–70. doi:10.1038/nature11412.
43. Gyorffy B, Lanczky A, Eklund AC, Denkert C, Budczies J, Li Q, et al. An online survival analysis tool to rapidly assess the effect of 22,277 genes on breast cancer prognosis using microarray data of 1,809 patients. Breast Cancer Res Treat. 2010;123(3):725–31. doi:10.1007/s10549-009-0674-9.
44. Yao TT, Mo SM, Liu LY, Lu HW, Huang ML, Lin ZQ. 5-Aza-2'-deoxycytidine may influence the proliferation and apoptosis of cervical cancer cells via demethylation in a dose- and time-dependent manner. Genet Mol Res. 2013;12(1):312–8. doi:10.4238/2013.February.4.5.

45. Gomyo Y, Sasaki J, Branch C, Roth JA, Mukhopadhyay T. 5-aza-2'-deoxycytidine upregulates caspase-9 expression cooperating with p53-induced apoptosis in human lung cancer cells. Oncogene. 2004;23(40):6779–87. doi:10.1038/sj.onc.1207381.
46. Zhu WG, Hileman T, Ke Y, Wang P, Lu S, Duan W, et al. 5-aza-2'-deoxycytidine activates the p53/p21Waf1/Cip1 pathway to inhibit cell proliferation. J Biol Chem. 2004;279(15):15161–6. doi:10.1074/jbc.M311703200.
47. Hackanson B, Daskalakis M. Decitabine. Recent Results Cancer Res. 2014;201:269–97. doi:10.1007/978-3-642-54490-3_18.
48. Hirasawa Y, Arai M, Imazeki F, Tada M, Mikata R, Fukai K, et al. Methylation status of genes upregulated by demethylating agent 5-aza-2'-deoxycytidine in hepatocellular carcinoma. Oncology. 2006;71(1–2):77–85. doi:10.1159/000100475.
49. Zhao L, Wang H, Deng YJ, Wang S, Liu C, Jin H, et al. Transgelin as a suppressor is associated with poor prognosis in colorectal carcinoma patients. Mod Pathol. 2009;22(6):786–96. doi:10.1038/modpathol.2009.29.
50. Murria R, Palanca S, de Juan I, Egoavil C, Alenda C, Garcia-Casado Z, et al. Methylation of tumor suppressor genes is related with copy number aberrations in breast cancer. Am J Cancer Res. 2015;5(1):375–85.
51. Gormally E, Caboux E, Vineis P, Hainaut P. Circulating free DNA in plasma or serum as biomarker of carcinogenesis: practical aspects and biological significance. Mutat Res. 2007;635(2–3):105–17. doi:10.1016/j.mrrev.2006.11.002.
52. Jeronimo C, Costa I, Martins MC, Monteiro P, Lisboa S, Palmeira C, et al. Detection of gene promoter hypermethylation in fine needle washings from breast lesions. Clin Cancer Res. 2003;9(9):3413–7.
53. Krassenstein R, Sauter E, Dulaimi E, Battagli C, Ehya H, Klein-Szanto A, et al. Detection of breast cancer in nipple aspirate fluid by CpG island hypermethylation. Clin Cancer Res. 2004;10(1 Pt 1):28–32.
54. Antill YC, Mitchell G, Johnson SA, Devereux L, Milner A, Di Iulio J, et al. Gene methylation in breast ductal fluid from BRCA1 and BRCA2 mutation carriers. Cancer Epidemiol Biomarkers Prev. 2010;19(1):265–74. doi:10.1158/1055-9965.EPI-09-0359.
55. Van De Voorde L, Speeckaert R, Van Gestel D, Bracke M, De Neve W, Delanghe J, et al. DNA methylation-based biomarkers in serum of patients with breast cancer. Mutat Res. 2012;751(2):304–25. doi:10.1016/j.mrrev.2012.06.001.
56. Shukla S, Mirza S, Sharma G, Parshad R, Gupta SD, Ralhan R. Detection of RASSF1A and RARbeta hypermethylation in serum DNA from breast cancer patients. Epigenetics. 2006;1(2):88–93.
57. Kim JH, Shin MH, Kweon SS, Park MH, Yoon JH, Lee JS, et al. Evaluation of promoter hypermethylation detection in serum as a diagnostic tool for breast carcinoma in Korean women. Gynecol Oncol. 2010;118(2):176–81. doi:10.1016/j.ygyno.2010.04.016.
58. Naito S, Pippin JW, Shankland SJ. The glomerular parietal epithelial cell's responses are influenced by SM22 alpha levels. BMC Nephrol. 2014;15:174. doi:10.1186/1471-2369-15-174.
59. Groger CJ, Grubinger M, Waldhor T, Vierlinger K, Mikulits W. Meta-analysis of gene expression signatures defining the epithelial to mesenchymal transition during cancer progression. PLoS One. 2012;7(12), e51136. doi:10.1371/journal.pone.0051136.
60. Thompson O, Moghraby JS, Ayscough KR, Winder SJ. Depletion of the actin bundling protein SM22/transgelin increases actin dynamics and enhances the tumourigenic phenotypes of cells. BMC Cell Biol. 2012;13:1. doi:10.1186/1471-2121-13-1.
61. Pang J, Liu WP, Liu XP, Li LY, Fang YQ, Sun QP, et al. Profiling protein markers associated with lymph node metastasis in prostate cancer by DIGE-based proteomics analysis. J Proteome Res. 2010;9(1):216–26. doi:10.1021/pr900953s.
62. Park GH, Lee SJ, Yim H, Han JH, Kim HJ, Sohn YB, et al. TAGLN expression is upregulated in NF1-associated malignant peripheral nerve sheath tumors by hypomethylation in its promoter and subpromoter regions. Oncol Rep. 2014;32(4):1347–54. doi:10.3892/or.2014.3379.
63. Mikuriya K, Kuramitsu Y, Ryozawa S, Fujimoto M, Mori S, Oka M, et al. Expression of glycolytic enzymes is increased in pancreatic cancerous tissues as evidenced by proteomic profiling by two-dimensional electrophoresis and liquid chromatography-mass spectrometry/mass spectrometry. Int J Oncol. 2007;30(4):849–55.
64. Klade CS, Voss T, Krystek E, Ahorn H, Zatloukal K, Pummer K, et al. Identification of tumor antigens in renal cell carcinoma by serological proteome analysis. Proteomics. 2001;1(7):890–8. doi:10.1002/1615-9861(200107)1:7<890::AID-PROT890>3.0.CO;2-Z.
65. Rho JH, Roehrl MH, Wang JY. Tissue proteomics reveals differential and compartment-specific expression of the homologs transgelin and transgelin-2 in lung adenocarcinoma and its stroma. J Proteome Res. 2009;8(12):5610–8. doi:10.1021/pr900705r.
66. Assinder SJ, Stanton JA, Prasad PD. Transgelin: an actin-binding protein and tumour suppressor. Int J Biochem Cell Biol. 2009;41(3):482–6. doi:10.1016/j.biocel.2008.02.011.
67. Yang Z, Chang YJ, Miyamoto H, Ni J, Niu Y, Chen Z, et al. Transgelin functions as a suppressor via inhibition of ARA54-enhanced androgen receptor transactivation and prostate cancer cell growth. Mol Endocrinol. 2007;21(2):343–58. doi:10.1210/me.2006-0104.
68. Ryu JW, Kim HJ, Lee YS, Myong NH, Hwang CH, Lee GS, et al. The proteomics approach to find biomarkers in gastric cancer. J Korean Med Sci. 2003;18(4):505–9.
69. Yu B, Chen X, Li J, Qu Y, Su L, Peng Y, et al. Stromal fibroblasts in the microenvironment of gastric carcinomas promote tumor metastasis via upregulating TAGLN expression. BMC Cell Biol. 2013;14:17. doi:10.1186/1471-2121-14-17.
70. Shapland C, Hsuan JJ, Totty NF, Lawson D. Purification and properties of transgelin: a transformation and shape change sensitive actin-gelling protein. J Cell Biol. 1993;121(5):1065–73.
71. Hall A. The cytoskeleton and cancer. Cancer Metastasis Rev. 2009;28(1–2):5–14. doi:10.1007/s10555-008-9166-3.
72. Shen J, Yang M, Ju D, Jiang H, Zheng JP, Xu Z, et al. Disruption of SM22 promotes inflammation after artery injury via nuclear factor kappaB activation. Circ Res. 2010;106(8):1351–62. doi:10.1161/CIRCRESAHA.109.213900.
73. Gimona M, Kaverina I, Resch GP, Vignal E, Burgstaller G. Calponin repeats regulate actin filament stability and formation of podosomes in smooth muscle cells. Mol Biol Cell. 2003;14(6):2482–91. doi:10.1091/mbc.E02-11-0743.
74. Gourlay CW, Carpp LN, Timpson P, Winder SJ, Ayscough KR. A role for the actin cytoskeleton in cell death and aging in yeast. J Cell Biol. 2004;164(6):803–9. doi:10.1083/jcb.200310148.
75. Kato Y, Salumbides BC, Wang XF, Qian DZ, Williams S, Wei Y, et al. Antitumor effect of the histone deacetylase inhibitor LAQ824 in combination with 13-cis-retinoic acid in human malignant melanoma. Mol Cancer Ther. 2007;6(1):70–81. doi:10.1158/1535-7163.MCT-06-0125.
76. Zhang R, Zhou L, Li Q, Liu J, Yao W, Wan H. Up-regulation of two actin-associated proteins prompts pulmonary artery smooth muscle cell migration under hypoxia. Am J Respir Cell Mol Biol. 2009;41(4):467–75. doi:10.1165/rcmb.2008-0333OC.
77. Kaverina I, Stradal TE, Gimona M. Podosome formation in cultured A7r5 vascular smooth muscle cells requires Arp2/3-dependent de-novo actin polymerization at discrete microdomains. J Cell Sci. 2003;116(Pt 24):4915–24. doi:10.1242/jcs.00818.
78. Yu H, Konigshoff M, Jayachandran A, Handley D, Seeger W, Kaminski N, et al. Transgelin is a direct target of TGF-beta/Smad3-dependent epithelial cell migration in lung fibrosis. FASEB J. 2008;22(6):1778–89. doi:10.1096/fj.07-083857.
79. Chunhua L, Donglan L, Xiuqiong F, Lihua Z, Qin F, Yawei L, et al. Apigenin up-regulates transgelin and inhibits invasion and migration of colorectal cancer through decreased phosphorylation of AKT. J Nutr Biochem. 2013;24(10):1766–75. doi:10.1016/j.jnutbio.2013.03.006.
80. Ye J, Coulouris G, Zaretskaya I, Cutcutache I, Rozen S, Madden TL. Primer-BLAST: a tool to design target-specific primers for polymerase chain reaction. BMC Bioinformatics. 2012;13:134. doi:10.1186/1471-2105-13-134.
81. Gur-Dedeoglu B, Konu O, Bozkurt B, Ergul G, Seckin S, Yulug IG. Identification of endogenous reference genes for qRT-PCR analysis in normal matched breast tumor tissues. Oncol Res. 2009;17(8):353–65.
82. Winer J, Jung CK, Shackel I, Williams PM. Development and validation of real-time quantitative reverse transcriptase-polymerase chain reaction for monitoring gene expression in cardiac myocytes in vitro. Anal Biochem. 1999;270(1):41–9. doi:10.1006/abio.1999.4085.
83. Kumaki Y, Oda M, Okano M. QUMA: quantification tool for methylation analysis. Nucleic Acids Res. 2008;36(Web Server issue):W170–5. doi:10.1093/nar/gkn294.
84. McCarty Jr KS, Szabo E, Flowers JL, Cox EB, Leight GS, Miller L, et al. Use of a monoclonal anti-estrogen receptor antibody in the immunohistochemical evaluation of human tumors. Cancer Res. 1986;46(8):4244s–8s.
85. Mihaly Z, Kormos M, Lanczky A, Dank M, Budczies J, Szasz MA, et al. A meta-analysis of gene expression-based biomarkers predicting outcome after tamoxifen treatment in breast cancer. Breast Cancer Res Treat. 2013;140(2):219–32. doi:10.1007/s10549-013-2622-y.